Molecular mechanisms of neuronal death in glaucoma: development of a gene therapy approach for neuroprotection

Molecular mechanisms of neuronal death in glaucoma: development of a gene therapy approach for neuroprotection

Nitin Chitranshi

B.Pharm, M.Pharm

Faculty of Medicine and Health Sciences

Macquarie University

April 2017

Supervisors

Prof. Stuart L Graham
Faculty of Medicine and Health Sciences
Department of Clinical Medicine
Macquarie University

Dr. Vivek K Gupta
Faculty of Medicine and Health Sciences
Department of Clinical Medicine
Macquarie University

Dr. Yuyi You
Faculty of Medicine and Health Sciences
Department of Clinical Medicine
Macquarie University

MACQUARIE University
SYDNEY·AUSTRALIA

Copyright statement

‘I hereby allow Macquarie University or its agents the privilege to file and to make accessible my thesis or postulation in entire or part-in the University libraries in all types of media, subject to the provisions of the Copyright Act 1968. I hold every single restrictive right, such as patent rights. I likewise hold the privilege to use in future works (for example articles or books) all or some portion of this thesis or postulations. I have either utilized no considerable portions of copyright material in my thesis or I have obtained permission to use copyright material; where authorization has not been granted I have connected /will apply for a fractional confinement of the computerized duplicate of my thesis or postulation.’

Nitin Chitranshi

April 2017

Authenticity statement

`I confirm that the Library deposit digital copy is an immediate likeness the last authoritatively endorsed rendition of my thesis. No revisal of content has happened and if there are any minor variations in organizing, they are the aftereffect of the transformation to digital format.'

Nitin Chitranshi

April 2017

I would like to dedicate this thesis to my beloved wife and son and to my parents who have supported me throughout this process.

Originality statement

`I hereby declare that this thesis entitled “Molecular mechanisms of neuronal death in glaucoma: development of a gene therapy approach for neuroprotection” is my own work and to the best of my insight it contains no materials beforehand published or written by someone else, or generous extents of material which have been acknowledge for the award of some other degree or certificate at Macquarie University or if any other educational organization, with the exception of where due affirmation is made in the thesis. I additionally proclaim that the intellectual content of this thesis is the result of my own work, except to the extent that help from others in the project's outline and origination or in style, presentation and semantic expression is acknowledged.'

Nitin Chitranshi

April 2017

Acknowledgements

"Only in the darkness can you see the stars" – Martin Luther King.

Above all else, I'd get a kick out of the chance to thank my supervisor Professor Stuart L Graham, for the opportunity to join vision group and exceptional mentorship. I've had incredibly rewarding experience learning from him and working in the Graham Lab. He has always given support, consolation, feedback, and guidance. The atmosphere he encourages in his lab is one of the inspiration, coordinated effort, and collaboration, I am genuinely grateful for the open doors he's made feasible for me. His support of my ideas, including traveling to the United States for the world leading vision conference, ARVO, in my first year of PhD, gave me enthusiasm for glaucoma research and made the success of my graduate career possible. I am fortunate to have had such an exceptional mentor, and would like to have the capacity to emulate his footsteps as an outstanding scientist and mentor in future.

I'd likewise like to show my appreciation to my supervisor Dr. Vivek K. Gupta. Dr. Gupta has been a supportive mentor, companion, and colleague whose opinion on all scientific matters I value and trust. His direction has been an integral part of my work in the Graham lab and completing this thesis. He has been my teacher for many of the protocols used in these experiments. This work would have not been possible without him. His mastery of the numerous specialized techniques of these experiments such as viral construct design, intravitreal injection, intraocular injection, biochemistry and many other practical approaches was unimaginably useful. Dr. Yuyi You, my other co-supervisor, instructed me in many animal experimental techniques including electrophysiology, in the early years of my PhD.

I'd also like to thank Mrs. Yogita Dheer, Ms. Roshana Vander Wall, Mrs. Mojdeh Abbassi and Ms. Dana Georgevsky who has been the most essential source of support during my entire graduate career, presentations, long nights, weekends in the lab and this thesis. They had listened to, perused or edited much of what I've presented, as well as performed animal monitoring for me when I was unavailable. Overall the support they have provided has been priceless.

This study was supported by:

Macquarie University Research Excellence Scholarship (**iMQRES**)

Macquarie University Postgraduate Research Fund (**PGRF**)

Skipper Postgraduate / Early Career Researcher Travel Award

Travel grant from German Neuroscience Society (**GNS 2017**)

Translational vision summit award (**ARVO-ASIA 2017**)

Publications

This is a partially publication-based thesis. Declaration of contribution to papers containing submitted or published work.

Journal Articles published from the thesis

1. **Nitin Chitranshi**, Vivek Gupta, Stuart L Graham. (2016) Molecular determinants and interaction data of cyclic peptide inhibitor with the extracellular domain of TrkB receptor. *Data in Brief*, Mar; 6:776-782
2. **Nitin Chitranshi,** Vivek Gupta, Sanjay Kumar, Stuart L Graham. (2015) Exploring the Molecular Interactions of 7,8 Dihydroxyflavone and its derivatives with TrkB and VEGFR2 proteins. ***Int. J. Mol. Sci.*** 16, 21087-21108
3. Vivek Gupta, **Nitin Chitranshi**, Yuyi You, Veer Gupta, Alexander Klistorner, Stuart Graham. (2014) Brain derived neurotrophic factor is involved in the regulation of glycogen synthase kinase 3β (GSK3β) signaling. *Biochem Biophys Res Commun.* 454(3):381-386. (doi: 10.1016/j.bbrc.2014.10.087)

Manuscript under preparation/ submitted from the thesis

4. **Nitin Chitranshi,** Yogita Dheer, Roshan Vander Wall, Veer Gupta, Mojdeh Abbasi, Mehdi Mirzaei, Yuyi You, Roger Chung, Stuart L Graham, Vivek Gupta (2017) Adeno-associated virus mediated overexpression of PTPN11 induces TrkB dephosphorylation and increases endoplasmic stress in SH-SY5Y cells and rat retina (***submitted in Journal of Neurochemistry)***
5. TrkB signaling pathways in glaucoma: Focus on molecular basis, genetics and potential neuroprotection (**Manuscript under preparation**).
6. Downregulation of Shp2 in retinal ganglion cells protects retinal degeneration via TrkB activation in experimental glaucoma (**Manuscript under preparation**).

Other accepted/ published journal articles

7. Vivek Gupta, Mehdi Mirzaei, Veer Bala Gupta, **Nitin Chitranshi,** Yogita Dheer, Roshana VanderWall, Mojdeh Abbasi, Yuyi You, Roger Chung, Stuart Graham (2017) Glaucoma is associated with plasmin proteolytic activation mediated through oxidative inactivation of neuroserpin (***revision Scientific Reports***)
8. **Nitin Chitranshi,** Yogita Dheer, Roshana Vander Wall, Veer Gupta, Mojdeh Abbasi, Stuart L Graham, Vivek Gupta. (2016) Computalional analysis unravels novel destructive single nucleotide polymorphisms in the non-synonymous region of human caveolin gene. ***Gene Reports*** http://dx.doi.org/10.1016/j.genrep.2016.08.008
9. Vivek Gupta, Veer B Gupta, **Nitin Chitranshi**, Sumudu Gangoda, Roshana Vander Wall, Mojtaba Golzan, Yogita Dheer, Tejal Shah, Alberto Avolio, Roger Chung, Ralph Martins, Stuart L Graham. (2016) One protein, multiple pathologies: Multifaceted involment of amyloid β in neurodegenerative disorders of the brain and retina, 2016 ***Cell Moll. Life Sci***.; DOI 10.1007/s00018-016-2295-x
10. Vivek Gupta, **Nitin Chitranshi**, Veer B Gupta, Mojtaba Golzan, Yogita Dheer, Anna E King, James C Vickers, Roger Chung, Stuart L Graham. (2016) Amyloid β

accumulation and inner retinal degenerative changes in Alzheimer's disease transgenic mouse. 2016 ***Neurosci Lett***, Apr 28; 623:52-56.

11. Yuyi You, Vivek K Gupta, **Nitin Chitranshi,** Brittany Reedman, Alexander Klistorner, Stuart L Graham. (2015) Visual evoked potential recording in a rat model of experimental optic nerve demyelination. ***J. Vis. Exp.*** (101), e52934, doi:10.3791/52934.

Conference Presentations

1. **Nitin Chitranshi**, Vivek K Gupta, Yogita Dheer, Stuart L Graham, (2017) AAV mediated PTPN11 knockdown stimulates TrkB activity in neuronal cells in culture and in rat retina. **12th Gottingen Meeting of the German Neuroscience Society.**
2. **Nitin Chitranshi**, Vivek K Gupta, Yogita Dheer, Stuart L Graham, (2017) Adeno-associated virus knockdown of Shp2 phosphatase protect inner retinal structure and function in experimental glaucoma. **ASIA-ARVO 2017.**
3. Vivek K Gupta, Mehdi Mirzaei, Veer Gupta, Joel Chick, Yunqi Wu, **Nitin Chitranshi**, Roshana Vander Wall, Stuart L Graham, (2017) Proteomic profiles of normal and glaucoma eyes: Overlap with Alzheimer's Disease biomarkers. **ASIA-ARVO 2017.**
4. Yogita Dheer, **Nitin Chitranshi**, Roshana Vander Wall, Vivek K Gupta, Stuart L Graham (2017) Retinoid-X-receptor agonist Bexarotene treatment provides retinal functional protection in acute and chronic model of glaucoma. **ASIA-ARVO 2017.**
5. Roshana Vander Wall, Vivek K Gupta, **Nitin Chitranshi**, Yogita Dheer, Stuart L Graham (2017) New insights into Protease Inhibitor Activity of Neuroserpin in Glaucoma. **ASIA-ARVO 2017.**
6. Mojdeh Abbasi, Vivek K Gupta **Nitin Chitranshi,** Yogita Dheer, Anita Turner, Roshana Vander Wall, Stuart L. Graham (2016) Cav-1 ablation protects against loss of inner retinal function caused by PTPN11 overexpression. **ANS2016.**
7. **Nitin Chitranshi,** Roshana Vander Wall, Yogita Dheer, Stuart L. Graham, Vivek K Gupta. (2016) AAV Mediated Gene Therapy to Modulate Neurotropic Factors in the Retina and in Neuronal Cells in Culture. **19th Annual meeting of ASGCT**, **Mol. Therapy** 24: S321-S350; doi : 10.1038/mt.2016.80
8. **Nitin Chitranshi,** Vivek K. Gupta, Roshana Vander Wall, Yogita Dheer, Stuart L. Graham. (2016) SHP2 (PTPN11) over-expression by AAV gene delivery impairs neuronal cell growth in SH-SY5Y cells and induces neurodegeneration of SD rat retinal ganglion cells. **ARVO 2016, Invest. Ophthalmol. Vis. Sci.. 2016; 57(12):3997**.
9. Yogita Dheer, **Nitin Chitranshi,** Roshana Vander Wall, Stuart L. Graham, Vivek K. Gupta. (2016) Retinoid x receptor (RXR) expression in the rodent retina and effects of its modulation in neuronal cells. **ARVO 2016, Invest. Ophthalmol. Vis. Sci.. 2016; 57(12):1725**.
10. **Nitin Chitranshi,** Yuyi You, Vivek Kumar Gupta, Alexander Klistorner, Stuart L Graham. (2015) Effects of isoflurane on the visual evoked potentials in rats. **ARVO 2015**, **Invest. Ophthalmol. Vis. Sci.**; 56(7):468.
11. Stuart L. Graham, **Nitin Chitranshi,** Roger Chung, Vivek K. Gupta. (2015) Impaired inner retinal function and Amyloid β aggregation is demonstrated in a mouse model of Alzheimer's disease. **Invest. Ophthalmol. Vis. Sci..**; 56(7):2434.

Abstract

In glaucoma, loss of retinal ganglion cells (RGCs) and axons leads to blindness; preservation of RGC neurons is therefore a major therapeutic goal. Increasing pressure (intraocular pressure, IOP) is a major risk factor in primary open angle glaucoma (POAG). Therapeutic lowering of IOP has been shown to be protective against glaucoma. However, despite IOP lowering many patients continue to demonstrate progressive glaucomatous neuropathy thus warranting additional intervention strategies. Brain-derived neurotrophic factor (BDNF) and its high affinity receptor tropomyosin receptor kinase B (TrkB) are reported to play important role in preservation of RGCs. In this thesis, I have investigated BDNF-TrkB signaling in neuronal cells and have explored the binding pattern of agonist and antagonist to the neurotrophin receptors. I have also investigated TrkB activity by modulating Shp2 phosphatase (PTPN11) in SH-SY5Y cells, in both healthy rodents and an experimental glaucoma animal model, using viral vector gene therapy. The results show that BDNF regulates the GSK3β activity in RGC-5, PC-12 and animal RGCs. Shp2 modulation regulates TrkB phosphorylation and endoplasmic stress response in SH-SY5Y and in the RGCs of both healthy and experimental glaucoma animal models. Shp2 overexpression in SH-SY5Y cells and animal retina, was associated with TrkB antagonism, reduced neuritogenesis, loss of retinal structural & functional integrity and enhanced ER stress response leading to apoptotic changes. Conversely, Shp2 knock down in an animal model of elevated IOP resulted in protection of the retinal structural and functional integrity. These observations correlated with enhanced TrkB phosphorylation in RGCs in response to genetic knockdown of Shp2 expression in experimental animal glaucoma model. The current findings reinforce the role played by Shp2 in regulating signaling in neuronal cells and highlight that Shp2 dysregulation is detrimental for the inner retina. Based on these observations we propose that selective targeting of Shp2 in RGCs may be a promising therapeutic strategy in glaucoma.

TABLE OF CONTENTS

Copyright statement i
Authenticity statement ii
Originality statement iv
Acknowledgements v
Publications vii
Abstract ix
Table of contents x
List of Figures and Tables xv
List of abbreviations xvii

CHAPTER 1: INTRODUCTION

1.1 Motivation 1
1.2 Human visual system 3
1.2.1 Retina 3
1.2.2 Optic nerve 4
1.2.3 Lateral geniculate nucleus and visual cortex 5
1.3 Glaucoma 6
1.3.1 Definition and history 6
1.3.2 Epidemiology and risk factors 8
1.3.3 Genetic factors 9
1.3.4 Current management 11
1.3.5 Rodent models of glaucoma 14
1.4 Biochemical mechanism of neurotrophins in RGCs neuroprotection 17
1.4.1 Neurotrophin structure and function 17
1.4.2 Neurotrophin role in RGCs 20
1.4.3 Neurotrophin deprivation in glaucoma 22
1.4.4 BDNF-TrkB signaling 23
1.4.5 Glial BDNF-TrkB signaling 25
1.4.6 Pharmacological modulation of TrkB 26
1.4.7 TrkB regulation by endogenous phosphatase Shp2 28
1.5 Apoptosis in RGCs 31
1.5.1 ER stress and unfolded protein response 31
1.5.2 Signaling pathways of ER stress-associated apoptosis 33
1.6 Therapeutic targets in glaucoma 36
1.6.1 Can neurotrophins therapy scale down RGCs damage in glaucoma? 36
1.6.2 Targeting neurotrophin receptors in glaucoma therapy 38
1.6.3 Protective effects of inhibiting apoptotic pathway in RGCs in glaucoma 41
1.6.4 Targeting ER stress marker proteins as a strategy to halt the RGCs damage in glaucoma 43
1.6.5 Cross-talk with other receptor tyrosine kinase 44
Hypothesis 46
Aims 46

CHAPTER 2: MATERIAL AND METHODS

2.1 Ethics 48
2.2 List of materials 48
2.2.1 Animal experiments and electrophysiology 48
2.2.2 Histology study 49
2.2.3 Western blotting and immunoprecipitations 49
2.2.4 Cell cultures 49
2.2.5 Antibodies 50
2.3 Methods and protocols 51
2.3.1 Animals and anesthesia 51
2.3.2 AAV vector-Design and packaging 51
2.3.3 AAV2 intravitreal injections 55
2.3.4 Microbead Injection and IOP measurement 55
2.3.5 Animal recovery and follow up 56
2.3.6 Electroretinography 56
2.3.7 Tissue preparation and histology 57
2.3.7.1 Tissue fixation, embedding and section 57
2.3.7.2 Hematoxylin and eosin (H&E) staining 58
2.3.7.3 Bielschowsky's silver staining 58
2.3.7.4 TUNEL staining 58
2.3.7.5 Immunofluorescence 59
2.3.8 Biochemistry 60
2.3.8.1 Protein extraction 60
2.3.8.2 SDS-PAGE, Western Blot and Immunoprecipitations 60

CHAPTER 3: PROTECTIVE ROLE OF BRAIN DERIVED NEUROTROPHIC FACTOR IN NEURONAL CELLS

Abstract 63
3.1 Introduction 64
3.2 Materials and methods 66
3.2.1 Cell culture and treatments 66
3.2.2 Transfections 67
3.2.3 Drug treatments 67
3.2.4 SDS–PAGE and Western Blot analysis 68
3.2.5 Statistical analysis 68
3.3 Results 68
3.3.1 BDNF negatively regulates GSK3β activation in RGC-5 and PC12 cells 68
3.3.2 $BDNF^{+/-}$ mice depict reduced GSK3β phosphorylation with age 68
3.3.3 TrkB agonist enhances GSK3β phosphorylation in vivo 72
3.3.4 BDNF knockdown along with TrkB inhibition augments GSK3β activation 73
3.4 Discussion 75

CHAPTER 4: MECHANISTIC INSIGHTS INTO THE PHARMACOLOGICAL TARGETING OF TrkB RECEPTOR

Part A 79
Abstract 79
4A.1 Introduction 80
4A.2 Materials and methods 82
4A.2.1 Selection and Preparation of Macromolecule 82
4A.2.2 Selection and Preparation of dihydroxy flavones derivatives 83
4A.2.3 Molecular docking 83
4A.2.4 Molecular dynamics simulations 84
4A.2.5 Cell culture and treatment regimens 85
4A.2.6 Western Blot and Immunoprecipitations 86
4A.2.7 Statistical analysis 86
4A.3 Results 86
4A.3.1 Molecular determinants of 7,8 DHF binding with TrkB and VEGFR2 86
4A.3.2 Binding interactions of TrkB and VEGFR2 receptors with 7,8-DHF derivatives 88
4A.3.3 Molecular dynamics (MD) of 7,8-DHF-TrkB and 7,8-DHF-VEGFR2 Complex 97
4A.3.4 7,8-DHF treatment leads to loss of VEGFR2 activity 103
4A.4 Discussion 104
4A.5 Conclusion 109

Part B 112
Abstract 112
4B Data, Experimental Design, Materials and Methods 113
4B.1 Selection and Preparation of Cyclotraxin B, TrkB Inhibitor 113
4B.2 Molecular modeling and generation of TrkB binding region 115
4B.3 Identification of CTXB binding site 115
4B.4 Peptide docking in the binding region 117

CHAPTER 5: EFFECT OF TrkB MODULATION BY PTPN11 GENE TARGETING IN SH-SY5Y CELLS

Abstract 121
5.1 Introduction 122
5.2 Materials and methods 125
5.2.1 Viral vector transduction and treatment regimen in SH-SY5Y cells 125
5.2.2 Cell survival analysis and MTT assay 126
5.2.3 TUNEL staining 127
5.2.4 SDS–PAGE and western blotting 127
5.2.5 Immunofluorescence 127
5.2.6 Statistical Analysis 127
5.3 Results 128
5.3.1 PTPN11 has a regulatory effect on TrkB phosphorylation 128
5.3.2 PTPN11 modulation influences the endoplasmic stress

marker response 131
5.3.3 BDNF effects on PTPN11 induced TrkB deactivation and ER stress response 134
5.3.4 PTPN11 effects on TrkB and ER stress response are alleviated by TrkB modulation 136
5.3.5 PTPN11 upregulation induces neuronal apoptosis and its loss is associated with increased neuritogenesis 140
5.4 Discussion 143

CHAPTER 6: SHP2 UPREGULATION IMPAIR INNER RETINAL ENVIORNMENT AND NEGATIVELY REGULATES TrkB RECEPTOR ACTIVITY

Abstract 151
6.1 Introduction 152
6.2 Materials and methods 154
6.2.1 AAV vectors-Design and packaging 154
6.2.2 AAV2 vectors intravitreal injections 154
6.2.3 Electroretinography 154
6.2.4 Histology 155
6.2.5 SDS–PAGE and western blotting 155
6.2.6 Immunofluorescence 155
6.2.7 Statistical Analysis 156
6.3 Results 156
6.3.1 Assessment of transgene expression in healthy animal eyes 156
6.3.2 Reduced GCL density and axonal loss in response to Shp2 upregulation 159
6.3.3 Shp2 upregulation impairs inner retinal electrophysiological response 161
6.3.4 Shp2 has regulatory effects on TrkB phosphorylation 164
6.3.5 Shp2 upregulation induces neuronal apoptosis and ER stress in retina 166
6.4 Discussion 168

CHAPTER 7: SHP2 GENE THERAPY IS EFFECTIVE IN RGC NEUROPROTCTION IN EXPERIMENTAL GLAUCOMA

Abstract 175
7.1 Introduction 176
7.2 Materials and methods 178
7.2.1 Microbead Injection and IOP measurement 178
7.2.2 AAV vectors-Design and packaging 178
7.2.3 AAV2 vectors intravitreal injections 178
7.2.4 Electroretinography 179
7.2.5 Histology 179
7.2.6 SDS–PAGE and western blotting 179
7.2.7 Immunofluorescence 179

7.2.8 Statistical Analysis 179
7.3 Results 180
7.3.1 Intravitreal injection of microbead induced intraocular pressure elevation in animal eyes 180
7.3.2 Assessment of transgene expression in glaucoma eyes 181
7.3.3 Reduced GCL density and axon loss in response to experiment induced-glaucoma 185
7.3.4 Downregulation of Shp2 protects the GCL and axon loss against experimental glaucoma 187
7.3.5 Loss of inner retinal function in response to glaucoma 189
7.3.6 Downregulation of Shp2 is protective against inner retinal functional loss in experimental glaucoma 190
7.3.7 Shp2 suppression augments TrkB phosphorylation in inner retina in glaucoma 192
7.4 Discussion 194

CHAPTER 8: CONCLUSION AND FUTURE DIRECTIONS 202

REFERENCES 207

Figures

Chapter 1
Figure 1.1. Schematic representation of two different aqueous humor flow pathways.
Figure 1.2. Anatomical organization of the eye and the retina.
Figure 1.3. Human visual pathway system
Figure 1.4. The neurotrophins and their receptors.
Figure 1.5. Schematic representation of BDNF/ TrkB signaling in normal and glaucomatous condition

Chapter 2
Figure 2.1. Map of the plasmid containing the mShp2 sequence used for overexpression.
Figure 2.2. Map of the plasmid containing the mShp2-shRNAmir sequence used for knockdown.

Chapter 3
Figure 3.1. BDNF knockdown leads to GSK3β activation by reducing its phosphorylation levels.
Figure 3.2. $BDNF^{+/-}$ animals depict a decrease in GSK3β phosphorylation with age.
Figure 3.3. Treatment with TrkB agonist leads to enhanced GSK3β phosphorylation *in vivo*.
Figure 3.4. Inhibition of TrkB receptor promotes dephosphorylation of GSK3β.

Chapter 4
Figure 4A.1. Interaction and binding mode of 7,8 dihydroxyflavone (7,8-DHF) with TrkB and VEGFR2.
Figure 4A.2. Molecular modelling showing interaction of 7,8-DHF derivatives with the TrkB
Figure 4A.3. Molecular modelling showing interaction of 7,8-DHF derivatives with the VEGFR2.
Figure 4A.4. RMSF of backbone and side chain during 10 ns MD simulations.
Figure 4A.5. Energy peak during 10 ns MD simulation.
Figure 4A.6. The MD simulation Time vs. RMSD of the backbone atoms.
Figure 4A.7. MD Simulation Time vs. RMSD of the heavy atoms.
Figure 4A.8. H-bonds formed during total course of 10,000 ps MD simulations.
Figure 4A.9. 7,8-DHF exerts an inhibitory effect on the VEGFR2.
Figure 4A.10. Sequence alignment of VEGFR2, TrkB, IGF1R, STK4, PK3CG and CDCP1 with space filled model of TrkB and VEGFR2
Figure 4B.1. Cyclotraxin B stuructre
Figure 4B.2. Predicted binding sites of CTXB peptide ‘‘CNPMGYTKEG’’ core motif
Figure 4B.3. Interacting residues and binding mode of CTXB with TrkB-D5 domain.

Chapter 5
Figure 5.1. Schematic representation of AAV2 viral vector system used for PTPN11 overexpression and knockdown.
Figure 5.2. PTPN11 modulation negatively affects TrkB Y515 phosphorylation in SH-SY5Y cells.
Figure 5.3. Effect of PHPS1 on SH-SY5Y neuronal cells.
Figure 5.4. PTPN11 upregulation is associated with enhanced ER stress marker response.
Figure 5.5. Densitometric quantification indicating no significant changes in ER stress marker response on PTPN11 downregulation.
Figure 5.6. Effect of BDNF on PTPN11 mediated TrkB changes and ER stress response
Figure 5.7. Effects of pharmacological modulation of TrkB on PTPN11 mediated TrkB changes and ER stress response on 7,8 DHF treatment
Figure 5.8. Effects of pharmacological modulation of TrkB on PTPN11 mediated TrkB changes and ER stress response on CTX-B treatment.
Figure 5.9. *PTPN11* upregulation induces cell apoptosis.
Figure 5.10. Cell viability and MTT Assay.
Figure 5.11 *PTPN11* upregulation suppresses neuritogenesis

Chapter 6
Figure 6.1. Expression of GFP in the inner retina of rat following intravitreal injection.
Figure 6.2. Transgene (GFP and Shp2) expression in normal rat eyes under healthy condition
Figure 6.3. Retinal and optic nerve morphometric changes induced by *Shp2* upregulation.
Figure 6.4. Shp2 upregulation in RGCs induces inner retinal functional loss.

Figure 6.5. Effect of Shp2 overexpression and knock down on scotopic ERG.
Figure 6.6. IOP graph
Figure 6.7. *Shp2* modulation negatively affects TrkB Y^{515} phosphorylation in rat ONH.
Figure 6.8. Cryosections of rat retina showed expression of RGCs.
Figure 6.9. *Shp2* upregulation induces cell apoptosis.
Figure 6.10. *PTPN11* (or *Shp2*) upregulation is associated with enhanced ER stress marker response.

Chapter 7
Figure 7.1. Effect of IOP on intravitreal AAV2 injections and microbead injection in rat eyes.
Figure 7.2. Transgene expression in animal glaucoma eyes
Figure 7.3. GFP and Shp2 expression in control and glaucoma optic nerve head (ONH) lysate.
Figure 7.4. Retinal and optic nerve morphometric changes experimentally induced high ocular pressure.
Figure 7.5. Retinal and optic nerve morphometric changes induced by AAV2-Shp2 knockdown in high intraocular pressure.
Figure 7.6. Effect of microbead on animal electrophysiology.
Figure 7.7. Effect of AAV mediated Shp2 KD on electrophysiology under high IOP experimental glaucoma model.
Figure 7.8. Anti- pTrkB Y^{515} immunostaining in control, microbead and microbead+AVV viral treated retinas.

Chapter 8
Figure 8.1. Schematic representation of BDNF-TrkB downstream signaling altered by Shp2. Misfolded protein accumulation brings changes in endoplasmic reticulum stress markers (IRE1α, ATF6 and PERK) which are possibly implicated in progression of RGCs axon damage in glaucoma

Tables

Table 1.1. Demographic statistics of estimated glaucoma in 2040
Table 1.2. Pharmacological agents used in the management of POAG
Table 1.3. Summary of rodent glaucoma models
Table 4A.1. Structural parameters of thirty seven di-hydroxy flavonoid derivatives including 7,8-DHF.
Table 4A.2. 7,8-DHF and 36 di-hydroxy flavonoid derivatives with corresponding energies against TrkB-D5
Table 4A.3. 7,8-DHF and 36 di-hydroxy flavonoid derivatives with corresponding energies against VEGFR2
Table 4A.4. Toxicity prediction of 37 di-hydroxy flavanoid derivatives including 7,8DHF
Table 4B.1..The chemical property and the calculation of Cyclotraxin B
Table 4B.2. PepSite2 binding score prediction of selected Cyclotraxin B
Table 4B.3. The top 20 docking scores

AAV2	adeno-associated virus, serotype 2
AD	Alzheimer's disease
AdV	adenovirus
AKT	RAC-alpha serine/threonine-protein kinase
AMD	age related macular degeneration
ASK1	apoptotic-signaling kinase-1
ATF4/6	activating transcription factor 4/6
Bcl-2	B-cell lymphoma 2
BDNF	brain-derived neurotrophic factor
BiP	binding immunoglobulin protein
CAG	chicken β-actin globulin
cAMP	cyclic adenosine monophosphate
CAV1/2/3	caveolin 1/ 2/ 3
CHOP	C/EBP-homologous protein
CRE	cAMP response elements
CMV	cytomegalovirus
CNS	central nervous system
CNTF	ciliary neurotrophic factor
CREB	cyclic adenosine monophosphate-responsive element-binding protein
CtBP2	c-terminal binding protein 2
CTX-B	cyclotraxin-B
DAPI	4',6-diamidino-2-phenylindole
dLGN	dorsal lateral geniculate nucleus
DMEM	Dulbecco modified Eagle medium
eGFP	enhanced green fluorescent protein
eIF2α	elongation initiation factor 2α
ER	endoplasmic reticulum

ERG	electroretinography
ERSE-1	ER stress-response elements
GABA	γ-aminobutyric acid
GC	genome copies
GCL	ganglion cell layer
GADD153	growth arrest and BDA-damage-inducible protein 153
GDNF	glial cell line-derived neurotrophic factor
GFAP	glial fibrillary acidic protein
GFP	green fluorescence protein
GRP78	glucose-regulated protein 78
CtBP2	C-terminal binding protein 2
HO-1	heme oxygenase 1
HRP	horse radish peroxidase
IHC	immunohistochemistry
IOP	intraocular pressure
IPL	inner plexiform layer
INL	inner nuclear layer
IRE1α	inositol-requiring protein-1α
ITRs	inverted terminal repeats
JNK	c-Jun N-terminal kinases
LGN	lateral geniculate nucleus
LINGO1	Leucine rich repeat and Immunoglobin-like domain-containing protein 1
MAPK/ERK	mitogen-activated protein kinase/extracellular signal-regulated kinase
mBDNF	mature brain-derive neurotrophic factor
MYOC	myocilin
NeuN	neuronal nuclei
NGF	nerve growth factor
NMDA	N-methyl-D-aspartate
NRF2	nuclear erythroid 2 p45-related factor 2

NT-3	neurotrophin-3
NT-4	neurotrophin-4
OCT	optical coherence tomography
OHT	ocular hypertension
ON	optic nerve
ONH	optic nerve head
ONL	outer nuclear layer
OPTN	optineurin
p75NTR	p75 neurotrophin receptor
PBS	phosphate-buffered saline
PDGFR	platelet-derived growth factor receptor
P-PERK	phospho-protein kinase RNA
PFA	paraformaldehyde
PI3K/PKB	phosphatidylinositol 3-kinase/protein kinase B
PLC/IP3	phospholipase C/inositol 1,4,5-triphosphate
POAG	primary open angle glaucoma
PVDF	polyvinylidene difluoride
RGC	retinal ganglion cell
RMSF	root mean square fluctuations
RNFL	retinal nerve fiber layer
SC	superior colliculus
SHP2	SH2 domain containing protein-tyrosine phosphatase 2C
STAT3	signal transducer and activator of transcription 3
TB	trabecular meshwork
TNF	tumor necrosis factor
Trk	tropomyosin-related kinase receptor
TrkA	tropomyosin receptor kinase A
TrkB	tropomyosin receptor kinase B
TrkC	tropomyosin receptor kinase C

TrkB-D5	tropomyosin receptor kinase B domain 5
TrkB-FL	tropomyosin receptor kinase B full length form
TrkB-T1	tropomyosin receptor kinase B truncated form 1
TTBS	tri Tris-buffered saline
UPR	unfolded protein response
VEGF	vascular endothelial growth factor
VEGFR	vascular endothelial growth factor receptor
VEP	visual evoked potentials
XBP-1	X-box binding protein 1
7,8-DHF	7,8-di-hydroxyflavone

CHAPTER 1

Introduction

1.1 Motivation

Untreated glaucoma causes blindness and it has been projected to affect approximately 60 million people by 2020, translating to more than 8.4 million cases of irreversible blindness worldwide (Davis et al., 2016). The danger of becoming visually impaired from the disease is more likely in developing countries in comparison to developed countries (Frenk, 2006). It has been recorded that adults over 40 years of age with a family history of glaucoma, a history of complicated cardiovascular disease or diabetes, run a higher risk of developing glaucoma and therefore, the ageing population generally forms the majority of sufferers of this disease (Jamison and Mosley, 1991). The major signs of glaucoma are elevated intra ocular pressure (IOP), optic nerve head (ONH) damage, optic disc cupping and visual field loss (Boland et al., 2012). Blockage or reduction in aqueous humor fluid outflow causes an increase in IOP in many cases. The conventional schematic flow of aqueous humor is shown in Figure 1.1. An increase in IOP is associated with destruction of the optic nerve and is responsible for the occurrence of irreversible vision loss in humans (Dimovska-Jordanova, 2012). There is no cure for this pathological condition, however, its management is limited to lowering IOP medically by means of pharmacological agents or surgery (Shaarawy et al., 2004). Many subjects never manifest an elevated IOP and there have been records of the glaucoma advancement under normal IOP levels, as in the case of normal tension glaucoma (NTG) (Mallick et al., 2016). The condition is not noticed by the patient until a critical loss in

vision occurs. The loss of vision is not accompanied by pain or discomfort and there is the danger of the condition deteriorating unless careful monitoring and treatment of IOP is performed (Colligris et al., 2012). Regardless of the rigorous approach to treatment and monitoring techniques made accessible to glaucoma patients, there is still a risk of disease progression (Heijl et al., 2002, Wu et al., 2017). This ongoing risk of progression highlights the need to develop other forms of treatment apart from lowering IOP.

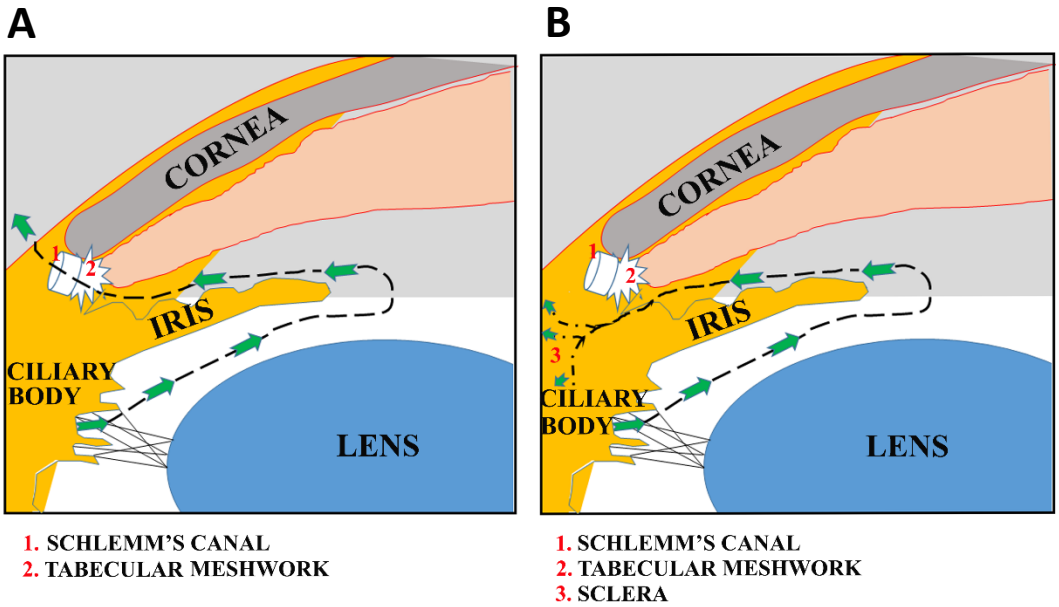

Figure 1.1 Schematic representation of two different aqueous humor flow pathways. Ciliary body produce the aqueous humor and fills both the anterior and posterior chamber of the eye (A) Diagram showing the conventional pathway, the fluid flows out through the trabecular meshwork in Schlemm's canal and is subsequently absorbed into the episcleral veins. (B) Second pathway is the uveoscleral pathway in which the aqueous humor flows through the ciliary body and muscles towards the suprachoroidal space, from where it is absorbed by the venous system via collector channels of the ciliary body, choroid and sclera.

1.2 Human visual system

Extension of central nervous system (CNS) gives ability to visualize and enable many functions and reflexes of the visual pathway (eg: light reflexes, balance, movement etc). The human visual system detects information from visible light and delivers it to CNS to produce a processed representation of the surrounding information. The visual system, via complicated pathways and binocular input allows identification and classification of the image; distance evaluation and adjustment in contrast needed to perceive the object. The human visual system comprises 3 important parts; the retina, optic nerve, lateral geniculate nucleus (LGN) and visual cortex.

1.2.1 Retina

The retina is an exceptional specialized sensory organ formed of complex multi-layered neural circuit where visual perception begins. Contrary to other sensory structures located in peripheral nervous system, the retina is considered to be part of CNS because during embryonic development it is extended from the diencephalon (London et al., 2013). Like human retinas, the mouse retina has similar prototypic structure consisting of 5 different types of neurons (retinal ganglion cells (RGCs), amacrine, bipolar, horizontal and photoreceptor) that are highly organized in anatomical structure (Figure 1.2). Despite different morphology, RGC show the typical properties of CNS neurons and mostly comprise a cell body, dendrite and an axon (Peterson and Dacey, 2000). Bipolar, amacrine and horizontal cells form the inner nuclear layer (INL) whereas outer nuclear layer (ONL) has photoreceptor cells, the rods and cones. INL and ONL are separated by two plexiform layers. Phototransduction, the mechanism of converting light into electrical signal, is carried out by the rods and cones (Williams, 2016). The rods are

highly sensitive to light and responsible for night vision, while cones function capability is higher in the day light. In the mouse retina, the 145 million photoreceptor population is rod cell dominated (approximately 97%) (Cunea and Jeffery, 2007) and the cones are packed in the center of retina that process color vision (Conway, 2009). The cells in the INL modify and transfer the signal to RGC, destination within retina. The cascades of visual information from photoreceptors output, terminates within the visual cortex.

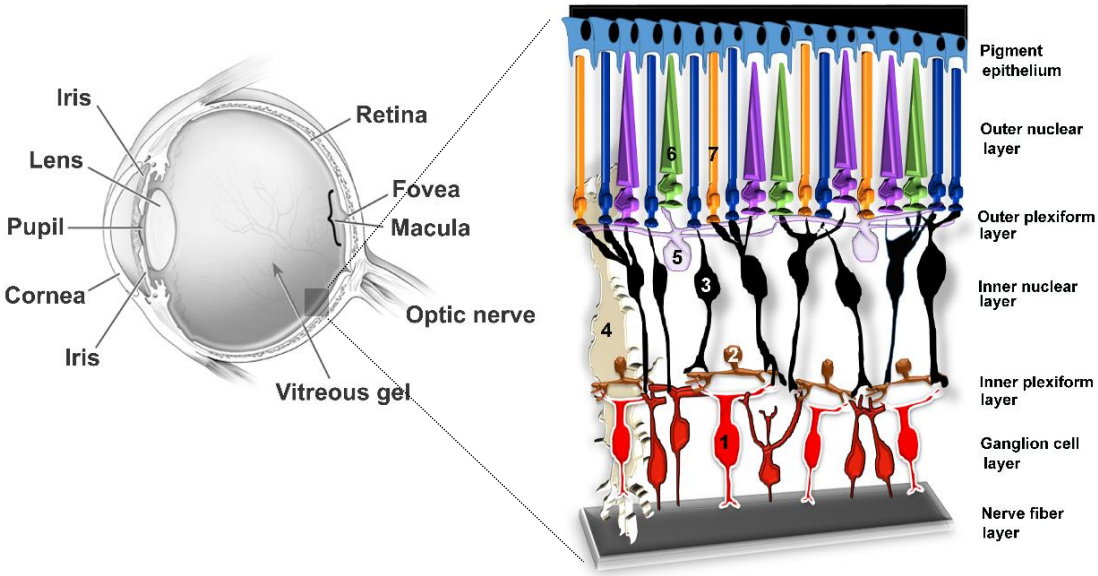

Figure 1.2 Anatomical organization of the eye and the retina. Light entering the eye is focused onto the retina due to the combined refractive power of the cornea and the lens. Light passes through the upper layers of the retina before light energy is captured by the photoreceptor outer segments, transferring this energy into neuronal signals. (1) retinal ganglion cells, (2) amacrine cells, (3) bipolar cells, (4) muller cells, (5) horizontal cells, (6) cones and (7) rods.

1.2.2 Optic nerve

Visual information detected in photoreceptor cells are transmitted through one million optic nerve (ON) fibers to higher visual centers. In mice approximately, 45,000 axons bundle together forming the ON, compared to ~1.7 million in humans (Alur et al., 2008,

Mikelberg et al., 1989). There are four different regions in ON; (1) ONH (2) lamina region (3) myelinated and (4) unmyelinated region (Oyama et al., 2006). ON also contains a variety of glial cells in addition to the RGC axons. Glial cell population and diversity is based upon the region of the ON. They provide support and nutrition to maintain the axonal health (Butt et al., 2004). In mice and other mammals, the ON from each eye meets at the optic chiasm. At this region, most of the axons partially cross over and project to the contralateral side of the brain while the remaining axons project to the ipsilateral side (crossed and uncrossed projection) (Petros et al., 2008). Upon exiting the optic chiasm, these axons project to one of three major subcortical targets: LGN, the pretectal nuclei and superior colliculus (SC) (Gupta and Yucel, 2003).

1.2.3 Lateral geniculate nucleus and visual cortex

The next information processing center in the visual transduction pathway is the LGN, which begins to integrate information from both eyes into a binocular representation of visual space. Once retinal signals arrive within the LGN, they can be impacted by a wide variety of other inputs as well as the complex feedforward and feedback circuits to and from the higher visual centers. These inputs include not only visual data, but also nonvisual data that comes from cortical areas, SC, pretectum, parabigeminal nucleus, reticular nucleus and other brain stem pathways (Huberman, 2007). The LGN neurons mainly project to the primary visual cortex (striate cortex or V1) (Figure 1.3). Area V1 is located in the occipital lobe at the back of the head and from here the information is distributed to several higher cortical centers for further processing (Grill-Spector and Malach, 2004).

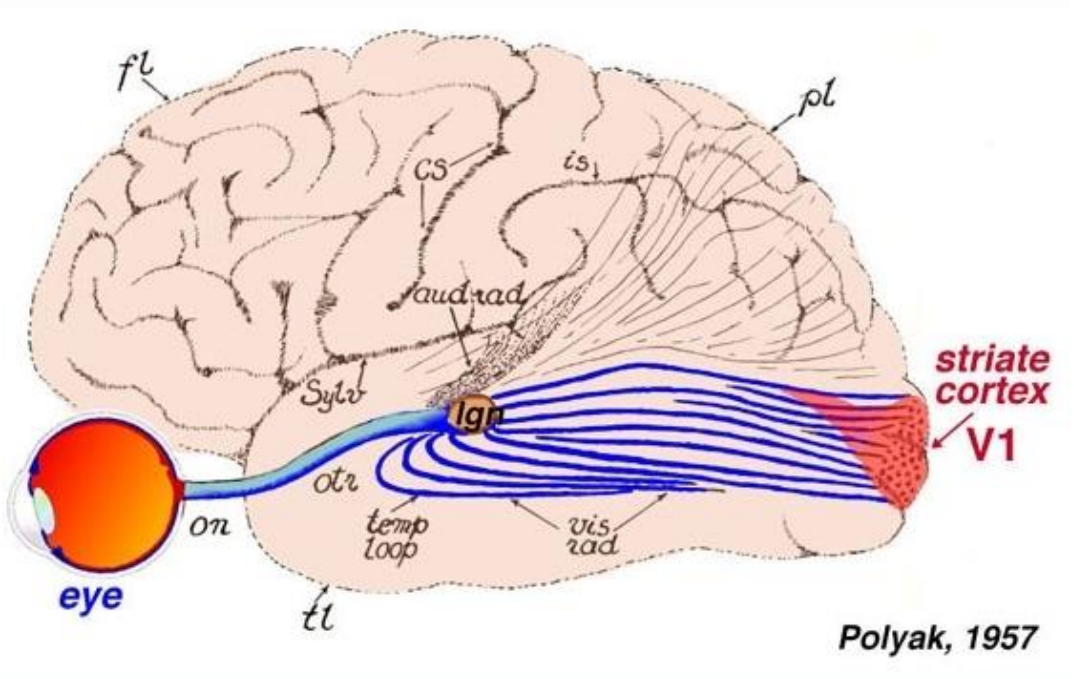

Figure 1.3 Human visual pathway system. Visual information to the brain goes from eye to LGN and then to primary visual cortex, or V1, located in the posterior of the occipital lobe (Polyak, 1957)

1.3 Glaucoma

1.3.1 Definition and history

There is some debate over the true meaning of the term "glaucoma". In 17th century, the Greeks defined glaucoma as clouded or blue-green hue, most likely describing a person with a swollen cornea or who was rapidly developing cataract, both of which may be used to describe long-term elevated pressure inside the eye. Cataract and glaucoma were not distinguished until 1705. In the beginning of 18th century Dr. Antoine-Pierre Demours (1818) for the first time described glaucoma as raised ocular tension. Thereafter the central concept of a rise in the IOP became fully established. Later, Dr. G. J. Guthrie (1823), recognized a characteristic feature of eye hardness which he termed as glaucoma. A Scottish clinician in 1835, Dr. William Mckenzie, finally established the feature of

raised eye tension in both chronic and acute glaucoma. Taking forward Dr. Mckenzie's work, Dr. Donders (1862) described his clinical observation an incapacitating increased eye tension occurring without any inflammatory symptoms as simple glaucoma (Tsatsos and Broadway, 2007). More refined definition of glaucoma has come about over the last 100 years. During 20th century, the definition of glaucoma has been refined as a disease of the optic nerve (an optic neuropathy).

The term "glaucoma" describes a heterogeneous group of dynamic optic neuropathies, defined as a slow progressive neurodegeneration of RGCs and axons, bringing about a characteristic appearance in the optic disc structure (cupping) and associated functional damage in the visual field (Perdicchi et al., 2007, Davis et al., 2016, Wojcik-Gryciuk et al., 2015). Types of glaucoma include primary open angle glaucoma (POAG), as well as congenital glaucoma, angle closure glaucoma and secondary glaucoma. In POAG, the progressive degeneration of RGCs leads to nerve fiber layer loss, characteristic optic disc changes and reduced visual field sensitivity. The diagnosis of glaucoma therefore includes evaluation of the auxiliary characteristics of the ONH, measurement of IOP and assessment of central and peripheral visual function using standard automated perimeters. Although raised IOP is an important risk factor in glaucoma, as mentioned above patients can at times present with IOP within the normal range (10-21 mmHg), known as normal-tension glaucoma, NTG (Anderson, 2011). Changes in ONH structure are commonly identifiable before reductions in visual field sensitivity (Bartz-Schmidt et al., 1999, Jonas and Grundler, 1997, Emdadi et al., 1999). Recent advances in imaging innovations take into consideration objective and quantitative structural assessment of the retinal nerve fiber layer (RNFL) entering the optic nerve head, utilizing non-invasive optical techniques, such as optical coherence tomography (OCT). These RNFL losses

correlate with visual field defects, providing a structure/function correlation (Trip et al., 2006, Pula et al., 2011).

1.3.2 Epidemiology and risk factors

The number of people with glaucoma worldwide will increase to 79.76 million in 2040, disproportionally affecting people residing in Asia and Africa. Studies estimated that around 3% of the Australian population aged 60 years or older will have glaucoma by 2030 (Rochtchina and Mitchell, 2000). Data from other countries like United States also suggest that glaucoma affected more than 2 million people in the year 2004, whereas this number is set to increase by 50% by the year 2020 (Friedman et al., 2004). These statistics are important for preparing strategies to design, screen and make treatment available for glaucoma. A projection of the number of people affected by overall POAG in 2020 and 2040 is presented below in table 1.1 (With permission from Prof. Cheng).

World region	POAG	
	2020	2040
Asia	28.29 (21.99-35.75)	42.32 (33.03-53.34)
Africa	8.73 (5.28-13.17)	16.26 (9.86-24.59)
Europe	5.67 (4.21–7.51)	6.39 (4.79–8.42)
North America	3.52 (2.31–5.08)	4.24 (2.80–6.10)
Latin America and the Caribbean	6.22 (3.36–11.01)	10.20 (5.52–17.97)
Oceania	0.25 (0.12–0.40)	0.35 (0.18–0.58)
Worldwide	52.68 (37.27–72.92)	79.76 (56.18–111.0)

Table 1.1 Number of people (aged 40-80 years) in 2013 was estimated based on World Population (Tham et al., 2014). POAG; primary open angle glaucoma.

Most clinical investigations show that glaucoma is frequently associated with abnormal elevation of IOP as the major risk factor (Kaufman, 2017). However, 25% to 50 % of glaucoma patients have the IOP within the normal range (<21 mm Hg) (Anderson, 2011). Other unequivocally supported risk factors include age progression (Sawada et al., 2015), low diastolic perfusion pressure (Zheng et al., 2010), near-sightedness (Chen et al., 2012) and moderately thinning in central cornea (Galgauskas et al., 2014). More systemic risk factors including diabetes mellitus, hypertension and migraine are less predictable (Zhou et al., 2014, Langman et al., 2005, Chen et al., 2016).

1.3.3 Genetic factors

A family history of POAG has also been well-established, suggesting that genetic mutations are associated with pathogenesis of glaucoma (Mabuchi et al., 2015). Up to now there have

been over 20 genetic loci and 4 genes have been linked to POAG including; *MYOC* (Kim et al., 2001), *OPTN* (Sarfarazi and Rezaie, 2003), *WDR36* (Skarie and Link, 2008) and *Cav1/Cav2* (Wiggs et al., 2011). The MYOC gene was first examined *in vitro* in trabecular meshwork (TM) as response of glucocorticoid-induced gene while studying the effects of dexamethasone on TM cell cultures (Polansky et al., 1997). The gene encodes myocilin protein and intracellular accumulation of the misfolded form of its mutant increases the IOP (Kasetti et al., 2016). Unlike myocilin, optineurin (*OPTN*) was shown to have a protective role in glaucoma progression in response to TM stress, though there is contradictory evidence in transgenic mice model overexpressing *OPTN* in the lens, where it failed to protect against transforming growth factor-β1–induced apoptosis (Kroeber et al., 2006). The role of this gene in glaucoma pathogenesis requires further studies. Another gene associated with POAG is *WDR36*. The abnormalities in *WDR36* alone are not sufficient to cause POAG however, the relationship of *WDR36* sequence variants with more severe disease in affected individuals propose that deformities in the *WDR36* gene can add to POAG (Hauser et al., 2006). *WDR36* encodes protein thought to be involved with T-cell activation and proliferation and in ribosomal RNA processing (Mao et al., 2004). The loss of *WDR36* in zebrafish line with viral insert wdr36^{hi3630aTg} showed reduction in WDR36 protein but lead to activation of the p53 stress response pathway without alteration in *bax,* a pro-apoptotic gene (Skarie and Link, 2008). Genome-wide association study (GWAS) resulted in discovery of caveolin genes (*cav1/ cav2*) isoform that are associated with POAG (Thorleifsson et al., 2010b).

Cav1 and cav2 are known to involve in the formation of caveolae, specific invaginations of the plasma membrane that are rich in cholesterol and other lipids and take part in transcytosis. Cav1 and cav2 are expressed in most human cell types, including tissues such as the TM (Surgucheva and Surguchov, 2011), scleral spur cells (Thorleifsson et al., 2010a)

and RGCs (Thorleifsson et al., 2010a), however changes in these tissues are assumed to play a critical role in the POAG pathology, leading to death of RGC axons, along with supportive glia and vasculature. We further discuss in detail the role of cav1 and cav2 in glaucomatous stress in section *1.4.7* "*TrkB regulation by endogenous phosphatase Shp2*".

1.3.4 Current management

Treatment and management of POAG involves patient education, compliance with therapy and management by an ophthalmologist. High IOP is the only risk factor that can be pharmacologically or clinically modified, apart from management of co-existing illnesses such as cardiovascular disease and diabetes. Pharmacological administration of drugs used to lower IOP in a patient with ocular hypertension may slow but cannot always arrest the progression of glaucoma (Law, 2007). Traditionally, glaucoma treatment begins with pharmacological intervention, proceeding to laser therapy and surgery when necessary. Though designed to maximize the benefit of treatment while minimizing risk to the patient, the pharmacological approach has been challenged as less effective than surgery (Noecker, 2006) but the latter is associated with potential complications. Some glaucoma patients may require all three treatment options and because glaucoma is a chronic, progressive disease with no known cure, all treatments should be made available to each patient. The treatment of POAG includes the use of topical and orally administered agents (Table 1.2).

S.No	Pharmaceutical agent	Drugs	Adverse reactions	Contraindications
1	Prostaglandin analogs (Linden and Alm, 1999)	1. Bimatoprost 2. Latanoprost 3. Travoprost	*Ocular:* Blurred vision Stinging, burning, hyperemia, foreign body sensation, itching, increased iris pigmentation, eyelash changes, punctate epithelial keratitis, cystoid macular edema, iritis and Herpes simplex keratitis *Systemic:* Headaches and upper respiratory tract symptoms	*Ocular:* History of uveitis, CME, herpes simplex, keratitis and complicated cataract surgery *Systemic:* None
2	Alpha2-adrenergic agonists (Apatachioae and Chiselita, 1999)	*Nonselective* 1.Epinephrine 2. Dipivefrin *Selective* 1.Apraclonidine 2. Brimonidine	*Ocular:* Allergic sensitivity, minimal mydriasis, lid retraction, conjunctival vasoconstriction, stinging, burning, foreign body sensation, hyperemia and conjunctival follicles. *Systemic:* Gastrointestinal discomfort, taste abnormalities, headache, fatigue/drowsiness, oral dryness and severe heaches	Only with Epinephrine *Ocular:* Aphakia/ pseudophakia and narrow angles *Systemic:* Systemic hypertension, heart disease, hyperthyroidism, diabetes mellitus and certain medications
3	Beta-blocking agents (Brooks and Gillies, 1992)	*Nonselective* 1.Carteolol 2. Levobunolol 3. Metipranolol 4. Timolol *Selective* 1. Betaxolo	*Ocular:* Stinging, burning, superficial punctate keratitis, allergic sensitivity, decreased corneal sensitivity and uveitis. *Systemic:* COPD, systemic hypotension, bradycardia, diabetes mellitus, Myasthenia gravis and certain medications	*Ocular:* Narrow angles *Systemic:* Chronic obstructive pulmonary disease, systemic hypotension, bradycardia, diabetes mellitus, Myasthenia gravis and certain medications

4	Carbonic anhydrase inhibitors (Mincione et al., 2007)	*Systemic, oral* 1.Acetazolamide injection or sustained release 2.Dichlorphenamide 3.Methazolamide	*ORAL CARBONIC ANHYDRASE INHIBITORS* *Ocular:* None *Systemic:* Malaise depression, confusion, metallic taste, anorexia, diarrhea, paresthesia, kidney stones, metabolic acidosis and blood dyscrasia.	*ORAL CARBONIC ANHYDRASE INHIBITORS* *Ocular:* None *Systemic:* History of kidney stones, liver disease, sulfonamide allergy, cardiac disease, Addison's disease, renal disease and severe chronic obstructive pulmonary disease.
		Topical 1. Dorzolamide 2. Brinzolamide	*TROPICAL CARBONIC ANHYDRASE INHIBITORS* *Ocular:* Stinging, burning, allergic sensitivity, blurred vision, superficial punctate keratitis and corneal edema. *Systemic:* Altered taste	*TROPICAL CARBONIC ANHYDRASE INHIBITORS* *Ocular:* Corneal endothelium compromise *Systemic:* Sulfonamide allergy
5	Cholinergic agonists—miotics (Marquis and Whitson, 2005)	1. Pilocarpine, 2. Carbachol	*Ocular:* Stinging, irritation, ciliary spasms (myopia), miosis (vision), pupillary block and retinal detachment *Systemic:* Headache, pain, sweating, vomiting, diarrhea, salivation, bradycardia, arrhythmia and dyspnea.	*Ocular:* History of retinal detachment, severe myopia, cataracts, inflammation/infection and Ahakia/pseudophakia *Systemic:* Asthma, ulcers, bladder dysfunction and Parkinson's disease

Table 1.2 Pharmaceutical agents for management of POAG along with major adverse reactions and contraindications

Unfortunately, despite effective IOP lowering, some patients still develop vision impairment and optic neuropathy. This damage indicates that an IOP-independent mechanism may be involved in mediating the RGC degeneration in glaucoma disease (Guo et al., 2005). Consequently, IOP is no longer regarded as the only potential target for glaucoma treatment and more effective strategies are required to protect RGCs. In recent years, several new techniques have been examined in preclinical models to create neuroprotective treatments for glaucoma to prevent RGC death and further ON injury. If successful, these neuroprotective strategies may gradually find applications in the clinical management of the disease, along with current IOP lowering therapies (Song and Caprioli, 2014, Parikh et al., 2008). Nevertheless, currently no alternative therapy has been demonstrated in humans for clinical application to prevent glaucoma damage. The lack of treatment strategies is largely because we do not completely comprehend the molecular basis of the disease and how it influences retinal structure and function (Robin and Grover, 2011, Gessesse and Damji, 2013). Therefore, the main principle of POAG treatment remains reducing IOP either by means of pharmacological agent, laser or surgery (Crawley et al., 2012, Perry et al., 2003, Topouzis et al., 2007).

1.3.5 Rodent models of glaucoma

Like many clinical diseases, it is very difficult to study the pathophysiology of glaucoma in human patients. The researchers heavily depend on animal models that replicate important aspects of condition to study the disease mechanism and to develop new therapies. A variety of animal models of glaucoma are available. The rodent models are highly attractive for several reasons including their potential for trial (including but not constrained to genetic) manipulation, short life expectancy, and minimal cost. The similarity of the visual structure

and physiology to humans have been mentioned (Kass et al., 2002, Lambert et al., 2017, Rovere et al., 2016, Vidal-Sanz et al., 2015, You et al., 2014) (Table 1.3). The mouse does not develop connective tissue bundles through the optic nerve head at the level of sclera (Tansley, 1956, May and Lutjen-Drecoll, 2002) where as in the rat with optic nerve head a single collagen bundles are present forming a lamina-cribrosa (Morrison et al., 1995, Hildebrand et al., 1985). In genetic rodent models of glaucoma, ocular hypertension occurs naturally, however it can also be induced experimentally in wild-type rodents either by surgical procedures or by gene manipulation (Nair et al., 2016, Anderson et al., 2001, Junglas et al., 2012), providing an opportunity to explore molecular mechanism in the progression of disease. The IOP-independent rodent models of glaucoma come under the category of acute models, such as optic nerve crush or transection (Templeton and Geisert, 2012), intraocular injection of toxins (Guo et al., 2006), pressure induced ischemia/ reperfusion (Adachi et al., 1996) and endothelin-1 minipump (Orgul et al., 1996). The acute models of glaucoma are fast and RGC death is induced in short period of time. The laser-damaged near retinal ganglion cell layer is also IOP independent. In contrast, chronic glaucoma rodent models (or IOP-dependent), the aqueous outflow pathway (episcleral vein and TM) is blocked, resulting in moderate increase in IOP, mimicking the pathophysiology in glaucoma patients. Chronic IOP elevation can be achieved experimentally in rodents by laser induced photocoagulation of episcleral vein (Li et al., 2006), episcleral vein injection of hypertonic saline (Jia et al., 2000), cauterization (Danias et al., 2006), TM obstruction (Lambrou et al., 1989) and S-antigen administration (Bakalash et al., 2003). Recently, we and others have demonstrated the model of microbead injection in the anterior chamber to block the aqueous flow in the rodent eye (Gupta et al., 2014b, You et al., 2014, Krishnan et al., 2016, Yang et al., 2016b, Weber and Zelenak, 2001, Sappington et al., 2010). We have used the microbead model in this thesis with details presented in chapter 7. In addition to *in vivo* models, cell

culture systems are also widely used to study the RGC survival and apoptosis. RGC-5 cell line was originally characterized as cells isolated from rat but later this cell line were believed to be murine (*Mus musculus*) and not of rat (*Rattus norvegicus*) origin (Sippl and Tamm, 2014). The RGC specific marker, Thy1 can be employed to confirm the origin of these retinal cell line. RGC-5 cell line expresses Brn3C, TrkA, TrkB, BDNF, NT-3 and other neurotrophic factors (Agarwal et al., 2007). The cell line morphologically appears as glial but does not express glial fibrillary acid protein and electrophysiological ion channels (Frassetto et al., 2006). Retinal explant culture also serves as a model of glaucoma and it requires all axons within the optic nerve followed by the significant degeneration of RGCs. This experiment cannot be performed *in vivo* due to limitations involving tissue access, microenvironment or systemic factors (Seigel, 1999).

Genetic mouse models
Point mutation (eg. DBA/2J, myocilin, optineurin)
Multiple point mutation (eg. YBR/EiJ, Collagen type-I α1 subunit, CTGF overexpression)
Knock out (eg. GLAST, EAAC1, CYP1B1, FOXC1, FOXC2, PITX2, LMX1B, PAX6, BMP4)
Acute (IOP-independent)
Optic nerve crush or transection
Intraocular injection of toxins (eg. glutamate, staurosporine)
Retinal ischemia and reperfusion
Endothelin-1 minipump
Chronic (IOP-dependent)
Anterior chamber injection of microbeads
Laser induced photocoagulation of episcleral vein
Episcleral vein injection of hypertonic saline
Episcleral vein cauterization (2–3 veins)
Intracameral injection and trabecular meshwork obstruction
S-antigen administration
Cell cultures
Primary RGC culture
RGC-5 cell line culture
Retinal explant culture

Table 1.3 Summary of rodent glaucoma models

1.4 Biochemical mechanism of neurotrophins in RGCs neuroprotection

1.4.1 Neurotrophin structure and function

Neurotrophins are a family of growth factors, secreted proteins that support the survival, development and function of neurons (Hempstead, 2006, Luther and Birren, 2009, Reichardt, 2006). As per the neurotrophic theory, the amount of released survival factors is limited to and dependent on the size of the target organ and number of neurons receiving neurotrophic factors (Oppenheim, 1989). For instance, it has been suggested that neurotrophins are produced in the brain (eg. neurons and glial cells) and act either by retrograde, anterograde, paracrine or autocrine manner to support other sensory neurons (Noga et al., 2003, Binder and Scharfman, 2004). The first such factor to be discovered during the search for survival factors was nerve growth factor (NGF) (Levi-Montalcini, 1987). There are four different types of neurotrophins reported in mammals; (1) brain-derived neurotrophic factor (BDNF), (2) NGF, (3) neurotrophin-3 (NT-3) and (4) neurotrophin-4 (NT-4) (Binder and Scharfman, 2004). There are other proteins that have been reported to have role in development, structural, functional and survival in the nervous system such as cytokines and glial cell-derived neurotrophic factor (GDNF) (Ibanez and Andressoo, 2016, Stolp, 2013). However, these neurotrophins exert their biological functions on neurons through two transmembrane receptors: p75 neurotrophin receptor (p75NTR) and tropomyosin kinase receptors family (Trk), TrkA, TrkB, and TrkC. BDNF has high binding affinity to TrkB and p75NTR receptor, NGF binds to TrkA receptor, NT-3 shows prominent binding with TrkC receptor and NT-4/5 exhibit specificity towards TrkB receptor (Figure 1.4) (Huang and Reichardt, 2003, Benedetti et al., 1993). Both Trk family and p75NTR receptors are often present on the same cells. Neurotrophins arise from precursors, as pro-forms (30-35kDa) and are later processed by protease cleavage, mainly by the serine protease (Gray and Ellis, 2008), plasmin (Gray and Ellis, 2008), to generate

their mature forms (12-13kDa). These neurotrophin receptors are important and show diverse functions such as during development of nervous system or regenerating injured neurons for survival. Interestingly, different functions are attributed to these two neurotrophin receptors; p75NTR transfers positive and negative signals leading to cell survival or cell death, whereas the Trk family receptors transmit predominantly positive signals that augment the signaling cascade. p75NTR and Trk family receptors have a contradictory relationship: either suppression or enhancement actions on the cellular signaling and survival. The pro-form of neurotrophins binds to Trk receptors in a similar fashion but with low affinity and its cleavage to active form is important for the neurotrophin action (Figure 1.4) (Bothwell, 2016, Ding et al., 2016). The binding of neurotrophin to Trk receptor is very important because it promotes the formation of Trk dimers, this interaction then promotes the phosphorylation of the intracellular cytoplasmic domain, with further activation of the adapter protein and enzymes to the submembrane area and subsequent pathway activation (Chitranshi et al., 2015). Downstream signaling pathways for neuronal survival are activated by Trk receptors in response to neurotrophin binding. The mitogen-activated protein kinase/extracellular signal-regulated protein kinase (MAPK/ERK) pathway (Gupta et al., 2013a), the phosphatidylinositol 3-kinase/protein kinase B (PI3K/PKB) pathway (Guo et al., 2014) and the phospholipase C/inositol 1,4,5-triphosphate (PLC/IP3) pathway (Guo et al., 2014) are the three important pathways by which Trk receptors foster survival signaling. Contradictory to the specificity of mature neurotrophin-Trk receptor family signaling, all pro- or uncleaved neurotrophins activate p75NTR receptor with high affinity. However, the mature neurotrophins show low binding affinity to the p75NTR receptor. The catalytic motif is absent in p75NTR receptor but it interacts with other intracellular proteins that are activated downstream upon uncleaved neurotrophin binding (Sebastiani et al., 2015). “Yin and yang” neurotrophin model propensity has been

proposed as an on/ off model in which pro- and mature forms of neurotrophin can stimulate either class of the neurotrophin receptors (Trk family or p75NTR) (Lu et al., 2005). Hempstead et. al demonstrated that the pro form of neurotrophin (unprocessed form) binding to p75NTR has the capability to act independently and promote cell death in developing neurons (Bamji et al., 1998, Hempstead et al., 1991). Cell death was also noted in oligodendrocytes (Beattie et al., 2002), Schwann cells (Teng et al., 2005), photoreceptors (Srinivasan et al., 2004), smooth muscle cells (Lee et al., 2001), corticospinal neurons (Harrington et al., 2004), and superior cervical ganglion cells (Teng et al., 2005). p75NTR receptor has high affinity to proneurotrophin. p75NTR downstream activation can also be achieved through ceramide signaling and initiate signal transduction by forming cluster within the membrane (DeFreitas et al., 2001). Dobrowsky and colleagues proposed that p75NTR activates sphingomyelinase-2 (nSMase2) activity in the inner part of the plasma membrane, but how nsMase2 coupled to p75NTR is still not well understood (Dobrowsky et al., 1994, Milhas et al., 2010). Upon activation, sphingomyelinase hydrolyzes sphingomyelin to ceramide. Ceramide then activates c-Jun N-terminal kinases (JNK), which is linked to the apoptotic cascade in mitochondria of neuronal cells (Casaccia-Bonnefil et al., 1996, Heumann, 1994, Kaplan and Miller, 2000). In addition, studies on JNK knock-out mice suggested a dual role of JNK in death of neuronal cells in the developing spinal cord and its survival in developing neocortex (Kuan et al., 1999). Upon binding to their membrane receptors at presynaptic terminals, the activated neurotrophin-receptor complexes are activated and retrogradely transported towards the cell body, where they regulate nuclear and cytosolic events important for the survival or apoptosis of these neurons (Campenot and MacInnis, 2004, Bartlett et al., 1998). Neurotrophin deprivation happens after CNS trauma or in diseases like glaucoma and Alzheimer's disease, detrimental to neuronal functioning and survival.

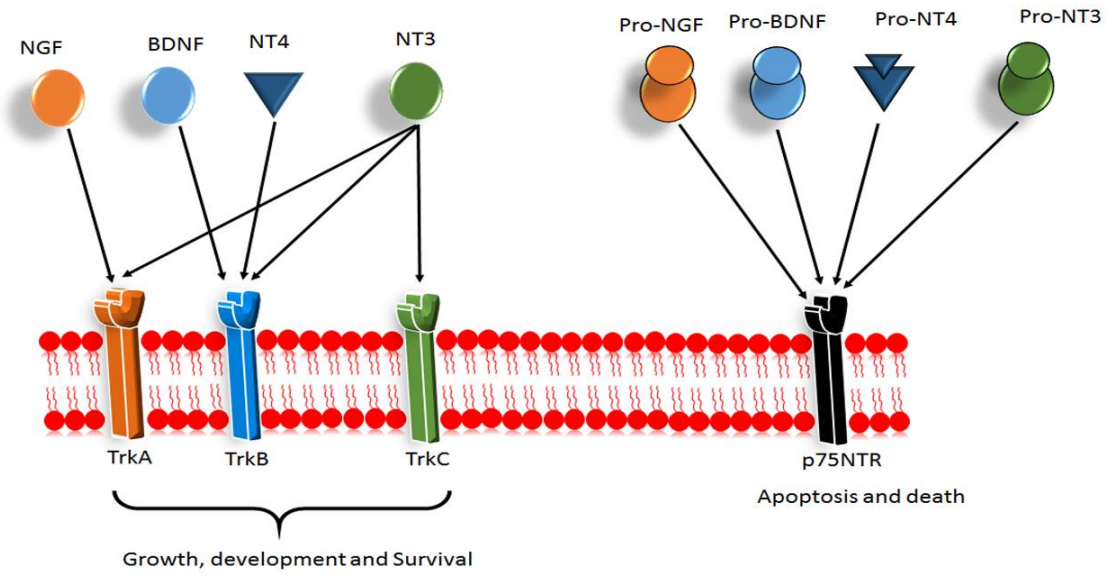

Figure 1.4 The neurotrophins and their receptors. Mature neurotrophins bind preferentially to specific Trk receptors, whereas unprocessed pro-neurotrophins bind to p75NTR. NGF, nerve growth factor; BDNF, brain-derived neurotrophic factor; NT-4, neurotrophin-4; NT3, neurotrophin-3; Trk, tropomyosin-related kinase; p75NTR, p75 neurotrophin receptor

1.4.2 Neurotrophin role in RGCs

The mature form of neurotrophin plays a key role in neuronal cell survival. In healthy or normal conditions, RGCs get neurotrophins from Muller cells (Seki et al., 2005) or retrograde axonal transport from the brain directly, visualized using live-cell imaging *in vitro* (Takihara et al., 2011). Human and mouse adult RGCs not only express Trk family receptors but also abundantly express p75NTR receptor during retinal development (Lebrun-Julien et al., 2010). The p75NTR receptor is predominantly expressed in Müller glial cells (Lebrun-Julien et al., 2010, Ibanez and Simi, 2012). The immature form of neurotrophin, such as pro-NGF binding to p75NTR leads to its activation and programmed cell death *via* tumor necrosis factor-alpha (TNFα) production in glial cells (Kimura et al., 2016). NGF binding to the p75NTR receptor in the absence of TrkA leads to apoptosis in developing RGCs (Harada et al., 2006), but there is some controversy about the level of p75NTR expression in adult

RGCs (Harada et al., 2006, Mysona et al., 2014). Lack of neurotrophin support has been suggested as a reason for RGCs degeneration and death in glaucoma (Dekeyster et al., 2015). A significant question is where does neurotrophin originate, and how do neurotrophins function upon engaging receptors on RGCs? Differential activation of neurotrophin receptors can occur when neurotrophins actions at the axonal terminal (retrogradely transported) or at the neuronal cell body (locally produce) (Quigley et al., 2000, Feng et al., 2016). Neurotrophins are retrogradely transported from the SC in the CNS. Retrograde transportation of neurotrophin takes place from SC to RGCs cell bodies. However, in neurotrophin deprivation conditions, one aspect could be absence of retrograde transport of neurotrophin which stimulates the apoptotic signaling pathway and ultimately RGCs death. Studies in rats demonstrated that acute IOP elevation inhibits the retrograde transport of BDNF from SC to the RGCs soma. Deprivation of BDNF among the RGCs contributes to the loss of visual signal (Quigley et al., 2000). In another example, NGF is produced in several different neurons in the peripheral nervous system (PNS) but also in the CNS. Following release, NGF diffuses to presynaptic axon terminals of neurons such as the cholinergic neurons where it binds its receptor TrkA, bringing its dimerization, phosphorylation and the formation of an extended complex of proteins involved in signaling pathways. These complexes are then internalized in part by clathrin-coated membranes and moved to early endosomes that are then retrogradely transported from axons to the cell body through dynein-microtubule based mechanism. When the signaling endosome reaches the cell body, the signal is communicated to the cytoplasm and the nucleus, triggering gene expression. Lysosomes promote the degradation of this signaling complex. The model proposed for NGF may well apply for other neurotrophins. Many studies have led to the conclusion that BDNF is also locally synthesized in the retina. The RGCs and neighboring amacrine cells also produce BDNF that may act in a paracrine fashion. The RGCs themselves

act in autocrine fashion, these neurons can survive in absence of additional BDNF from the brain and are able to express it in culture (Vecino et al., 2002, Garcia et al., 2003). However, there is insufficient confirmatory findings regarding the existence of neurotrophins source in retina during high IOP. Additionally, other neurotrophic factors such as ciliary neurotrophic factor (CNTF) and GDNF have also been suggested to be involved in RGCs maintenance and survival (Pease et al., 2009, Hauck et al., 2006).

1.4.3 Neurotrophin deprivation in glaucoma

Neurotrophins are transported to the retina by retrograde manner. They are responsible for regulation of neuronal growth, function and survival. The long-range retrograde (from brain to RGCs) neurotrophin transportation is probably facilitated through endosome signaling. As discussed earlier, neurotrophin binds to the Trk receptors and this complex activates the Trk receptor at axon terminals which is then taken up by cell body retrogradely. In glaucomatous conditions, due to high IOP the retrograde transport is thought to be blocked at the ONH region and neuronal RGCs fail to receive BDNF and TrkB support for survival (Pease et al., 2000, Quigley et al., 2000). This deprivation causes an alteration of axoplasmic transport of neurotrophins from target neurons in the SC and LGN in the brain (Tanaka et al., 2009). RGCs, as well as all other neurons in CNS, require the support of neurotrophins, as these small peptides regulate cellular metabolism by the activation of neuronal cell receptors. RGCs seem to be especially dependent upon BDNF, NT-4, CNTF, and GDNF (Feng et al., 2016, Ma et al., 1998, Wen et al., 2012, Yan et al., 1999). Pease and colleagues demonstrated that experimental glaucoma induces abnormal TrkB axonal distribution, focal accumulation of TrkB and BDNF, increased levels of TrkB in ganglion cell layer (GCL), and increased TrkB in glia (Pease et al., 2000). The ability of RGCs to survive in culture

with the lack of exogenous BDNF has also been demonstrated (Garcia et al., 2003) suggesting that the deprivation of extrinsic BDNF because of retrograde transport interruption is not the only reason for RGCs death in glaucoma. This is important because BDNF/ TrkB interactions and downstream signaling is involved in apoptosis inhibition and has been shown to supports survival of retinal explants and cultures. It has also been shown to increase the rate of axonal elongation but only when it is present in the axonal terminals (Thanos et al., 1989, Frade et al., 1997, de Rezende Correa et al., 2015). The presence of TrkB and BDNF in the all sub-populations of the RGCs has been demonstrated in the retina (Vecino et al., 2002). It is believed that neurotrophin deprivation in neurons exerts stress and initiates apoptotic pathways with in the cell through activated JNK which stimulates expression of BH-3-containing proteins that facilitate the actions of a proapoptotic proteins causing mitochondrial dysfunction (BAX) (Virdee et al., 1997, Tsuruta et al., 2004). In summary, neurotrophin deprivation is one conceivable reason of cell death and auxiliary therapy can potentially be an imminent approach in glaucoma treatment.

1.4.4 BDNF-TrkB signaling

There is evidence for the protective role of BDNF in maintaining the survival of RGCs under conditionally induced apoptosis like optic nerve injury or glaucoma (Mansour-Robaey et al., 1994). In regenerating RGCs neurons, BDNF initiates neuritogenesis (Cohen-Cory and Fraser, 1995), and can repair damaged optic nerve and RGCs (Mansour-Robaey et al., 1994, Chen and Weber, 2001). Our recent studies have established the role of BDNF in structural, functional and molecular neurodegenerative variations in inner retina that are exacerbated with age and in glaucoma in $BDNF^{+/-}$ mice (Gupta et al., 2014b). TrkB activation leads to an enhanced PI3K/Akt and Erk1/2 signaling in the RGCs and Erk1/2 appears to be

responsible for promoting the survival of RGCs (Cheng et al., 2002) (Figure 1.5). BDNF/ TrkB signaling has been shown to mediate retinal neuroprotection by activating TrkB receptor activity (Turner et al., 2006, Trifunovic et al., 2012). Previous studies have shown that BDNF mediated TrkB signaling modulates glycogen synthase kinase 3β (GSK3β) activity in retinoic acid differentiated neuroblastoma, SH-SY5Y cells (Mai et al., 2002). BDNF binds to the TrkB receptor to initiate multiple signaling cascades as discussed above, including the PI3K which in turn leads to the stimulation of the Ser/Thr kinase Akt (Patapoutian and Reichardt, 2001). Akt is a major upstream regulator of GSK3β and regulates GSK3β signaling by its phosphorylation at Ser^9, thereby inactivating it (Hu et al., 2013). The active form of GSK3β (GSK3β phosphorylation) inhibits collapsin response mediator protein-2 (CRMP-2) binding to tubulin and promotes microtubule dynamics along with regulating axonal transport and outgrowth in neurons. In order to understand the mechanism of BDNF/ TrkB signaling in RGCs, we have demonstrated *in vitro* that activation of the BDNF-TrkB signaling in neuronal RGC-5 and PC-12 cell lines regulate GSK3β activity which is involved in cellular survival, cell fate determination and proliferation (Gupta et al., 2014a). BDNF knockdown in RGC-5 and PC-12 cell lines resulted in marked downregulation of GSK3β phosphorylation in normal cells. In addition, ONH of $BDNF^{+/-}$ mice illustrates reduced GSK3β phosphorylation with age. Further studies to stimulate BDNF-TrkB signaling can have a direct impact on RGCs neuroprotection that may lead to effective treatment therapies for glaucoma (Chapter 3).

1.4.5 Glial BDNF-TrkB signaling

From previous studies, it has been established that BDNF-TrkB signaling promotes cell survival by the activation of pro-survival pathways (Kimura et al., 2016, Liu et al., 2007). Notably the expression of TrkB is relatively higher in inner retinal cells like Müller glial cells and RGCs than outer retinal cells such as photoreceptor cells (Cui et al., 2002, Harada et al., 2011, Kimura et al., 2016). This leads to the suggestion that the neuroprotective roles of BDNF-TrkB signaling in the inner and outer retina is different. Indeed, Kimura et al, reported a direct neuroprotective action of glia on photoreceptor cells. BDNF treated Muller glia cells *in vitro* show upregulated CNTF levels, while upregulation of basic fibroblast growth factor by glia protects the photoreceptor cells undergoing damage (Harada et al., 2002). BDNF-TrkB signaling in glial cells produces neuroprotective effects. Two different TrkB knockout mice models were used to confirm the positive role of BDNF-TrkB signaling in RGC survival. These models are $TrkB^{flox/flox}$ mice crossed with *GFAP*-Cre mice to produce $TrkB^{GFAP}$ KO mice (TrkB is selectively deleted from Muller glial cells) and $TrkB^{c-kit}$ KO mice (TrkB is deleted only from RGCs). With these KO mice models, ie $TrkB^{GFAP}$ KO mice and $TrkB^{c-kit}$ KO mice a similar degree of neuronal damage from glutamate neurotoxicity was observed. Likewise, apoptosis in the photoreceptor cells induced by methylnitrosourea (MNU), was augmented in $TrkB^{GFAP}$ KO mice. In addition, an ON damage model demonstrated that $TrkB^{GFAP}$ KO mice had a higher percentage of RGC loss in comparison to the wild-type (WT) mice (Harada et al., 2011, Harada et al., 2002). $TrkB^{GFAP}$ KO mice cultured Muller glial cells were treated with BDNF to determine the expression of neurotrophic factors like BDNF, CNTF and GDNF. Unfortunately, these neurotrophic factors were absent in $TrkB^{GFAP}$ KO mice cultured Muller glial cells whereas WT cultured mouse Muller glial cells showed upregulation of BDNF, CNTF and GDNF (Harada et al., 2011). TrkB.T1 is the truncated isoform of TrkB receptor and BDNF binding

to this truncated isoform in Muller cells demonstrated protection of photoreceptor cells against light-induced damage (Liu et al., 1997). Localization of BDNF and TrkB along with other adaptor protein like Src homology 2 domain containing (Shc) and phospholipase Cγ1 (PLC-γ1) in the endosomes potentially making it possible for TrkB to be transported within the cell (Huang and Reichardt, 2003). This could be a reason of BDNF-TrkB translocation in the optic nerve axons. Taken altogether, these discoveries establish the neuroprotective role of glial BDNF-TrkB signaling in retinal cells by activating the downstream pro-survival cascades.

1.4.6 Pharmacological modulation of TrkB

Even though BDNF is accepted to be neuroprotective in RGCs, its impact on RGC survival has been observed to be transient. While BDNF at first enhances RGC survival, it loses its protective effect over time (Klocker et al., 1998). On repeated TrkB activation by higher doses or multiple applications, the pathway becomes desensitized to BDNF. Considering different caveats of BDNF, for example, its short half-life, cross-reactions connected with the prolonged use or expanded doses, and difficulty of delivery, the clinical prospect of utilizing BDNF for neuroprotective therapy has been disappointing (Jang et al., 2010b).

There are not many natural or synthetic compounds that can act as an agonist to the TrkB receptor and mimic the function of BDNF with minimal side effects. For example, TrkB agonist antibody 29D7 enhanced RGCs survival in culture in a dose-dependent manner and enhanced the cAMP elevation, consistent with prior observations on the ability of cAMP to enhance the RGC response to BDNF for the survival and axon growth (Hu et al., 2010). Hua et al also demonstrated the ability of antibody 29D7 to enhance RGCs survival and regeneration *in vivo* after intravitreal injection of 29D7 antibody. The density of surviving

RGCs was increased by single antibody 29D7 injection but to a lesser degree than in the BDNF-treated retinas. The tricyclic antidepressant Imipramine also demonstrated RGC protection against oxidative stress-induced apoptosis. RGC-5 cell exposed to oxidative stress, Imipramine treatment resulted in activation of TrkB pathways through Erk/ TrkB phosphorylation and also it ameliorated in H_2O_2-induced apoptosis in culture (Han et al., 2016).

We and others have shown that naturally occurring flavonoid, 7,8-dihydroxyflavone (7,8-DHF) has potential to activate the TrkB receptor extracellular domain (ECD) triggering conformational changes in the receptor and stimulating phosphorylation of the TrkB receptor intracellular domain (ICD) which is critical for the tyrosine kinase activity of the TrkB receptor and it's downstream signaling events (Chitranshi et al., 2015, Gupta et al., 2013b). The binding of 7,8-DHF and BDNF to TrkB is shown to be different sites (Chapter4). 7,8-DHF binds specifically to the ECD of the TrkB receptor and induces TrkB phosphorylation at Tyr^{515}, Try^{706} and Tyr^{816} in ICD in neurons. In neuronal lysates, the BDNF-triggered phosphorylattion activity of TrkB and in return TrkB was highly ubiquitinated (Makkerh et al., 2005, Arevalo et al., 2006). In contrast, 7,8-DHF rapidly elicited TrkB phosphorylation in the retinal ganglion cells (Gupta et al., 2013a). Remarkably, no TrkB ubiquitination was detected in 7,8-DHF induced TrkB receptor activation (Liu et al., 2014). Another small molecule that mimics the neurotrophic activity of BDNF is deoxygedunin. It is a tetranortriterpenoid present in the Indian neem tree (Azadirachta indica) (Liu et al., 2016). Deoxygedunin also binds to the ECD of TrkB and elicited strong TrkB activation in hippocampal neurons of rat. Deoxygedunin is also found to stimulate downstream signaling activation of both Erk1/2 and Akt in neuronal culture and prevent neurons from undergoing apoptosis (Jang et al., 2010a, Liu et al., 2014).

1.4.7 TrkB regulation by endogenous phosphatase Shp2

Protein tyrosine phosphatase (PTP) is the Src homology 2 (SH2) domain containing phosphatase Shp2 (Lorenz, 2009). It is expressed ubiquitously and plays a key role in several cellular signaling pathways affiliated with cell growth, differentiation, mitotic cycle, metabolic control, transcription regulation and cell migration, along with positive or negative regulatory role in TrkB receptor signaling and neural fate in retina (Figure 1.5) (Tsang et al., 2012, Neel et al., 2003, Kontaridis et al., 2008) . Shp2 binds to tyrosine kinase receptors like platelet-derived growth factor receptor (PDGFR) and epidermal growth factor receptor (EGFR) *via* its SH2 domains directly or indirectly (Agazie and Hayman, 2003). In addition, Shp2 has been found in the receptor complexes in which the Jak/Tyk family of receptor-associated tyrosine kinases phosphorylate tyrosine residues in response to stimulation with CNTF, leukemia inhibitory factor, oncostatin M and interleukin-6 (Schaper et al., 1998). Shp2 acts either as an adaptor protein (Hanafusa et al., 2004) or as a modulator of tyrosine phosphorylation (Agazie and Hayman, 2003) in these signaling complexes. It has also been shown that Shp2 acts as a mediator of BDNF-activated signaling (Rusanescu et al., 2005). The presence of BDNF in cerebral cortical neurons is suggested to promote the the phosphorylation of Shp2 (Gupta et al., 2013a, Easton et al., 1999, Zhou et al., 2015). Although, Shp2 enhances the survival effect of BDNF in these neurons (Araki et al., 2000), it also acts as a negative regulator of BDNF-activated signaling during neuronal excitotoxicity (Rusanescu et al., 2005, Kim et al., 2007). Cai *et al*, demonstrated that Shp2 is essential for the initiation of retinal neurogenesis but is not crucial for tissue differentiation (Cai et al., 2011). However, *Shp2* deletion in embryonic stages resulted in retinal degenerative changes including optic nerve dystrophy in mice, further explaining its role in retinal development. Also, Shp2 mediated tyrosine dephosphorylation is reported in Semaphorin-4D (Sema4D) induced axonal repulsion in RGCs and hippocampus neurons

(Kruger et al., 2005, Fuchikawa et al., 2009). Shp2 has been shown to be predominantly expressed in the inner retina including GCL, although it also regulates photoreceptor differentiation and is suggested to protect the outer retina indirectly through the Muller glial cell involvement (Cai et al., 2011, Pinzon-Guzman et al., 2015). The studies in our group have demonstrated interaction of TrkB with Shp2 is increased in the RGCs by 2-3 fold in ON axotomy and microbead injected glaucoma animal models. Further, primary culture of rat RGCs and RGC-5 cell line showed high TrkB and Shp2 interaction when subjected to glutamate excitotoxic and hydrogen peroxide (H_2O_2) induced mild oxidative stress conditions. Interestingly, increased dephosphorylation of TrkB was observed in the RGC stress models *in vivo.* Not much is known about how Shp2 regulation of TrkB activity affects the RGC survival in healthy and disease conditions. Therefore, Shp2 may serve as a potential target to explore and understand the mechanisms of RGC death. It also offers an opportunity to explore the potential for Shp2 gene therapy as a therapeutic target in glaucoma conditions.

Caveolins or cav are integral membrane adaptor proteins that form the principal components of the omega-shaped caveolar structures in the plasma membrane. The various form of cav are caveolin-1 (cav1), caveolin-2 (cav2), and caveolin-3 (cav3). These variants differ with respect to tissue distribution and their specific function. Origin of ancestry is similar for cav1 and cav2 and are expressed in smooth muscle cells, neuronal cells, endothelial cells, adipocytes and fibroblast in abundance (Okamoto et al., 1998, Galbiati et al., 1998). Previously, it was shown that cav3 expression is limited to muscle (Okamoto et al., 1998), despite the fact it has also been observed in astroglial cells and vegetative ganglion neurons (Nishiyama et al., 1999, Kiss et al., 2002). Cav1 is linked to diseases with significant retinal pathologies including diabetic retinopathy and glaucoma (Klaassen et al., 2013, Thorleifsson et al., 2010a) but its role in retinal neuroprotection is still a mystery. Recently, Reagan and colleagues demonstrated the neuroprotective role of cav1 in the retina. Cav1 is involved in

recruiting circulating leukocytes during inflammation and these cytokines activate the JAK/STAT pathway, which downregulates apoptotic factors to prevent retinal neuronal death (Reagan et al., 2016, Chucair-Elliott et al., 2012).

Other receptors in retina on which cav1 has a positive impact are toll-like receptors (TLRs) that recognize and respond to pathogenic stimuli and initiate pro-inflammatory cytokine responses. Cav1 associates with TLRs and regulates TLR signaling (Jiao et al., 2013). Recently, we have shown molecular evidence that Shp2-TrkB interaction in RGC is mediated through cav. Under ON axotomy and glaucomatous stress cav1 and cav3 undergoe hyperphosphorylation and interacts with Shp2 in the RGCs. Cav may bind to the SH2 domain of Shp2 and thus dimnishes the auto-inhibition of Shp2 and enhance its phosphatase activity (Pawson et al., 2001). There might be the possibility of pooled recruitment of Shp2 by cav acting as a signaling platform in close proximity of ICD of TrkB receptor, thereby increasing dephosphorylation of TrkB and cessation of cell survival downstream signaling mediated through BDNF/ TrkB activation. Cav1$^{-/-}$ mice show an enhanced Erk1/2 phosphorylation in the hippocampus (Takayasu et al., 2010). Our findings in RGCs under stress are consistent with previous studies that cav1 undergoes hyper-phosphorylation in oxidative and osmotic cellular stress in fibroblast cultures (Volonte et al., 2001, Sanguinetti et al., 2003). TM cell lines from POAG patients treated with dexamethasone show a decline in cav1 phosphorylation (Surgucheva and Surguchov, 2011), implicating that cav phosphorylation in glaucoma in the RGCs. Cav is also reported to play a critical in Shp2 activation in astrocytes, retinal homeostasis, preservation of blood retinal barrier permeability and outer retinal functions (Jo et al., 2014, Li et al., 2012b, Tian et al., 2012).

1.5 Apoptosis in RGCs

Apoptosis is cell death and ganglion cells undergo apoptosis in glaucoma leading to irreversible loss of vision in visual diseases, such as glaucoma, uveitis and diabetic retinopathy. This mechanism of cell death is controlled by specific gene modulation. Specifically, the misfolded proteins are activated and accumulated in the dying cell. The loss of RGCs is the principal endpoint in experimental glaucoma (Vrabec and Levin, 2007).

Pro-apoptotic factor can arise in retina from various factors such as ischemia, inflammation, excitotoxicity, oxidative stress and hyperglycemia (Gupta et al., 2013b, Osborne et al., 2004, Barot et al., 2011, Wang et al., 2012, Ientile et al., 2001, Feenstra et al., 2013). Recent evidence suggests that abnormal protein aggregation stress may lead to unfolded protein response in endoplasmic reticulum (ER) (Jing et al., 2012). Furthermore, some of the ER stress signaling proteins control cell fate either by activating pro-apoptotic, Bcl2 or anti-apoptotic Bax molecules in response to cell burden (Wang et al., 2011).

1.5.1 Endoplasmic reticulum stress and unfolded protein response

Intracellular synthesized protein is further processed by ER. As protein folding, maturation, and trafficking are some of the important functions of this organelle. The folded membranes of ER help the newly synthesized proteins to undergo posttranslational modification and correctly fold in their three-dimensional (3D) conformations (Figure 1.5). However, only mature (correctly folded) proteins can be taken up by the Golgi bodies for further targeting. ER is the major intracellular organelle that senses environmental changes, cellular stresses, coordinates signaling pathways and controls cell function/ survival (Schwarz and Blower, 2016). Different pathological and physiological conditions, nutrient scarcity, change in redox status and viral infection can influence the ER ability to facilitate protein folding,

resulting in unfolded or misfolded protein accumulation in the ER lumen and consequently increased ER stress. The unfolded proteins form insoluble protein aggregates that are toxic to the cell. This has been reported in neurodegenerative diseases like glaucoma, Parkinson's disease and Alzheimer's disease (Cornejo and Hetz, 2013, Varma and Sen, 2015, Anholt and Carbone, 2013). Within the cell, an adaptive mechanism is activated that comprises various intracellular signaling pathways in response to removing toxic protein counterparts, termed the unfolded protein response (UPR). In order to maintain protein homeostasis within the cell, the UPR alleviates ER stress by three different strategies; (1) induced ER-related molecular chaperons to stimulate re-folding of the folding proteins; (2) inhibit mRNA translation so that no more generation of unfolded proteins take place and (3) stimulate the retrograde transport of the misfolded proteins from the ER lumen into the cytosol for ubiquitination by activation of ER-associated protein degradation (ERAD) (Bravo et al., 2013).

Recently, research groups have reported that the ER stress is associated with neuronal cell death in neurodegenerative diseases like glaucoma (Peters et al., 2015). In an animal model of chronic glaucoma and acute ON traumatic injury, researchers demonstrated an increase in ER stress proteins in the RGCs (Doh et al., 2010, Hu, 2016). Intravitreal injection of tunicamycin (0.1 µg/eye an ER stress inducer) in mice resulted in the loss of RGCs but no change was observed in the inner plexiform layer (IPL). A higher dose of tunicamycin (1 µg/eye) resulted in the loss of RGCs as well as thinning of IPL. Intravitreal injection of N-methyl-D-aspartate (NMDA) given in ischemic insult animal model resulted in increased ER stress protein expression in the inner retinal cells like RGCs, amacrine and microglia. Activation of Bip, ATF4, and CHOP by tunicamycin or NMDA-induced apoptosis in mouse primary RGCs suggest an imperative role of ER stress in neuronal cell death in the retina (Kang and Ryoo, 2009). An antipsychotic drug, Valproate demonstrated neuroprotective

actions in the ischemic retina from ER stress-induced apoptosis by inhibiting histone deacetylase activity (Zhang et al., 2011). Neuronal ER stress is therefore a promising therapeutic target for glaucoma and potential for other types of neurodegeneration diseases.

1.5.2 Signaling pathways of ER stress-associated apoptosis

Cell death often occurs if ER stress is chronic, the protein burden on ER is unable to fold the protein dimension accurately and outperforms cellular function. The three-major proteins involved in UPR are (1) protein kinase RNA (PKR)-like ER kinase (PERK), (2) ATF6 and (3) IRE1α (Figure 1.5). Under normal biological conditions, BiP, an ER local chaperon, binds PERK and ATF6 which keeps these ER stress proteins idle. Upon aggregation of ER misfolded proteins, BiP is set free from these complexes and helps in folding of accumulated proteins (Gardner and Walter, 2011). The function of PERK is to regulate mRNA translation and to prevent the entry of newly formed unfolded protein to the ER compartment already experiencing stress. PERK phosphorylates the elongation initiation factor 2α (eIF2α) and nuclear erythroid 2 p45-related factor 2 (NRF2). Phosphorylated eIF2α stops polypeptide synthesis and phosphorylated NRF2 induces oxidative stress by cell reinforcement genes such as heme oxygenase 1 (HO-1) (Marciniak et al., 2006, Cullinan et al., 2003). Another transcription factor, ATF6 ER stress signal, are taken up by Golgi apparatus upon UPR and cleaved into luminal domain by serine protease site-1, whereas site-2 protease cleaves the N-terminal domain. The separated N-terminal domain of ATF6 then moves into nucleus and form complex with ATF/cAMP response elements (CRE) and ER stress-response elements (ERSE-1), ATF6-CRE-ERSE-1 complex initiates transcription of BiP, Grp94 and CHOP (Sano and Reed, 2013). The IRE1α promotes apoptosis by stimulating apoptotic-signaling kinase-1 (ASK1) and its downstream signaling activation of stress kinases JNK and p38

MAPK (Wang et al., 2015b). Environmental stress, such as ultra violet radiation stimulated mitochondrial apoptosis-inducing substrates of JNK, Bcl-2 (antiapoptotic) is inhibited while Bim (proapoptotic) is activated (Lei and Davis, 2003). Anti-apoptotic marker, Bcl-2 expression downregulates and Bim upregulates on p38 MAPK activation, moreover, the translocation of apoptotic and anti-apoptotic marker is initiated in mitochondria and triggers the transcription factor CHOP (Szegezdi et al., 2006). Dual action of IRE1α has also been reported. It triggers survival signaling pathways by upregulating the expression of spliced XBP1, the product of the translational frame shift (Yoshida et al., 2001). Genetic removal of IRE1α and XBP1 causes embryonic mortality (Lee and Ozcan, 2014), signifying that IRE1α and XBP1 are required during the development stages. However, the activated IRE1α causes the decay of ER-localized spliced XBP1 in *Drosophila* and mammals (Hollien et al., 2009, Hollien and Weissman, 2006). Further investigations are required to understand how the dual functions IRE1α are regulated.

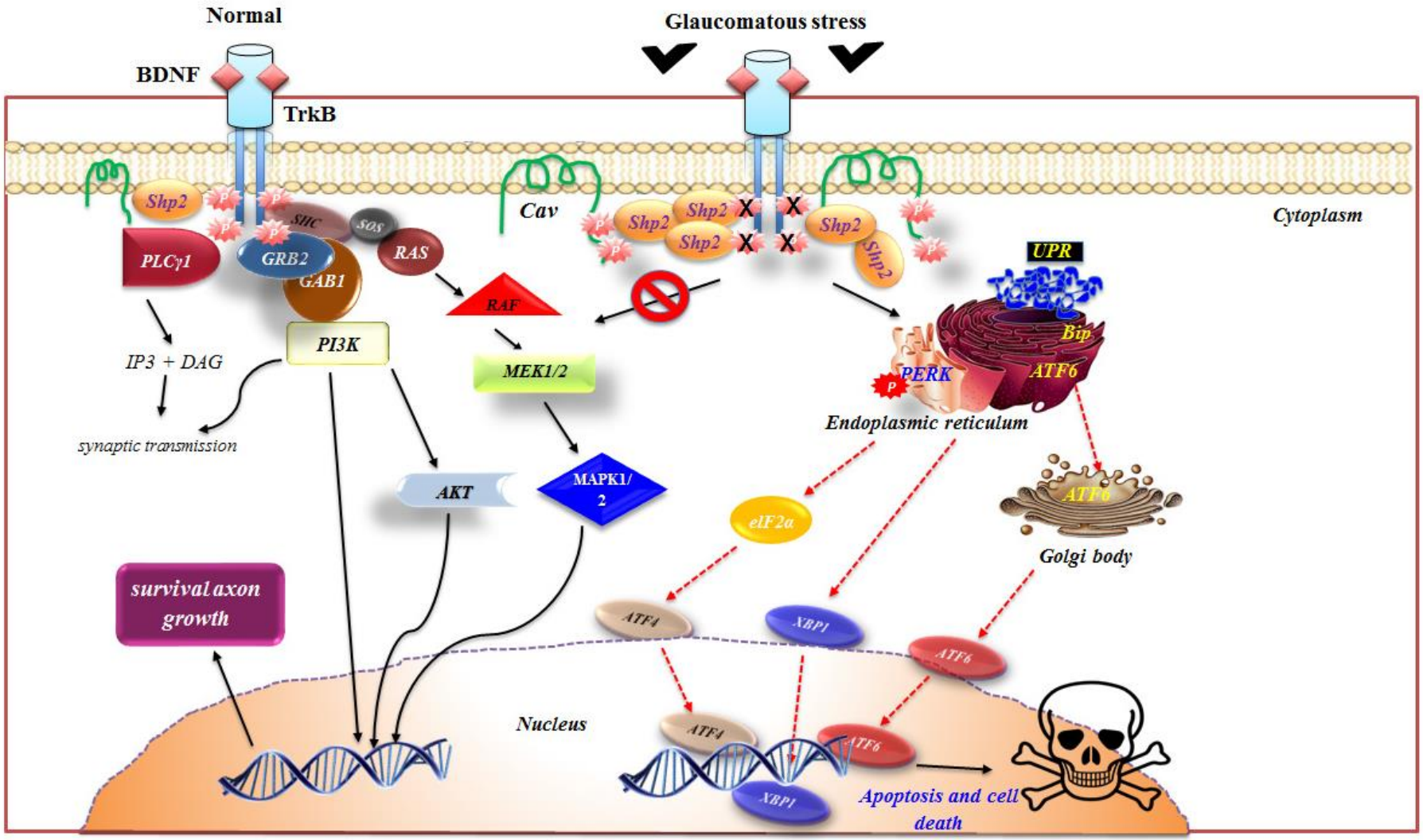

Figure 1.5 Schematic representation of the BDNF/ TrkB signaling in normal and glaucomatous conditions. The downstream cellular effects of BDNF-TrkB complex in normal condition promote neuronal survival. Under glaucomatous stress, the downstream survival pathway ceases and induces ER stress and promote cell apoptosis.

1.6 Therapeutic targets in glaucoma

This section outlines the difficulties connected with evolving treatments and strategies related to the tyrosine kinase family receptor that offer the potential to protect RGCs with a new target based approach.

1.6.1 Can neurotrophins therapy scale down RGCs damage in glaucoma?

Many studies have shown the effect of neurotropic factor supplemention on protecting the RGCs in ocular hypertension (OHT) animal models of glaucoma by intravitreal injection of human recombinant BDNF (Domenici et al., 2014). The disadvantage of using BDNF is that it requires repeated intravitreal injections to achieve a recognizable neuroprotective effect (Ko et al., 2000). Ko and colleagues have shown an increase in RGC protection after four intravitreal injections of BDNF therapy. BDNF enhances and prolongs RGCs survival both *in vivo* (Mansour-Robaey et al., 1994, Mey and Thanos, 1993, Pernet and Di Polo, 2006) and *in vitro* (Takihara et al., 2011, Thanos et al., 1989) after optic nerve injury and axotomy. However, TrkB expression in RGCs is down-regulated after axotomy, making the cells less sensitive to the neuroprotective actions of BDNF. TrkB gene transfer to RGCs coupled with intravitreal BDNF administration significantly increased RGC survival after axotomy (Pollock et al., 2003). The neuroprotective effects of BDNF can be enhanced by associative administration of other growth factors, for example, FGF2 and NT-3 (Blanco et al., 2008, Park and Poo, 2013). FGF2 administrated to the ON after ON injury can increase BDNF and TrkB expression in RGCs (Blanco et al., 2008). Several other growth factors also have protective effects on the RGCs. Recombinant CNTF intravitreal injections exhibit neuroprotective effects in OHT animal model. A single intravitreal injection of low dose (2 μg CNTF) exerts a neuroprotective effect with 15% less RGC loss with 15% in weeks (Pease

et al., 2009). This effect correlated with upregulation of STAT3 in cells within the RGC layer and the inner nuclear layer (Bok et al., 2002). Of note is the observation made by McGill and colleagues that improvement in retinal electrophysiology function is observed in animal models of retinal degeneration at a very high dose of CNTF (McGill et al., 2007). While short-term advantageous effects have been shown at times for single intraocular administrations of NGF, long-term neuroprotection in glaucoma patients will likely require sustained NGF supply.

The concept of gene therapy could be applied to neurotrophin factor supplementation for glaucoma to meet the requirements for sustained delivery. By using viral vectors to increase endogenous retinal production of select NGF(s), it might be possible to reduce the RGC damage over the long period. For example, adenovirus (AdV) vector mediated over-expression of BDNF in Müller glial prolongs the survival of RGCs in a rat model of optic nerve transection (Di Polo et al., 1998). In another approach, repeated intravitreal injection of AdV vector used to deliver GDNF prior to optic nerve axotomy lead to 125%-fold increase in RGC survival at 14 days post axotomy (Schmeer et al., 2002). However, the efficacy of AdV-mediated gene transfer is limited by its relatively short duration of expression and by the fact that AdV triggers significant inflammatory reactions. AdV have been found to be very immunogenic in clinical trials, when an 18-year old boy died due to systemic inflammatory response syndrome (Raper et al., 2003). The adeno-associated virus (AAV), has proven to be an effective alternative. Like AdV, AAV vectors do not integrate into the genome. Furthermore, an advantage is that they do not elicit a string immune response. AAV-FGF2 transduction of the retina protected RGCs in models of optic nerve crush and excitotoxicity (Sapieha et al., 2003). Martin and colleagues used AAV to transduce retinal cells in the laser-induced OHT model of glaucoma (Martin et al., 2003). They used a hybrid promoter of cytomegalovirus (CMV), chicken β-actin (CAG) enhancer and the

woodchuck hepatitis post-transcriptional regulatory element (WPRE) to deliver BDNF gene incorporated in an AAV viral vector. The promoter was able to efficiently transduce more than 70,000 cells within the RGC layer per eye. A single intravitreal injection of AAV-BDNF gene therapy reduced the axonal loss in the ON from 52.3% to 32.3% (relative to uninjured contralateral eyes) four weeks after the laser induced experimental model of glaucoma in rodents. Likewise, CNTF gene therapy also promoted long term survival and regeneration of rat RGCs after 7 weeks of ON crush (Leaver et al., 2006). Using a similar vector, Leaver and colleagues showed increase in RGCs protection in retinas injected with CNTF compared to viral vector containing no CNTF. RGC survival was not enhanced by AAV-GFP but was increased in AAV-CNTF (mean RGCs/retina: 17450+/-358 s.e.m). However, a combination of CNTF-BDNF had no significant improvement in RGC axon survival in laser induced rat glaucoma model and the reason for lack of improved effect was not clear (Pease et al., 2009). One of the first major successes for gene therapy with AAV vectors has been the treatment of Leber congenital amaurosis, a severe form of retinal degeneration that leads to vision loss in early childhood (Cideciyan et al., 2013). A replication-deficient AAV vector was used to deliver a gene for isomerohydrolase activity (AAV-hRPE65v2). The vector was injected subretinally and vision gains were found in younger patients (Simonelli et al., 2010, Hauswirth et al., 2008). Furthermore, recent advances in recombinant AAV engineering have led to the development of vectors that are less susceptible to ubiquitin-mediated degradation (Yan et al., 2013).

1.6.2 Targeting neurotrophin receptors in glaucoma therapy

NGF signaling pathways are often subject to complex regulation and accordingly primary increase of neurotrophic factor levels does not always benefit neuronal survival. As

discussed previously, in addition to promoting cell survival via Trk family receptor, NGF can bind to p75NTR receptor and trigger pro-apoptotic signals. Indeed, it has been suggested that cause of failure of NGF in glaucoma may be related to over-activation of p75NTR due to administration of a selective Trk family agonist. In that capacity, design of modified receptor-defined ligands as compared to naturally occurring neurotrophic factors, is being investigated as an approach to achieve greater neuroprotection. Interesting work has been demonstrated by Lebrun-Julien et al in survival of RGCs following optic nerve injury through combined effect of TrkA activation and p75NTR inhibition in p75NTR null mice. The major outcome of this study gives an impression that the deleterious effect of p75NTR in Muller cells may regulate neuronal death directly by emancipating neurotoxins or indirectly by diminishing their sympathetic functions. Also, p75NTR activation could attenuate the beneficial effects of BDNF delivery and inhibition of p75NTR was shown to unmask a potent neuroprotective effect of NGF (Lebrun-Julien et al., 2009). BDNF combined with CNS-specific leucine –rich repeat protein LINGO-1 (LINGO-1 negatively regulates p75NTR signaling) antagonists have been found to promote long-term RGC survival after laser-induced OHT rat model (Fu et al., 2009). Fu et al demonstrated that LINGO-1-TrkB receptor complex adversely controls its activation in the retina after OHT injury. Antibody-1A7 or soluble LINGO-1 (LINGO-1-Fc) commonly used as LINGO-1 antagonist, protects RGCs from death by activating the BDNF-TrkB signaling pathway in animal models of OHT (Fu et al., 2010). Alternatively, novel ligands which specifically activate TrkB and not p75NTR might be of interest. A monoclonal antibody and a natural flavonoid, 7,8-DHF which specifically activates TrkB have shown RGC neuroprotection in the optic nerve transection and OHT animal model (Hu et al., 2010, Gupta et al., 2013b). In light of these outcomes, it is conceivable that selectively activating multiple Trk receptors

while blocking p75NTR using synthetic receptor ligands may create a great deal more robust neuroprotective effect than just delivering the conventional neurotrophic factors.

Recently, our group has demonstrated that Shp2 (discussed earlier) interacts with the TrkB receptor in RGCs and negatively affects its action in ON transection and chronically elevated IOP in rodents. The Shp2-TrkB binding is mediated through the adapter protein, caveolin. Under stress conditions, caveolin isoforms 1 and 3 undergo hyperphosphorylation in RGCs and further bind to Shp2 phosphatase. The expansion in phosphatase activity of Shp2 in glaucomatous stress simultaneously reduces the phosphorylation action of TrkB (Gupta et al., 2012b). The increased dephosphorylation of the TrkB also downregulates its cell survival signaling. As an alternative, it might be advantageous to circumvent neurotrophic receptor activation by advancing downstream pro-survival pathways directly instead of developing new ligands with higher specificity. Added benefits of this approach include the possibility of activating regulatory pathways to multiple neurotrophic factors at the same time and circumventing the problems associated with change in receptor expression in glaucoma. Pernet et al., used AAV to transduce RGCs with genes encoding MEK1, the upstream activator of Erk1/2. MEK1 activation induced *in vivo* phosphorylation of Erk1/2 in RGC bodies and axons. Single injection of AAV encoding MEK1 gene increased RGC survival at 2 weeks after axotomy (Pernet et al., 2005). We have also shown the neuroprotective effect of sphingosine-1-phosphate analogue fingolimod (FTY720) in a chronic OHT animal model. Administration of FTY720 reduced the loss of electrophysiological responses and protected against GCL and ON loss. It was determined that the action of fingolimod was facilitated by increased activation of phosphorylated level of Akt and Erk1/2. Both SIP1 and SIPR receptors were found to be expressed in the experimental glaucomatous condition (You et al., 2014).

1.6.3 Protective effects of inhibiting apoptotic pathway in RGCs in glaucoma

Apoptosis is a programmed cell death that has essential roles in physiological processes but also is a feature in the pathogenesis and pathophysiology of various diseases. Different signals and factors add to apoptosis such as Bax, Bcls, and caspases, play important roles in promoting or inhibiting apoptosis effects. Apoptosis may be mediated through either intrinsic or extrinsic pathway. Initiation of intrinsic pathway is from mitochondria after efflux of cytochrome c, whereas FAS receptor or TNF receptor mediate extrinsic apoptotic pathway. Downstream signaling of intrinsic and extrinsic pathways activates caspases, isoform 3, 6 and 7 and initiate the programmed cell death by degradation of intracellular proteins through the proteolytic action of these caspases. Antiapoptotic Bcl-2 like proteins, for example Bcl-2, Bcl-X, Bcl-w, Mcl-1 and A1/Bfl-1, either interact with antiapoptotic proteins to inhibit their function or directly inhibit mitochondria apoptosis protein (Martinou and Youle, 2011). Dkhissi et al confirmed the DNA fragmentation using the terminal deoxynucleotidyl transferase dUTP nick end labelling (TUNEL) method in the GCL and INL in an avian glaucoma-like disorder model (Dkhissi et al., 1999). The apoptosis in RGCs was also studied in experimental glaucoma animal models by activation of the tumor suppressor protein, p53, which functions to activate the proapoptotic pathways (Nickells, 1999). Considering these observations, anti-apoptotic molecules may preserve the phenotype damage of ON in glaucoma. Etanercept, TNF-α inhibitor, when given intraperitoneally, blocked the TNF-α activity in experimental OHT produced due to activation of microglia and reduced axonal degeneration and loss of RGCs. Clinically, a new therapy was investigated in glaucoma using TNF-α antagonist as suppressors of inflammation (Roh et al., 2012). Recently, it has been shown that a type of 20-24 nucleotide non-coding RNA called microRNAs (miRNAs) are reported in eye diseases (Raghunath and Perumal, 2015). Zhang et al have demonstrated that miRNA-187 negatively regulated the

cell survival via inhibiting cell apoptosis and promoting cell proliferation in RGC-5 line (Zhang et al., 2015). Furthermore, intravitreal injection of second-generation tetracycline, minocycline, has been shown to exhibit neuroprotection in experimental glaucoma and optic nerve transection animal models. It was reported that minocycline increased the expression of antiapoptotic gene Bcl-2 and at the same time decreased the expression of apoptotic gene Bax. Also, TNF-α, inhibitor of apoptosis protein (IAP1) and Gadd45α was upregulated in retinas with optic nerve transection (Levkovitch-Verbin et al., 2014). Calcineurin inhibitor, FK506 administered orally, showed RGC and ON protection from apoptosis by decreasing Bad dephosphorylation and inhibiting mitochondrial cytochrome c release under experimentally induced high IOP (Huang et al., 2005). In addition, agents that alter the expression of endogenous anti-apoptotic proteins can also be employed for neuroprotection function in injured ON. For instance the use of brimonidine, an α2 adrenergic receptor agonist decreases the level of Bcl-2 and also reduces mitochondrial-dependent apoptosis in RGCs of post-mortem eyes from glaucoma individuals (Tatton et al., 2001). Equally, suppressing pro-apoptotic downstream signaling may likewise give a possibility for RGC neuroprotection. Indeed C-terminal binding protein 2 (CtBP2) was recently shown to be neuroprotective in CNS injury and repair in DBA/2J mice. Lentivirus mediated overexpression of CtBP2 in L-glutamate-induced apoptosis of primary cultured RGCs showed decrease in expression of Bax and caspase-3 (Wang et al., 2015a). Cobalt chloride induced hypoxia in primary rat RGCs treated with GABA receptor agonist baclofen, prevented the RGC apoptosis through Akt activation (Fu et al., 2016). Various systemically-administered compounds have additionally been proposed to activate pro-survival pathways or suppress pro-apoptotic pathways downstream of neurotrophic factors and may be considered for neuroprotective treatment in glaucoma.

1.6.4 Targeting ER stress marker proteins as a strategy to halt the RGCs damage in glaucoma

Several studies have concentrated on utilizing the therapeutic application of synthetic chaperons to subdue ER retention of the misfolded proteins, minimized generation of misfolded proteins and amend the ER folding capacity. UPR are triggered in ON axotomy resulting in RGCs death. RGCs shown to have upregulated CHOP in ON injury and promote neuronal apoptosis. CHOP knockout (KO) mice have demonstrated increased RGCs survival by 24% after two weeks of ON axotomy (Hu et al., 2012). Alternatively, the overexpression of XBP-1 in RGCs was carried out using intravitreal AAV injection in WT and CHOP KO mice. AAV viral vector expressing *XBP-1s,* showed considerably increased in RGCs survival in both WT and transgenic mice. Comparing the results in WT treated with AAV-GFP and AAV-XBP-1s at 2 weeks after ON injury, there was significant increase in RGCs survival by 64% in animal overexpressing *XBP-1s* whereas AAV-GFP control mice demonstrated only 20% RGC survival. RGCs survival was increased to 82% in transgenic mice (CHOP KO mice) overexpressing XBP-1s following ON crush injury compared to the wild type animals. Altogether, this experiment suggested an opposite action of XBP-1s and CHOP in controlling RGCs survival and apoptosis after ON injury (Hu et al., 2012, Hu, 2016). Recently, Nakano et al succeeded in designing two novel compounds KUSs (Kyoto University Substances), KUS121 and KUS187 and treated with PC12 cells with these two substances. Both of these compounds inhibited the cellular ATP levels under mitrochondrial respiratory chain complex III and V inhibition. CHOP expression was reduced in culture PC12 cells upon treatment with these KUSs inhibitors. *In vivo* neuroprotective effect on RGCs was also demonstrated by KUSs inhibitor in mice in ON axotomy model and model of glaucoma with high IOP. The rescue of RGCs in ON axotomy and high IOP was initiated by the low expression level of Grp78 or Bip, and ER stress marker apoptosis (Nakano et al.,

2016). RGCs death was also reported recently by the activation of chemokines (CXCL10) and CXCR3 (chemokines receptor). Experimentally induced ischemia and retinal stress modulate the expression on CXCL10 and CXCR3. Upregulation of chemokines and its receptor increases the expression of Grp78, CHOP and ATF4 in RGCs. However, when the mice were treated with ER stress blockers 4-pheylybutyric acid and taurousodeoxycholic (Ozcan et al., 2006), the chemokines expression was attenuated by 61% and 43% respectively. Moreover, in CXCR3 KO mice, the ER stress inhibitor did not transform the expression of ER stress markers, suggesting that the downstream event of CXCR3 activation is not associated with ER stress (Ha et al., 2015). It may therefore be essential to comprehend the dual biological functions of UPR signaling both in survival and apoptosis before exploring therapeutic application focusing ER stress. Alternatively, a conceivable approach could be employing the activation of IRE1α that doesn't activate JNK pathway but induces the activation of XBP-1 mRNA splicing without initiating the apoptosis or by upregulating the UPR gene transcription of chaperons.

1.6.5 Cross-talk with other receptor tyrosine kinase

Vascular endothelial growth factor (VEGF) plays an important role both in physiological and pathological angiogenesis. BDNF signaling is identified as potential proangiogenic factor and stimulates VEGF expression through PI3K pathway for promotion of endothelial cell survival in neuroblastoma cells (Nakamura et al., 2006, Zhang et al., 2010). Similarly, VEGF, an angiogenic factor, was also shown to stimulate axonal outgrowth from dorsal root ganglia by acting as a neurotrophic factor (Sondell et al., 2000). Apart from angiogenesis function, VEGF can also stimulate non-vascular cells such as Tenon's fibroblasts, a target for antifibrotic treatment in glaucoma filtration surgery (Fischer et al., 2016). VEGF is

usually released after retinal ischemia, and can further spread through the aqueous humor to the anterior segment of the eye. The latter results in neovascularization of the iris and angle, causing secondary closed angle glaucoma (Simha et al., 2013). Inhibition of VEGF signaling remains a noteworthy focus for the treatment of retinal and choroid neovascularization and in retina edema. Although VEGF binds to both of its receptor forms (VEGFR1 and VEGFR2). VEGFR1 may be important in development by sequestering VEGF, preventing its interaction with VEGFR2, which is responsible for endothelial cell mitogenesis, survival and permeability (Holmes et al., 2007). Therapeutically targeting VEGF has been successful in clinical studies of ranibizumab, a recombinant monoclonal antibody Fab fragment that binds and neutralizes VEGF. Monthly intravitreal injections of this agent prevent vision loss and improved visual activity in age-related macular degeneration (AMD) patients (Comparison of Age-related Macular Degeneration Treatments Trials Research et al., 2012). In addition, ranizumab therapy also protects retinal thickness and improved visual acuity in patients with diabetic macular edema (Bressler et al., 2012). VEGF is expressed by retinal cells *in vitro* and is upregulated by hypoxia (Marti et al., 2000). Although VEGF is currently an important therapeutic target for the treatment of retinal and choroidal neovascularization and retinal edema, it is important to remember that VEGF does not have only pathogenic effects. In addition to its role in angiogenesis, VEGF is also neurogenic and neuroprotective (Storkebaum and Carmeliet, 2004). RGCs in transgenic mice overexpressing VEGF in neurons were protected from axotomy-induced degeneration (Kilic et al., 2006). It will be interesting to see how neurotrophin factor signaling overlaps with angiogenic factors and how manipulating one pathway would affect the other (Chapter 4).

Hypothesis

Previous studies from our group and the literature showed that BDNF/ TrkB signaling is important in neuronal cells, specifically to RGCs, to maintain homeostasis and prevent the neurons undergoing cell death. TrkB undergoes de-phosphorylation by adaptor protein phosphatase, Shp2 (or PTPN11) and this phosphatase negatively regulates the downstream TrkB signaling in RGCs. So, in this context we hypothesized that downstream consequences of alterations in BDNF/ TrkB signaling by manipulating Shp2 can be a molecular cell mechanism behind RGC loss and the injury to the optic nerve in glaucoma.

Aims

The aims of this thesis are:

1. To investigate the understanding of TrkB receptor and its role in BDNF/ TrkB signaling.
2. To determine the effect of manipulating Shp2 using AAV viral vector in neuronal cells.
3. To investigate the therapeutic applications for glaucoma treatment using gene therapy in rodents.

CHAPTER 2

Material and methods

2.1 Ethics

All procedures involving animals were conducted in accordance with the Australian Code of Practice for the Care and Use of Animals for Scientific Purposes and the guidelines of the ARVO statement for the Use of Animals in Ophthalmic and Vision Research, and were approved by the Animal Ethics Committee of Macquarie University, NSW, Australia. (ARA: 2012/031 and 2014/058)

2.2. List of materials

2.2.1. Animal experiments and electrophysiology

Ketamine 100 mg/ml (Ketamil, Troy Laboratories); Medetomidine 1 mg/ml (Domitor, Pfizer); Atipamezole hydrochlorine 5 mg/ml (Antisedan, Pfizer); Cephazolin sodium (Hospira); Carprofen 50mg/ml (Norbrook); Tropicamide 1.0% (Mydriacyl, Alcon); Proparacaine hydrochloride 0.5% (Alcaine, Alcon); Dexamethasone 0.1% (Maxidex, Alcon); Ciprofloxacin hydrochloride 0.3% (Ciloxan, Alcon Laboratories, NSW, Australia); 0.3% Tobramycin (3mg/ml, Tobrex, Alcon); Homoeothermic blanket system (Harvard Apparatus); Goldring corneal electrode (3103RC, Roland Consult, Brandenburg, Germany); Hand-held multi-species electroretinograph (HMsERG) (OcuScience); ERG viewer

software (OcuScience); Hamilton syringe (Hamilton); FluoSpheres polystyrene microspheres (F-8834, Invitrogen); TonoLab tonometer (Icare Tonovet, Helsinki, Finland).

2.2.2 Histological study

Paraformaldehyde (Sigma); Automatic tissue processor (ASP200S, Leica); Rotary microtome (Microm); Tissue Tek TEC tissue embedding console (Sakura Finetek); Cryostat (CM1950, Leica); Tissue Tek OCT cryostat embedding medium (Sakura Finetek); Hematoxylin (Sigma); eosin (Sigma); Silver nitrate (Sigma); Normal horse serum (Sigma); DeadEnd colorimetric Terminal deoxynucleotidyl transferase dUTP nick end labelling (TUNEL) system (Promega); Vectashield HardSet mounting medium (Vector Laboratories); Axio Imager Z1 fluorescence microscope (Zeiss).

2.2.3. Western blotting and immunoprecipitations

Bicinchoninic acid assay (BCA) protein assay kit (Pierce, Rockford, USA); NuPAGE 10% Bis-Tris gel (Invitrogen); MOPS SDS running buffer (Invitrogen); iBlot gel transfer PVDF membrane (Invitrogen); Supersignal West Pico Chemiluminescent substrate (Pierce); Automated luminescent image analyzer (ImageQuant LAS 4000, GE Healthcare); ImageJ software (NIH Image); Protein A-Sepharose (GE Healthcare).

2.2.4 Cell cultures

The SH-SY5Y neuronal cells, PC-12 (ATCC® CRL-1721™) was obtained from American type culture collection (ATCC, VA, USA). RGC-5 and 661W was kindly gifted from University of Oklahoma. Neurobasal-A media (Life Technologies); B-27 supplement (Life

Technologies); 7,8-Dihydroxyflavone (7,8 DHF) was purchased from Tocris Bioscience, UK. Shp2 or PTPN11 inhibitor, PHPS1 (c-222226) were obtained from Santa Cruz Biotechnology, INC. TrkB receptor antagonist Cyclotraxin-B (CTX-B) was procured from Life Research Ltd, Australia. Dulbecco's modified Eagle's medium (DMEM) and Fetal bovine serum (FBS) from Life Technologies. Recombinant human brain derived neurotrophic factor (BDNF) (ab9794) was purchased from Abcam, VIC, Australia. Poly-D-lysine, Glutamate, Trypan blue dye, Neubauer micro-chamber, MTT assay kit and Hydrogen peroxide were purchased from Sigma-Aldrich, St. Louis, MO, USA. DAPI (4',6-diamidino-2-phenylindole) from Molecular Probes and cell counter from Wertheim, Germany. All other analytical grade chemicals and reagents from purchased either from Sigma (St. Louis, MO, USA) or Invitrogen (Carlsbad, CA, USA).

2.2.5. Antibodies

Anti-BDNF (sc-546), anti-TrkB (sc20542), anti-GADD-153 (sc-7351), anti-XBP-1 (sc-7160), anti-p-PERK (sc-3257) antibodies were obtained from Santa Cruz Biotechnology, CA, USA. Anti-Akt (11E7); anti-pAkt (Ser473) (193H12); anti-GSK3β (27C10); anti-pGSK3 β (Ser9) (5B3); anti-p44/42 MAPK (Erk1/2) (137F5); anti-p-p44/42 MAPK (Erk1/2 Thr202/Tyr204) (D13.14.4E); and anti-VEGFR2 antibodies were purchased from Cell Signaling, MA, USA. Anti-Shp2 or anti-PTPN11 (6D9) from purchased from Pierce. Anti-pTrkBY^{515} (ab51187 and ab131483); GFP (ab290); anti-beta III Tubulin (ab78078); anti-NeuN (ab104225) and anti-VEGF (ab46154) were obtained from Abcam, VIC, Australia. β-Actin antibody (AC-40) were from Sigma. Alexa-Fluor 488 goat anti-rabbit IgG; Alexa-Fluor 555 goat anti-mouse IgG and Alexa-Fluor 594 goat anti-mouse IgG were used from Life Technologies, Australia.

2.3. Methods and protocols

2.3.1. Animals and anesthesia

Male Sprague-Dawley rats with a body weight of 300-350 g (10-12 weeks, Animal Research Centre, Perth), BDNF+/- and wid-type (WT) control mice (both male/female) were obtained from Mental Health Research Institute (Parkville, VIC, Australia) and genotyped using standard PCR methodology were used. All animals were maintained in an air-conditioned room with controlled temperature (21 ± 2℃) and fixed daily 12-hour light/dark cycles. The animals were anaesthetized with an intraperitoneal injection of ketamine (75 mg/kg) and medetomidine (0.5 mg/kg) in all eye injections and electrophysiology recording. At the end of the procedure, anesthesia was reversed using atipamazole (0.75 mg/kg) subcutaneous injection, and 0.3% ciprofloxacin drops (Ciloxan) and 0.1% dexamethasone eye drops (Maxidex, Alcon Laboratories) were instilled in both eyes. An ointment (Lacri-lube; Allergan, NSW, Australia) was also applied to protect against corneal drying until the animal recovered (Chapter 3,4, 6 and 7).

2.3.2 AAV vector-Design and packaging

The murine Shp2 or PTPN11 cDNA (BC057398, isoform-a) was placed under the transcriptional control of the cytomegalovirus (CMV) β-actin (CAG2) hybrid promoter and inserted into the commercially available Adeno-associated virus, serotype 2 (AAV2) basic green fluorescence protein (GFP) vector (AAV2-CAG2-GFP-T2A-mPTPN11 or AAV2-PTPN11) for PTPN11 over expression (Vector Biolabs, USA). Both, GFP and PTPN11 sequences were driven by the CAG2 promoter with 2A linker in between. For PTPN11 gene

silencing, shRNAmir was used to knock down the PTPN11 sequence (AAV2-CAG-GFP-mPTPN11shRNAmir or AAV2-PTPN11KD). AAV2 containing shRNAs targeting PTPN11 coding sequences (NM_001109992.1) starting at nucleotide 1296 (5'-CCTGATGAGTATGCGCTCAAA-3') was used to achieve PTPN11 knockdown and 5'-GTCTCCACGCGCAGTACATTT-3' sequence was used as scramble shRNAmir control. AAV2 vector containing shRNA also included an upstream enhanced green fluorescent protein (eGFP) reporter cassette flanked by a viral CAG promoter and a V5 epitope tag/polyA sequence. To increase the cloning capacity of hybrid CAG2 promoter was used that contains smaller chicken β-actin intron from the original CAG promoter. AAV2-CAG2-GFP was used as control for PTPN11 over expression and AAV2-CAG-GFP-shRNA as control for PTPN11 knockdown (Chapter 5, 6 and 7).

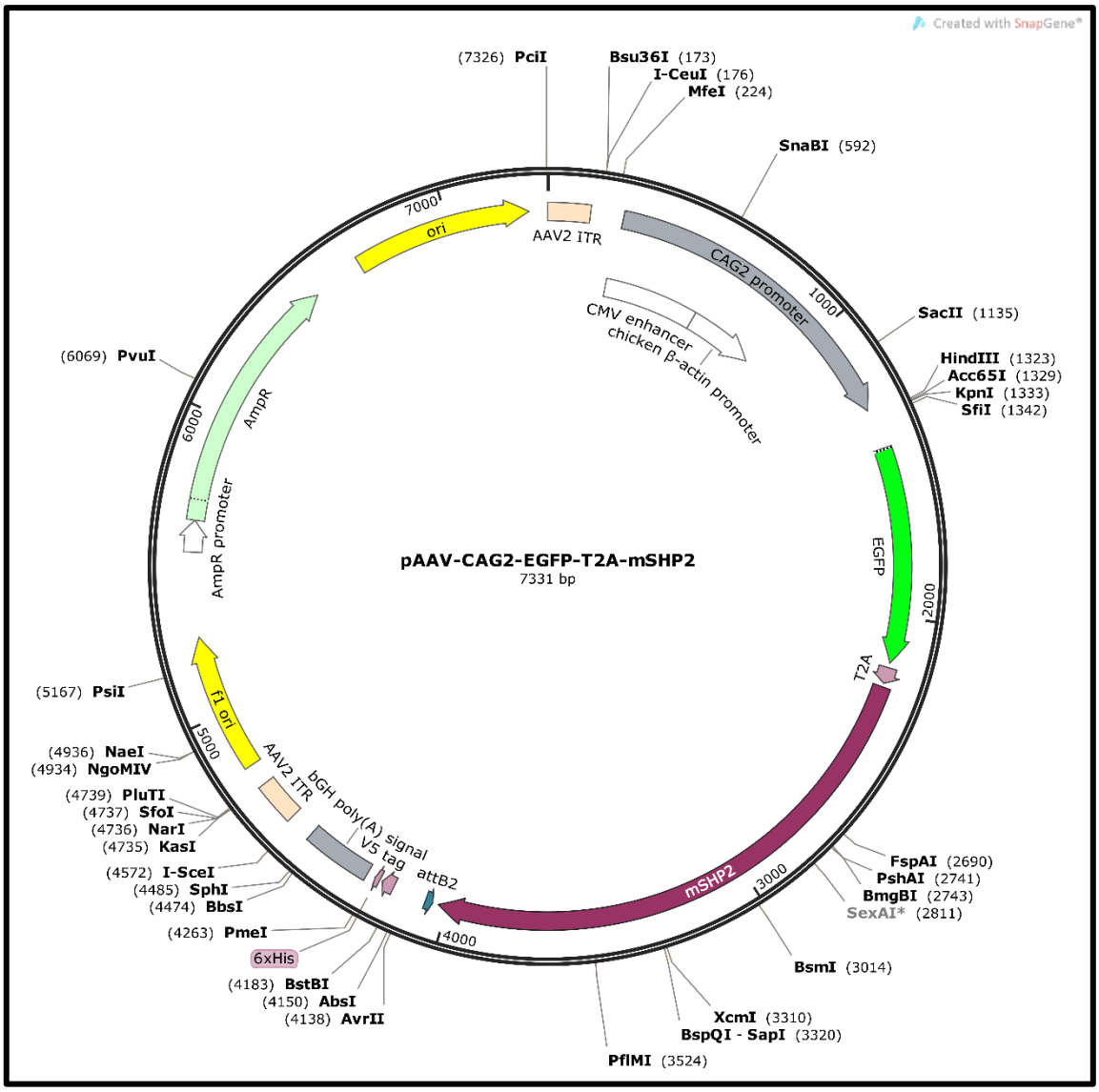

Figure 2.1 Map of the plasmid containing the mShp2/ mPTPN11 sequence used for overexpression. Adeno-associated vector plasmid delivering the *PTPN11(Shp2)* gene construct. AmpR, ampicillin resistance gene; Ori, origin of replication; bGH poly(A), bovine growth hormone polyA sequence; ITR, inverted terminal repeat. Transgenes enhanced green fluorescence protein (eGFP) or murine *PTPN11* was under the control of the cytomegalovirus and chicken β-actin (CAG2) hybrid promoter. GFP and mPTPN11 genes are separated by poly 2A linker protein. The control viral vector containing only eGFP.

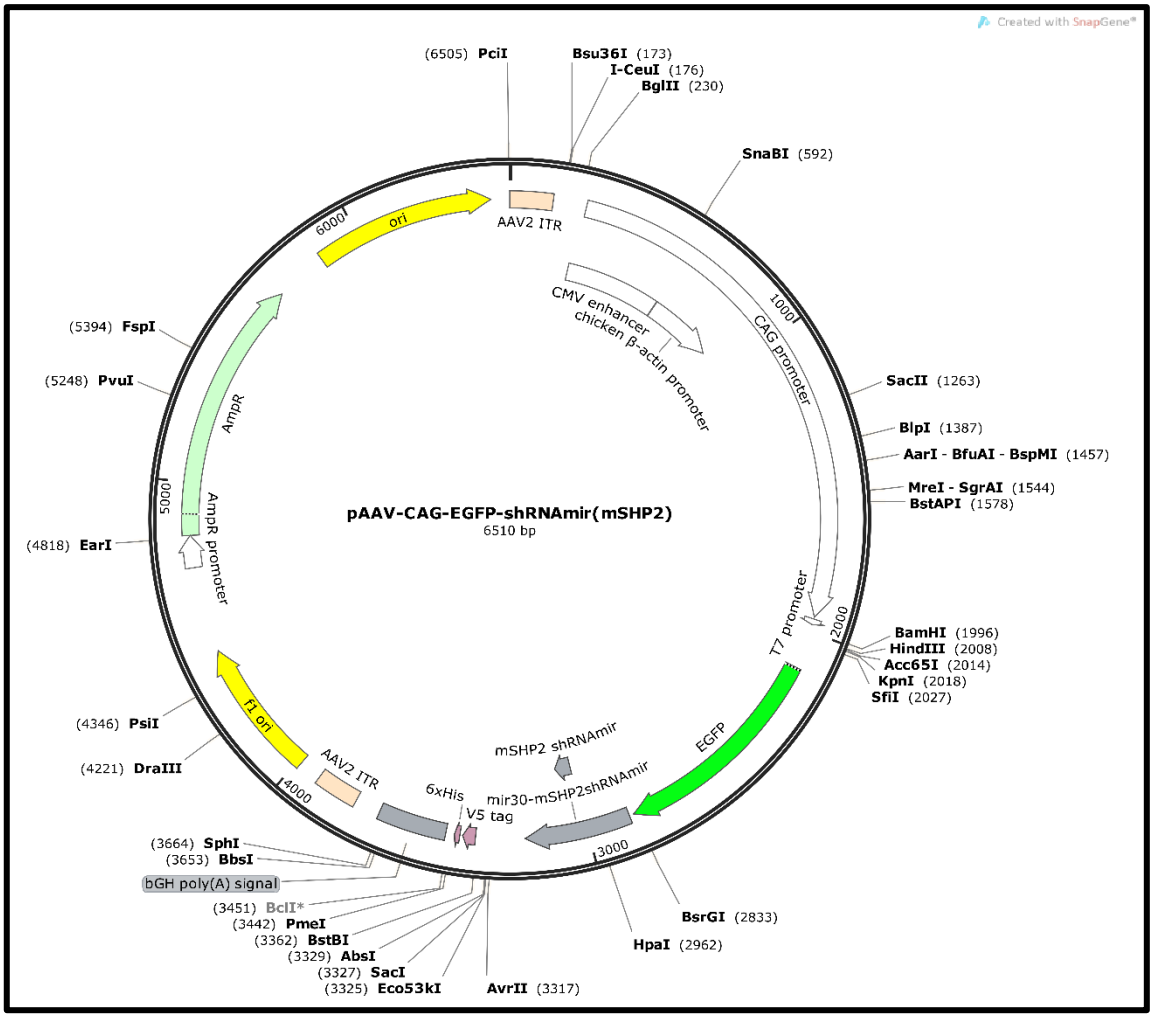

Figure 2.2 Map of the plasmid containing the mPTPN11shRNAmir sequence used for knockdown. Adeno-associated vector plasmid delivering the shRNA sequence. AmpR, ampicillin resistance gene; Ori, origin of replication; bGH poly(A), bovine growth hormone polyA sequence; ITR, inverted terminal repeat. Transgenes enhanced green fluorescence protein (eGFP) or murine *PTPN11*-shRNA were under the cytomegalovirus and chicken β-actin (CAG) hybrid promoter. The control viral vector has eGFP along with scramble sequence of shRNAmir (mPTPN11).

2.3.3 AAV2 intravitreal injections

Animals were anesthetized as described above with intraperitoneal mixture of ketamine medetomidine. Pupillary dilation was achieved with 1% tropicamide and 2.5% phenylephrine eye drops. For the AAV2 injections, a 33-gauge needle was used for injections (5 μL) injected temporally and nasally at a 45° angle 2 mm behind the corneoscleral limbus into the vitreous body without touching the lens. All injections were carefully carried out under an operating microscope (OPMI-11 Vario S88; Carl Zeiss, Oberkochen, Germany). After the injection, the needle was left in place for another minute to allow dispersion of the AAV2 solution into the vitreous. Control eyes were either injected with AAV2 expressing GFP, scrambled sequences or treated with vehicle. The animals were maintained for 2 months after the AAV2 injection (Chapter 6 and 7).

2.3.4 Microbead Injection and IOP measurement

A chronic RGC degeneration model was established by a producing a chronic increase of IOP in rats by microbead (Fluospheres, Molecular Probes, 10 μm) injections in the anterior chamber and anesthetized using isoflurane. After anesthesia both pupils were dilated with topical tropicamide 1%. Weekly intraocular injections (3.6×10^6 microbeads/mL) were made until a sustained increase in IOP was observed. The contralateral eye was used as control. Eyes were injected using a 25-μL Hamilton syringe connected to a disposable 33-gauge needle (TSK Laboratory, Tochigi, Japan). All ocular procedures were performed under magnification using an operating microscope with care taken to avoid needle contact with the iris or lens. The needle was inserted bevel down, tangentially beneath the corneal surface, to facilitate self-sealing of the puncture wound. Once the needle tip was visualized within the anterior chamber, 10 μL microbead solution was injected. During anesthesia and

prior to each injection, IOP was measured by using a handheld electronic tonometer. The IOP displayed on the tonometer was the mean of six consecutive measurements. Three consecutive IOP readings were obtained from each eye and the average number was taken as the IOP (Chapter 7).

2.3.5. Animal recovery and follow up

For microbead or viral vector injection, dexamethasone and 0.3% Tobramycin along with 2% povidone-iodine were administered to prevent ocular inflammation and infection after the treatment. 5% carprofen was administered subcutaneously (50mg/ml) as pain relief. The animals were allowed to recover on a warming pad. Routinely monitored for two consecutive days after the injection. The animals were also monitored weekly thereafter over a 2-month period (Chapter 6 and 7).

2.3.6 Electroretinography

Animals were dark-adapted overnight and anaesthetized as mentioned above and pupils were dilated using 1% tropicamide and topical anesthetic (1% alcaine) were applied to the cornea. Animals were positioned on a heated sliding stage to maintain body temperature during anesthesia and recording sessions. Ground and reference electrodes were placed subcutaneously in the tail and forehead of the animal, respectively. A solid custom-made gold ring recording electrode was placed on each eye in contact with the cornea and a thin layer of methylcellulose was used to maintain contact between the cornea and the electrode and to decrease the recording noise. ERGs were recorded using a flash intensity of 3 log $cd \cdot s/m^2$ (Ocusciences, Xenotec, Inc., MO, USA). For all ERG recordings, a-wave amplitude

was measured from baseline to the a-wave trough; b-wave amplitude was measured from the a-wave trough to the peak of b-wave. For positive scotopic threshold responses (pSTRs) dim stimulation using flash intensities of − 3.4 log cd·s/m^2 was delivered 30 times at a frequency of 0.5 Hz. For all positive STR responses, amplitudes were measured from baseline to the positive peak observed around 120 ms (Chapter 6 and 7).

2.3.7. Tissue preparation and histology

2.3.7.1. Tissue fixation, embedding and section

Animals were euthanized humanely with an overdose of intraperitoneal injection of sodium pentobarbitone (100 mg/kg Lethabarb, Virbac Pty, Australia) and then perfused transcardially with 4% paraformaldehyde (PFA, Sigma). Tissues (eyes and ON) were harvested for morphometric and immunofluorescent studies and the marking dye (polysciences) was used to mark orientation of excised eyes. For morphometric analysis, the eyes were fixed for 2 hours in 4% PFA and then incubated in 70% ethanol overnight at 4°C. Eyeballs were placed in embedding cassette and processed *via* automatic tissue processor (ASP200S, Leica). Eyes were subsequently embedded in molten paraffin wax. Using a rotator microtome, 7 µm thick paraffin embedded sections involving the whole retina as well as the optic disc, were cut from the vertical meridian of each eye and mounted onto Superfrost Plus slides (Menzel-Glaser Lomb). Sections were made using a rotary microtome. For immunofluorescent study (see below), eye and ON tissues were kept in 4% PFA for 1-2 hours at room temperature, followed by three subsequent washings with 1X- PBS. Tissues were cryopreserved in 30% sucrose solution (in 1x PBS with 0.01% sodium azide) in 4°C until the tissue sank completely. Then after the samples was embedded in OCT cryostat

embedding medium and the 10 μm thick cryosections were made using the cryostat (Chapter 4 and 5).

2.3.7.2. Hematoxylin and eosin (H&E) staining

H&E staining was performed on paraffin embedded sections after standard procedures of deparaffinization (xylene) and dehydration (graded ethanol, 100%, 95%, 75%, 50%). Sections were then incubated in 0.005% hematoxylin solution for 4 min, followed by 0.1% eosin solution for 1 min (Chapter 6 and 7).

2.3.7.3. Bielschowsky's silver staining

Bielschowsky's silver staining was carried out to evaluate axonal density in the optic nerve. Slides were pre-treated in 10% silver nitrate at 40 °C for 15 min, and then incubated in ammonium silver solution for 30 min. Next, sections were placed directly into the developer working solution (0.08% formaldehyde, 0.005% citric acid, 0.005% nitric acid and 1% concentrated ammonium hydroxide) for 30 sec, followed by incubation in 5% sodium thiosulfate solution for 5 min (Chapter 6 and 7).

2.3.7.4. Terminal deoxynucleotidyl-transferase-mediated biotin-dUTP nick end labelling (TUNEL) staining

DNA fragmentation as a marker of apoptosis was detected by TUNEL using the DeadEnd colorimetric TUNEL assay kit according to the manufacturer's instructions. To detect cell apoptosis, SH-SY5Y cells and retina tissues were stained with TUNEL System. Briefly, cells

were grown to 50–60% confluency. Following viral transduction and fixed with 4% paraformaldehyde solution in PBS, pH 7.4 for 1 h. Fixed frozen retinal sections were also subjected to PBS, pH 7.4 for 1 h. Permeabilization was carried out using 0.1% Triton X-100 in 0.1% sodium citrate on ice for 10 min. Cells and retinal sections were then independently washed twice with PBS and incubated with TUNEL reaction mixture at 37°C for 1 h in a humidified atmosphere in the dark. Following incubation, slides were washed with PBS, mounted with prolong antifade dapi, and directly analyzed for apoptotic cell staining using epi-fluorescence microscopy (Chapter 5, 6 and 7).

2.3.7.5. Immunofluorescence

Animals were euthanized with an overdose of anesthetics and then perfused transcardially with 4% PFA. Orientation of the eyes was demarcated using tissue marking dye and eyes were harvested and fixed in 4% PFA. Following fixation for 2 hrs in 4% PFA, the eyes were washed incubated in 30% sucrose overnight and embedded in OCT cryostat embedding medium as described previously (Gupta et al., 2016). Tissue sections 12 µm were prepared using a cryostat and sections were permeabilized in 0.1 % Triton X-100 in PBS (You et al., 2014). This was followed by incubating the sections with the appropriate primary antibodies overnight at 4°C: anti-PTPN11 (1:150), anti-GFP (1:150), anti-GADD 153 (1:200), anti-pTrkB Y^{515} (1:100) or anti-TrkB (1:100). Further, slides were incubated with either of the secondary AlexaFluor-488, 555 or 644 conjugated anti-mouse, anti-goat or anti-rabbit antibodies (1:400) for 1 h at room temperature followed by extensive washing and mounting using anti-fade mounting media with dapi. Cells were similarly fixed for 10 min, permeabilised and treated with respective primary and secondary antibodies. Images were acquired using a Zeiss fluorescence microscope (Rajala et al., 2013). Fluorescent images

were inverted and thresholded and relative fluorescence intensity and pixel density was quantified and plotted using ImageJ (Chapter 5,6 and 7).

2.3.8. Biochemistry

2.3.8.1 Protein extraction

The cells were washed with 1X PBS and lysed with TN buffer (50 mM Tris–HCl pH 7.5, 150 mM NaCl, 0.1 % SDS) with 1 % protease inhibitor (Sigma), followed by incubation on ice for 10 min. The SDS soluble protein fraction was collected by centrifugation at 16 100 g for 10 min. For immunoblotting, the cells were also treated with 0.125 % trypsin for 2 min at room temperature before lysis (Chapter 3, 4, 5, 6 and 7).

2.3.8.2 SDS-PAGE, Western Blot and Immunoprecipitations

The tissues or cells were mixed in lysis buffer (20 mM HEPES, pH 7.4, 1 % Triton X-100, 2 mM EDTA) containing protease inhibitors (10 µg/ml aprotinin, 10 µM leupeptin, 1mM phenymethyl sulfonyl fluoride) and phosphatase inhibitors (1 mM $NaVO_3$, 100 mM NaF, 1mM Na_2MoO_4 and 10mM $Na_2P_2O_7$ (Gupta et al., 2012a)) and sonicated. The proteins were separated by 10% SDS-PAGE and transferred to PVDF membrane as explained previously (Gupta et al., 2014b). The blots were washed 3 times for 5 min with TTBS (20 mM Tris-HCl [pH 7.4], 100 mM NaCl, and 0.1% Tween 20) and blocked with 5% non-fat dry milk (Bio-Rad) in TTBS buffer for 1 h at room temperature (Gupta et al., 2010). Membranes were incubated overnight with anti-GFP (1:1000), anti-PTPN11 (1:1000), anti-pTrkB Y^{515} (1:1000), anti-TrkB (1:1000), anti-GADD 153 (1:200), anti-XBP-1 (1:200), anti-p-PERK (1:200), anti-actin (1:5000) overnight at 4°C (Chapter 3, 4 and 5), anti-BDNF (1:1000), anti-

TrkB (1:1000), anti-pTrkB (Tyr^{515}) (1:1000), anti-Akt (1:1000), anti-pAkt (Ser273) (1:1000), anti-Erk (1:1000), anti-pErk (Thr202/Tyr204) (1:1000), anti-GSK3β (1:1000), anti-pGSK3β (Ser9) (1:1000) or anti-actin (1:5000) either for 1 h (actin) at room temperature or overnight at 4 ^{0}C (Chapter 7). Actin was used to ensure a comparable loading was made in each case (Basavarajappa et al., 2011). Following primary antibody treatment, immunoblots were incubated with horseradish peroxidase (HRP)-linked secondary antibodies and after extensive washing, antibody detection was accomplished with Supersignal West Pico Chemiluminescent substrate (Pierce). Signals were detected using an automated luminescent image analyser (ImageQuant LAS 4000, GE Healthcare). Band intensities were quantified using ImageJ software (NIH, USA).and densitometric analysis of the band intensities performed (Image J, USA) (Gupta et al., 2014a, Gupta et al., 2010) (Chapter 3, 4, 5, 6 and 7).

CHAPTER **3**

Protective role of brain derived neurotrophic factor in neuronal cells

Published as:

Vivek Gupta, **Nitin Chitranshi,** Yuyi You, Veer Gupta, Alexander Klistoner, Stuart Graham**.** Brain derived neurotrophic factor is involved in the regulation of glycogen synthase kinase 3β (GSK3β) signalling. ***Biochemical and Biophysical Research Communications*** 454 (2014) 381–386.

Abstract

Glycogen synthase kinase 3β (GSK3β) is involved in several biochemical processes in neurons regulating cellular survival, gene expression, cell fate determination, metabolism and proliferation. GSK3β activity is inhibited through the phosphorylation of its Ser-9 residue. In this study, we sought to investigate the role of BDNF/TrkB signaling in the modulation of GSK3β activity. BDNF/TrkB signaling regulates the GSK3β activity both in vivo in the retinal tissue as well as in the neuronal cells under culture conditions. We report here for the first time that BDNF can also regulate GSK3β activity independent of its effects through the TrkB receptor signaling. Knockdown of BDNF lead to a decline in GSK3β phosphorylation without having a detectable effect on the TrkB activity or its downstream effectors Akt and Erk1/2. Treatment with TrkB receptor agonist had a stimulating effect on

the GSK3β phosphorylation, but the effect was significantly less pronounced in the cells in which BDNF was knocked down. The use of TrkB receptor antagonist similarly, manifested itself in the form of downregulation of GSK3β phosphorylation, but a combined TrkB inhibition and BDNF knockdown exhibited a much stronger negative effect. In vivo, we observed reduced levels of GSK3β phosphorylation in the retinal tissues of the $BDNF^{+/-}$ animals implicating mechanistic role of BDNF in the regulation of the GSK3β activity. Concluding, BDNF/TrkB axis strongly regulates the GSK3β activity and BDNF also exhibits GSK3β regulatory effect independent of its actions through the TrkB receptor signaling.

3.1. Introduction

Glycogen synthase kinase 3β (GSK3β) is a ubiquitously expressed and evolutionarily conserved intracellular protein serine/threonine kinase. It is constitutively active in most cells and plays a pivotal role in key cellular functions ranging from glycogen metabolism to important regulatory effects on the neural plasticity and survival. It is important regulatory protein that is subject to phosphorylation by growth factor-stimulated signaling pathways (Mai et al., 2002). Phosphorylation at Ser9 residue is the most well defined post-translational modification of GSK3β which regulates its activity (Mai et al., 2002). GSK3β activity is negatively regulated by several signal transduction cascades that protect neurons against apoptosis, including the phosphatidylinositol-3 kinase (PI-3K) pathway. Over-expression of GSK3β in specific regions of the brains in animals results in region specific neuronal cell death (Lucas et al., 2001).

Previous work has shown that Brain-derived neurotrophic factor (BDNF) mediated signaling modulates GSK3β activity in retinoic acid differentiated SH-SY5Y cells (Mai et al., 2002).

BDNF exerts neurotrophic effects primarily through its high affinity receptor tropomyosin receptor kinase B (TrkB), which upon stimulation undergoes dimerization and phosphorylation of its specific intracellular tyrosine residues and activates various cell signaling pathways linked to growth, differentiation, and survival (Patapoutian and Reichardt, 2001, Bartkowska et al., 2010). BDNF binds to the TrkB receptor to initiate multiple signaling cascades, including the PI-3K which in turn leads to the activation of the Ser/Thr kinase Akt (Patapoutian and Reichardt, 2001, Gupta et al., 2013a). Akt is a major upstream regulator of GSK3β and regulates GSK3β signaling by its phosphorylation at Ser^9, thereby inactivating it (Hu et al., 2013). GSK-3β activity changes have been reported to be associated with several psychiatric and neurodegenerative diseases, such as Alzheimer's disease, schizophrenia and autism spectrum disorders, in addition to several cellular proliferative disorders and it is becoming increasingly clear that GSK3β might serve as a potential therapeutic target in several of these disorders (Namekata et al., 2012, Luo, 2009). It is also possibly associated with ageing related cellular effects. GSK-3β phosphorylation inhibits CRMP-2 binding to tubulin and promotes microtubule dynamics along with axonal transport and outgrowth in neurons. It also plays a role in regulating the polarity of the neurons (Namekata et al., 2012). Enhanced GSK3β activity is involved in the CREB protein inactivation and promotes cell death and degeneration (Grimes and Jope, 2001).

In retina, BDNF has been shown to play a vital role in maintaining the health of retinal ganglion cells (RGCs) and protecting them from apoptosis caused by glaucoma or injury (Mansour-Robaey et al., 1994). BDNF is shown to stimulate the growth of neurites from regenerating RGCs (Cohen-Cory and Fraser, 1995), and protect optic nerve and RGCs from damage (Mansour-Robaey et al., 1994, Chen and Weber, 2001). The higher susceptibility of $BDNF^{+/-}$ mice to development of neurodegenerative changes in the inner retina with age

indicates that these might be arising due to the disruption of BDNF/TrkB axis leading to possible activation of GSK3β (Gupta et al., 2014b). An enhanced GSK3β activity has been observed in the inner retinas of animal models of experimental glaucoma as well as post-mortem samples of human glaucoma subjects (Hu et al., 2013). The present study investigates the regulatory effects of BDNF impairment on GSK3β activity in vivo using wild type and $BDNF^{+/-}$ animals. As GSK3β phosphorylation and activation can be regulated in a cell and tissue dependent manner; to rigorously investigate the role played by BDNF in regulating the GSK3β activity we used two neuronal RGC-5 and PC12 cell lines and evaluated the role of BDNF and TrkB in regulating the GSK3β activity and also determined the relevance of the findings in vivo. The results provide novel data that raise the prospects of using TrkB agonist treatment to regulate the potential deleterious effects of GSK3β activity. Further, we show here for the first time that BDNF regulates Ser^9 residue phosphorylation of GSK3β independent of its effects through high affinity receptor TrkB and subsequent PI3K/Akt and Erk1/2 activation.

3.2. Materials and methods

Used of animals and chemicals are described in chapter 2

3.2.1. Cell culture and treatments

RGC-5 and PC12 neuronal cells were maintained in DMEM medium containing 10% foetal bovine serum (FBS) at 37^0C with 5% CO2. Approximately 2.0 x 10^5 cells were seeded in each 60 mm culture dish 6–12 h before subjecting them to transient transfections. After transfections and subjecting the cells to serum starvation for a period of another 12 h, the cells were either treated with TrkB receptor agonist, 7,8DHF (100nM, 6 h) or a cyclic peptide

CTX-B, which is a TrkB antagonist with 1–11 Cys residue disulphide linkage (CNPMGYTKEGC; 5 lM, 6 h). 7,8-DHF was dissolved in phosphate-buffered saline containing 17% dimethylsulfoxide. Subsequently, cells were harvested, lysed and the cell lysates subjected to Western blotting for biochemical analysis.

3.2.2. Transfections

RGC-5 and PC12 cells were subjected to transient BDNF knockdown using the BDNF siRNA (Santa Cruz Biotechnology; sc42122) which is a combination of 3 target-specific 20–25 nucleotide siRNA sequences designed to knockdown gene expression. It was resuspended in RNAse free water to obtain a 10 lM solution in Tris–HCl, pH 8.0, 20 mM NaCl, 1 mM EDTA. Briefly the siRNA was mixed with the Lipofectamine RNAiMAX (Invitrogen) reagent and cells transfected (Gupta et al., 2012b). Control cells were treated with the control siRNA sequences (Santa Cruz biotechnology; sc37007). It consisted of a scrambled sequence that is not known to lead to specific degradation of any known cellular mRNA. The cells were subjected to serum starvation by excluding FBS from the culture media, approximately 12 h after the transient transfections were performed and allowed to grow for another 18–24 h.

3.2.3. Drug treatments

The animals were treated chronically (2 mg/kg) with a TrkB agonist 7,8DHF. 7,8-DHF is a potent and selective TrkB receptor agonist that provokes receptor autophosphorylation and dimerization and has been shown to activate the TrkB signaling in the RGCs (Gupta et al., 2013b, Jang et al., 2010b, Liu et al., 2010a)]. 7,8DHF was administered fortnightly for a period of 2 months through intraperitoneal injections. Animals were sacrificed and tissues

harvested 2 h after the last drug treatment. $BDNF^{+/-}$ mice were healthy with normal behavior, and had no visible phenotype different from WT mice.

3.2.4. SDS–PAGE and Western Blot analysis

Following enucleation of the eyes and retinal dissection, ONH regions of the retina were excised under a surgical microscope, lysed in lysis buffer as described in chapter 2, *section 2.3.8.2*. Blots were then incubated with anti-BDNF (1:1000), anti-TrkB (1:1000), anti-pTrkB (Tyr515) (1:1000), anti-Akt (1:1000), anti-pAkt (Ser273) (1:1000), anti-Erk (1:1000), anti-pErk (Thr202/Tyr204) (1:1000), anti-GSK3β (1:1000), anti-pGSK3β (Ser9) (1:1000) or anti-actin (1:5000) either for 1 h (actin) at room temperature or overnight at 4 ^{0}C. Rest of the procedure followed as mentioned in chapter 2, *section 2.3.8.2.*

3.2.5. Statistical analysis

Data were analyzed and graphed using commercially available Graphpad Prism software (version 6.0) (GraphPad Software, San Diego, CA). All values with error bars are presented as mean ± SD and compared by Student's t test for unpaired data. Grouped data was analyzed using ANOVA. The significance was set at $p < 0.05$.

3.3. Results

3.3.1. BDNF negatively regulates GSK3β activation in RGC-5 and PC12 cells

The role of BDNF knockdown on the TrkB and its downstream signalling comprising Akt, Erk1/2 and GSK3β was investigated in the RGC-5 and PC12 neuronal cells. The cells were

also subjected to either treatment with the TrkB receptor agonist 7,8DHF or incubated with 7,8DHF subsequent to BDNF knockdown and downstream signalling changes analysed (Figure 3.1 A and E). Quantification of the band intensities revealed that siRNA mediated knockdown was successful in significantly reducing the BDNF expression in both cell types ($p < 0.03$) (Figure 3.1 B and F). A basal level of TrkB phosphorylation indicated that it was constitutively active in both cell lines. BDNF knockdown was not observed to have any significant effect on the phosphorylation levels of TrkB receptor. To decipher the relative contributions of BDNF and its high affinity receptor TrkB, the cells were treated with TrkB receptor agonist 7,8DHF. Treatment of cells with 7,8DHF produced significant activation of the TrkB receptor in both cell types ($p < 0.05$) (Figure 3.1 C and G). We also observed a corresponding activation of the Akt ($p < 0.005$) and Erk2 proteins ($p < 0.01$) which are downstream of the TrkB receptor. BDNF knockdown by itself did not have any detectable effect on the phosphorylation levels of any of these proteins. Interestingly, BDNF knockdown resulted in marked downregulation of GSK3β phosphorylation in the normal untreated cells ($p < 0.05$) as well as those treated with 7,8DHF ($p < 0.05$) indicating that BDNF also has a regulatory effect on GSK3β signalling independent of its effects through the TrkB activation (Figure 3.1 D and H). 7,8DHF treatment was not shown to have any effect on the expression of BDNF, TrkB, Akt, Erk1/2 or GSK3β proteins.

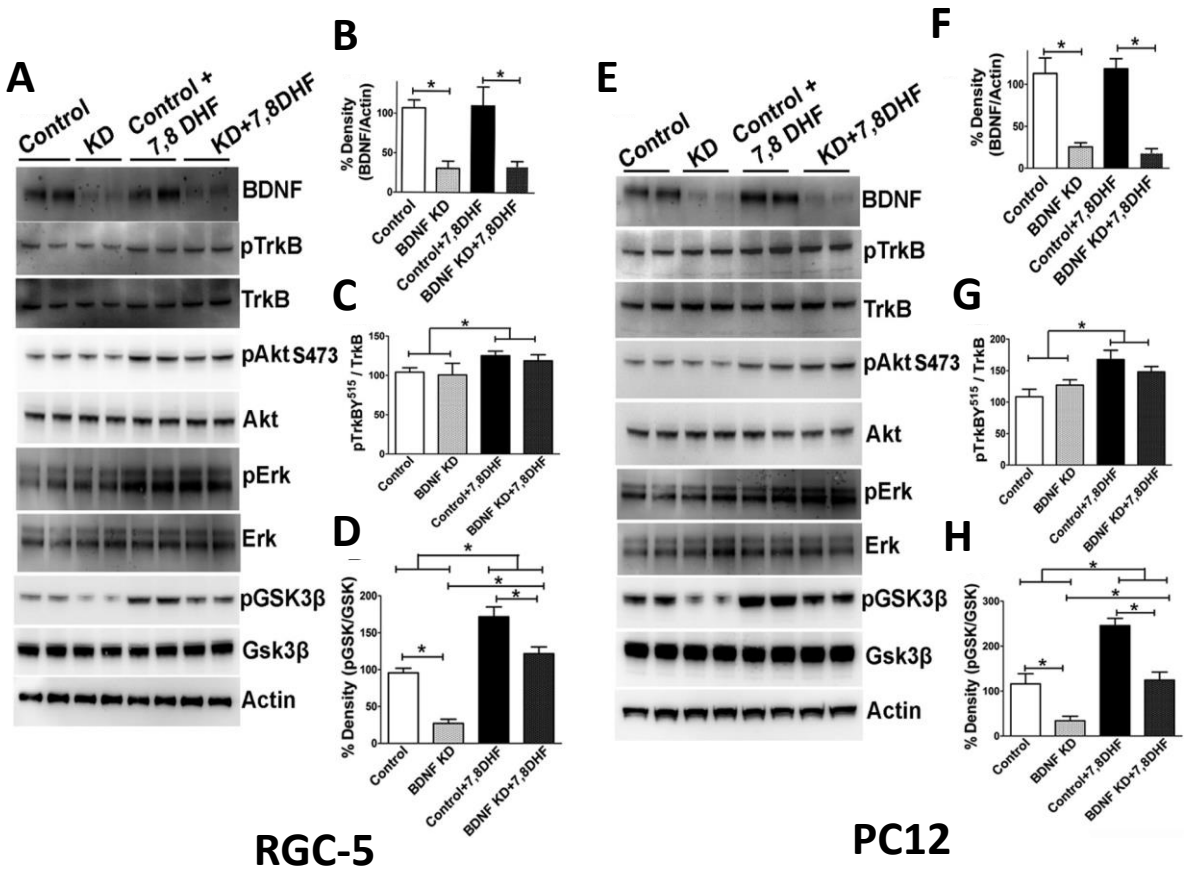

Figure 3.1. BDNF knockdown leads to GSK3β activation by reducing its phosphorylation levels. (A) RGC-5 cells were subjected to BDNF knockdown, treatment with 7,8DHF (100 nM) or BDNF knockdown and then incubation with 7,8DHF and Western blotting performed. Band intensities were analysed and plotted for (B) BDNF (C) pTrkB (Tyr515) and (D) pGSK3β (Ser9) proteins using actin, TrkB and GSK3β as controls respectively. (E) PC12 cells were subjected to either knockdown of BDNF, treatment with 7,8DHF (100 nM) or BDNF knockdown and subsequent incubation with 7,8DHF followed by Western blotting. Band intensities were quantified and plotted for (F) BDNF (G) pTrkB (Tyr515) and (H) pGSK3β (Ser9) proteins using actin, TrkB and GSK3β as controls respectively. *$p < 0.05$ in each case.

3.3.2. BDNF$^{+/-}$ mice depict reduced GSK3β phosphorylation with age

In order to determine whether BDNF mediated regulation of GSK3β is reflected under in vivo conditions, we investigated changes in the GSK3β phosphorylation in optic nerve head (ON) of the retinas of WT and BDNF$^{+/-}$ animals. No changes in the phosphorylation status of GSK3β were observed at 2 m time point (Figure 3.2 A). Our previous studies have shown that aged BDNF$^{+/-}$ animals depict reduced levels of BDNF in the ONH at 1 year (Gupta et al., 2014b). We therefore also evaluated any changes in GSK3β phosphorylation levels at

this time point and interestingly observed a significant level of GSK3β activation ($p < 0.01$) (Figure 3.2 B). There was no detectable change in the expression levels of total GSK3β protein. Actin was used as loading control in each case. These results indicate that BDNF loss modulates the GSK3β signaling in vivo by promoting its activation.

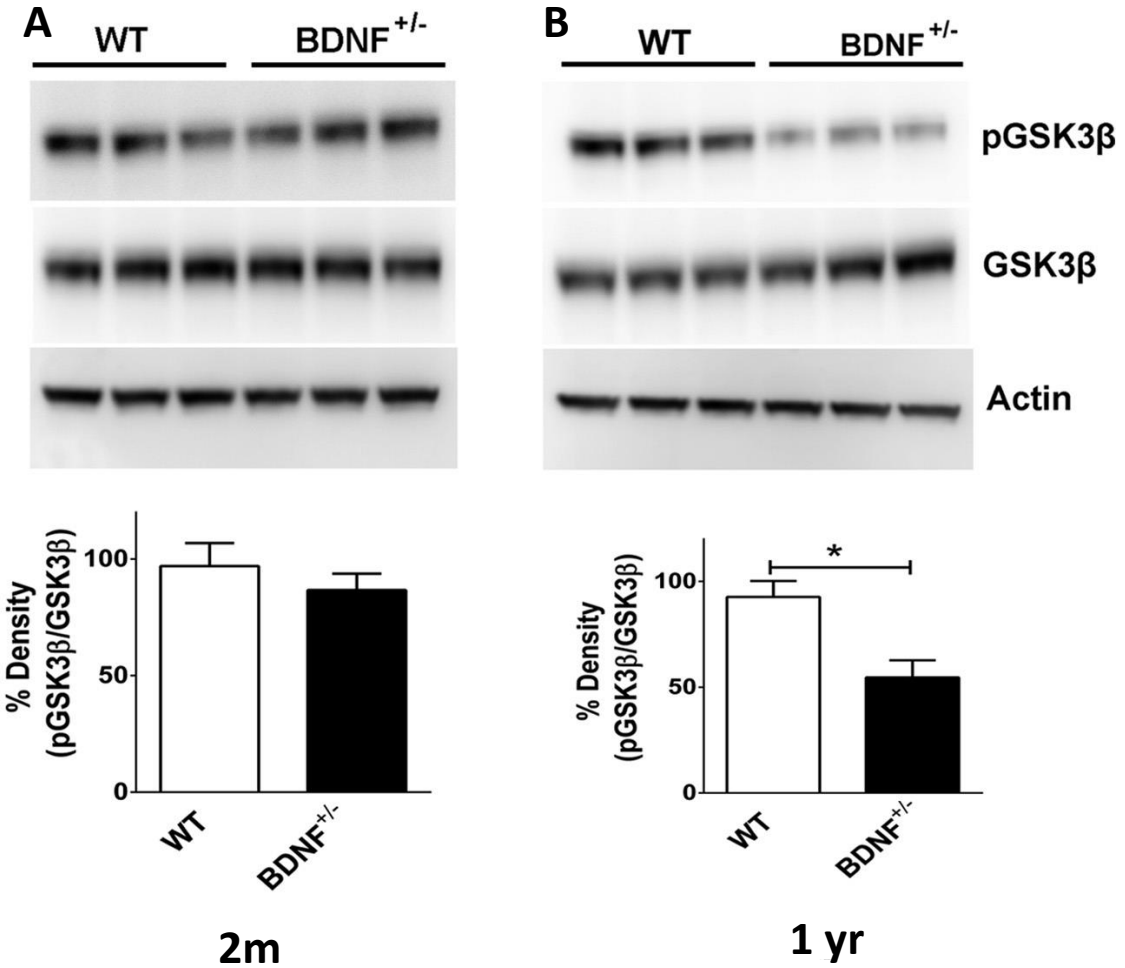

Figure 3.2. BDNF$^{+/-}$ animals depict a decrease in GSK3β phosphorylation with age. (A) Optic nerve head region was excised from the retinas of 2 month old WT and BDNF$^{+/-}$ mice and subjected to Western blotting. Changes in the phosphorylation levels of GSK3β protein (Ser9) were plotted by quantification of the band intensities. (B) Optic nerve head region was excised from the retinas of 1 year old WT and BDNF$^{+/-}$ mice and subjected to Western blotting. GSK3β was assessed for any changes in the phosphorylation levels (Ser9) by quantification of the band intensities ($^{*}p < 0.01$). Actin was used as loading control in each case.

3.3.3. TrkB agonist enhances GSK3β phosphorylation in vivo

BDNF is a high affinity ligand for the TrkB receptor. We explored the role of TrkB receptor activation in mediating GSK3β phosphorylation in vivo by chronic administration of TrkB receptor agonist to the WT and BDNF$^{+/-}$ mice (2 mg/kg) fortnightly for 2 months. At the end point, ONH tissues of the mice retina were excised, lysates subjected to Western blotting and probed for changes in the GSK3β phosphorylation profile. 7,8DHF treatment was able to significantly promote the GSK3β phosphorylation in both the WT ($p < 0.05$) and BDNF$^{+/-}$ ($p < 0.05$) mice (Figure 3.3 A and B). The results suggest that TrkB agonist action can lead to inhibition of GSK3β activity in vivo independent of the status of BDNF impairment. We did not observe any alterations in TrkB or BDNF expression in the ONH in response to 7,8DHF treatment. No changes in the total protein levels of GSK3β were observed. Actin served as the loading control.

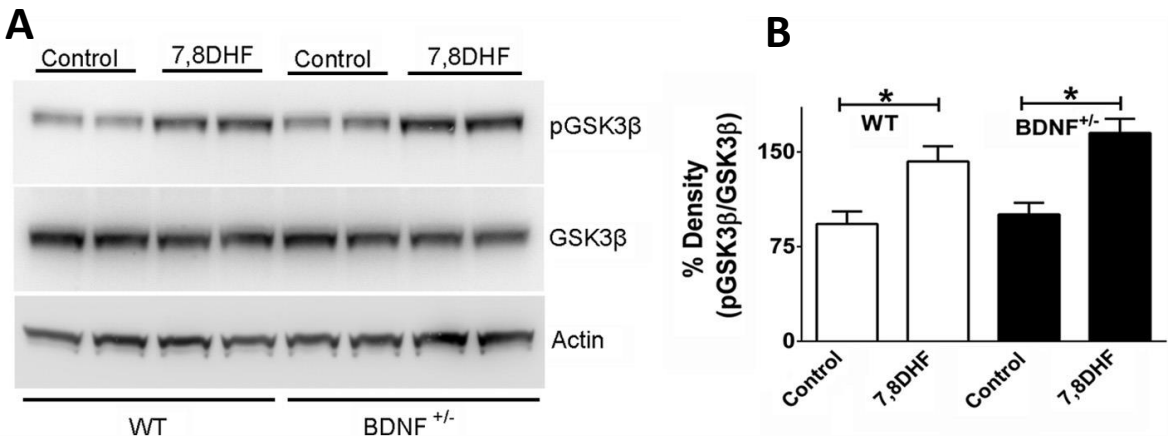

Figure 3.3. Treatment with TrkB agonist leads to enhanced GSK3β phosphorylation *in vivo*. (A) ONH tissues from WT and BDNF$^{+/-}$ mice which were treated with 7,8DHF (2 mg/kg) or vehicle control, were excised, lysed and subjected to Western blotting. Blots were probed for changes in GSK3β phosphorylation using anti-pGSK3β and GSK3β antibodies. Actin was used as loading control. (B) Band intensities were quantified and values plotted as shown ($^{*}p < 0.05$).

3.3.4. BDNF knockdown along with TrkB inhibition augments GSK3β **activation**

Our experimental paradigm suggested that BDNF knockdown can produce GSK3β dephosphorylation (Ser^{9}) without producing corresponding changes in phosphorylation of TrkB receptor (Tyr^{515}) or its downstream effectors Akt (Ser^{473}) and Erk1/2 (Thr^{202}/Tyr^{204}) (Figure 3.1). The involvement of TrkB in BDNF induced regulation of GSK3β activity was further elucidated by treating the cells with TrkB antagonist and evaluating changes in GSK3β phosphorylation as a consequence of BDNF knockdown. The levels of knockdown achieved by BDNF siRNA were consistent (Figure 3.4 A and C) with that observed in previous experiment ($p < 0.05$) (Figure 3.1). Treatment with CTX-B resulted in significant reduction in the TrkB activation in both cell types ($p < 0.02$). CTX-B treatment also produced a significant downregulation of GSK3β phosphorylation in both the RGC-5 ($p < 0.03$) and PC12 ($p < 0.05$) cells. Importantly, when the cells were subjected to treatment with CTX-B subsequent to BDNF knockdown, there was a further reduction in the GSK3β phosphorylation in both the neuronal cell types ($p < 0.05$) (Fig. 3.4a-d). CTX-B treatment did not result in any changes in the BDNF, TrkB or GSK3β expression compared to the corresponding controls. BDNF knockdown also did not produce any alterations in the TrkB or GSK3β protein expression. This experiment further suggested that BDNF may have a regulatory effect on GSK3β activity independent of its effects on TrkB and that combined BDNF knockdown and TrkB inhibition has a reinforcing outcome on the GSK3β activation.

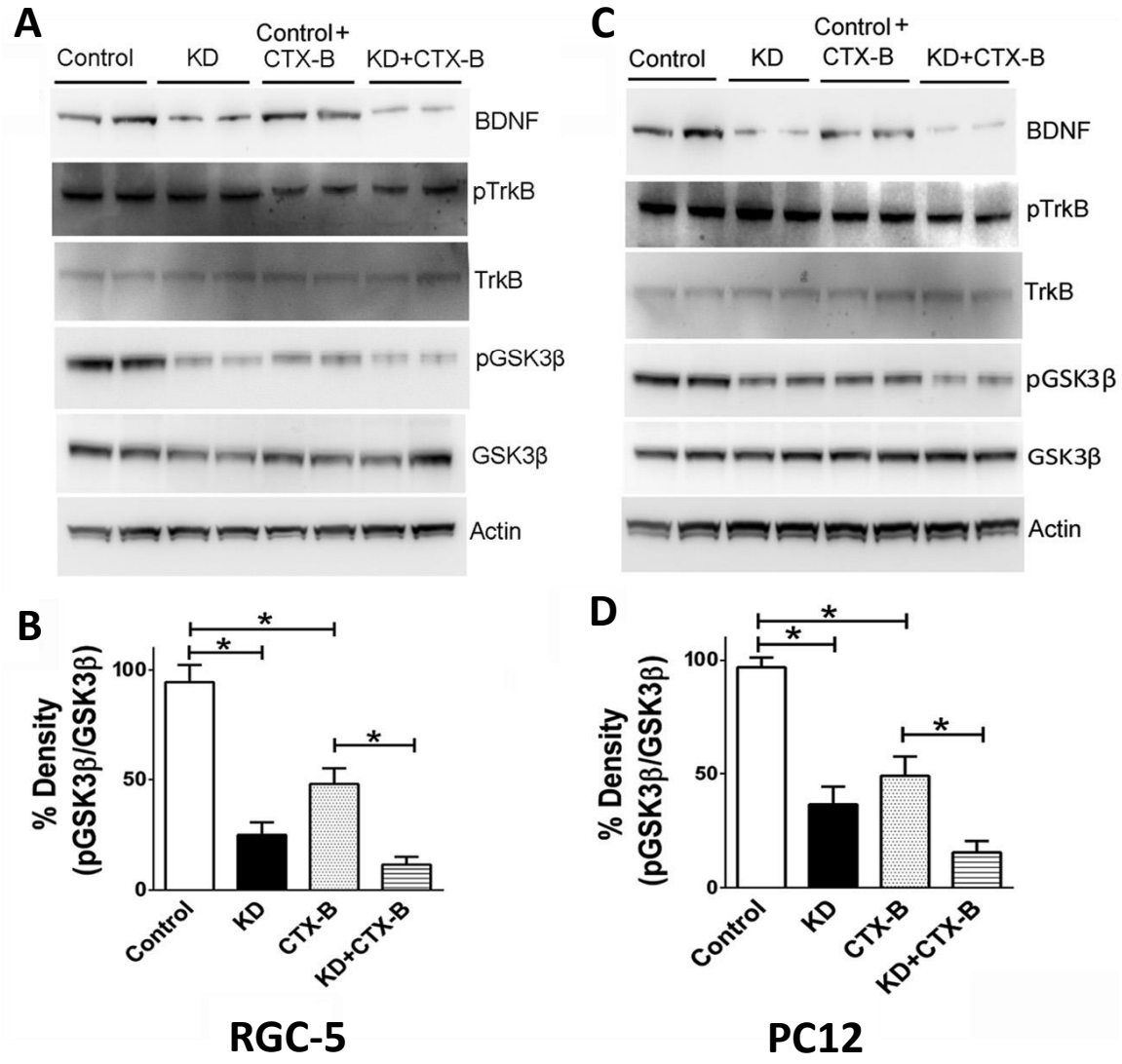

Figure 3.4. Inhibition of TrkB receptor promotes dephosphorylation of GSK3β. (A) RGC-5 cells were subjected to either BDNF knockdown, treatment with CTX-B (5 lM) or BDNF knockdown followed by incubation with CTX-B and immunoblotting performed. The blots were probed to evaluate changes in BDNF, pTrkB and pGSK3β reactivity. (B) Quantification of the pGSK3β band intensities normalised to total GSK3β protein was plotted ($^{*}p < 0.03$). (C) In a similar experiment, PC12 cells were subjected to BDNF knockdown, incubation with CTX-B (5 lM) for TrkB inhibition or BDNF knockdown followed by CTX-B treatment paradigms. Cell lysates were analysed by Western blotting using BDNF, pTrkB (Tyr515), TrkB, pGSK3β (Ser9), GSK3β and actin specific antibodies. (D) Quantification of the pGSK3β band intensities normalised to total GSK3β protein ineach case ($^{*}p < 0.05$).

3.4. Discussion

An interruption in BDNF availability and transport has been proposed to be responsible for RGC apoptosis in various models of optic nerve injury including glaucoma (Gupta et al., 2014b, Mey and Thanos, 1993, Peinado-Ramon et al., 1996). This study confirmed that BDNF/TrkB signaling plays an important role in regulation of the GSK3β activity both in the neuronal cells in culture as well as in the retina *in vivo*. GSK3β is a key protein involved in neuronal survival and has been regarded as a converging point for N-methyl-D-aspartate, BDNF and P2X7 purinergic receptor signaling (Ortega et al., 2010). We found that BDNF regulates the GSK3β activity independent of its effects *via* the high affinity receptor TrkB and downstream Akt and Erk1/2 signaling modules. A downregulation of the GSK3β (Ser^9) phosphorylation, which is generally downstream of PI3K/Akt pathway has previously been observed in animal models of glaucoma as well as in human post-mortem glaucoma tissues (Gupta et al., 2014b). Activation of GSK3β has been shown to promote the phosphorylation and degradation of β-catenin (Miller and Moon, 1996). Its activation inhibits mitochondrial pyruvate dehydrogenase and thereby promotes neuronal death (Hoshi et al., 1996). GSK3β activity has also been implicated in PI3K inhibition dependent apoptosis induced in neuronal like PC12 cells (Pap and Cooper, 1998).

Here we show that siRNA mediated knockdown of BDNF in the RGC-5 and PC12 cell lines lead to significant downregulation of the GSK3β phosphorylation. Cellular knockdown of BDNF did not produce any detectable effect on the TrkB, Akt or Erk1/2 activation or expression (Figure 3.1 and 3.4). This indicated that BDNF plays a novel role in the regulation of GSK3β activity independent of these signaling pathways. In further experimental paradigms, we treated the cells independently with a known TrkB agonist 7,8DHF (Figure 3.1) or antagonist CTX-B (Figure 3.4), which resulted in the modulation of the TrkB activity

(Gupta et al., 2013b) and also induced changes in the GSK3β phosphorylation. Results corroborate our previous observations that 7,8DHF and CTX-B treatments affect TrkB receptor phosphorylation in the RGCs (Gupta et al., 2013b). Treatment of cells with a TrkB agonist following BDNF knockdown rescued the GSK3β phosphorylation to a significant extent while combined treatment with TrkB antagonist induced a further decline in the Ser^9 phosphorylation of GSK3β. Overall, these results support the hypothesis that GSK3β Ser^9 phosphorylation is regulated through multiple molecular pathways and is common target of both the TrkB receptor mediated signaling as well as BDNF effects independent of the TrkB and downstream Akt and Erk1/2 signaling.

We sought to further correlate our findings *in vivo* by investigating alterations in GSK3β activity in the $BDNF^{+/-}$ animals. $BDNF^{+/-}$ mice are more prone to inner retinal degeneration when exposed to high intraocular pressure (IOP) (Gupta et al., 2014b). A higher vulnerability of $BDNF^{+/-}$ mice to degenerative changes in the inner retina caused by elevated IOP may be attributed to possible exacerbation of GSK3β activation subsequent to BDNF insufficiency. The regulatory effects of BDNF impairment were not evident in the younger animals but follow up revealed that GSK3β was significantly activated in the retinal tissues in aged $BDNF^{+/-}$ mice compared to their WT counterparts (Figure 3.2). These findings indicated that BDNF impairment has a progressive age-related effect on the GSK3β activation. This corresponds with our previous observations that decreased BDNF levels were observed in the ONH of aged $BDNF^{+/-}$ animals (Gupta et al., 2014b). Because BDNF/TrkB signaling has a noticeable effect on the GSK3β activity, its activation under various conditions may reflect an impaired status of BDNF/TrkB signaling. In previous studies, exogenously applied BDNF was shown to induce the dephosphorylation of collapsin response mediator protein-2 (CRMP2) and phosphorylation of GSK3β in hippocampal neurons. BDNF through its

interactions with dedicator of cytokinesis-3 (Dock3) protein was also shown to be involved in recruitment of GSK3β to cell membrane and induce its phosphorylation and inactivation (Namekata et al., 2012).

Long term chronic treatment of the animals with the TrkB agonist 7,8DHF resulted in significantly enhanced phosphorylation of the GSK3β in the ONH tissues in both the WT and $BDNF^{+/-}$ animals further confirming that this pathway regulates the GSK3β signaling (Figure 3.3). The efficacy of 7,8DHF is supported by previous observations that a single dose of 7,8DHF could produce a significant reduction in β-secretase-1 (BACE1) expression in the brain (Devi and Ohno, 2012). 7,8DHF treatment induced phosphorylation of the GSK3β highlighted the pharmacological potential of TrkB agonists to enhance the neuroprotective biochemical signaling pathways in the retina. Increased RGC survival observed with the use of highly specific TrkB agonistic antibodies both *in vitro* and *in vivo* conditions, may be attributed to its effects on the GSK3β signaling observed in this study (Hu et al., 2010, Qian et al., 2006). These findings provide a proof of concept that chronic pharmacological activation of retinal and optic nerve TrkB receptors with non-peptide agonists such as 7,8-DHF may represent an efficacious therapeutic approach to promote GSK3β inhibition, which may find therapeutic uses in several neurodegenerative diseases including glaucoma and other optic nerve disorders. In summary, this study sheds new light on the complex network of pathways through which GSK3β activity is regulated by the BDNF/TrkB signaling axis, and identifies it as a potential therapeutic target.

CHAPTER **4**

Mechanistic insights into the pharmacological targeting of TrkB receptor

Part A published as:

Nitin Chitranshi, Yogita Dheer, Veer Gupta, Roshana Vander Wall, Stuart Graham**.** Exploring the Molecular Interactions of 7,8-Dihydroxyflavone and Its Derivatives with TrkB and VEGFR2 Proteins. ***Int. J. Mol. Sci.*** 2015, 16, 21087-21108.

Abstract

7,8 dihydroxyflavone (7,8-DHF) is a TrkB receptor agonist and treatment with this flavonoid derivative brings about an enhanced TrkB phosphorylation and promotes downstream cellular signaling. Flavonoids are also known to exert an inhibitory effect on vascular endothelial growth factor receptor (VEGFR) family of tyrosine kinase receptors. VEGFR2 is one of the important receptors involved in the regulation of vasculogenesis and angiogenesis and has also been implicated to exhibit various neuroprotective roles. Its upregulation and uncontrolled activity is associated with a range of pathological conditions such as age-related macular degeneration and various proliferative disorders. In this study, we investigated molecular interactions of 7,8-DHF and its derivatives with both TrkB receptor as well as VEGFR2. Using a combination of molecular docking and computational mapping tools involving

molecular dynamics approaches we have elucidated additional residues and binding energies involved in 7,8-DHF interactions with TrkB Ig2 domain and VEGFR2. Our investigations have revealed for the first time that 7,8-DHF has dual biochemical action and its treatment may have divergent effects on the TrkB *via* its extracellular Ig2 domain and on the VEGFR2 receptor through the intracellular kinase domain. Contrary to its agonistic effects on the TrkB receptor, 7,8-DHF was found to downregulate VEGFR2 phosphorylation both in the 661W photoreceptor cells and in retinal tissue.

4A.1 Introduction

Flavonoids are a naturally occurring class of chemicals, which are abundant in fruits and vegetables and exert diverse biological effects. Recent studies have identified that a flavonoid derivative, 7,8-DHF acts as a high-affinity tropomyosin related kinase receptor B (TrkB) agonist that provokes receptor dimerization and autophosphorylation and activation of downstream signaling *in vivo* (Jang et al., 2010b). This compound has been shown to be highly neuroprotective in several disease conditions such as Alzheimer's disease (Castello et al., 2014) , Parkinson's disease (Jang et al., 2010b) , Rett syndrome (Chapleau et al., 2013) , and Huntington's disease (Jiang et al., 2013). It can readily penetrate the blood–brain barrier and is bioavailable orally (Liu et al., 2010b). We have shown that 7,8-DHF can play a role in the protection of retinal ganglion cells from excitotoxicity and oxidative stress mediated degeneration (Gupta et al., 2013b). TrkB is a receptor tyrosine kinase which is well expressed in retina and is important in the development of the inner retinal network (Gupta et al., 2013b). 7,8-DHF can activate the TrkB receptor several fold and can induce the activation of downstream pro-survival signaling cascades such as Akt and MAPK/Erk pathways. While several studies have shown that neuroprotective actions of 7,8-DHF are

mediated through the TrkB receptor, the exact comprehensive molecular basis of 7,8-DHF action is not explicitly clear. 7,8-DHF is known to bind to the TrkB extracellular domain in the region of the cysteine cluster 2 (CC2) and the leucin rich region (LRR) (Jang et al., 2010b, Liu et al., 2010b). Our study suggests that 7,8-DHF may also interact with and additionally bind to the Ig2 domain on TrkB-D5 extracellular domain. This additional binding site could mediate at least in part the 7,8-DHF binding affinity to the TrkB. Our findings are in agreement with previous observations that another TrkB ligand, brain derived neurotrophin factor (BDNF) binding to TrkB is partly mediated through the Ig2 domain in TrkB receptor which contributes to the receptor dimerization (Jiang et al., 2013). Ig2 domain possesses an N-glycosylation site which could potentially mediate the ligand receptor interaction (Haniu et al., 1995).

VEGF receptor super-family is another class of tyrosine kinase receptors which play a critical role in the retina. In addition to its involvement in neovascularization associated with several proliferative disorders, abnormal VEGF expression is implicated in several ocular disease conditions such as macular edema associated with diabetic retinopathy (Shibuya, 2006), choroidal neovascularization associated with age-related macular degeneration (Hagstrom et al., 2014), neovascular glaucoma and fibrotic complications of glaucoma filtration surgery etc (Daneshvar, 2013). VEGFR2 is well expressed in the retina and is believed to predominantly regulate the cellular actions of VEGF (Holmes et al., 2007, Nishiguchi et al., 2007). Flavonoids have been reported to play a role in the inhibition of VEGFR2 and thus suppress angiogenesis and proliferation of vascular endothelial cells (He et al., 2011, Wang et al., 2013). VEGFR2 is thus important target to study the biological effects of 7,8-DHF and other similar flavonoid compounds.

We report here for the first time a dual action of compound 7,8-DHF on TrkB and VEGFR2 receptor. Using a combination of bioinformatics and biochemical approaches we have provided critical additional insights into the molecular interactions of 7,8-DHF with both the TrkB and the VEGFR2 receptor. Structurally related derivatives of 7,8-DHF are extensively compared to determine the interactions and binding parameters with the TrkB and VEGFR2 receptors. This study also illustrates the effects of 7,8-DHF treatment on the activity of VEGFR2 in both the 661w photoreceptor cells as well as in the rat retina.

4A.2 Materials and methods

Used of animals and chemicals are described in chapter 2

4A.2.1 Selection and Preparation of Macromolecule

Crystal structure of the TrkB-D5 domain bound to Neurotrophin-4/5 (PDB id: 1HCF) (Banfield et al., 2001) and VEGFR2 protein (PDB id: 1Y6B) (Harris et al., 2005) from human was retrieved from protein databank (Berman et al., 2003) . TrkB-D5 domain contains four chains A, B, X and Y. The A & B chains constitute Neurotrophin 4 which forms homodimer. The chains X & Y form BDNF/ NT-3 protein. Only chain X of PDB id 1HCF is considered for these studies. On the other hand, VEGFR2 contain only one chain A bounded to 2-anilino-5-aryl-oxazole inhibitor. The selection of two proteins was carried out on the basis of resolution and organism derived. Resolution for TrkB-D5 and VEGFR2 was 2.70 Å and 2.10 Å respectively. The optimization of proteins was carried out using UCSF Chimera software, implying amber parameters, followed by minimization with MMTK method in 500 steps with a step size of 0.02 Å (www.cgl.ucsf.edu/chimera/). The

active site residues of the binding pocket were determined from Castp server (Dundas et al., 2006) in case of TrkB-D5 domain and bounded ligand in case of VEGFR2.

4A.2.2 Selection and Preparation of dihydroxy flavones derivatives

The three-dimensional (3D) structure of dihydroxy flavones derivatives were collected from pubchem database (Sayers et al., 2011). In total, 37 derivatives were collected including 7,8 dihydroxy flavones, 7,8 DHF (Table 4a.1) and was built using ChemDraw Ultra 8.0 (http://www.cambridgesoft.com). The energy minimization was performed using Austin Model-1 (AM1) (Chitranshi et al., 2013) until the root mean square (RMS) gradient value became smaller than 0.100 kcal/mol Å and then molecules were subjected to re-optimization via MOPAC (Prasanna et al., 2005) (Molecular Orbital Package) method until the RMS gradient attained a value lesser than 0.0001 kcal/mol Å using MOPAC.

4A.2.3 Molecular docking

The docking of the 37 dihydroxy derivatives to the binding site of TrkB-D5 and VEGFR2 was performed using the AutoDock v.4.2 (Morris et al., 2009). In order to compare the results from docking protocols, water molecules and other ligand (2-anilino-5-aryl-oxazole) were excluded for better docking score. The rotatable bonds of the ligands were set to be free and the protein was treated as a rigid body (Chitranshi et al., 2013). Crystal structure of the TrkB-D5 and VEGFR2 protein (1HCF and 1Y6B) was retrieved from protein databank (http://www.pdb.org/). Rigid docking was performed for studying protein-ligand interactions through AutoDock tools. The atom types and bond types were assigned (Bikadi and Hazai, 2009, Labute, 2009) . The polar hydrogen atoms of the enzymes were added, the non-polar hydrogen atoms were merged, Gasteiger charges were assigned and solvation

parameters were added. For all ligands, including 7,8-DHF, the non-polar hydrogen atoms were merged, and the Gasteiger charges were assigned. The auxiliary program AutoGrid generated the grid maps. The grid box dimensions were 60×60×60 Å and 52×46×56 Å around the active site and the grid spacing was set to 0.375 Å for TrkB-D5 and VEGFR2 protein respectively. The starting positions of all ligands were outside the grid box (>20 Å away from the centre of the binding pocket). Docking was performed using the empirical free energy function together with the LGA (Li and Li, 2010). The LGA protocol applied a population size of 150, while 250,000 energy evaluations were used for the 20 LGA runs. In addition, the maximum number of evaluations was set to 27,000; the mutation rate to 0.02; the crossover rate to 0.8; and the elitism rate to 1.0. Estimated inhibition constants (*Ki*) were used for determination of binding energies of different docking conformations, ranking in accordance to their binding scores (Morris et al., 2009) . The calculated properties of K_i, binding free energy, electrostatic energy, van der Waals, hydrogen bond, desolvation energy, total intermolecular and torsional energy for 37 DHF derivatives are given in Table 3 and Table 4 for TrkB-D5 and VEGFR2 respectively. Chimera (Pettersen et al., 2004), Discovery Studio (DS) Visualizer2.5 (O'Brien et al., 2005) and LigPlot$^+$ software (Laskowski and Swindells, 2011) were used for visualization and calculation of protein-ligand interactions.

4A.2.4 Molecular dynamics (MD) simulations

MD simulations were performed for the complex of 7,8-DHF-TrkB and 7,8 DHF-VEGFR2 using Desmond 3.2 software (Guo et al., 2010), incorporating OPLS_2005 force field for 10,000 ps (picoseconds) simulation time. The salvation system was maintained in a 100×100×100 Å orthorhombic box with periodic boundary conditions by adding SPC water molecules (Sun et al., 2006) for both the complexes. The whole system was neutralized by adding counter ions Na^+ and Cl^- to balance the net charge of the system. In Desmond,

equilibration of the whole system was carried out using default protocol made up of a series of restrained minimizations and MD simulations. During simulation, initial coordinates of the protein molecules were slowly relaxed without deviation. The minimized system was relaxed with NPT (number of atom, pressure, and temperature) ensemble restraining non-hydrogen solute atom for 10 ns simulation time. The full system was composed of 17346 atoms for TrkB-D5 and 36979 for VEGFR2 complex respectively. The temperature was maintained at 300 K and pressure at 1.01325 bars. Long-range electrostatic interactions were computed using particle-mesh Ewald method (Cerutti et al., 2009, Strahan et al., 1998) and van der waals (VDW) cut-off was set to 9 Å. The SHAKE algorithm was used to satisfy the hydrogen bond geometry constraints during simulation (Sun et al., 2006). The full system was simulated to analyse the stability of the 7,8-DHF-TrkB-D5 and 7,8-DHF-VEGFR2 complexes. The dynamic behavior and structural changes of the complex were analyzed by calculating the RMSD and energy fluctuation. The root mean square fluctuations (RMSF) for the backbone and side chain of each residue of TrkB-D5 and VEGFR2 protein were analyzed. The 7,8-DHF-TrkB-D5 and 7,8-DHF-VEGFR2 complexes were analyzed and monitored for the stability in hydrogen bond interactions.

4A.2.5 Cell culture and treatment regimens

Photoreceptor derived 661W cells were maintained in DMEM culture media containing 10 % fetal bovine serum and 1% penicillin/streptomycin at 37°C at 5 % CO_2. Approximately, 2.0×10^5 cells were seeded in each culture dish 6–12 h before treatment (Basavarajappa et al., 2011, Gupta et al., 2012a). Cells were treated with 7,8 DHF (100 nM) and allowed to grow for a period of 24 hours before harvesting. For *in vivo* experiments, 7,8-DHF (2mg/kg) was administered intraperitoneally to the rats. The rat retinas were harvested, flash frozen and sonicated in the lysis buffer for further analysis.

4A.2.6 Western Blot and Immunoprecipitations

661W cells and retinal tissues were lysed in lysis buffer as mentioned in chapter 2, *section 2.3.8.2*

4A.2.7 Statistical Analysis

Data were analyzed and graphed using GraphPad Prism software (GraphPad Software, CA). All values with error bars are presented as mean ± SD from given n sizes and compared by student's t test for unpaired data. The significance was set at $p<0.05$.

4A.3 Results

4A.3.1 Molecular determinants of 7,8 DHF binding with TrkB and VEGFR2

The interactions of 7,8-DHF with TrkB and VEGFR2 receptor were analysed by using a molecular docking approach. TrkB-domain5 (TrkB-D5) and VEGFR2 structures were subjected to 7,8-DHF binding *in silico* using AutoDock4.2 to reveal the best binding modes of 7,8-DHF. Our studies revealed that the binding site of TrkB-D5 comprised of Lys^{312}, Pro^{313}, Ala^{314}, Leu^{315}, Trp^{317}, Ile^{323}, Leu^{324}, Glu^{326}, Cys^{331}, Thr^{332}, Lys^{333}, Ile^{334} and Tyr^{342} residues. Hydrogen bonding with Leu^{315} and Ile^{334} indicated these to be critical residues involved in interaction with 7,8-DHF (Figure 4A 1A and B). In the case of 7,8-DHF docking with VEGFR2, the binding site was selected based on its previously reported interactions with 2-anilino-5-aryl-oxazole (AAX), a VEGFR2 inhibitor (PDB id. 1Y6B). The amino

acids Leu^{838}, Arg^{840}, Ile^{847}, Ala^{864}, Val^{865}, Lys^{866}, Glu^{883}, Ile^{913}, Val^{914}, Phe^{916}, Cys^{917}, Lys^{918}, Asn^{921}, Thr^{924}, Arg^{1030}, and Leu^{1033} were observed to comprise the binding site of VEGFR2 protein. AAX extraction and docking of 7,8-DHF showed key hydrogen bond interaction

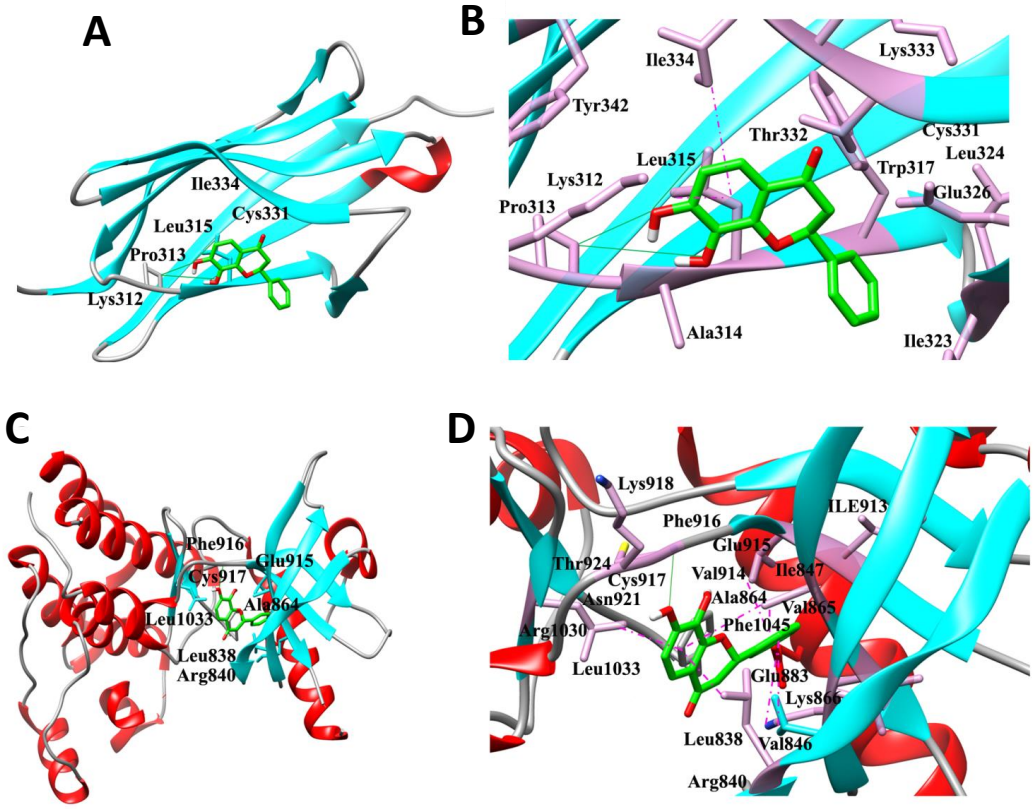

with Cys^{917} residues of VEGFR2 protein (Figure 4A 1C and D).

Figure 4A.1. Interaction and binding mode of 7,8 dihydroxyflavone (7,8-DHF) with TrkB and VEGFR2. (A) Docking of TrkB (ribbon structure) with the 7,8-DHF (wire-frame) showing critical residues involved in interaction. (B) Enlarged view of the interaction pocket within 5.5 Å around the ligand, 7,8-DHF-TrkB complex. (C) Docking of VEGFR2 (ribbon structure) with the 7,8-DHF (wire-frame) highlighting important residues involved in interaction. (D) Enlarged view of the interaction pocket within 5.5 Å around the ligand, 7,8-DHF-VEGFR2 complex. Green strong line denotes the hydrogen bonding and pink dashed line reflects pi-sigma interactions and stacking. The images were generated with the Discovery Studio 4.0 Client.

4A.3.2 Binding interactions of TrkB and VEGFR2 receptors with 7,8-DHF derivatives

In order to understand the mechanism of TrkB and VEGFR2 binding with 7,8-DHF, we evaluated various interaction parameters of several structural derivatives of 7,8-DHF (Table 4A.1). A panel of 37 dihydroxy flavonoid derivatives were selected and individually docked to both TrkB-D5 and VEGFR2 using Lamackrian Genetic Algorithms (LGA). The docking scores, predicted binding energies, inhibitory constants and other energies were calculated (Table 4A.2 and 4A.3). Among the TrkB–Flavone derivative complex clusters, the lowest binding energy complexes have been listed in Table 4A.2. A binding energy of −5.71 kcal mol^{-1} was observed to be associated with the binding of 7,8-DHF with human TrkB-D5. An inhibitory constant (K_i) of 64.79 μM was calculated for 7,8-DHF-TrkB complex binding which correlated well with its binding energy. In general, all 37 flavonoid derivatives could be divided into 2 parts: scaffold I comprises of 2, 3-dihydro-*4H*-chromen-4-one and scaffold II formed by 2-phenyl group (Table 4A.1). The study showed that 14 of dihydroxy flavonoid derivatives interacted through scaffold I (2,3-dihydro-*4H*-chromen-4-one), 7 dihydroxy flavonoid derivatives through scaffold II (phenyl ring) and the remaining 16 involved interactions through both scaffold I & scaffold II with the TrkB protein (Figure 4A 2A). Scaffold I binding and orientation was largely conserved amongst all the 7,8-DHF derivatives. Scaffold I moiety binding region comprised Lys^{312}, Ala^{314}, Glu^{326}, Thr^{332}, and Ile^{334} residues (Figure 4A 2B). In scaffold I, ring A formed a *pi*–alkyl and *pi*–sigma stacking interaction between Leu^{315} and Ile^{334} respectively while the 7,8-dihydroxy group interacted with the main chain O atom of Pro^{313} and N atom of Leu^{315} respectively through hydrogen bonding.

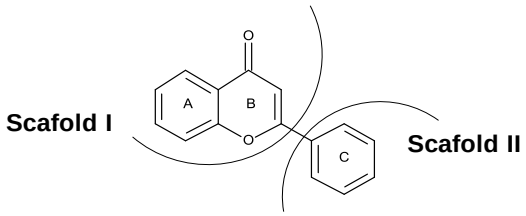

Compounds	Ring A	Ring B	Ring C	Scaffolds
7,8 DHF	7, 8 di-OH	-	-	I
C1	-	2, 3 di-OH	-	I
C2	-	-	2', 3' di-OH	II
C3	-	-	2', 5' di-OH	II
C4	5-OH	-	2'-OH	I and II
C5	-	-	2',5' di-OH, 5'-acetate	II
C6	5-OH	-	4'-OH	I and II
C7	-	3-OH	2'-OH	I and II
C8	-	3-OH	4'-OH	I and II
C9	-	-	3', 4' di-OH	II
C10	-	-	3', 4' di-OH, 4'-glucoside	II
C11	5 OH, 6, 7 di-methoxy	3-methoxy	3'-OH, 4'-methoxy	I and II
C12	3, 5 di-OH	-	-	I
C13	-	-	3', 5' di-OH	II
C14	3, 6 di-OH	-	-	I
C15	3, 7 di-OH	-	-	I
C16	6-OH	-	4'-OH	I and II
C17	7-OH	-	4'-OH	I and II
C18	5-OH	-	3'-OH	I and II
C19	5-OH, 7-methoxy	-	4'-OH, 3'-methoxy	I and II
C20	5, 6 di-OH	-	-	I
C21	5, 7 di-OH	-	4'-methoxy	I and II
C22	5, 7 di-OH	-	-	I
C23	5, 7 di-OH	-	7-benzoate	I and II
C24	5, 7 di-OH, 7 β-monoglucoside	- -	- -	I
C25	5, 8 di-OH	-	-	I
C26	6, 7 di-OH	-	-	I
C27	6, 8 di-Cl	-	3', 5' di-OH	I and II
C28	5-OH, 6-methoxy, 7 O-glucoside	-	4'-OH	I and II
C29	7-OH	-	2'-OH	I and II
C30	7-OH, 7-glucoside	-	2'-OH	I and II
C31	7-OH	-	3'-OH	I and II
C32	7-OH, 7-glucoside	-	4'-OH	I and II
C33	7-OH, 7-rutinoside	-	4'-OH	I and II

C34	5, 6-OH, 7-D-glucuronic acid	-	-	I
C35	8-OH	-	2'-OH	I and II
C36	7-OH, 8-β-D-glucopyranosyl	-	4'-OH	I and II

Table 4A.1 Structural parameters of thirty seven di-hydroxy flavonoid derivatives including 7,8-DHF.

C.Name	*BE*^{e} *(kcal/mol)*	*Ki* *(µM)*	*IME*^{e} *(kcal/mol)*	V_{dw}-H_b-D_s *(kcal/mol)*	*E*^{e} *(kcal/mol)*	*IE*^{e} *(kcal/mol)*	*TFE*^{e} *(kcal/mol)*
7, 8 DHF	**-5.71**	**64.79**	**-5.84**	**-5.6**	**-0.24**	**-0.69**	**0.82**
C1	-5.94	44.35	-5.97	-5.91	-0.06	-0.8	0.82
C2	-5.91	46.34	-6.57	-6.12	-0.45	-0.16	0.82
C3	-5.28	133.89	-5.54	-5.34	-0.2	-0.57	0.82
C4	-6.13	32.06	-6.28	-5.94	-0.34	-0.67	0.82
C5	-5.96	43.12	-6.84	-6.41	-0.43	-0.21	1.10
C6	-5.65	71.59	-5.77	-5.63	-0.13	-0.71	0.82
C7	-5.63	75.12	-6.09	-5.71	-0.38	-0.36	0.82
C8	-5.52	89.37	-5.95	-5.85	-0.09	-0.4	0.82
C9	-6.02	38.62	-6.7	-6.51	-0.19	-0.14	0.82
C10	-7.10	6.21	-6.33	-6.08	-0.25	-3.24	2.47
C11	-7.42	3.62	-7.67	-7.49	-0.17	-1.68	1.92
C12	-6.43	19.41	-6.36	-6.01	-0.35	-0.89	0.82
C13	-5.18	158.66	-5.85	-5.6	-0.25	-0.15	0.82
C14	-5.24	143.46	-5.51	-5.37	-0.14	-0.56	0.82
C15	-5.36	118.3	-5.86	-5.58	-0.28	-0.32	0.82
C16	-5.28	135.23	-5.94	-5.76	-0.18	-0.16	0.82
C17	-5.49	94.66	-6.14	-5.97	-0.18	-0.17	0.82
C18	-5.81	55.47	-5.95	-5.67	-0.28	-0.68	0.82
C19	-6.17	30.1	-6.37	-5.99	-0.38	-1.17	1.37
C20	-6.00	39.92	-5.81	-5.52	-0.29	-1.01	0.82
C21	-5.97	42.38	-6.30	-6.11	-0.19	-0.76	1.10
C22	-5.46	98.9	-5.56	-5.36	-0.20	-0.73	0.82
C23	-6.47	18.12	-6.68	-6.51	-0.17	-1.16	1.37
C24	-6.85	9.56	-7.02	-6.88	-0.13	-2.3	2.47
C25	-6.08	35.18	-5.82	-5.78	-0.04	-1.08	0.82
C26	-6.11	33.05	-6.31	-6.07	-0.24	-0.62	0.82
C27	-6.29	24.48	-6.92	-6.72	-0.2	-0.19	0.82
C28	-7.90	1.61	-8.31	-8.05	-0.27	-2.61	3.02
C29	-5.41	108.5	-6.05	-5.76	-0.29	-0.18	0.82
C30	-6.53	16.21	-7.06	-6.84	-0.22	-1.94	2.47
C31	-5.62	76.09	-6.29	-5.91	-0.38	-0.15	0.82
C32	-5.89	47.88	-6.25	-5.99	-0.26	-2.11	2.47
C33	-6.16	4.82	-4.05	-3.86	-0.19	-2.68	3.57

C34	-7.50	3.18	-6.97	-6.38	-0.6	-3.27	2.74
C35	-5.64	72.83	-5.68	-5.26	-0.42	-0.79	0.82
C36	-6.77	10.99	-7.78	-7.15	-0.63	-1.45	2.47

Table 4A.2 7,8-DHF and 36 di-hydroxy flavonoid derivatives with corresponding energies obtained from docking with TrkB-D5 using AutoDock program. BE^e Estimated binding free energy in kcal mol^{-1}; *Ki* Inhibitory constant in micro-molar; IME^e Final Intermolecular Energy in kcal mol^{-1}; V_{dw}–H_b–D_s Van der waals-hydrogen bond-desolvation energy component of binding free energy in kcal mol^{-1}; E^e Electrostatic energy in kcal mol^{-1}; IE^e Final total internal energy in kcal mol^{-1}; TFE^e Torsional free energy in kcal mol^{-1}

Further, we investigated the interactions of these flavones derivatives with VEGFR2. The study indicated interactions of 18 dihydroxy flavonoids by scaffold I, 7 dihydroxy flavonoids through scaffold II and remaining 12 dihydroxy flavonoid derivatives through both the scaffold I & scaffold II with VEGFR2 (Table 4A.3). The binding pocket of VEGFR2 comprised of Val^{846}, Ala^{864}, Val^{865}, Lys^{866}, Glu^{883}, Val^{914}, Glu^{915}, Phe^{916}, and Leu^{1033} residues (Figure 4A 3A and B). In scaffold I, ring A formed a *pi*–alkyl and *pi*–sigma stacking interaction with Ala^{864} and Leu^{1033} respectively. The scaffold II also showed 3 *pi*–alkyl interactions with Val^{846}, Ala^{864}, Lys^{866} and one *pi*–sigma stacking interaction with Val^{914}. The 7,8-dihydroxy group interacted with the carboxyl O and amino N atom of Cys^{917} and amino N atom of Leu^{315} through hydrogen bonding. Scaffold I binding and orientation was approximately conserved amongst all the 7,8-DHF derivatives (Figure 4A 2 and 3). With respect to 7,8-DHF interaction, a binding score of -7.76 kcal mol^{-1} and K_i of 2.04 μM were observed when compared to that calculated for AAX, a known VEGFR2 inhibitor with binding score of -9.68 kcal mol^{-1} and K_i 0.08 μM (Table 4A.3). Potential carcinogenicity and mutagenicity of various dihydroxyflavone derivatives in cells and rodents was predicted using ToxPredict tool (Hardy et al., 2010) (Table 4A.4). ToxPredict studies demonstrated 7,8-DHF to be a non-carcinogenic and non-mutagenic flavonoid with minimal toxicity potential compared to all other derivatives.

C.Name	*BE*[e] *(kcal/mol)*	*Ki* *(μM)*	*IME*[e] *(kcal/mol)*	V_{dw}-H_b-D_s *(kcal/mol)*	*E*[e] *(kcal/mol)*	*IE*[e] *(kcal/mol)*	*TFE*[e] *(kcal/mol)*
AAX	**-9.68**	**0.08**	**-10.43**	**-10.42**	**-0.01**	**-1.44**	**+2.20**
7, 8 DHF	**-7.76**	**2.04**	**-8.09**	**-7.97**	**-0.12**	**-0.50**	**+0.82**
C1	-6.69	12.49	-6.49	-6.49	+0.00	-1.03	+0.82
C2	-7.01	7.29	-7.28	-7.18	-0.10	-0.56	+0.82
C3	-6.66	13.11	-6.91	-6.86	-0.05	-0.57	+0.82
C4	-6.97	7.72	-7.17	-7.09	-0.08	-0.62	+0.82
C5	-7.44	3.51	-8.27	-8.08	-0.19	-0.27	+1.10
C6	-7.27	4.66	-7.39	-7.23	-0.15	-0.71	+0.82
C7	-7.08	6.44	-7.09	-6.97	-0.11	-0.82	+0.82
C8	-7.19	5.41	-7.52	-7.25	-0.27	-0.49	+0.82
C9	-7.07	6.52	-7.76	-7.59	-0.17	-0.14	+0.82
C10	-9.41	0.13	-9.64	-9.20	-0.44	-2.24	+2.47
C11	-6.33	22.82	-6.69	-6.49	-0.20	-1.56	+1.92
C12	-7.41	3.71	-7.16	-7.13	-0.03	-1.07	+0.82
C13	-7.25	4.84	-7.91	-7.58	-0.33	-0.17	+0.82
C14	-7.31	4.41	-7.61	-7.48	-0.14	-0.52	+0.82
C15	-7.30	4.46	-7.69	-7.56	-0.13	-0.44	+0.82
C16	-7.27	4.69	-7.93	-7.68	-0.25	-0.17	+0.82
C17	-7.54	2.99	-8.19	-7.89	-0.30	-0.17	+0.82
C18	-7.08	6.48	-7.19	-6.88	-0.31	-0.71	+0.82
C19	-7.73	2.16	-7.92	-7.79	-0.13	-1.18	+1.37
C20	-7.75	2.10	-7.87	-7.73	-0.14	-0.70	+0.82
C21	-7.23	5.03	-7.56	-7.48	-0.08	-0.77	+1.10
C22	-7.53	3.02	-7.61	-7.55	-0.06	-0.74	+0.82
C23	-8.34	0.77	-8.61	-8.56	-0.05	-1.10	+1.37
C24	-8.17	1.03	-8.47	-8.23	-0.24	-2.17	+2.47
C25	-7.17	5.54	-7.04	-6.99	-0.05	-0.95	+0.82
C26	-7.60	2.68	-7.77	-7.58	-0.19	-0.65	+0.82
C27	-7.50	3.17	-8.14	-7.85	-0.29	-0.19	+0.82
C28	-8.76	0.38	-9.01	-8.76	-0.25	-2.77	+3.02
C29	-6.93	8.28	-7.16	-7.12	-0.04	-0.59	+0.82
C30	-7.96	1.47	-8.23	-7.81	-0.42	-2.20	+2.47
C31	-7.46	3.40	-8.11	-7.65	-0.47	-0.17	+0.82
C32	-8.43	0.66	-9.03	-8.68	-0.36	-1.86	+2.47
C33	-8.14	1.09	-7.83	-7.65	-0.18	-3.88	+3.57
C34	-9.22	0.174	-9.45	-8.47	-0.98	-2.52	+2.74
C35	-6.73	11.57	-6.60	-6.56	-0.04	-0.96	+0.82
C36	-8.29	0.84	-8.21	-8.07	-0.14	-2.55	+2.47

Table 4A.3. 7,8-DHF and 36 di-hydroxy flavonoid derivatives with corresponding energies obtained from redocking validation followed by docking with VEGFR2 protein using AutoDock program. *BE*[e] Estimated

binding free energy in kcal mol^{-1}; *Ki* Inhibitory constant in micro-molar; IME^e Final Intermolecular Energy in kcal mol^{-1}; V_{dw}–H_b–D_s Van der waals-hydrogen bond-desolvation energy component of binding free energy in kcal mol^{-1}; E^e Electrostatic energy in kcal mol^{-1}; IE^e Final total internal energy in kcal mol^{-1}; TFE^e Torsional free energy in kcal mol^{-1}

S.No	C.No	Pubchem CID	M.W	Carcinogenic Potency DBS Mouse	Carcinogenic Potency DBS MultiCellCall	Carcinogenic Potency DBS Mutagenicity	Carcinogenic Potency DBS Rat	Carcinogenic Potency DBS SingleCellCall	Eye irritation
1	7,8-DHF	CID_44335549	256.25	non-carcinogen	non-carcinogen	non-mutagenic	non-carcinogen	non-carcinogen	No
2	C1	CID_17874507	256.25	non-carcinogen	non-carcinogen	non-mutagenic	non-carcinogen	non-carcinogen	No
3	C2	CID_676289	254.24	non-carcinogen	carcinogen	mutagenic	carcinogen	carcinogen	No
4	C3	CID_44257593	254.24	non-carcinogen	carcinogen	mutagenic	carcinogen	carcinogen	No
5	C4	CID_688660	254.24	non-carcinogen	carcinogen	mutagenic	non carcinogen	carcinogen	No
6	C5	CID_44257596	296.27	non-carcinogen	carcinogen	mutagenic	non carcinogen	carcinogen	No
7	C6	CID_165521	254.24	non-carcinogen	carcinogen	mutagenic	non carcinogen	carcinogen	No
8	C7	CID_455313	254.24	non-carcinogen	carcinogen	mutagenic	carcinogen	carcinogen	No
9	C8	CID_688715	254.24	non-carcinogen	carcinogen	mutagenic	carcinogen	carcinogen	No
10	C9	CID_145726	254.24	non-carcinogen	carcinogen	mutagenic	carcinogen	carcinogen	No
11	C10	CID_44257601	416.38	non-carcinogen	carcinogen	mutagenic	non-carcinogen	carcinogen	Yes
12	C11	CID_5315263	374.34	non-carcinogen	carcinogen	mutagenic	carcinogen	carcinogen	No
13	C12	CID_5393151	254.24	non-carcinogen	carcinogen	mutagenic	non-carcinogen	carcinogen	No
14	C13	CID_45933941	254.24	non-carcinogen	carcinogen	mutagenic	carcinogen	carcinogen	No
15	C14	CID_688659	254.24	non-carcinogen	carcinogen	mutagenic	non-carcinogen	carcinogen	No
16	C15	CID_5393152	254.24	non-carcinogen	carcinogen	mutagenic	non-carcinogen	carcinogen	No
17	C16	CID_182362	254.24	non-carcinogen	carcinogen	mutagenic	non-carcinogen	carcinogen	No
18	C17	CID_5282073	254.24	non-carcinogen	carcinogen	mutagenic	carcinogen	carcinogen	No
19	C18	CID_676030	254.24	non-carcinogen	carcinogen	mutagenic	non-carcinogen	carcinogen	No
20	C19	CID_5464381	314.29	non-carcinogen	carcinogen	mutagenic	non-carcinogen	carcinogen	No
21	C20	CID_14349487	254.24	non-carcinogen	carcinogen	mutagenic	non-carcinogen	carcinogen	No

22	C21	CID_5280442	284.26	non-carcinogen	carcinogen	mutagenic	non-carcinogen	carcinogen	No
23	C22	CID_5281607	254.24	non-carcinogen	carcinogen	mutagenic	non-carcinogen	carcinogen	No
24	C23	CID_5575368	358.34	non-carcinogen	non-carcinogen	non-mutagenic	non-carcinogen	non-carcinogen	No
25	C24	CID_5490092	416.38	non-carcinogen	carcinogen	mutagenic	carcinogen	carcinogen	Yes
26	C25	CID_11055	254.24	non-carcinogen	carcinogen	mutagenic	non-carcinogen	carcinogen	No
27	C26	CID_5353357	254.24	non-carcinogen	carcinogen	mutagenic	non-carcinogen	carcinogen	No
28	C27	CID_57368355	322.16	non-carcinogen	carcinogen	mutagenic	carcinogen	carcinogen	Yes
29	C28	CID_5318083	462.4	non-carcinogen	carcinogen	mutagenic	non-carcinogen	carcinogen	Yes
30	C29	CID_5391149	254.24	non-carcinogen	carcinogen	mutagenic	carcinogen	carcinogen	No
31	C30	CID_44257565	416.38	non-carcinogen	carcinogen	mutagenic	non-carcinogen	carcinogen	Yes
32	C31	CID_5391140	254.24	non-carcinogen	carcinogen	mutagenic	carcinogen	carcinogen	No
33	C32	CID_44257571	416.38	non-carcinogen	carcinogen	mutagenic	non-carcinogen	carcinogen	Yes
34	C33	CID_44257573	562.52	non-carcinogen	carcinogen	mutagenic	non-carcinogen	carcinogen	Yes
35	C34	CID_64982	446.36	non-carcinogen	non-carcinogen	mutagenic	non-carcinogen	carcinogen	Yes
36	C35	CID_14034267	254.24	non-carcinogen	carcinogen	mutagenic	non-carcinogen	carcinogen	No
37	C36	CID_44257569	416.38	non-carcinogen	non-carcinogen	non-mutagenic	non-carcinogen	non-carcinogen	Yes

Table 4A.4. Toxicity prediction of 37 di-hydroxy flavonoid derivatives including 7,8DHF using ToxPredict program.

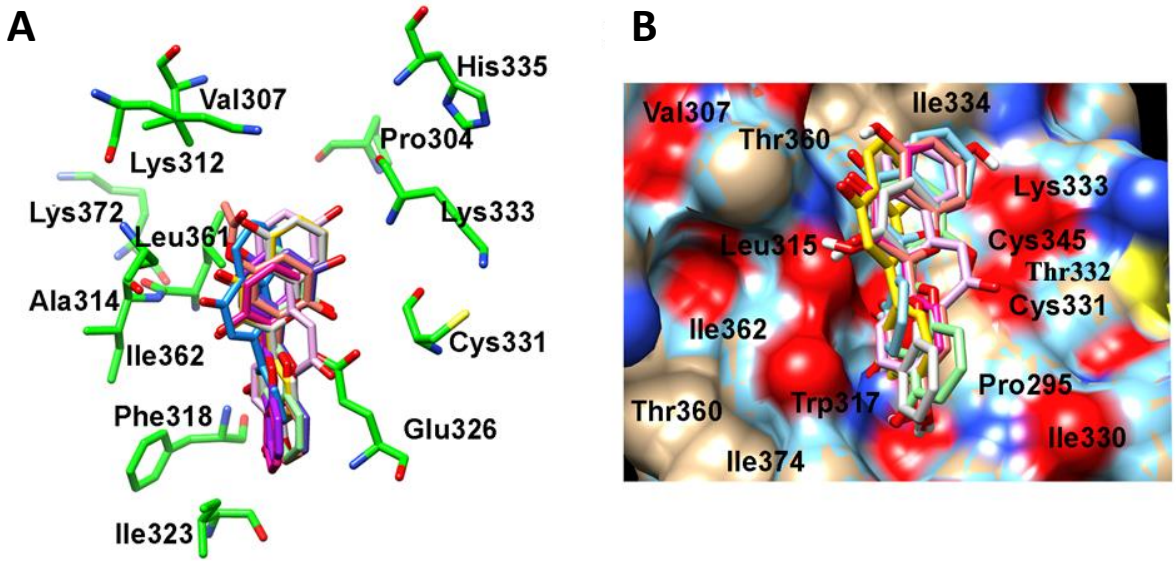

Figure 4A.2. Molecular modelling showing interaction of 7,8-DHF derivatives with the TrkB. (A) Amino acid interactions with the 7,8-DHF derivatives (B) Space filled model to depict the binding pocket of 7,8-DHF derivatives in TrkB domain.

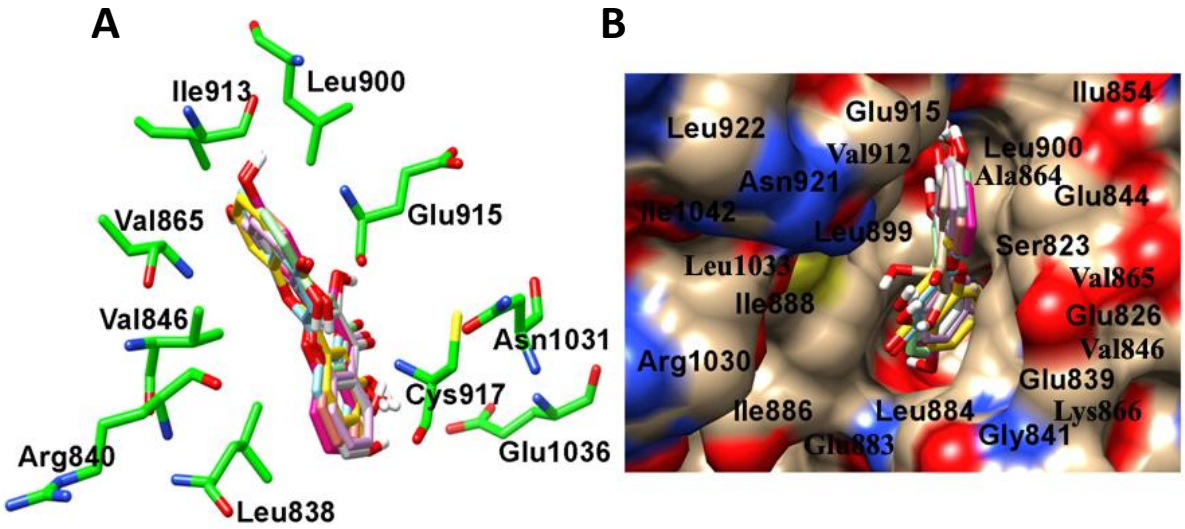

Figure 4A.3. Molecular modelling showing interaction of 7,8-DHF derivatives with the VEGFR2. (A) Amino acid interactions of VEGFR2 binding site with the 7,8-DHF derivatives (B) Space filled model to depict the binding pocket of 7,8-DHF derivatives in VEGFR2.

4A.3.3 Molecular dynamics of 7,8-DHF-TrkB and 7,8-DHF-VEGFR2 complex

MD simulation provides information about the internal motions of the receptor–ligand complex treated in a flexible condition in the solvent with respect to time. In order to confirm the binding mode of 7,8-DHF-TrkB-D5 and 7,8-DHF-VEGFR2 docking complexes, MD simulation was performed using the Desmond program 3.2 (Shan et al., 2011) . MD simulations were carried out in an *in-silico* environment mimicking physiological condition of pH and molarity. The dynamic properties of 7,8-DHF-TrkB-D5 and 7,8-DHF-VEGFR2 docking complexes were analyzed using trajectory data obtained from 10 ns MD simulations indicating effective receptor–ligand binding under above conditions. The trajectory of 7,8-DHF with TrkB-D5 and VEGFR2 docking complexes were plotted for root mean square fluctuation (RMSF) (Figure 4A 4A and B), energy (Figure 4A 5A and B) and root mean square deviation (RMSD) (Figures 4A 6 and 7).

RMSD plot for backbone and heavy atoms (Figures 4A 6 and 7) indicated a subtle rearrangement in the initial conformation of the docking complex that eventually stabilized following molecular simulation. The overall range of RMSD of 7,8-DHF-TrkB-D5 and 7,8-DHF-VEGFR2 complex was 0.3-1.7 Å and 0.2–2.3 Å for backbone atoms (Figure 4A 6A and B) respectively. For heavy atoms the average RMSD for the 7,8-DHF-TrkB-D5 and 7,8-DHF-VEGFR2 complex was observed to be 0.2-2.8 Å and 0.2–2.5 Å respectively (Figure 4A 7A and B). The RMSF of the residues were approximated by averaging all the atoms of the given protein. RMSF analysis indicated that all backbone (blue) and most of the side chain residues (red) were within the acceptable limit of 2.5 Å. Fluctuations for some of the side-chain residues for TrkB complex exceeded 2.5 Å but was below 3.0 Å (Figure 4A 4A). Similar pattern of RMSF was evident with respect to VEGFR2, where most of the backbone (blue) and side chain (red) residues were within the limit of 2.5 Å (Figure 4A 4B).

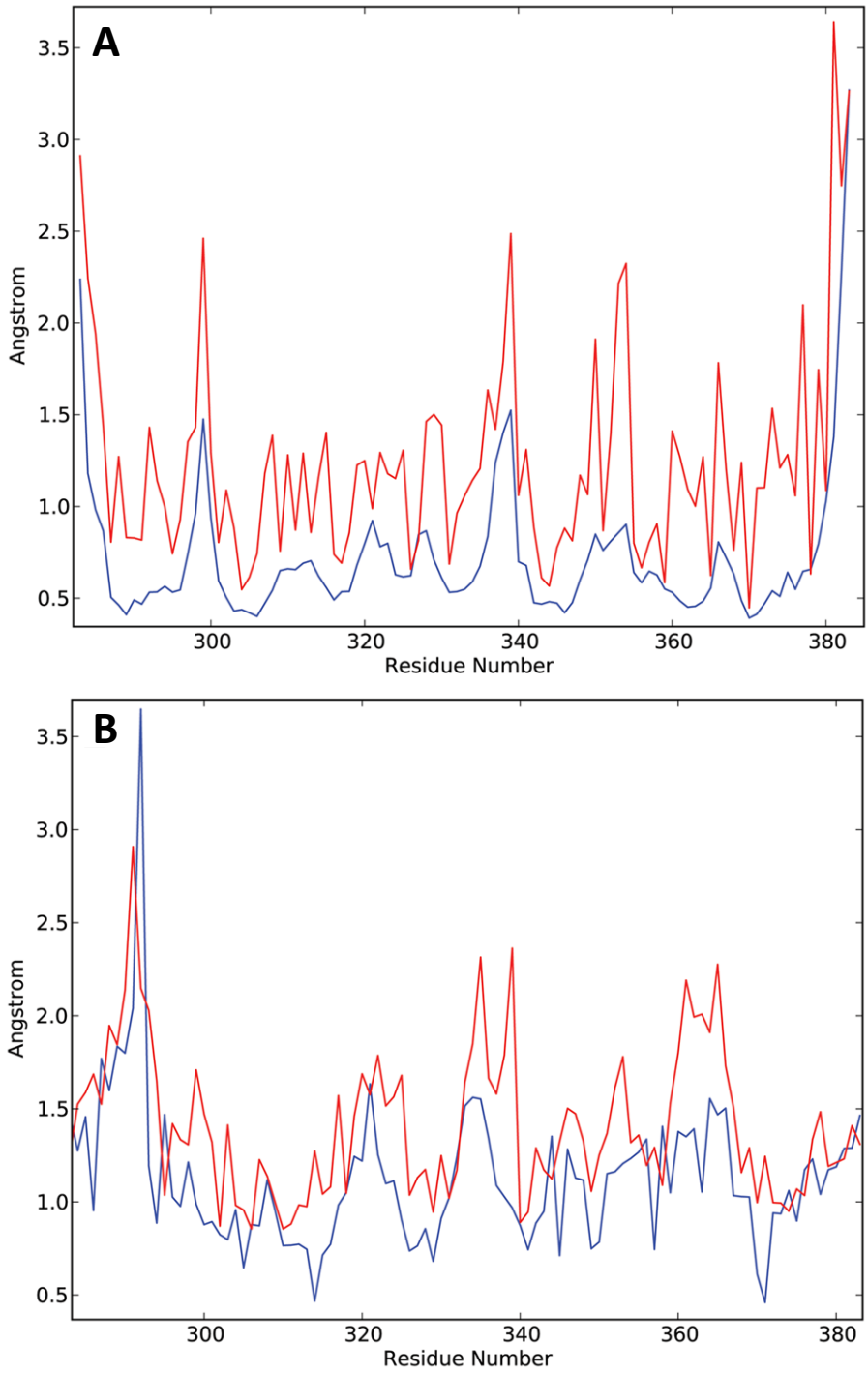

Figure 4A.4. RMSF of backbone and side chain during 10 ns MD simulations. Blue color indicates backbone and red color indicates side chains (A) 7,8DHF-TrkB complex (B) 7,8DHF-VEGFR2 complex

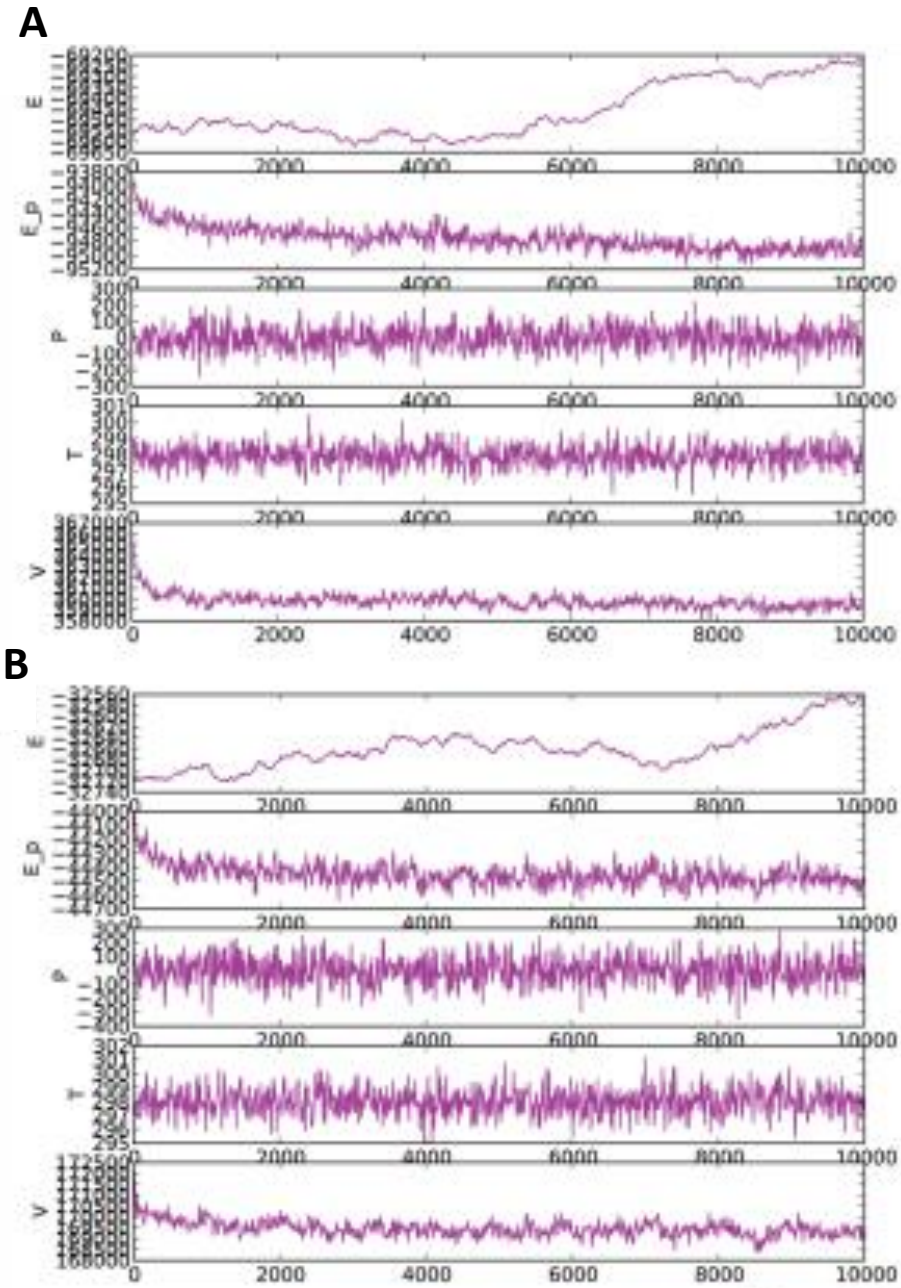

Figure 4A.5. Energy peak during 10 ns MD simulation (A) 7,8DHF-TrkB complex. (B) 7,8DHF-VEGFR2 complex.

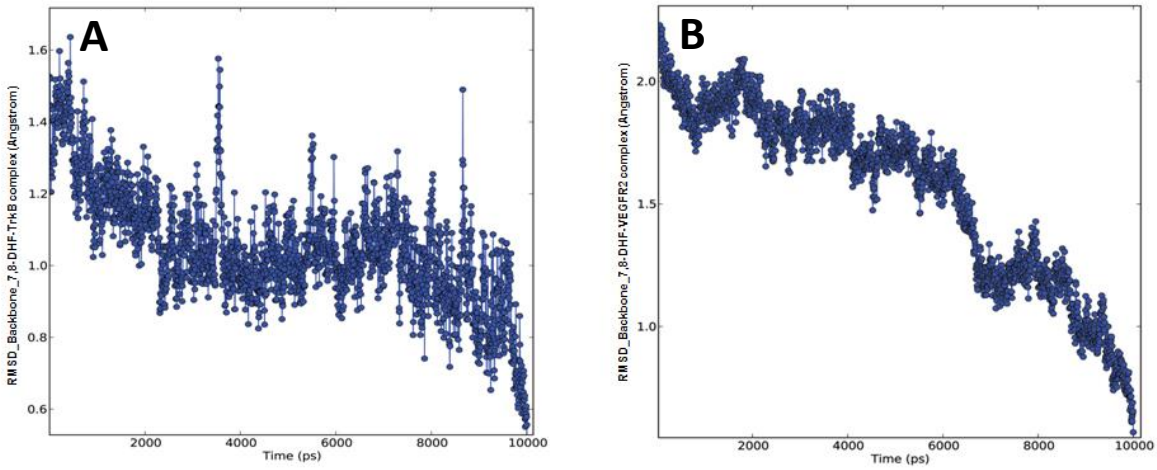

Figure 4A.6. The MD simulation Time vs. RMSD of the backbone atoms (A) 7,8-DHF-TrkB protein complex (B) 7,8-DHF-VEGFR2 protein complex.

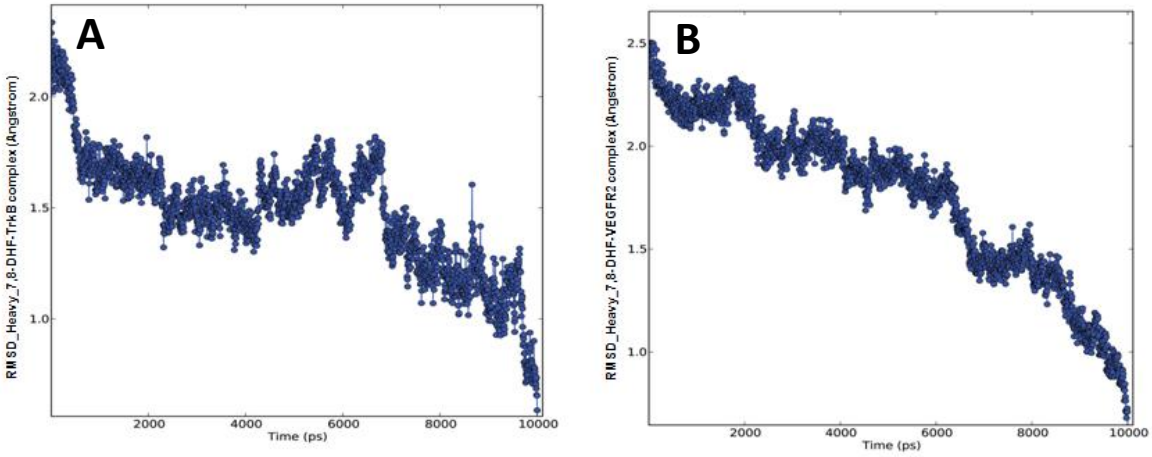

Figure 4A.7. MD Simulation Time vs. RMSD of the heavy atoms (A) 7,8-DHF-TrkB protein complex (B) 7,8-DHF-VEGFR2 protein complex.

The lower atomic fluctuation for active site residues reflected small conformational changes. The energy, RMSD and RMSF plots illustrated that the 7,8-DHF-TrkB-D5 and 7,8-DHF-VEGFR2 docking complex were observed to be stable throughout MD simulation. 7,8-DHF-TrkB-D5 and 7,8-DHF-VEGFR2 molecular interactions were also monitored to assess the structural flexibility of the docked complex (Figure 4A 8). Molecular analysis of 7,8-DHF complex with TrkB-D5 showed 18 (O) and 20 (O) atoms of 7,8-DHF to be involved in hydrogen bonding with 250 (N) of Leu^{315} and 236 chiral (C) atom of Lys^{312} respectively (Figure 4A 8A). The trajectory analysis of MD simulation further showed hydrogen bond formation between atom 19 H11 of 7,8-DHF and atom 241 (O) of Pro^{313} as well as atom 21 (H) of 7,8-DHF and atom 241 (O) Pro^{313}. In addition *pi*-sigma interaction was also observed between the B ring of 7,8-DHF and atom 265 (C) of Leu^{315}. Hydrogen bonding and *pi*-sigma bonding with the residues Pro^{313} and Leu^{315} in MD simulation may indicate a potential conformational change in TrkB (Figures 4A 1B and 8A). In VEGFR2 complex simulation, atom 20 (O) of 7,8-DHF was observed to form hydrogen bonds with atom 743 (N) of Cys^{917} and atom 746 (O) of Cys^{917} (Figure 4A 8B). The trajectory analysis of MD simulation showed hydrogen bonding between atom 19 H11 of 7,8-DHF and atom 726 (O) of Glu^{915} as well as atom 18 (O) of 7,8-DHF and atom 733 (H) Phe^{916} which was additional to that of Cys^{917} hydrogen bond interaction observed in molecular docking analysis (Figures 4A 1D and 8B).

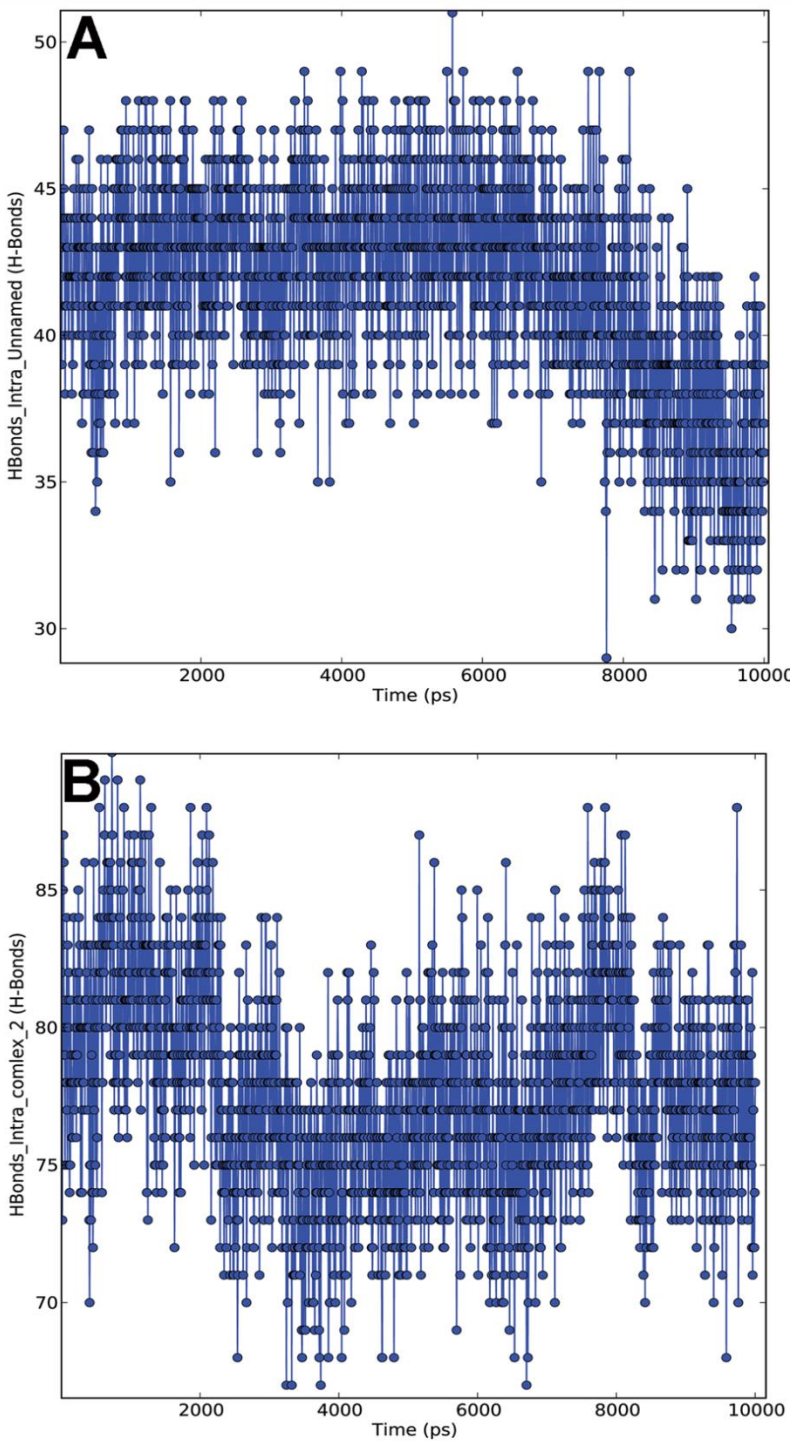

Figure 4A.8 H-bonds formed during total course of 10,000 ps MD simulations (A) 7,8DHF-TrkB complex (B) 7,8DHF-VEGFR2 docking complex.

4A.3.4 7,8-DHF treatment leads to loss of VEGFR2 activity

7,8-DHF is known to bring about substantial activation of the TrkB receptor both *in vitro* and *in vivo* (Zeng et al., 2012) . Here we investigated whether 7,8-DHF has any effect on the activation of the VEGFR2 receptor. The VEGFR2 was immunoprecipitated from the 661w cell lysates and the blots probed with the pY100 antibody to detect the changes in phosphorylation status of the VEGFR2 receptor. Contrary to that, observed in the case of 7,8-DHF effects on TrkB receptor, we observed a dephosphorylation of the VEGFR2 in the cells which were pre-treated with the flavonoid derivative. Quantification of the band intensities showed a significant loss of the VEGFR2 activity ($P<0.04$) (Figure 4A 9A and B). The effects of the drug on VEGFR2 *in vivo* were investigated by immunoprecipitating VEGFR2 from the rat retinal lysates. Samples from animals treated with 7,8-DHF demonstrated a loss of VEGFR2 phosphorylation using the pY100 antibodies compared to the control retinal samples ($p<0.05$) (Figure 4A 9C and D). Non-immune IgGs were used as control for immunoprecipitations. The band intensities were normalized to the total amount of VEGFR2 immunoprecipitated in each case to ensure that phosphorylation changes are not attributed to differences in amounts of total immunoprecipitated protein.

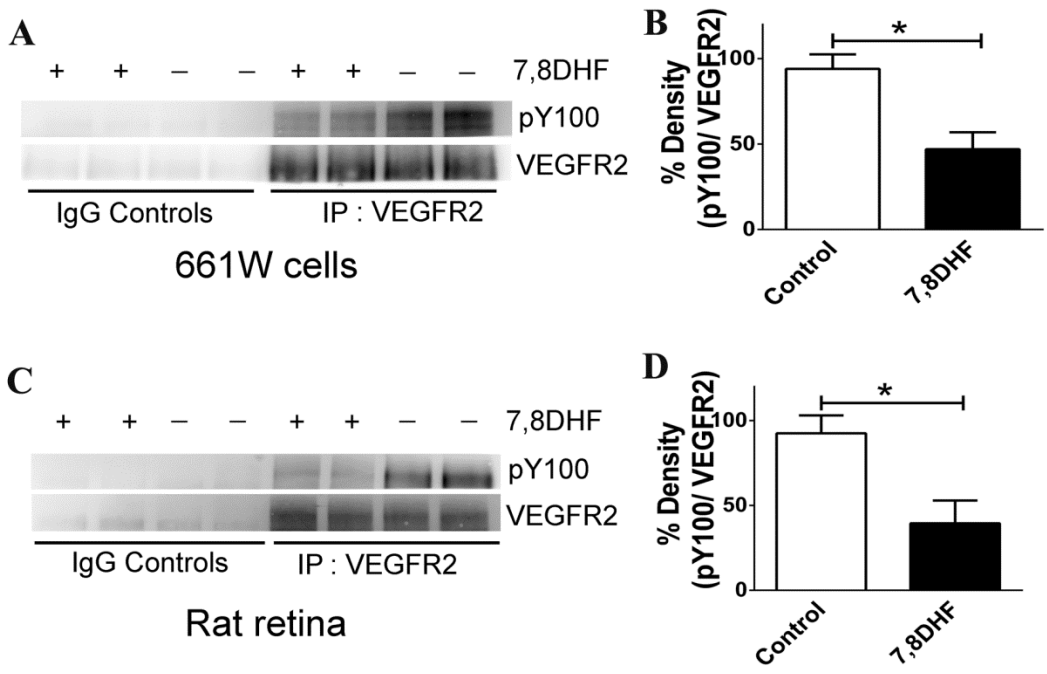

Figure 4A.9. 7,8-DHF exerts an inhibitory effect on the VEGFR2. (A) Immunoprecipitation of VEGFR2 was carried out from 661W cell lysates followed by probing with the VEGFR2 and PY100 antibodies. (B) Quantification illustrated a decline in VEGFR2 phosphorylation upon treatment with 7,8-DHF ($p<0.04$). (C) Immunoprecipitation of VEGFR2 from retinal lysates followed by probing with the VEGFR2 and PY100 antibodies. (D) Quantification illustrated a decline in VEGFR2 phosphorylation from rats treated with 7,8-DHF ($p<0.05$).

4A.4 Discussion

This study investigated the molecular interactions underlying 7,8-DHF and various other dihydroxyflavone derivatives with the TrkB receptor using a combination of molecular docking and dynamics studies. We also examined for first time molecular interactions between various flavonoid derivatives including 7,8-DHF with the VEGFR2. 7,8-DHF is an agonist of TrkB receptor and its treatment leads to upregulation in the tyrosine phosphorylation on TrkB residues and activate its downstream signaling (Gupta et al., 2013b). Intriguingly, a combination of molecular modelling and biochemical approaches has revealed that 7,8-DHF could act as an inhibitor of the VEGFR2. This suggestion corresponded with the previous observations that flavonoids inhibit the VEGFR2 activity in

human umbilical vein endothelial cells (Kim, 2003). The inhibitory constant of 7,8-DHF for VEGFR2 was calculated and found to be 2.04 μM indicating a ~32 fold higher inhibitory constant for the VEGFR2 as compared to a theoretical value of K_i 64.79 μM for TrkB. The high *in silico* K_i suggested that 7,8-DHF did not have a significant inhibitory effect on TrkB (Le Bail et al., 1998, Jang et al., 2010b) as compared to that observed in the case of VEGFR2 (Lin et al., 2012, Paramashivam et al., 2015).

The *in silico* docking approaches based on topological surface geometry complementarities for 7,8-DHF-TrkB and 7,8-DHF-VEGFR2 complexes indicated formation of hydrogen bond networks between surface amino acid residues (Gupta and Gowda, 2008). The stable behavior of the both the complexes could be attributed to van der waals forces and atomic contact energies (Camacho and Vajda, 2001). Molecular docking of 7,8-DHF with TrkB showed presence of 3 H-bonds between 7,8-DHF and TrkB protein at the Ig2 domain of extracellular region (Haniu et al., 1995). Interestingly, these interactions are in addition to already known interactions of 7,8-DHF with the cysteine cluster 2 (CC2) region of TrkB which is formed by the disulfide linkage of Cys145-Cys121 and Cys123-Cys163 residues and the leucine rich region (LRR) (Haniu et al., 1995). Jang *et. al*, showed using truncated binding assay that 7,8-DHF strongly associated with CC2 domain and also partially interacted with leucine-rich motif domain. This additional binding site at Ig2 may play a role in stabilizing or further enhancing the 7,8-DHF binding to the TrkB. Similar involvement of TrkB Ig2 domain in interactions with BDNF were observed with potential contributions to the TrkB receptor dimerization (Jiang et al., 2013). The N-glycosylation site in the Ig2 domain could also play a role in ligand receptor interaction but further studies are required to establish it (Haniu et al., 1995).

Molecular simulations revealed presence of additional H-Bonds increasing the total number to 5 and also indicated formation of *pi*-sigma bonds. 7,8-DHF-VEGFR2 complex also

showed formation of 2 hydrogen bonds with Cys^{917} after molecular docking. Molecular simulations further showed additional 5 H-bonds involving Glu^{915}, Phe^{916} and Cys^{917} residues. Detection of additional bonds and interactions following molecular simulations indicated that the protein-ligand complexes acclimatize and achieve a more stable configuration over a period of time. No significant changes were observed in the total energy of the either of the protein-ligand complexes within the 10ns simulation period indicating that the complexes attained a stable conformation (Figure 4A 5A and B).

The differential effects of 7,8-DHF on TrkB and VEGFR2 were on expected lines as the two membrane receptors belong to two independent superfamilies of receptor tyrosine kinases. VEGFR2 in addition to its several other unique structural features does not possess either the CC2 or LRR domains in its extracellular region. Further, the VEGFR2 ATP binding site has Val^{914}, Phe^{916}, and Cys^{917} residues which are critically involved in the hydrogen bond and pi-sigma interactions with the ligand; these residues are not present in TrkB. These residues are also absent in other kinases such as Insulin-like growth factor 1 receptor (IGF1R), Serine/threonine-protein kinase 4 (STK4), Phosphatidylinositol 4,5-bisphosphate 3-kinase (PK3CG) and CUB domain-containing protein 1 (CDCP1) (Figure 4A 10A). Further, tertiary structural analysis revealed that Val^{568} (TrkB) which corresponds to Val^{846} (VEGFR2) is buried in the TrkB and is not surface accessible for development of bond formation. These observations suggested that the absence of these structural motifs in TrkB could be the reason underlying exclusion of 7,8-DHF interactions with the ATP binding site of TrkB in contrast to that observed in VEGFR2 (Figure 4A10). Together these findings suggest that the inhibitory effects observed in VEGFR2 are not generic in nature and may not be generalized across different kinase families.

A

```
sp|VEGFR2_HUMAN    MSELKILIHIGHHLNVVNLLGACTKPGGPLMVIVEFCKFGNLSTYLRSKR
932
sp|TrkB_HUMAN      QREAELLTMLQHQH-IVRFFGVCTE-GRPLLMVFEYMRHGDLNRFLRSHG
605
sp|IGF1R_HUMAN     LNEASVMKEFNCHH-VVRLLGVVSQ-GQPTLVIMELMTRGDLKSYLRSLR
1095
sp|STK4_HUMAN      MDSGTMVRAVGDEMGTVRVASTMTD-GANTMIEHDDTLPSQLGTMVINAE
373
sp|PK3CG_HUMAN     WLEFKCADPTALSNETIGIIFKHGDDLRQDMLILQILRIMESIWETESLD
861
sp|CDCP1_HUMAN     WNISVPRDQVACLTFFKERSGVVCQTGRAFMIIQEQRTRAEEIFSLDEDV
625
```

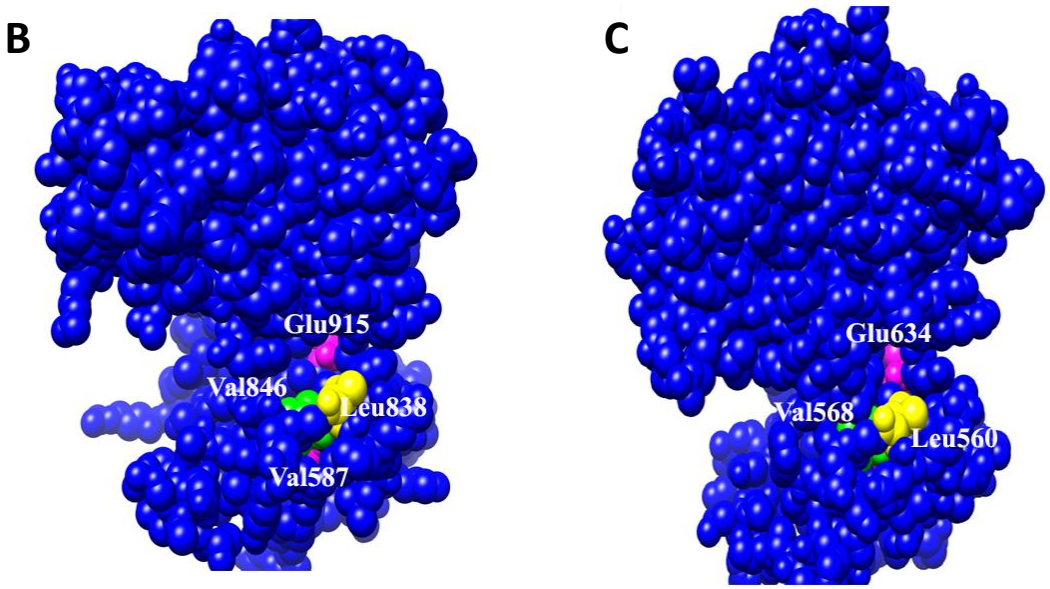

Figure 4A.10 (A) Multiple sequence alignment of 7,8DHF interacting residue at ATP binding site of VEGFR2 with corresponding residues from various other kinases. Space filled models highlighting the 7,8DHF interacting residues of (B) VEGFR2 (Left) and its topological comparison with (C) TrkB (Right).

The relevance of the predictive value of our *in-silico* studies was investigated in the photoreceptor 661w cells in culture as well as in the rat retina under *in vivo* conditions. 7,8-DHF treatment has been shown to activate the TrkB signaling and reduce apoptosis by activating the downstream processes of Akt and Erk1/2 pathways (Gupta et al., 2013c) . We choose 661w cells as these have been shown to express VEGFR2 (Tsui et al., 2013). Our previous studies have convincingly established that 7,8-DHF treatment can activate the TrkB and its downstream signaling in the retinal ganglion cells as well as in RGC-5 cells (Gupta et al., 2013c). VEGFR2 is known to undergo tyrosine (Tyr) autophosphorylation at residues 951/996 and 1054/1059 in response to ligand binding and undergo activation (Meyer et al., 1999). Phosphorylation leads to rapid recruitment of intracellular adapter proteins which is essential process to execute the VEGF stimulated signaling as well as mediate survival of endothelial cells and regulate angiogenesis process (Kroll and Waltenberger, 1997, Karkkainen and Petrova, 2000, Claesson-Welsh, 2003). In order to evaluate whether 7,8-DHF treatment had any effect on the activity of the VEGFR2, we evaluated changes in the Tyr phosphorylation of VEGFR2 in both the 661W cells in culture as well as in the rat retinal tissue. Immunoprecipitation of VEGFR2 followed by probing the blots with pY100 antibody demonstrated that Tyr phosphorylation was significantly reduced upon treatment with 7,8-DHF. The experiments were conducted on immunoprecipitated proteins using specific VEGFR2 antibodies and not whole lysates to eliminate possible interfering signals from other proteins. Appropriate controls were maintained in the form of non-immune IgGs for both the control as well as 7,8-DHF treated samples. This experiment established that 7,8-DHF has a dual effect in suppressing the VEGFR2 actions by reducing its activity in addition to its known agonistic effects on TrkB. These experimental observations corroborate our *in-silico* predictions. Briefly, the fact that similar inhibitory effect was observed in the rat retinal tissues upon 7,8-DHF treatment validate our 661W results and reassure that the inhibitory

effects are not an experimental artefact or not a cell specific phenomenon. The loss in VEGFR2 activity can potentially be attributed to 7,8-DHF interactions with key active site residues Glu^{915}, Phe^{916}, and Cys^{917} that may give rise to conformational changes in the geometry of the protein as observed in the molecular dynamic studies (Figure 4A 4 and 5).

Concurrent effects of a TrkB agonist as an inhibitor of VEGFR2 actions could have great application in the development of innovative therapeutics. In wet AMD for example, 7,8-DHF may enhance TrkB signaling and promote critical neuroprotective pathways while simultaneously downregulating VEGFR2, thereby inhibiting unregulated neovascularization in the retina. The data also suggested that treatment with 7,8-DHF may have clinical importance in other retinal vascular diseases including diabetic retinopathy and associated macular edema in retinal vein occlusions, based on its ability to activate TrkB and inhibit VEGFR2 receptors at the same time. Since many patients have co-existing pathologies of glaucoma, AMD and diabetes, an agent with these properties could provide additional benefits.

4A.5 Conclusion

Inhibition of VEGF/VEGFR signaling may be critical in several disorders involving unregulated angiogenesis. A poorly monitored treatment on the other hand may give rise to unwarranted complications. In the context of retina for example, excess of anti-VEGF treatment may give rise to onset of dry AMD leading to gradual neurodegeneration. In contrast, activation of the neurotrophic factor signaling such as TrkB may play a critical role in protecting against several neurodegenerative disorders including retinal disorders. In this study, we have evaluated the potential of flavonoid derivatives to act as VEGFR2 inhibitor and the same time evaluated their potential as an activator of neurotrophic factor signaling

via activation of the TrkB receptor with emphasis on examining additional interactions with 7,8-DHF. The interactions of 7,8-DHF and several of its derivatives with the extracellular domain of TrkB receptor using a combination of molecular docking and dynamics tools was determined. Potential interactions of 7,8-DHF and its derivatives with VEGFR2 were also evaluated. Computational studies indicated 7,8-DHF to be an inhibitor of the VEGFR2. Effects of 7,8-DHF on photoreceptor cells in culture revealed that 7,8-DHF downregulated the VEGFR2 activity. Similar results were obtained in the *in vivo* study where 7,8-DHF administration lead to a decrease in the activity of VEGFR2 in the retina. This combined *in silico*, cell culture and *in vivo* studies suggest emergence of 7,8-DHF as a dual action compound which in addition to its known agonistic effects on TrkB receptor can suppress the VEGFR2 actions.

Part 4B published as:

Nitin Chitranshi, Vivek Gupta, Yogita Dheer, Veer Gupta, Roshana Vander Wall, Stuart Graham**.** Molecular determinants and interaction data of cyclic peptide inhibitor with the extracellular domain of TrkB receptor. ***Data Brief.*** 2016 Mar; 6: 776–782.

Abstract

TrkB is a high affinity receptor for the brain derived neurotrophic factor (BDNF) and its activation leads to further activation of several cell signaling pathways linked to cellular growth, differentiation and maintenance. Identification and understanding the binding mechanisms of various activators and inhibitors of the TrkB receptor is critical to elucidate the biochemical, pharmacological pathways and analyse protein crystallization studies. The data presented here is related to the research article entitled "Brain Derived neurotrophic factor is involved in the regulation of glycogen synthase kinase 3β (GSK3β) signalling". Cyclotraxin B (CTXB) is cyclic peptide molecule linked by disulphide bridge and has been reported to interact with TrkB receptor and inhibit the BDNF TrkB signaling. This article reports for the first time the binding mechanism and interaction parameters of CTXB with the TrkB receptor. The molecular model of CTXB has been generated and it's docking with TrkB domain carried out to determine the critical residues involved in the protein peptide interaction.

4B. Data, Experimental Design, Materials and Methods

4B.1 Selection and Preparation of Cyclotraxin B, TrkB Inhibitor

Cyclotraxin B (CTXB) is a cyclic peptide chain of 10 amino acid linked by a disulphide bridge (Gupta et al., 2013b). It is an inhibitor of the TrkB activation and its downstream signaling pathway mediated by BDNF binding (Gupta et al., 2012b, Gupta et al., 2013a, Gupta et al., 2014b). Cyclization is important to provide stability to the peptide macromolecule. The primary structure of the peptide is known and in this manuscript, we report for the first time the putative three-dimensional structure of the peptide (Figure 4b 1A). The two-dimensional (2D) and three dimensional (3D) structure of the CTXB was built using ChemDraw Ultra 8.0 (Cambridgesoft, Waltham, MA, USA) (Figure 4B 1B and C). Extensive energy minimization was performed using the Austin Model-1 (AM1) programme until the root mean square (RMS) gradient value became smaller than 0.100 kcal/mol Å. The molecule was further subjected to re-optimization *via* MOPAC (Molecular Orbital Package) method (Chitranshi et al., 2015) until the RMS gradient attained a value lesser than 0.0001 kcal/mol Å. The chemical properties of CTXB was calculated by ACD (Advanced Chemistry Development, Canada) labs Chemsketch software and the data is presented in Table 4b.1 (Raj et al., 2014).

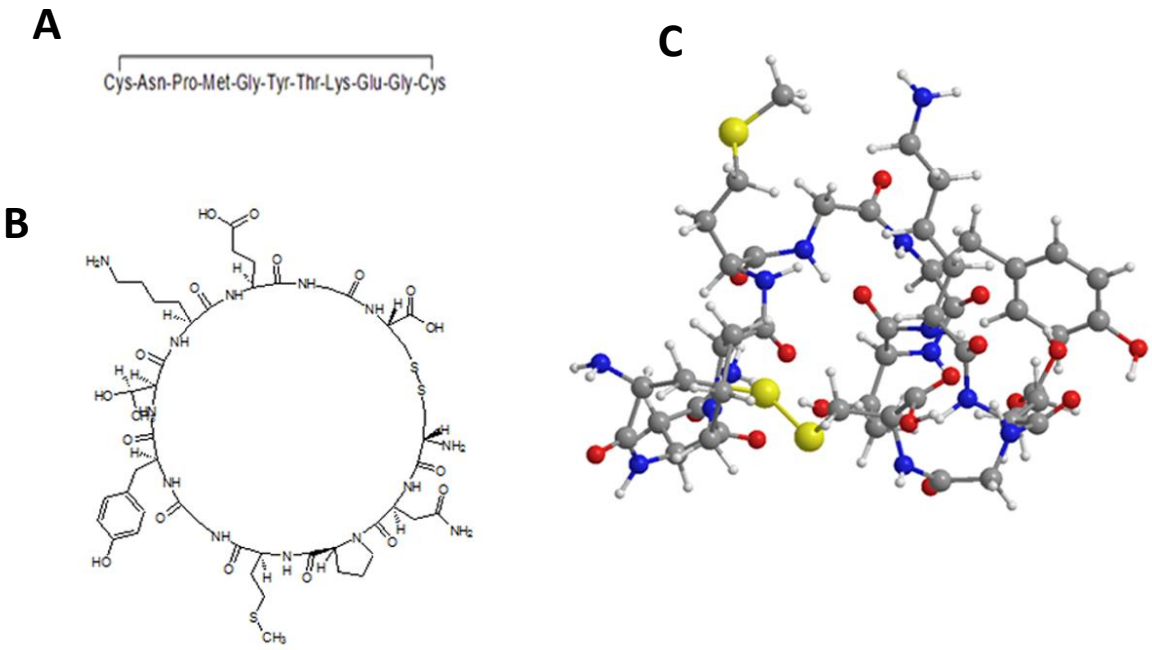

Figure 4B.1. Cyclotraxin B structure (A) One dimensional (B) Two dimensional and (C) Three dimensional view.

Chemical Properties	**Calculations**
Molecular Formula	$C_{48}H_{73}N_{13}O_{17}S_3$
Formula Weight	1200.36512
Composition	C(48.03%) H(6.13%) N(15.17%) O(22.66%) S(8.01%)
Molar Refractivity	296.25 ± 0.4 cm3
Molar Volume	805.8 ± 5.0 cm3
Parachor	2467.9 ± 6.0 cm3
Index of Refraction	1.656 ± 0.03
Surface Tension	87.9 ± 5.0 dyne/cm
Density	1.48 ± 0.1 g/cm3
Dielectric Constant	Not Available
Polarizability	117.44 ± 0.5 10-24cm3
Monoisotopic Mass	1199.440948 Da

Nominal Mass	1199 Da
Average Mass	1200.3651 Da

Table 4B.1. The chemical property and the calculation of Cyclotraxin B (CTXB) as evaluated using ACD labs Chemsketch software

4B.2 Molecular modeling and generation of TrkB binding region

The primary structure of TrkB receptor and its various domains were examined (Basavarajappa et al., 2011). Crystal structure of the extracellular D5 domain of the TrkB which exhibits binding with the human Neurotrophin-4/5 ligand (PDB id: 1HCF) was selected from the protein databank (Berman et al., 2003). This region contains two protein chains X and Y. The chains X and Y are known to interact with the BDNF/ NT-3 protein. Only chain X of PDB id 1HCF was considered in the present study for its potential interactions with the CTXB. The optimization of proteins was carried out using well characterized UCSF Chimera software (San Francisco, California, USA), implying amber parameters, followed by minimization with MMTK (Molecular Modeling Toolkit) method in 500 steps with a step size of 0.02 Å (Pettersen et al., 2004, Chitranshi et al., 2013).

4B.3 Identification of CTXB binding site

The protein motif was subjected to *in silico* assessment of the potential binding of selected CTXB residues to different regions on the TrkB D5 surfaces. This binding interactions were assessed in terms of probability of CTXB participating residues to the TrkB D5 receptor surface and theoretical scores determined using the PepSite2 server (Petsalaki et al., 2009). Peptide binding may also affect the tyrosine phosphorylation profile (Gupta et al., 2012a) of the TrkB receptor translating into its altered activity which can be assessed in future

investigations. Surface accessibility of the ligand to various binding pockets was also examined (Gupta and Gowda, 2008).

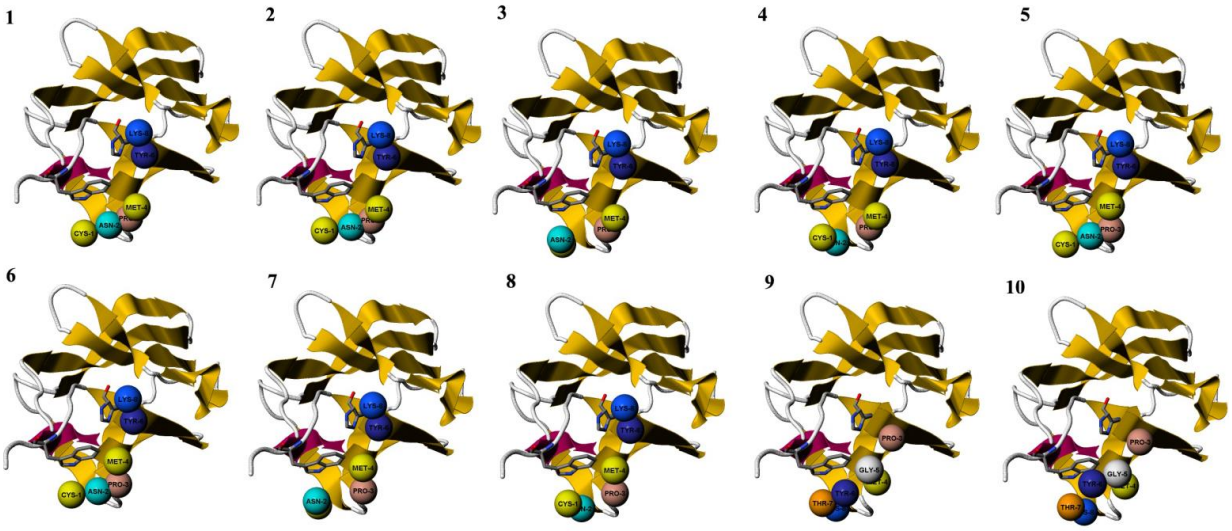

Figure 4B.2. Predicted binding sites of CTXB peptide ‘‘CNPMGYTKEG’’ core motif on the surface of TrkB-D5 domain as predicted by the PEPSITE2 program. The six ball shaped structures indicate the predicted locations of six residues from ‘‘CNPMGYTKEG’’. **(1-8)** distribution of 6 amino acids of the peptide predicted on the surface of TrkB-D5 in the sequence of Cys (C), Asn (N), Pro (P), Met (M), Tyr (Y) and Lys (K) (labeled) and **(9-10)** distribution of 6 selected amino acids of CTXB binding to TrkB-D5-Pro (P), Met (M), Gly (G), Tyr (Y), Thr (T) and Lys (K) (labeled).

PepSite2 is a computational tool that scans the surface of a given protein for patches or grooves that are likely to influence binding of individual amino acid residues or peptides up to ten amino acids and provides a score that reflects the propensity of the peptide to bind to that region. The PepSite score is expressed in relative units and the higher scores reflects superior binding. We applied PepSite in a sliding window of 10 residues to assess the binding of the TrkB-D5 domain and CTXB peptide sequence (CNPMGYTKEG). The scores of the CTXB binding to different regions of TrkB D5 domain are presented (Figure 4B 2A, Model 1, Table 4B 2).

Rank	Peptide sequence order	Pepsite2 Score
1.	CNPMYK	0.02733
2.	CNPMYK	0.03015
3.	CNPMYK	0.03266
4.	CNPMYK	0.03583
5.	CNPMYK	0.03719
6.	CNPMYK	0.04098
7.	CNPMYK	0.04435
8.	CNPMYK	0.04993
9.	PMGYTK	0.05985
10.	PMGYTK	0.06992

Table 4B.2. PepSite2 binding score prediction of selected Cyclotraxin B (CTXB) residue sequences to the TrkB-D5 domain.

4B.4 Peptide docking in the binding region

The protein-peptide docking was performed with the PatchDock software available in the public domain (Schneidman-Duhovny et al., 2005). The crystal structure of TrkB (PDB ID: 1HCF) was retrieved from Protein Data Bank. The single chain of TrkB-D5 as described previously was used for docking study under default complex-type settings. Molecular visualization and general analysis were done using the program PyMOL and Discovery Studio 4.0 software's (Simmons et al., 2014). The docking scores, atomic contact energies and geometrical parameters are compiled as Table 4B.3. The hydrogen bond between TrkB-D5 and CTXB (rank 1) was observed to be formed between the amino acid residues His353, Met354, Ala376, and His377 (Figure 4B 3A). The pi–sulpha interaction was also observed

between CTXB and Met354 (Figure 4B 3B). Surface binding of CTXB with TrkB-D5 domain is shown in figure 4B 3C.

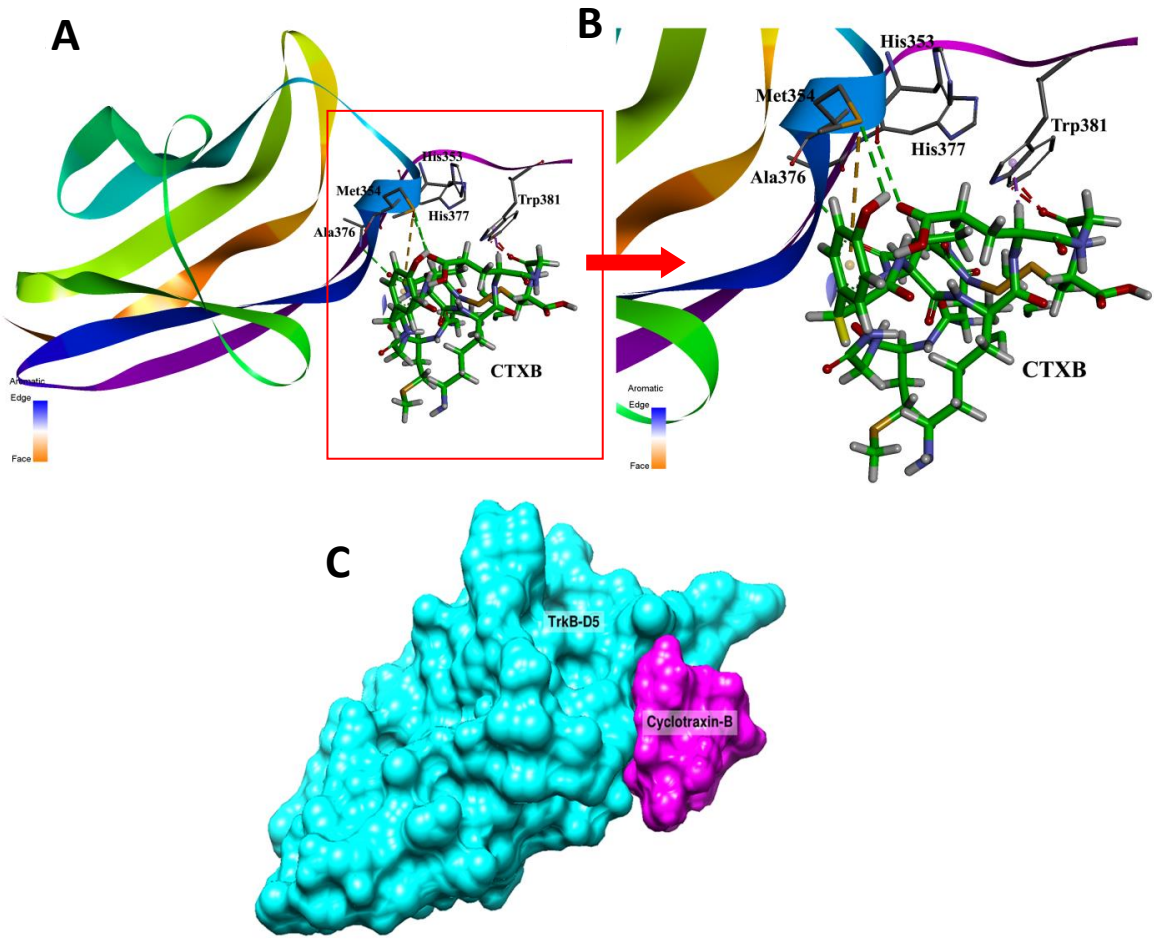

Figure 4B.3. Interacting residues and binding mode of CTXB with TrkB-D5 domain (A) Docking of TrkB (ribbon structure) with the CTXB (stick model) showing critical residues (rank 1) involved in interaction (B) Enlarged view of the interaction pocket within 5.5 Å region around the ligand, CTXB-TrkB-D5 complex and (C) Surface view showing the grove in TrkB-D5 domain (Cyan) locating CTXB peptide (pink). Green dashed line denotes the hydrogen bonding and brown dashed line reflects pi–sulpha interactions and stacking. The images were generated with the Discovery Studio 4.0 Client (Accelrys, Inc., San Diego, CA, USA).

Rank	Score	Area	ACE	Transformation
1	5538	652.1	-344.82	-0.57 -1.01 -2.62 -10.48 -3.78 29.57
2	5282	597.6	-272.85	-1.01 -0.26 0.32 -12.66 -4.68 28.84
3	5100	620	-330.86	-1.52 0.07 0.81 -11.83 -7.13 27.44
4	4966	528.9	-126.23	-0.31 -0.63 -2.16 -22.34 8.83 21.59
5	4878	623.4	-300.47	2.71 0.78 -1.27 -13.25 -4.12 29.20
6	4824	571.7	-214.66	-0.11 1.20 2.50 -5.75 11.23 7.03
7	4800	621.7	-217.57	-2.59 -0.46 0.54 -22.14 6.07 23.60
8	4678	531.9	-182.76	-0.67 -0.16 -1.87 -20.33 9.72 23.42
9	4654	512.8	-234.35	0.84 -0.57 0.51 -12.13 -2.05 31.89
10	4642	570.9	-250.43	-1.34 0.11 -1.76 -23.69 10.32 20.31
11	4606	539.9	-170.59	0.32 -1.01 2.51 -22.65 10.28 21.86
12	4536	521.6	-189.48	-3.07 -0.42 0.56 -20.13 9.32 24.74
13	4530	735.8	-436.61	-0.46 1.21 -2.78 -3.58 11.15 12.99
14	4522	622	-273.37	-1.99 -0.45 2.81 -8.24 -1.98 30.78
15	4358	547.6	-276.07	0.05 -0.96 2.97 -7.11 -6.08 31.48
16	4264	468.6	-196.84	2.26 -0.23 2.23 -1.86 14.82 14.52
17	4242	531.7	-154.98	-0.67 -0.38 -2.13 -16.81 14.23 21.56
18	4240	548.7	-304.69	0.50 -0.35 -0.24 -6.28 11.67 5.72
19	4234	458.8	-155.03	2.26 -0.60 -2.85 -2.98 13.89 13.16
20	4230	653.7	-351.22	-0.76 1.23 2.83 -5.51 13.82 10.66

Table 4B.3. The top 20 docking scores and geometrical parameters of the peptide CTXB with TrkB-D5 domain; ACE: Atomic Contact Energy.

CHAPTER 5

Effect of TrkB modulation by PTPN11 gene targeting in SH-SY5Y cells

Data presented in this chapter have been submitted for publication:

Nitin Chitranshi, Yogita Dheer, Roshana Vander Wall, Veer Gupta, Mojdeh Abbasi, Mehdi Mirzaei, Yuyi You, Roger Chung, Stuart L Graham, Vivek Gupta. Adeno-associated virus mediated overexpression of PTPN11 induces TrkB dephosphorylation and increases endoplasmic stress in SH-SY5Y cells and rat retina. Manuscript submitted to *Journal of Neurochemistry.*

This chapter was presented in ARVO 2016, Seattle, USA

Part of the abstract published as:

Nitin Chitranshi, Vivek K. Gupta, Roshana Vander Wall, Yogita Dheer, Stuart L. Graham. SHP2 (PTPN11) over-expression by AAV gene delivery impairs neuronal cell growth in SH-SY5Y cells and induces neurodegeneration of SD rat retinal ganglion cells. ***Invest. Ophthalmol. Vis. Sci.*** 2016; 57(12):3997.

Abstract

PTPN11, is associated with regulation of growth factor signaling pathways in the neuronal cells. Using SH-SY5Y neuroblastoma cells, we showed that adeno-associated virus (AAV) mediated *PTPN11* upregulation was associated with TrkB antagonism, reduced neuritogenesis and enhanced endoplasmic reticulum (ER) stress response leading to apoptotic changes. Genetic knock-down of *PTPN11* on the other hand lead to increased TrkB phosphorylation in SH-SY5Y cells. ER stress response induced by *PTPN11* upregulation was pharmacologically alleviated by a TrkB agonist and conversely, enhanced ER stress response induced by receptor antagonism was ameliorated by *PTPN11* suppression, providing additional evidence that PTPN11 effects are mediated through TrkB actions. BDNF treatment in SH-SY5Y cells also resulted in reduced ER stress protein markers. This study provides further evidence that support molecular cross-talk between PTPN11 and the TrkB receptor in SH-SY5Y cells. The results reinforce the role played by PTPN11 in regulating neurotrophin protective signaling in SH-SY5Y cells and highlight that PTPN11 overexpression in these cells culminates in apoptotic activation. Based on these findings we suggest that blocking *PTPN11* could potentially have beneficial effects to limit the progression of neuronal loss associated with other neurodegenerative disorders.

5.1 Introduction

Src homology 2-containing protein-tyrosine phosphatase 2 (Shp2; PTPN11) is ubiquitously expressed and plays a key role in several cellular signaling pathways affiliated with cell growth, differentiation, mitotic cycle, metabolic control, transcription regulation, and cell migration (Tsang et al., 2012). Missense mutations leading to PTPN11 hyperactivation or catalytic impairment are associated with genetic diseases such as cancers, cardiovascular disorders, Noonan syndrome, LEOPARD syndrome and neurodegenerative diseases of the brain and eye (Li et al., 2012a, Lauriol et al., 2015, Qiu et al., 2014, Pan et al., 2010, Gupta et al., 2012b). PTPN11 actions are demonstrated to modulate pro-survival neurotrophin signaling particularly BDNF/TrkB (brain-derived neurotrophic factor/ tropomyosin receptor kinase B), in addition to its regulatory effects on a broad range of other receptor tyrosine kinases, such as platelet-derived growth factor receptor (PDGFR), fibroblast growth factor receptor (FGFR) and epidermal growth factor receptor (EGFR). PTPN11 regulates the activation of the Ras/Erk pathway which is downstream of several receptor tyrosine kinases (Grossmann et al., 2009) and can have cell and tissue specific effects on PI3K/Akt signaling and Rho family small G-proteins (Yang et al., 2006, Kontaridis et al., 2004). PTPN11 can also regulate the sustained IL-1 induced ERK activation which is linked to integrin clustering in focal adhesions and is mediated possibly by PTPN11 cross talk with paxillin and Gab1 (Herrera Abreu et al., 2006).

PTPN11 dysregulation affects the development and molecular homeostasis of various organs like the central nervous system (CNS), the heart, and the mammary gland (Ke et al., 2007, Grossmann et al., 2009). The phosphatase plays a critical role in normal brain development and has been implicated in dorsal telencephalic neuronal and astroglia cell fate decisions (Grossmann et al., 2009). Its deletion in neuronal cultures reversed TrkB inhibition and

promoted neuronal survival (Rusanescu et al., 2005). Conditional loss of *PTPN11* in neural crest cells and in myelinating Schwann cells also resulted in deficits in glial development (Grossmann et al., 2009). PTPN11 regulates the downstream signaling of TrkB in mesencephalic and cortical neurons (Kumamaru et al., 2011) forming a critical switch in determining the fate of neural stem cells towards neuronal cells (Ke et al., 2007). In cerebral neuronal cultures, PTPN11 negatively regulates TrkB autophosphorylation and activation through BDNF in a calcium dependent manner (Rusanescu et al., 2005).

In the retina, Cai et al, (2011) demonstrated that *PTPN11* is essential for the initiation of retinal neurogenesis but is not decisive for tissue differentiation (Cai et al., 2011). *PTPN11* ablation in embryonic stages resulted in retinal degenerative changes including optic nerve dystrophy in mice further illustrating its role in retinal development. *PTPN11* has been shown to be predominantly expressed in the GCL and INL of the retina although it also regulates photoreceptor differentiation and is suggested to protect the outer retina indirectly through the Muller glial cell involvement (Cai et al., 2011, Pinzon-Guzman et al., 2015). These studies principally demonstrate the role of *PTPN11* in developing retina. To better understand the role of *PTPN11* in neuronal cells, we modulated *PTPN11* expression in differentiated SH-SY5Y cells using Adeno-associated virus, serotype 2 (AAV2). Using RGCs isolated from the retina, we have demonstrated previously that PTPN11 binds to TrkB and negatively regulates receptor activity in glaucomatous conditions (Gupta et al., 2012b). Pharmacological inhibition of PTPN11 restored TrkB activity in cultured neurons exposed to excitotoxic and oxidative stress (Gupta et al., 2012b). The potential role of BDNF/ TrkB axis in neuronal cells and particularly RGC survival is extensively explored; nevertheless, how it is regulated by PTPN11 is poorly understood.

To investigate the role played by PTPN11 in neuronal cells, this study evaluated cellular and molecular changes in neuroblastoma SH-SY5Y cells. The study describes role of PTPN11 in modulating TrkB activation in SH-SY5Y cells. Further, our study provides compelling evidence of PTPN11-dependent ER stress response elucidation in neuronal cells which in turn is regulated by TrkB activation. The significance of this non-canonical molecular regulation of TrkB activation and ER stress response elucidation by PTPN11 is reflected in concomitant apoptotic activation.

5.2 Materials and methods

Chemicals used, cell culture and AAV vector-design and packaging are described in chapter 2, *section 2.2.4* and *2.3.2.*

5.2.1 Viral vector transduction and treatment regimen in SH-SY5Y cells

The cells were grown in DMEM supplemented with 10% fetal bovine serum (FBS), penicillin (100 U/ml), streptomycin (100 U/ml) and 2 mM L−glutamine. The cells were at kept at 37˚C in a humidified atmosphere of air containing 5% CO_2. Approximately, 2.0×10^5 cells were seeded in each six well culture dish 6–12 h before treatment. Briefly, SH-SY5Y cells were grown to 80% confluency prior to transduction. Cells were pre-differentiated with 10 µM *all-trans* retinoic acid (Sigma) for 2 days. Medium was changed into retinoic acid medium without antibiotics and the viral transduction (1µl of virus+100µl culture media with retinoic acid) was carried out initially by incubating cells with either of the four-different viral construct (AAV2-GFP, AAV2-PTPN11, AAV2-Scramble-shRNAmir, and AAV2-shRNA-PTPN11mir) for 48 h. The transduction concentration of virus was 10^9 genome particles per well. After 48 h, transfection medium was replaced with fresh retinoic

acid medium (You et al., 2012a). For rhBDNF experiment, cells were pre-treated with rhBDNF (100 ng/ ml) at different time points 6, 12, 18 and 24 h prior to AAV2-PTPN11 or AAV2-PTPN11-shRNA transduction (Jaboin et al., 2002). Further, cells were pre-treated with 7,8 DHF (100 nM; 5 µl) 6 h prior to their exposure to AAV2-GFP and AAV2-PTPN11 viral constructs. For TrkB antagonist study cells were pre-treated with CTX-B (5 µM; 5µl; 6 h) and then transduced either with AAV expressing scramble control or PTPN11-shRNA. For PTPN11 inhibition studies, PTPN11 inhibitor, PHPS1 (5 µM; 5 µl) treatment was performed 6 h post- AAV-PTPN11 transduction.

5.2.2 Cell survival analysis and MTT assay

Following AAV viral transduction of SH-SY5Y cells, cell viability was evaluated using Trypan blue viability assay. Cells were diluted in sterile and filtered Trypan blue dye (0.4%) by preparing a 1.1 dilution of the cell suspension. Cell counter was used to evaluate the cell density using Neubauer micro-chamber to assess viable cell number. For MTT assay, SH-SY5Y cells were seeded into 96-well culture plates at a density of 2×10^3 cells/mL in DMEM supplemented with 10% FBS at 37˚C with 5% CO_2. Five different group of cells (control, AAV-GFP, AAV-PTPN11, AAV-Scramble-shRNAmir and AAV-PTPN11-shRNAmir) were analyzed. MTT reagent (5 mg/ml, 3-(4,5-dimethylthiazol-2-yl)-2,5-diphenyltetrazolium bromide) was added to the wells and allowed to incubate in dark at 37˚C for 3 h. The reaction was terminated by adding MTT solvent (0.1 N HCl in anhydrous isopropanol), MTT formazan crystals allowed to dissolve for 15 min and the plates gently agitated every 5 min. The amount of MTT formazan product was estimated by measuring absorbance at 570 nm (BioRad, CA, USA) (Ismail et al., 2012).

5.2.3 TUNEL staining

Described in chapter 2, *section 2.3.7.4*.

5.2.4 SDS PAGE and western blotting

SH-SY5Y cells were harvested and lysed in lysis buffer as mentioned in chapter 2, *section 2.3.8.2*. Membranes were incubated overnight with anti-GFP (1:1000), anti-PTPN11 (1:1000), anti-pTrkB Y^{515} (1:1000), anti-TrkB (1:1000), anti-GADD 153 (1:200), anti-XBP-1 (1:200), anti-p-PERK (1:200) and anti-actin (1:5000) overnight at 4°C. Secondary antibody treatment and signal detection with band intensities were determined as mentioned in chapter 2, *section 2.3.8.2*.

5.2.5 Immunofluorescence

Cells were fixed in 4% PFA for 15 min and were permeabilized in 0.1 % Triton X-100 in PBS (You et al., 2014). This was followed by incubating the cells with the appropriate primary antibodies overnight at 4°C: anti-PTPN11 (1:150), anti-GFP (1:150), anti-pTrkB Y^{515} (1:100), anti-TrkB (1:100), anti-GADD153 (1:200), anti-XBP-1 (1:200) or anti-pPERK (1:200). Secondary antibody treatment and signal detection with band intensities were determined as mentioned in chapter 2, *section 2.3.7.5*.

5.2.6 Statistical Analysis

Data including fluorescence changes were analysed and graphed using GraphPad Prism software (GraphPad Software, CA, v6.0). All values with error bars are presented as mean

± SD from given n sizes and compared by Student's t test for unpaired data and two-way ANOVA followed by Brown-Forsythe test. The significance was set at $p < 0.05$.

5.3 Results

5.3.1 PTPN11 has a regulatory effect on TrkB phosphorylation

To determine the regulatory effect of PTPN11 on the TrkB activation in neuronal cells, we investigated changes in TrkB Y^{515} phosphorylation in response to experimental modulation of *PTPN11* expression in the SH-SY5Y neuronal cells. *PTPN11* expression modulation was achieved using AAV2 constructs under the transcription control of hybrid CAG gene promoter (Martin et al., 2002) (Figure 5.1). AAV2 expressing eGFP alone was used as control for the *PTPN11* overexpression and eGFP along with scramble sequence was used as control for the *PTPN11* knockdown studies. Expression changes were evaluated using GFP and PTPN11 specific antibody immunostaining (Figure 5.2 A, panel 1). Immunoblotting of cell validated protein expression alterations in response to AAV transduction (Figure 5.2 B-E).

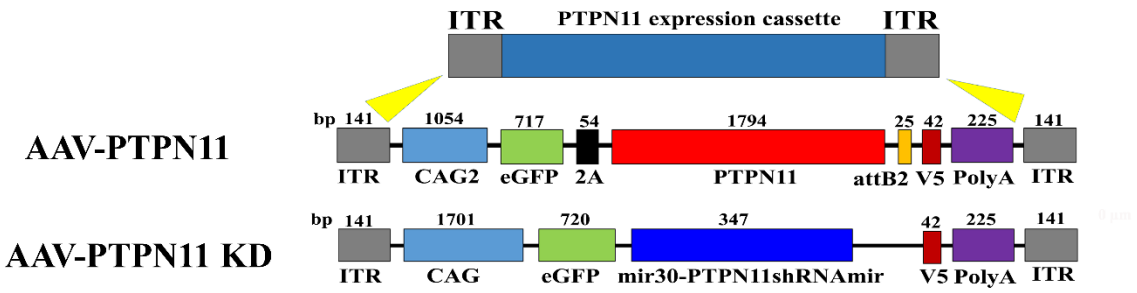

Figure 5.1 Schematic representation of AAV2 viral vector system used for PTPN11 overexpression and knockdown.

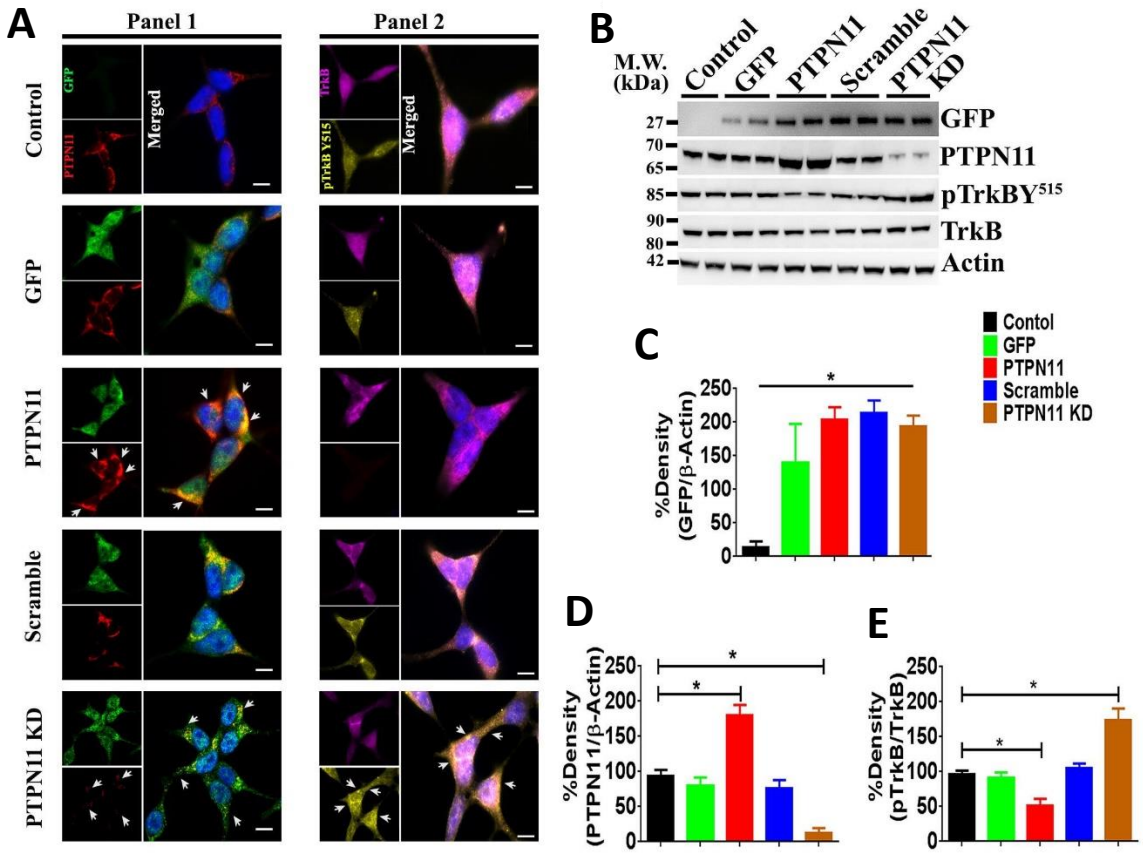

Figure 5.2. *PTPN11* modulation negatively affects TrkB Y^{515} phosphorylation in SH-SY5Y cells (A) Panel 1: Control and AAV transduced SH-SY5Y cells showing expression of GFP (green), PTPN11 (red). Cells were transduced either with AAV overexpressing GFP alone, PTPN11 (indicated by arrows), scrambled control or subjected to PTPN11 knockdown (indicated by arrows). Panel 2: Control and AAV transduced SH-SY5Y cells showing expression of TrkB (pink) and pTrkBY^{515} (yellow). Cells were subjected to either PTPN11 overexpression or knockdown as indicated. PTPN11 knockdown increases the expression of pTrkB Y^{515} (white arrow). Blue stain is 4',6-diamidino-2-phenylindoele (Dapi) for visualizing cell nuclei. Scale 5 µm. (B) Western blotting revealed expression of GFP in AAV treated SH-SY5Y cells, PTPN11 upregulated and pTrkB Y^{515} downregulated on AAV PTPN11, PTPN11 downregulated and pTrkB Y515 upregulated on AAV PTPN11 KD whereas normal expression of TrkB was observed, with β-actin as a loading control (C) Quantification of GFP protein expression in SH-SY5Y cells transduced with AAV viral construct (*$p<0.05$; ANOVA; Brown-Forsythe test). (D) Quantification of PTPN11 under PTPN11 overexpression and knockdown experiment shows significant changes compared to control. AAV expressing GFP and scramble sequence used as viral control (*$p<0.01$, *$p<0.009$; student t test). (E) Quantification of pTrkB Y^{515} relative to TrkB shows significant decrease in pTrkB Y^{515} in PTPN11 overexpression and significant increase in pTrkB Y^{515} under PTPN11 KD transduced neuronal cells (*$p<0.02$, *$p<0.03$; student t test). Graph data are expressed as mean ± SD. Protein molecular mass in kDa is indicated at the left of the blots.

Corroborating the previous evidence of PTPN11 mediated regulation of TrkB actions (Gupta et al., 2012b), we observed that *PTPN11* upregulation resulted in reduced TrkB Y^{515} phosphorylation in the SH-SY5Y cells (Figure 5.2 A, panel 2, B, E) (mean ± SD %;

96.88±3.12 vs 51.41±6.93; *p<0.03; n=3). Conversely, *PTPN11* knockdown lead to increased Y^{515} phosphorylation of TrkB compared to the scramble control in the SH-SY5Y cells in culture (mean ± SD %; 173±11.8; *p<0.03; n=3) (see Figure 5.2 A, panel 2). Analysis of TrkB expression in SH-SY5Y cells revealed that there was no compensatory change in total TrkB protein levels in response to AAV treatment or *PTPN11* modulation (Figure 5.2 A, panel 2, B, E), suggesting that loss of Y^{515} phosphorylation is mediated through the bonafide phosphatase activity of PTPN11. This is in accordance with previous observations that *PTPN11* deletion in neuronal cultures reverses TrkB inhibition and promote neuronal survival (Rusanescu et al., 2005). This hypothesis was further evaluated using PTPN11 specific pharmacological inhibitor, PHPS1 in the cultured neurons (Figure 5.3). Interestingly, PHPS1 treatment resulted in ablation of TrkB antagonism caused by *PTPN11* overexpression (Figure 5.3 A) (mean ± SD %; 106.1±6.12 vs 92.8±7.92, 91.33±14.34; n=6). Inhibitor treatment in GFP expressing cells was not associated with PTPN11 or TrkB protein expression changes (Figure 5.3 A, B). Overall, these results implicate that PTPN11 phosphatase activity negatively modulates the TrkB phosphorylation in neuronal cells *in vitro* systems.

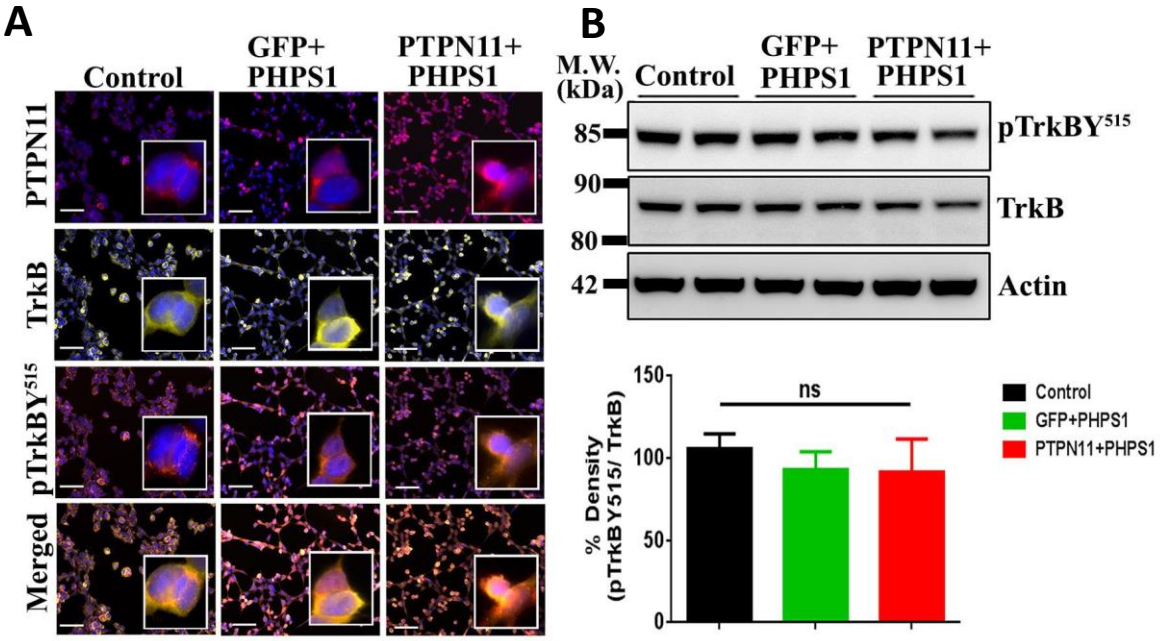

Figure 5.3. Effect of PHPS1 on SH-SY5Y neuronal cells (A) AAV expressing PTPN11 transduced SH-SY5Y cells were post treated (2h) with PTPN11 inhibitor, PHPS1 (5µM) to block the function of phosphatase. Immunostaining with antibody TrkB (yellow) shows the similar expression in control and GFP treated SH-SY5Y cells. Loss of pTrkB Y^{515} activity under PTPN11 overexpression (see Figure 5.1A, panel 2) reversed to normal as that of GFP and non-treated SH-SY5Y cells (n=6). Scale 200 µm (B) Western blot showing expression of TrkB and pTrkB Y^{515} after PHPS1 treatment in SH-SY5Y cells along with others viral construct, AAV-GFP and AAV-PTPN11. Quantification shows no significant change in pTrkB Y515 relative to TrkB under PTPN11 upregulation. Graph data are expressed as mean ± SD. Protein molecular mass in kDa is indicated at the left of the blots.

5.3.2 PTPN11 modulation influences the endoplasmic stress marker response

We then examined the effects of *PTPN11* modulation on ER stress response elucidation in the neuronal cells in culture. We found that *PTPN11* upregulation was associated with significant increase in reactivity of GADD153 (2.5 fold) (mean ± SD %; 115.9±15.88 vs 277.1±16.76; *p<0.02; n=3), XBP-1 (2.5 fold) (mean ± SD %; 89.22±10.78 vs 206.2±17.13; *p<0.03; n=3) and p-PERK (2 fold) (mean ± SD %; 97.96±2.04 vs 180.7±5.95; *p<0.006; n=3) which are markers of unfolded protein response from ER (Figure 5.4 A-D). *PTPN11* suppression, conversely, was not associated with any notable differences in expression of these markers. This experiment indicates that whereas *PTPN11* upregulation contributed to

enhanced ER stress, this response was not dependent on the loss of endogenous levels of PTPN11 in neurons. AAV expressing eGFP alone or scrambled sequence for *PTPN11* knockdown was used as controls (Figure 5.4 A and 5.5 A-C). To determine whether, ER stress response upregulation was mediated directly through the intrinsic PTPN11 activity or was potentially an indirect effect of its upregulation, we inhibited PTPN11 using PHPS1 and studied the effects on ER stress marker proteins. Selective inhibition of PTPN11 in the overexpression system resulted in normalisation of GADD153 (mean ± SD %; 84.35±15.65 vs 64.87±0.65; n=3), XBP-1 (mean ± SD %; 92.62±7.39 vs 107.5±9.44; n =3) and p-PERK (mean ± SD %; 99.97±0.03 vs 86.38±4.17; n=3) immunoreactivity (Figure 5.4 E-H). PHPS1 treatment alone or along with eGFP expression did not have any modulatory effects on ER

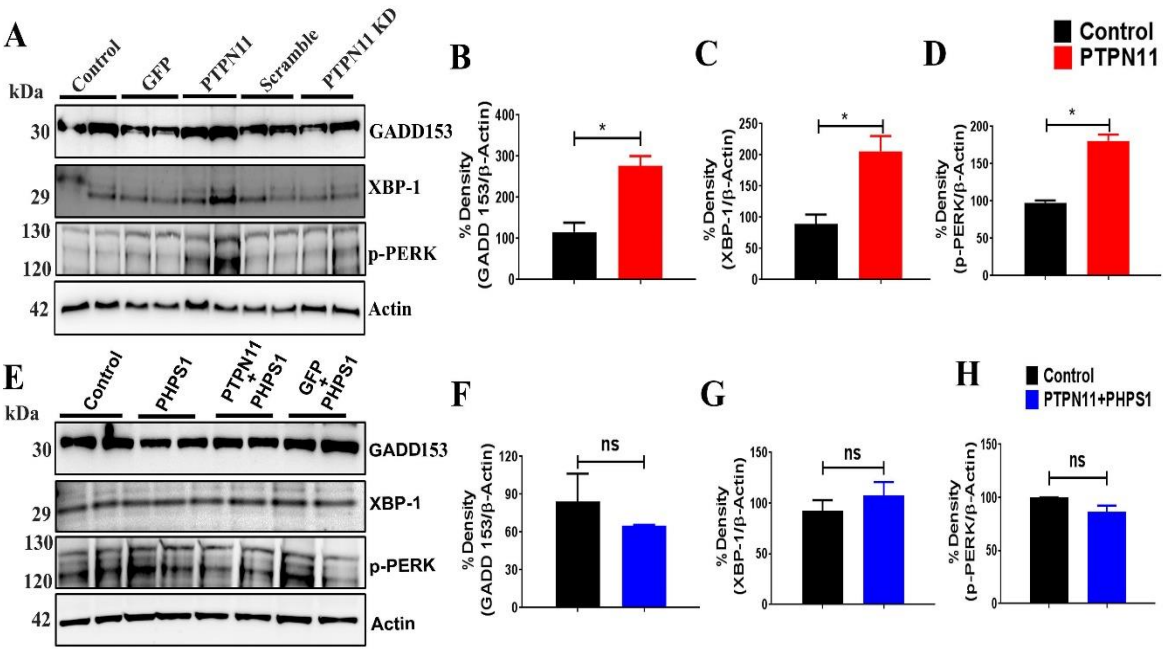

Figure 5.4. *PTPN11* upregulation is associated with enhanced ER stress marker response (A) Immunoblotting of SH-SY5Y cell lysates subjected to *PTPN11* expression modulation with anti- GADD153, XBP-1 and p-PERK antibodies. *β*-actin was used as loading control. (B-D) Densitometry analysis revealed significantly enhanced immunoreactivity of GADD, XBP-1 and p-PERK (*p<0.05) (E) SH-SY5Y cells overexpressing *PTPN11* and treated with PHPS1 inhibitor were evaluated for changes in ER stress markers and (F-H) western blots quantified by densitometry shows no significant changes in GADD153, XBP-1 and p-PERK under PHPS1 treatment (n=6).

stress proteins and these results reinforce *PTPN11* knockdown observations in Figure 5.4 A (Figure 5.4 E and 5.5 D-F). Together, these data argue that whereas a normal PTPN11 expression or activity may be dispensable to preserve ER homeostasis, an enhanced PTPN11 role disrupts the ER function promoting molecular stress response.

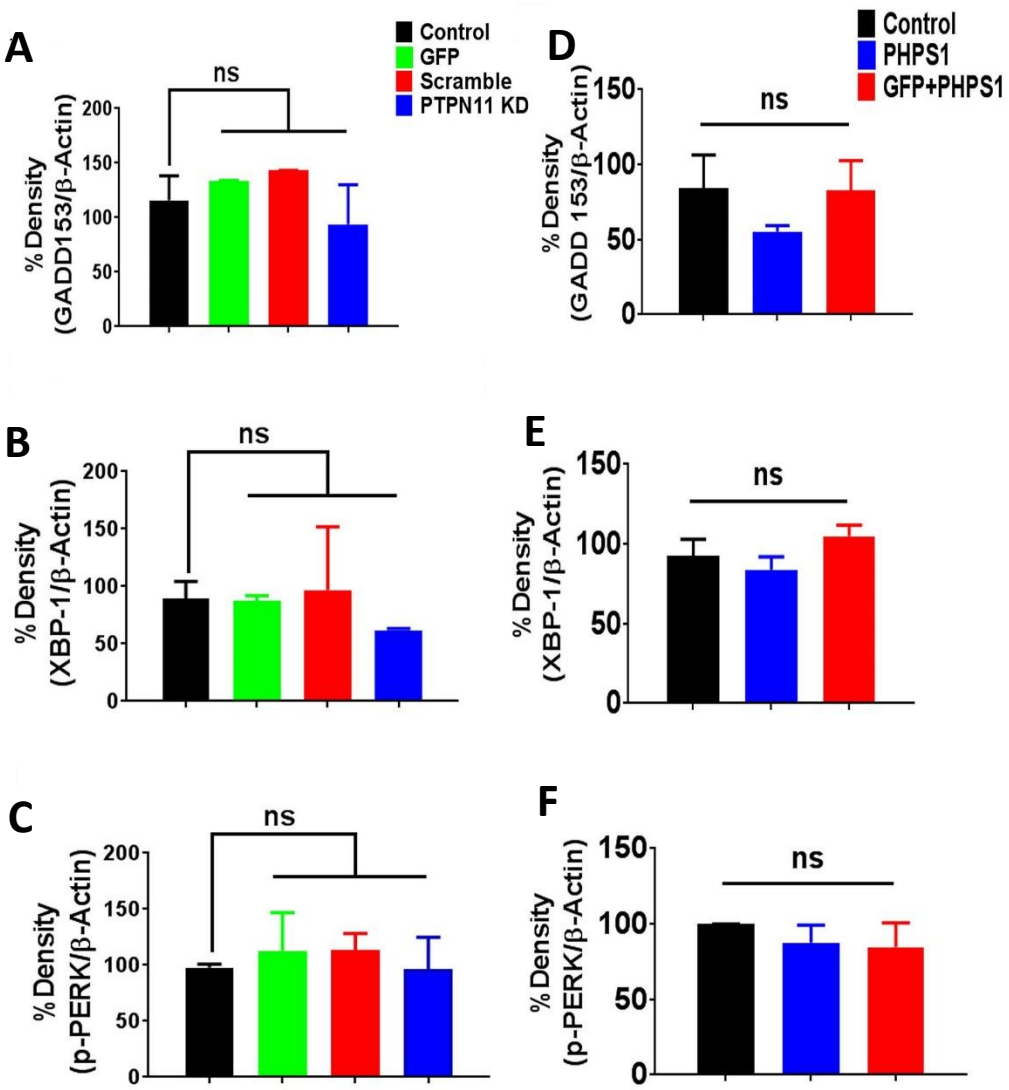

Figure 5.5 Densitometric quantification indicating no significant changes in ER stress marker response on PTPN11 downregulation (A) GADD (B) XBP-1 (C) p-PERK (n=4). No significant differences in ER stress protein expression (D) GADD 153, (E) XBP-1, (F) p-PERK under GFP, Scramble, PTPN11 KD and PHPS1, GFP+PHPS1 treated SH-SY5Y cells respectively as indicated. β-actin was used as loading control (n=4).

5.3.3 BDNF effects on PTPN11 induced TrkB deactivation and ER stress response

BDNF has high affinity ligand for TrkB receptor and therefore we sought to investigate the consequences of BDNF treatment on the PTPN11 regulatory effects on TrkB as well as on the downstream ER stress response elucidation. We and others have previously reported that TrkB receptor activation is mediated through BDNF in neuronal cells (Numakawa et al., 2010, Gupta et al., 2014b). SH-SY5Y neuronal cells pre-treated with BDNF at four different time intervals, for example 6, 12, 18 and 24 h and subjected either to PTPN11 overexpression or knockdown. BDNF treatment unable to induce activation of TrkB Y^{515} phosphorylation under PTPN11 overexpression condition at any time point. Conversely an augmentation of the pTrkB Y^{515} was observed upon PTPN11 knockdown following BDNF pre-treatment and continued up to 24h (Figure 5.6 A and B, $P<0.05$). No significant change was observed in the TrkB protein expression in any of the treatment groups. This experiment demonstrated that PTPN11 can modulate TrkB independent of BDNF treatment status and that regulatory effects of the two molecules can be partly attributed to mechanisms independent of each other. Further, the effects of BDNF on ER stress response elucidation following AAV mediated PTPN11 upregulation were investigated and results demonstrate that BDNF pre-treatment suppressed GADD153 (mean ± SD %; 107.8±7.77 vs 111.7±12.42; n=4), XBP-1 (mean ± SD %; 122.7±22.73 vs 96.48±4.65; n=4) and p-PERK (mean ± SD %; 132.4±32.36 vs 194.3±23.45; n=4) up-regulation (Figure 5.6 C-F). Transduction of AAV2 expressing eGFP and scramble sequence were used as control in each case (Figure 5.6). Data implicate that BDNF treatment can rescue the cells from entering into ER stress response mode caused by PTPN11 upregulation, thereby strengthening the argument that ER stress elucidation was not an artefact caused by PTPN11 overexpression but a result of subsequent downstream regulatory effects on TrkB.

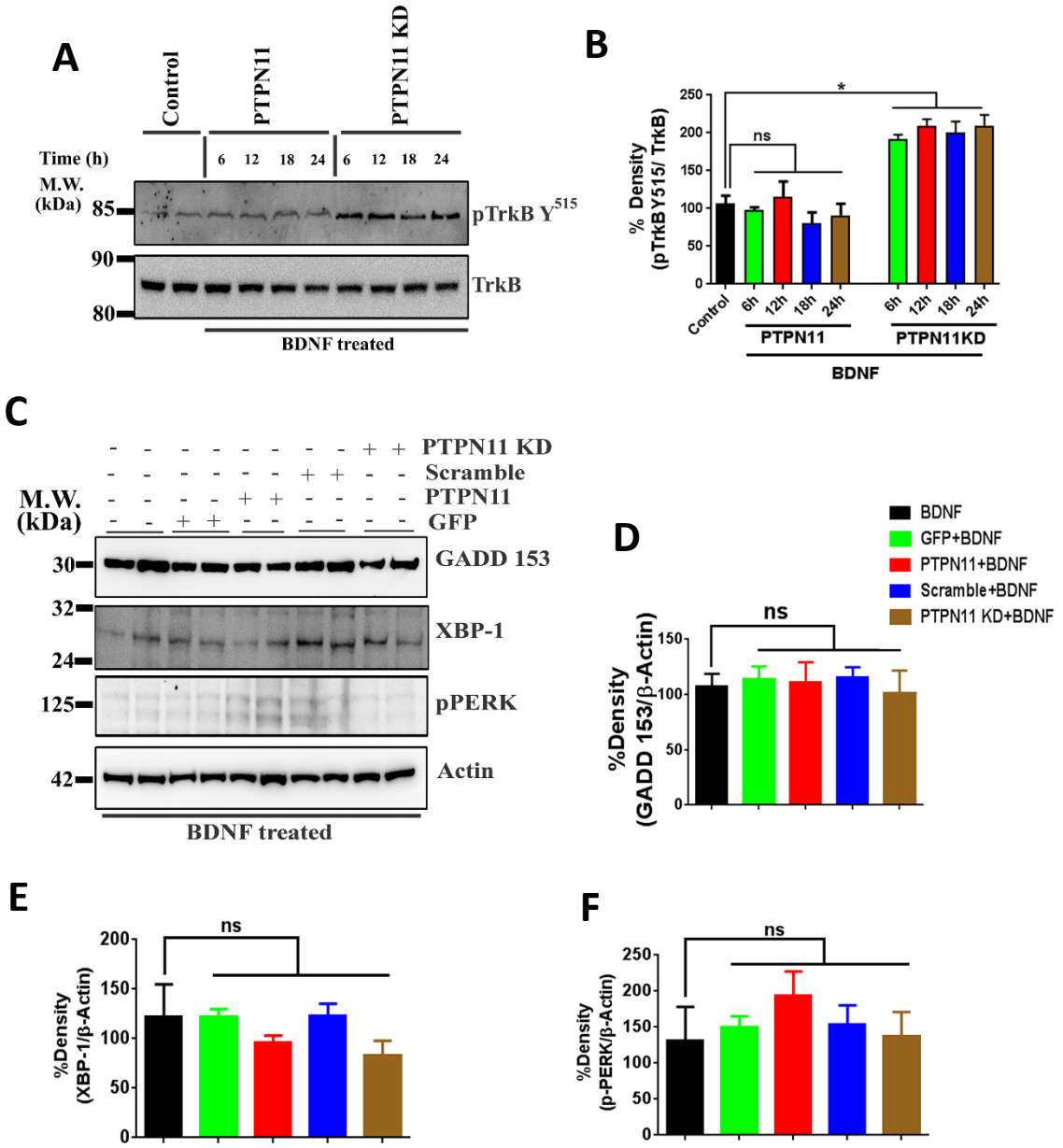

Figure 5.6. Effect of BDNF on PTPN11 mediated TrkB changes and ER stress response. SH-SY5Y cells were pre-treated with recombinant human BDNF (100 ng/ ml; 6,12,18 and 24h) prior to AAV2-GFP, AAV2-PTPN11, AAV2-Scramble and AAV2-PTPN11 KD transduction (A) Immunoblotting of SH-SY5Y cells depicts changes in pTrk Y^{515} immunoreactivity on PTPN11 upregulation and PTPN11 downregulation. No change in TrkB expression. Blots were cropped to show the relevant band. (B) Quantification of western blot showed significant decrease and increase in pTrkB Y^{515} immunoreactivity on PTPN11 overexpression and PTPN11 KD respectively (*$p<0.05$, n=4). (C) Western blot of BDNF induced TrkB activation for expression of ER stress marker, GADD 153, XBP-1 and p-PERK, and actin (loading control), SH-SY5Y neuronal cells treated with 4 different viral vector. Blots were cropped to show the relevant band. (D) Quantification of western blot showed no significant change in GADD 153 immunoreactivity (E) Densitometry quantification showed no significant XBP-1 immunoreactivity in neuronal cells either expression PTPN11 or PTPN11 KD (n=4) (F) Quantification of western blot indicating no significant change in p-PERK expression on BDNF treatment in SH-SY5Y cells transduced to AAV expressing GFP, PTPN11, Scramble and PTPN11 KD sequence (n=4). Graph data are expressed as mean ± SD. Protein molecular mass in kDa is indicated at the left of the blots.

5.3.4 PTPN11 effects on TrkB and ER stress response are alleviated by TrkB modulation

Finding that *PTPN11* modulation has a regulatory effect on TrkB activation and ER stress response in neurons, inspired us to investigate a correlation between these two processes. AAV2 mediated *PTPN11* overexpressing cells were pre-treated with TrkB agonist (7,8 DHF, 100 nM, 1hr) and immunostaining demonstrated that TrkB Y^{515} dephosphorylation caused by *PTPN11* over-expression (see Figure 5.2) was rescued by TrkB agonist 7,8 DHF treatment (Figure 5.7 A). Conversely, pre-treatment of the neuronal cells with TrkB antagonist, CTX-B, ablated the enhanced phosphorylation of TrkB Y^{515} induced by *PTPN11* knockdown as seen in Figure 5.2. CTX-B treatment of scrambled sequence transduced SH-SY5Y cells as control resulted in loss of TrkB Y^{515} phosphorylation (Figure 5.8 A). TrkB agonistic and antagonistic effects of 7,8 DHF and CTX-B respectively have been reported previously (Gupta et al., 2013b). A comparable TrkB immunostaining was observed in all cases indicating that pharmacological treatments or PTPN11 modulation as such did not result in any changed TrkB expression compared to the corresponding controls (Figure 5.7 A and 5.8 A). These data highlight the predominance of direct pharmacological modulation of TrkB activation over PTPN11 mediated antagonistic regulation of TrkB Y^{515} phsophorylation. Further, the effects of TrkB activation by 7,8 DHF on PTPN11 induced ER stress response (Figure 5.7 B) were evaluated by analysing changes in GADD153, XBP-1 and p-PERK expression (Figure 5.7 B-E). Loss of ER stress marker upregulation indicate that PTPN11 mediated ER stress response elucidation is mediated directly through TrkB (mean ± SD %; GADD153, 104.2±3.39; XBP-1, 134.5±3.96; p-PERK, 151.2±25.14; n=4) (Figure 5.7 B-E). These findings were further evaluated in another experimental paradigm by treating the cells with TrkB antagonist CTX-B, which resulted in upregulation of ER stress proteins (Figure 5.8 B-E) (Control vs CTX-B; mean ± SD %; GADD153, 84.31±15.69 vs 215.8±11.15, *p<0.03; n=4; XBP-1, 94.63±5.37 vs 153.5±3.59; *p<0.02; n=4 and p-

PERK, 100.7±0.73 vs 155.3±10.12; *p<0.05; n=4). Interestingly, the ER stress response associated with CTX-B treatment was abated upon subsequent AAV mediated *PTPN11* knockdown (Figure 5.8 B-E). This experiment suggests that while ER stress response induced by PTPN11 is mediated *via* its effects on TrkB, ER stress associated with TrkB antagonism can be alleviated by *PTPN11* suppression. Taken all together, our results implicate that both PTPN11 and TrkB mutually and negatively regulate ER stress response associated with their perturbations.

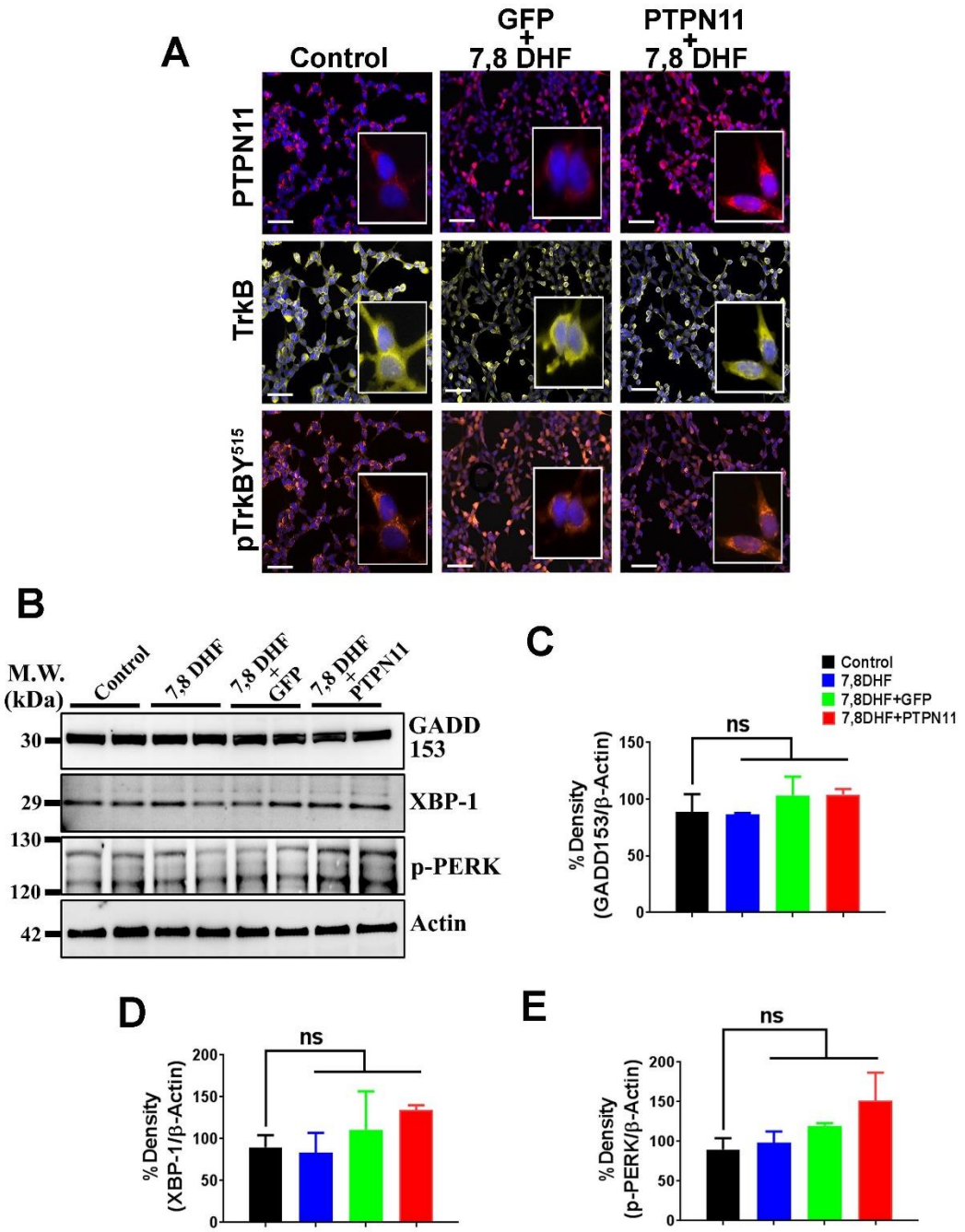

Figure 5.7. Effects of pharmacological modulation of TrkB on PTPN11 mediated TrkB changes and ER stress response on 7,8 DHF treatment (A) SH-SY5Y cells expressing *PTPN11* were pre-treated with TrkB agonist, 7,8 DHF (100 nM; 1h) and immunostained against PTPN11 (red), TrkB (yellow) and pTrkB Y^{515} (orange) antibodies. 7,8 DHF treatment resulted in re-gain in pTrkB Y^{515} activity in *PTPN11* expressing SH-SY5Y cells. GFP expressing and vehicle treated cells were used as controls. Scale 200 µm. (B) Normal expression of GADD153, XBP-1 and p-PERK was observed in western blotting of *PTPN11* overexpressing cells pre-treated with 7,8 DHF. (C-E) Densitometric quantification indicating no significant differences in ER stress protein expression on 7,8 DHF treatment in SH-SY5Y cells transduced to AAV expressing GFP and PTPN11 (n=4).

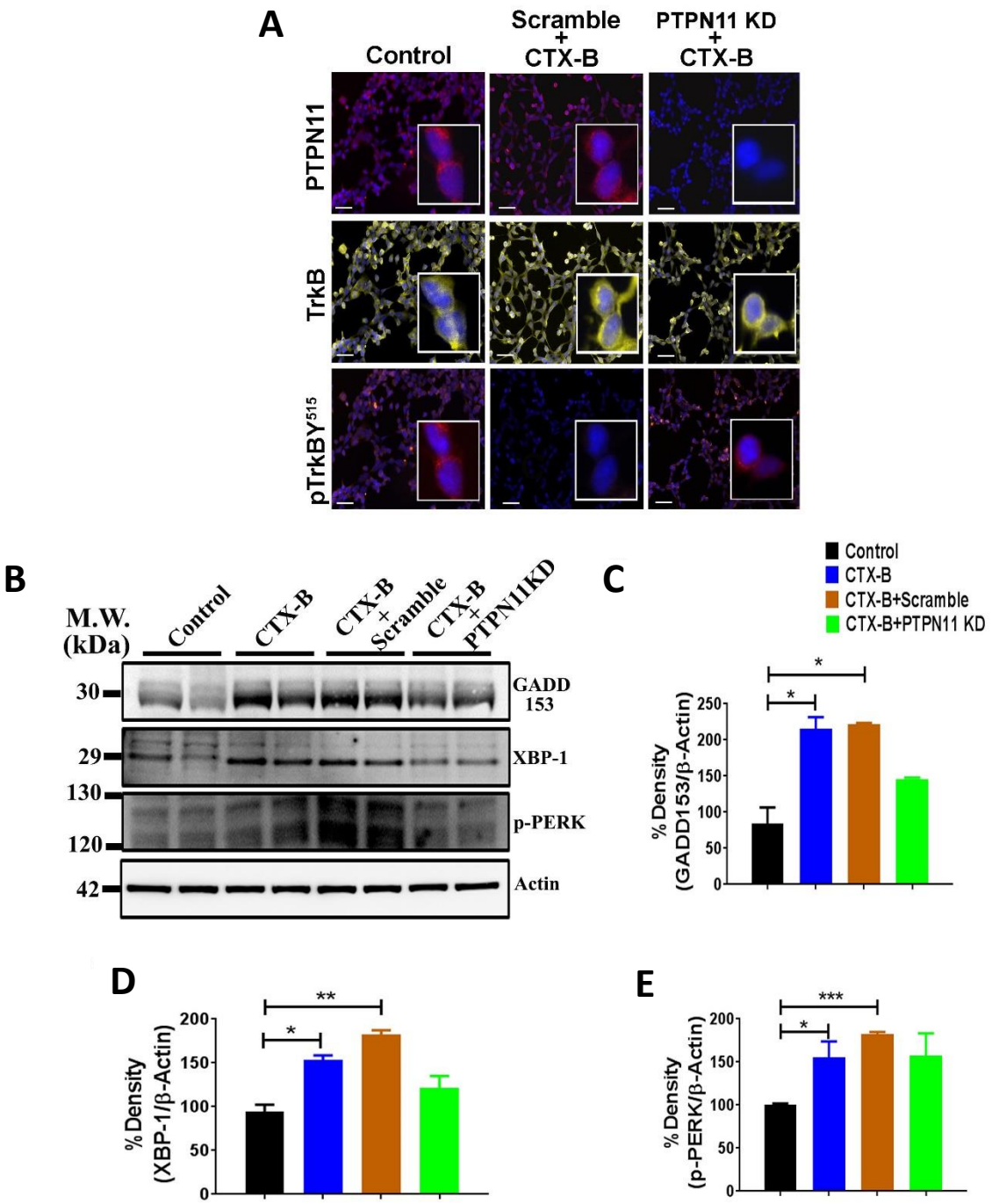

Figure 5.8. Effects of pharmacological modulation of TrkB on PTPN11 mediated TrkB changes and ER stress response on CTX-B treatment (A) SH-SY5Y cells pre-treated with TrkB antagonist, CTX-B (5 µM; 6 h) were subjected to *PTPN11* knockdown and cells stained against PTPN11 (red), TrkB (yellow) and pTrkB Y^{515} (orange) antibodies. CTX-B treatment in AAV scramble transduced SH-SY5Y cells resulted in loss of pTrkB Y^{515} activity. On the other side this loss in phosphorylation activity of TrkB was recovered in PTPN11 KD transduced neuronal cells. Scale 200 µm (B) Immunoblotting indicated an activation of ER stress marker in CTX-B and CTX-B+AAV scramble treated neuronal cells whereas ER stress immonoreactivity was downregulated in CTX-B+PTPN11 KD treated SH-SY5Y cells. (C-E**)** Densitometric quantification of SH-SY5Y cells shows significant changes in GADD153, XBP-1 and p-PERK expression under treatment of TrkB antagonist, CTX-B (*$p < 0.0001$; n=4). AAV Scramble, CTX-B alone and vehicle treated cells were used as control. *β*-actin was used as loading control.

5.3.5 PTPN11 upregulation induces neuronal apoptosis and its loss is associated with increased neuritogenesis

Due to increase in ER stress associated with PTPN11 overexpression, PTPN11 over-expressing neuronal cells were analyzed for differences cellular survival and apoptotic changes. Upregulation of ER stress markers has been suggested to promote apoptotic changes in several studies (Szegezdi et al., 2006, Sano and Reed, 2013). TUNEL assay was carried out 36 hrs post AAV2 transduction and results demonstrated increased TUNEL positive cells in this group compared to GFP and PHPS1 treated cells (Figure 5.9 A).

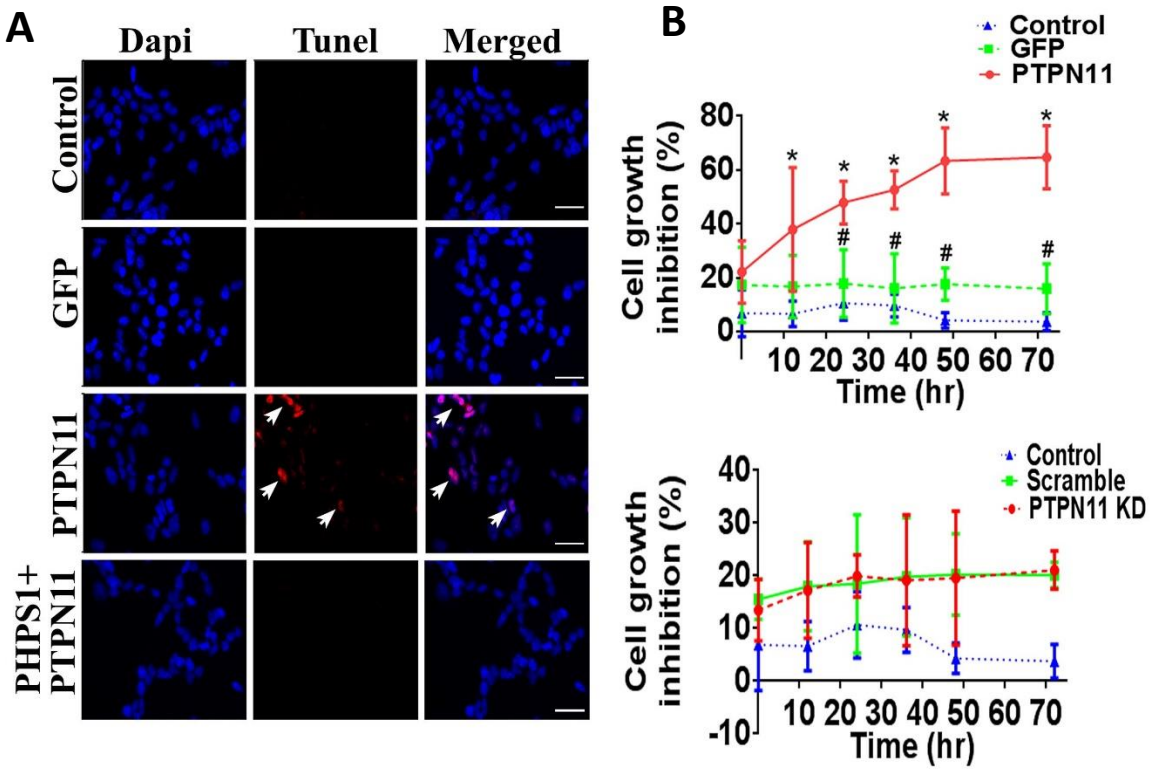

Figure 5.9. *PTPN11* upregulation induces cell apoptosis (A) SH-SY5Y cells overexpressing PTPN11 depicted enhanced TUNEL staining (red). GFP expressing and vehicle treated cells were used as controls. Scale 10 µm (B) An MTT proliferation assay was used to determine the ability of AAV to suppress SH-SY5Y cell proliferation at 0, 12, 24, 48 and 72 h after transduction. PTPN11 over-expression resulted in significant cell growth inhibition of SH-SY5Y cells. Absorbance was measured at 570 nm (mean ± SD; n=4; *p<0.05). Vehicle, GFP and Scrambled sequence treated neuronal cells were used as control.

PTPN11 inhibition remarkably eliminated the TUNEL staining in SH-SY5Y cells thereby establishing the role of PTPN11 upregulation in inducing cell apoptosis (Figure 5.9 A). These results matched with overall reduction in cellular viability as measured by Trypan blue assay in response to AAV2 mediated PTPN11 upregulation. No significant changes were observed in response to either PTPN11 knockdown, scramble or GFP control transduced cells (Figure 3.10).

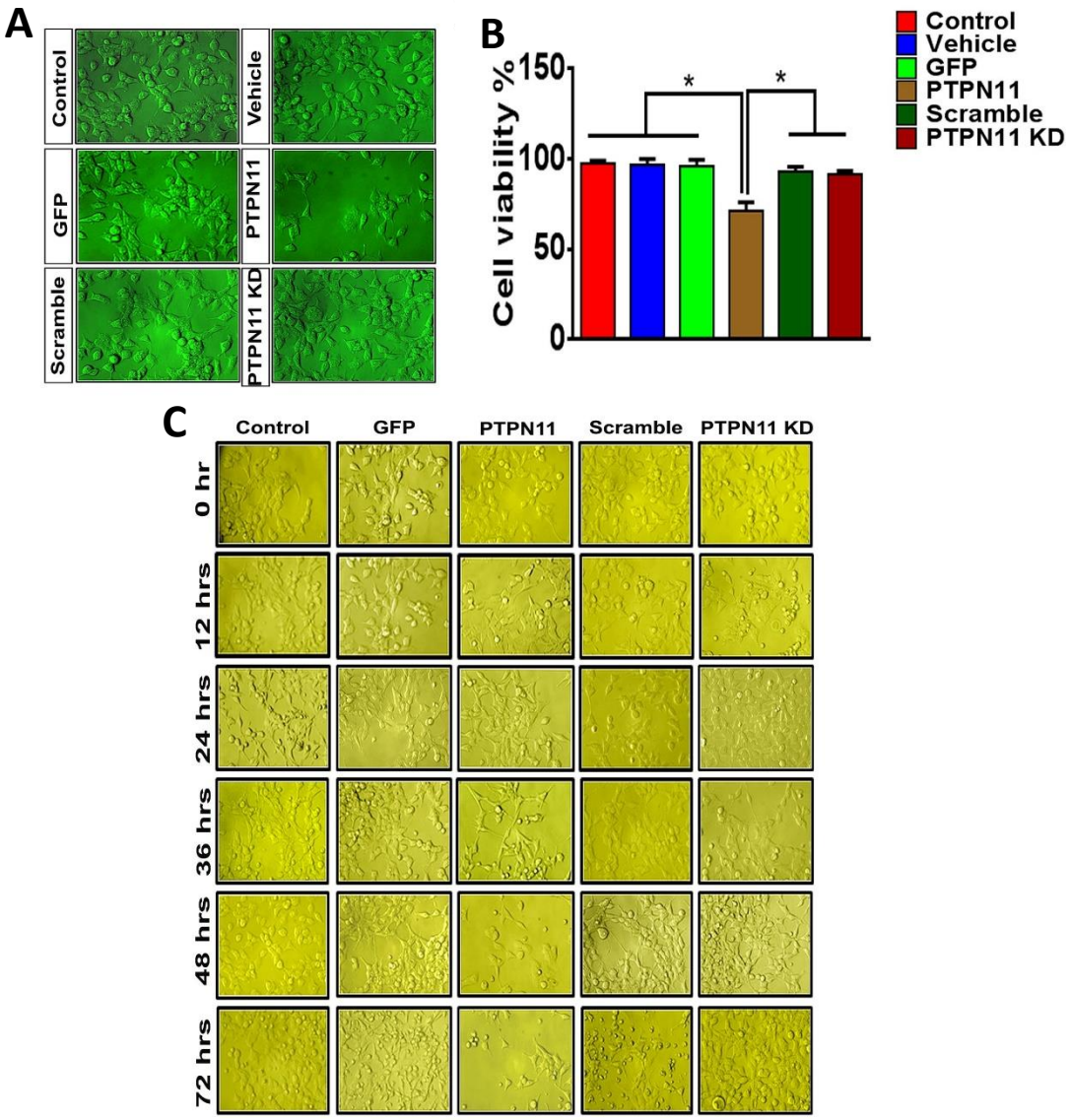

Figure 5.10 Cell viability and MTT Assay. **(**A**)** Total cell viability was evaluated on SH-SY5Y cells on different AAV viral construct. Non-treated, vehicle treated, GFP and scramble neuronal cells were used as control. (B) Cell viability was analysed by trypan blue exclusion assay. Significant decrease in cell viability percentage was observed under AAV expressing PTPN11 sequences. Data is presented mean±SD, n=4,

*p<0.05. (C) MTT assay demonstrating that PTPN11 over-expression resulted in significant cell growth inhibition of SH-SY5Y cells. Vehicle, GFP and Scrambled sequence treated neuronal cells were used as control.

MTT assay supported these findings and established time dependent inhibition of cell growth in PTPN11 upregulation system, while no significant changes were observed in PTPN11 knockdown, GFP and scrambled sequence transduced cells (Figure 5.9 B and 5.10 C). Furthermore, as ER extends into the dendrites and loss of TrkB is suggested to be associated with neuritogenesis (Salminen et al., 2009, Peng et al., 1995), we sought to delineate the differential effects of PTPN11 expression modulation on SH-SY5Y cell neuritogenesis. Results show that neuronal cells subjected to PTPN11 over-expression manifested in significant decline in neurite outgrowth compared to GFP transduced cells. On the other hand, significant increase in neurite outgrowth was detected in neuronal cells subjected to PTPN11 suppression compared to control cells (Figure 5.11). Together, these experiments unequivocally highlight the negative effects of PTPN11 upregulation on neuritogenesis and neuronal survival in culture.

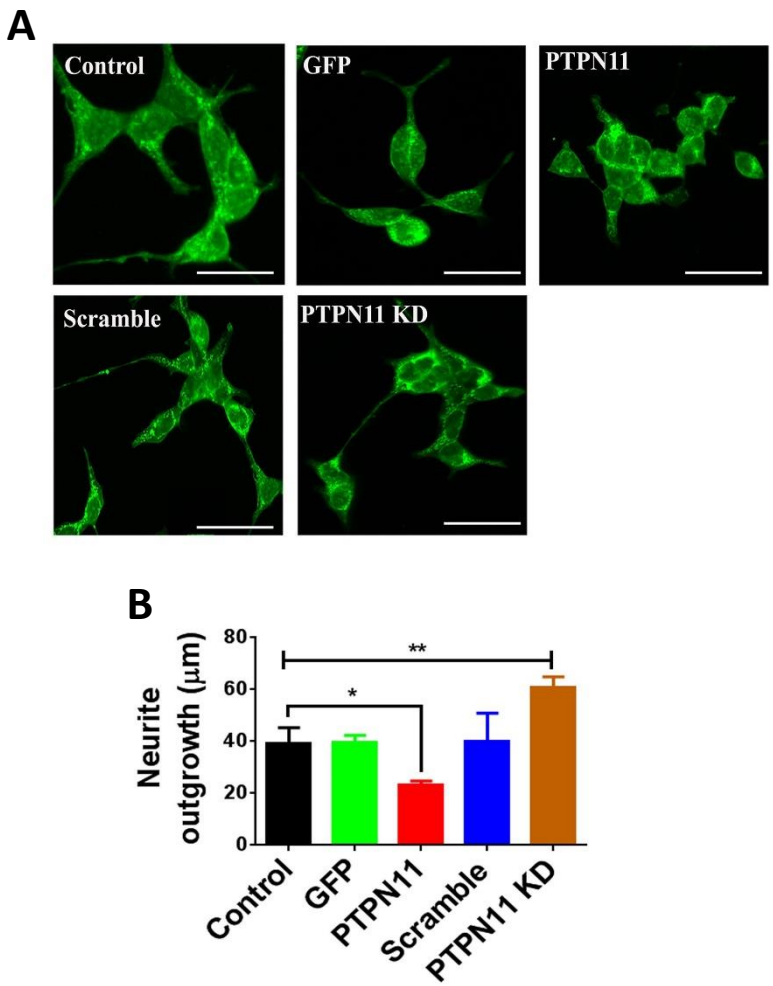

Figure 5.11. *PTPN11* upregulation suppresses neuritogenesis (A) Neuronal cells were immunostained with *β*III tubulin for neurite outgrowth in both overexpression and knockdown conditions. (Scale 100 µm). (B) A significantly reduction in neurite growth (*p<0.01) was observed in *PTPN11* over-expression system while an increase was observed in PTPN11 KD conditions (*p<0.01,**p<0.05; n=6). AAV GFP and scrambled expressing cells were used as controls. MTT assay supported these findings in time dependent cell growth inhibition in upregulation of PTPN11.

5.4 Discussion

PTPN11 both negatively and positively regulates various cellular signaling pathways through its scaffold function and phosphatase activity in a cell and tissue dependent manner (Li et al., 2012a). Missense mutations leading to PTPN11 hyperactivation or catalytic impairment are associated with genetic diseases (Qiu et al., 2014). This study established

that TrkB activation as demonstrated by receptor phosphorylation at Tyr^{515} in the neuronal cells in general is negatively regulated by PTPN11 actions. TrkB phosphorylation is associated with subsequent activation of downstream Shc-Ras-MAPK, PI3K/Akt, and PLCγ1 signaling cascades (Huang and McNamara, 2010, Gupta et al., 2013a). BDNF and its high affinity receptor TrkB contributes to neuronal survival, synapse formation and neural development in the central nervous system. In the retina, we reported previously (Chapter 3) that impairment of this signaling pathway is associated with age related inner retinal degenerative phenotype and exacerbation of experimental glaucoma induced RGC deficits (Gupta et al., 2014b). PTPN11 has been shown to be predominantly expressed in the GCL and INL of the retina although it also plays a role in indirectly supporting the photoreceptors survival through the Muller cells (Cai et al., 2011, Kinkl et al., 2002). We and others have previously demonstrated that PTPN11 interacts with TrkB in RGCs and other neuronal cells (Rusanescu et al., 2005, Gupta et al., 2012b).

In this study, we report that AAV mediated *PTPN11* overexpression in the cultured SH-SY5Y neuronal cells lead to loss of TrkB activation while its knockdown resulted in enhanced TrkB activation. PTPN11 regulatory effects on TrkB in neuronal cells were detectable independent of the BDNF treatment status. These results corroborate previous observations of PTPN11 co-immunoprecipitations with TrkB in neuronal cells (Rusanescu et al., 2005). This TrkB -PTPN11 interaction was suggested to be mediated through the adapter functions of caveolin (Cav) protein (Jo et al., 2014). As an adapter protein Cav binding may provide a signaling platform to PTPN11 and facilitate phosphatase mediated TrkB dephosphorylation by enhanced proximity effect. In order to further investigate the PTPN11 induced TrkB regulation, we pharmacologically inhibited the phosphatase using PHPS1 in the neuronal cells subjected to PTPN11 upregulation. Importantly, blocking

PTPN11 rescued TrkB phosphorylation highlighting potentially a direct involvement of the enzyme in coordinating TrkB activity. Pathological activation of PTPN11 can therefore impede TrkB actions induced by BDNF/NT-4 trophic factors or other agonists which may partially explain why the strategies to target TrkB directly have largely been unable to demonstrate protective effects in the long term. Dysregulation of the BDNF/TrkB axis is a critical factor underlying progressive and preferential loss of RGCs in healthy and disease conditions (Gupta et al., 2014b) and is suggested to constrain neurite arborisation and axonal regeneration (Hollis et al., 2009). Accordingly, PTPN11 upregulation was observed to inversely modulate neurite outgrowth in cultured neurons and result in apoptosis.

Secondly, we observed enhanced ER stress response elucidation in neuronal cells upon *PTPN11* upregulation as indicated by enhanced reactivity of various ER stress markers. ER disturbances are associated with unfolded protein responses (UPR) aimed to restore normal ER functioning, however prolonged stress and diminished adaptive response is associated with cellular dysfunction culminating in apoptotic activation (Fonseca et al., 2013). We found that pharmacologically inhibiting PTPN11 resulted in suppression of various ER stress markers indicating that PTPN11 activity underlies the neuronal ER stress response. Similar alterations in ER stress response caused by phosphatase modulation have previously been reported in liver cells (Nagata et al., 2012) and shown to augment Ca^{2+} release from ER in fibroblasts (Wang et al., 2006). Enhanced ER stress is observed in several neurodegenerative and acute disorders of the brain (Southwood et al., 2002). In the retina, enhanced ER stress has been implicated in macular degeneration, glaucoma and diabetic retinopathy (Zhang et al., 2014). Targeting ER stress in neuronal cells is suggested as a useful therapeutic target for glaucoma and other neurodegenerative disorders (Yang et al., 2016a). Neurotrophins have previously been implicated in preventing neuronal apoptosis and cell

death *via* suppressing ER stress response (Chen et al., 2007, Hetz, 2012). Our results underscore that BDNF pre-treatment protected neuronal cells from onset of ER stress response. BDNF was previously shown to protect neurons from apoptosis in tunicamycin-induced ER stress by selectively blocking activating transcription factor 6 (ATF6)/ GADD 153 pathway (Chen et al., 2007). This study supports that PTPN11 effects on ER stress can be rescued by BDNF mediated TrkB stimulation.

Several studies have previously shown BDNF/TrkB axis to be protective in ER stress response induced cell death in cerebral neurons *via* its opposing effects on GADD153 expression and nuclear translocation in neurons (Chen et al., 2007). Also, GADD153 ablated mice were more resistant to apoptosis induced by deprivation of neurotrophins (Tajiri et al., 2006). Other neurotrophins like NGF are also shown to attenuate ER stress mediate cell death (Shimoke et al., 2004). Here, we aimed to investigate whether enhanced ER stress is directly caused by PTPN11 increase or alternatively by TrkB effects subsequent to *PTPN11* dysregulation. Results support that ER stress elucidation by *PTPN11* is indeed dependent on cross-talk with TrkB signaling. TrkB agonist treatment effectively blocked PTPN11 induced ER stress and reciprocally *PTPN11* knockdown rescued the cells against ER stress caused by TrkB antagonist treatment. Thus, we propose an interdependent and coordinated activity of PTPN11 and TrkB in mediating ER stress response. Pharmacological blocking experiments and rescue by TrkB agonist also implicate that ER stress is induced by the upregulated PTPN11 activity and not emanating *per se* from excessive protein accumulation or increased synthesis rates of the PTPN11.

In neuronal cells, ER extends into dendrites, dendritic spines and synaptic terminals in neurons and therefore ER stress can affect neuritogenesis and axonal preservation (Murakami et al., 2007). On the other hand, axonal injury is shown to induce neuronal ER

stress and accordingly ON injury induced ER stress resulted in enhanced RGC death while its downregulation is demonstrated to protect RGCs against glaucomatous neurodegeneration (Yang et al., 2016a). We observed reduced cell viability, increased cell growth inhibition and onset of apoptotic changes associated with *PTPN11* over-expression in the culture SH-SY5Y cells. These apoptotic changes were also remarkably accompanied by reduced neurite length while neurons subjected to PTPN11 downregulation exhibited slight increase in neurite outgrowth. Persistent ER stress initiates apoptotic response via cJNK and caspase 4/12 pathways (Fonseca et al., 2013). For instance, apoptosis is suggested to be induced by GADD153 upregulation that has an activation effect on GADD34 that further increases oxidation in stressed ER (Marciniak et al., 2004). Xbp-1 is similarly synchronous with upregulation of several proteins linked to UPR (Sriburi et al., 2004) and PERK targets eIF2α inhibiting protein synthesis (Laszlo and Wu, 2009). Cellular apoptosis in different retinal layers particularly the GCL was previously reported in PTPN11 mutant transgenic mice (Cai et al., 2011). Although the details of the mechanism by which PTPN11 and TrkB dysregulation induce ER stress and their involvement in neurite preservation are not well understood, ER Ca^{2+} release may be an early event that precedes ER stress and associated neurite loss (Li et al., 2013b). PTPN11 was indeed shown to predispose neuronal cells to excitotoxic damage through negative regulation of TrkB activity while PTPN11 ablation augmented TrkB phosphorylation that corresponded with increased cellular survival against Ca^{2+} excitotoxicity (Rusanescu et al., 2005). Neuritogenesis changes may also be mediated through the PTPN11 associated TrkB signaling as its selective deletion has been reported to attenuate neurite outgrowth (Hollis et al., 2009). Moreover, we have already demonstrated that flavonoid agonist of TrkB- 7,8 DHF promotes neuritogenesis in retinal neuronal cells by stimulating neurite outgrowth, suggesting a possible therapeutic strategy for protection of RGCs in various optic neuropathies.

In conclusion, the present study highlighted that PTPN11 is part of tightly regulated signaling network that connects TrkB dysregulation with ER stress and apoptosis. The findings implicate a pathological impact that prolonged *PTPN11* activation may have on the neurons in general and form the molecular basis of several neurodegenerative disorders implicating PTPN11 as an attractive drug target.

CHAPTER **6**

Shp2 upregulation impair inner retinal environment and negatively regulates TrkB receptor activity

This chapter was presented in 19th Annual Meeting of American Society of Gene and Cell Therapy, ASGCT 2016, Washington DC, US

Manuscript is in preparation

Part of the abstract published as:

Nitin Chitranshi, Roshana Vander Wall, Yogita Dheer, Stuart L. Graham, Vivek K Gupta. AAV Mediated Gene Therapy to Modulate Neurotropic Factors in the Retina and in Neuronal Cells in Culture. ***Mol. Therapy*** 24: S321-S350; doi: 10.1038/mt.2016.80

Abstract

In the recent time, ocular gene therapy approaches have gained popularity in a variety of retinal diseases. In particular, clinical trials for RPE65 mutations, linked to inherited retinal dystrophy, and retinitis pigmentosa due to MERTK mutations have been conducted at different centers, showing that adeno-associated virus (AAV)- mediated gene therapy is safe. Gene therapy to modulate brain derived neurotrophic factor (BDNF) and its high affinity receptor, tropomyosin receptor kinase B (TrkB) in retinal ganglion cells (RGCs) has been largely unsuccessful due to short-lived protective effects on the RGCs and yet not been studied the failure mechanism in detail. In this study, retinal morphology, functions and apoptotic changes were examined in healthy rat retinas following AAV mediated modulation of *Shp2* gene using intravitreal injection with AAV2.CAG.GFP.2A.mShp2 (overexpression) or AAV2.CAG.GFP.shRNAmir (knockdown). Inner retinal morphology was assessed by histology analysis and immunohistochemical labeling. *Shp2* upregulation in RGCs was associated with morphological alterations in the inner retinal laminar structure leading to reduced RGCs and optic nerve axonal count. Furthermore, prolonged *Shp2* upregulation also resulted in an impaired electrophysiological response in the inner retina. In agreement with these physiological observations, *Shp2* upregulation was associated with TrkB antagonism, and enhanced endoplasmic reticulum (ER) stress. Increased number of TUNEL labeling positive RGCs was observed in retina overexpressing *Shp2*. Post injection *Shp2* knockdown did not alter any inner retinal morphology and function, but showed increased TrkB Y^{515} phosphorylation and reduced ER stress. These observations support the negative role of Shp2 in RGCs in regulating BDNF/ TrkB signaling pathways and suggest that *Shp2* knockdown could have a beneficial effect in disease associated RGC degeneration.

6.1 Introduction

Neurodegeneration might be either a direct result of neuronal loss that occurs over a developed timeframe, resembling in Alzheimer's (AD) and Parkinson's diseases (PD), or to associate an acute neurological insult, as, in ischemia or trauma. Neurodegeneration is a important reason for illness and death, furthermore the reasons of extraordinary expenses not in the advantage of general wellbeing. (Cho et al., 2007). Yet, for most neurodegenerative issues there are relatively few effective therapies. One reason for the lack of therapeutic strategies is the inaccessibility of the complex brain because of the blood–brain barrier (BBB) and the skull. In assessment of the brain, neurons of the eye and the optic nerve, that is comprised of ganglion cell axons, are successively accessible and are thus suited to study neurodegeneration and neuroregeneration inside the central nervous system (CNS) (Esiri, 2007).

Src homology 2-containing protein-tyrosine phosphatase 2 (Shp-2 or PTPN11) is a controller of tyrosine kinase receptor signaling (Neel et al., 2003). Shp2 assumes an imperative role in cell signaling and diseases like, cancer, cardiovascular impairment, glaucoma, Noonan syndrome and other neurodegenerative diseases that are well examined (Pan et al., 2010, Jiang and Zhang, 2008, Lauriol et al., 2015, Gupta et al., 2012b, Gomez del Rio et al., 2013, Graham et al., 2009). *Shp2* is highly expressed in RGCs in rodent retina. Latest investigations reinforce that Shp2 is localized in retinal neurons and dorsal root ganglion neurons and also involved in the intracellular signaling of axon coordinating signals (Fuchikawa et al., 2009). Shp2 has likewise been seen to play an important role in mediating BDNF-activated signaling that advance the formation of dendritic spines (Kim et al., 2007). Cai *et. al* demonstrated the role of Shp2 in retinal degeneration in *Shp2* mutant mouse retina. ERK signaling, particularly in Müller cells, are disrupted and augment Stat3 in photoreceptors. However, neither inactivation of Stat3 nor stimulation of AKT signaling

could enhance Shp2 related retinal degeneration. Rather, constitutively actuated k-ras signaling not only rescued the RGCs count in the *Shp2* mutant, but additionally improved the electroretinogram recording (ERG) (Cai et al., 2011). Moreover, the protective role of Shp2 was demonstrated in retinal progenitor cells by the activation of Ras/ERK signaling during optic nerve vesicle patterning (Cai et al., 2010b).

TrkB has high affinity for ligand BDNF and upon TrkB activation downregulates neuronal cell survival signaling pathways. However, the activity of TrkB is regulated by Shp2 in RGCs. Under glaucomatous stress, Shp2-TrkB interaction is increased and contributes to dephosphorylation of TrkB and results in inhibition of downstream pro-survival signaling pathways involving PI3K, phospholipase C-γ1 and MAPK mediated TrkB activation (Gupta et al., 2012b, Gupta et al., 2013a). Exogenous administration of BDNF can sublunary activate TrkB and rescue RGCs transiently (Di Polo et al., 1998, Clarke et al., 1998). Under normal physiological conditions, receptor tyrosine kinase randomly undergoes phosphorylation and dephosphorylation to maintain the harmony in the downstream signaling for proper cell functioning (Huang and Reichardt, 2003). The mechanism underlying a change of sensitivity of BDNF treatment to TrkB needs more examination.

AAV vectors are considered optimal for ocular gene therapy because of their efficiency, persistence, site specific integration and low immunogenicity (Daya et al., 2009). Our hypothesis was that an AAV incorporating Shp2 would be useful in understanding the neurotrophic and TrkB signaling pathway. We tested this hypothesis using intravitreal injection of AAV viral vector overexpressing and knockdown *Shp2* in healthy rat RGCs. We report a marked and statistically significant decrease in RGC survival as estimated by axon counting and increase in ER stress after 8 weeks in rats treated with AAV-Shp2 compared with control virus without *Shp2*. The study also provides direct evidence for the involvement of Shp2 in molecular regulation of TrkB activity in the animal RGCs and ER stress

associated with its dysregulation. Impairment of inner retinal laminar structure, loss of axons and electrophysiological response along with induction of apoptosis in ganglion cell layer (GCL) upon *Shp2* upregulation provides "proof-of-concept" for the key contribution of *Shp2* homeostasis in influencing neuronal compliance in adult CNS in general and in retina.

6.2 Materials and Methods

Ethics, chemicals and animals used are described in chapter 2, *sections 2.1, 2.2* and *2.3.1*.

6.2.1 AAV vectors-Design and packaging

Chapter 2, *section 2.3.2* describes the detailed methodology of viral vector design and packaging.

6.2.2 AAV2 vectors intravitreal injections

Chapter 2, *section 2.3.3* describes the intravitreal injections of AAV2 expressing mShp2, eGFP, mShp2shRNA and shRNAScramble sequence in detail.

6.2.3 Electroretinography

Electroretinographic (ERG) recordings were performed as described previously (Richards et al., 2006). Detailed methodology is presented in chapter 2, *section 2.3.6*.

6.2.4 Histology

As described in chapter 2, *section 2.3.7.1*, animal eye and ON were fixed, embedded and sectioned. Animal eye tissue were stained with H & E as reported previously, chapter 2, *section 2.3.7.2* (You et al., 2014, Gupta et al., 2014b). GCL density was determined by counting the number of cells in the layer over a distance of 500 μm (100-600 μm from the edge of the optic disc) using light microscopy. Inner nuclear and inner plexiform layer thickness was also evaluated and compared between control and viral vector treated retinas. ON section were made 5 μm thick and subject to Bielschowsky's silver staining as reported previously, chapter 2, *section 2.3.7.3* (You et al., 2014) and number of axons counted (10^{-2} mm^2) to evaluate changes in axonal density (Gupta et al., 2016).

6.2.5 SDS PAGE and western blotting

For animal eyes, following enucleation and retinal dissection, optic nerve head (ONH) regions of the retina were surgically excised from the retina under a microscope and lysed in lysis buffer mentioned in chapter 2, *section 2.3.8.2*. Protein concentrations and SDS-PAGE was performed as described in chapter 2, *section 2.3.8.1* and *2.3.8.2* respectively Membranes were incubated overnight with anti-GFP (1:1000), anti-Shp2 (1:1000), anti-pTrkB Y^{515} (1:1000), anti-TrkB (1:1000), anti-GADD 153 (1:200), anti-XBP-1 (1:200), anti-p-PERK (1:200) and anti-actin (1:5000) overnight at $4^{\circ}C$. Further, followed as stated in chapter 2, *section 2.3.8.2*.

6.2.6 Immunofluorescence

Cryostat tissue sections were used for immunofluorescence. Detailed methodology is described in chapter 2, *section 2.3.7.5*.

6.2.7 Statistical Analysis

The ERG/STR amplitudes, fluorescence changes, and retinal thickness differences, axon density in optic nerve were plotted and analysed using GraphPad Prism software (version 6.0) (GraphPad Software, San Diego, CA). All values with error bars are presented as mean ± SD for given n sizes and compared by Student's t test and two-way ANOVA. The significance was set at $p < 0.05$.

6.3 Results

6.3.1 Assessment of transgene expression in healthy animal eyes

To investigate the effect of Shp2 up-or downregulation on RGCs and axonal survival in normal conditions, rats were intravitreally injected with AAV2 viral vectors. The tropism of AAV2 has been shown to selectively target RGCs in the rodent retina (Cheng et. al 2002; Fisher et al, 2004; Moore et al. 2009). Shp2 was experimentally over-expressed with AAV2 incorporating *Shp2* cDNA (AAV2-Shp2), whereas its downregulation was induced using AAV2 containing a shRNAmir sequence specific to rat Shp2 (AAV2-shRNAmir-Shp2 or AAV2-Shp2KD). Antibody NeuN is used to stained neuronal cells in GCL (Figure 6.1). AAV2-GFP and AAV2-Scramble virus vector were used as a corresponding control. The expression of GFP and Shp2 was monitored by immunofluorescence on intact (Figure 6.2 A, C) after AAV2 delivery. In intact retinae, compared with AAV2-GFP injection (Figure 6.2 A, ii, iii and 6.2 C, ii, iii), caused a significant upregulation of Shp2 after intravitreal injection of viral vector expressing *Shp2* (Figure 6.2 B; n=12 rats/group, $^{*}p<0.01$, unpaired t-test, 42-50 cells/rat). The significant downregulation of Shp2 was also observed in AAV2-Shp2KD injected retinae (Figure 6.2 C, v, d; n=12 rats/group, $^{*}p<0.01$, unpaired t-test, 4-8

cells/rat). No fluorescence detection of GFP was observed in control retinal section (Figure 6.2 A, i). GFP fluorescence detection in retinal sections (Figure 6.2 A, ii-v) revealed AAV2-mediated expression of the target gene in cells mostly located in the RGCL.

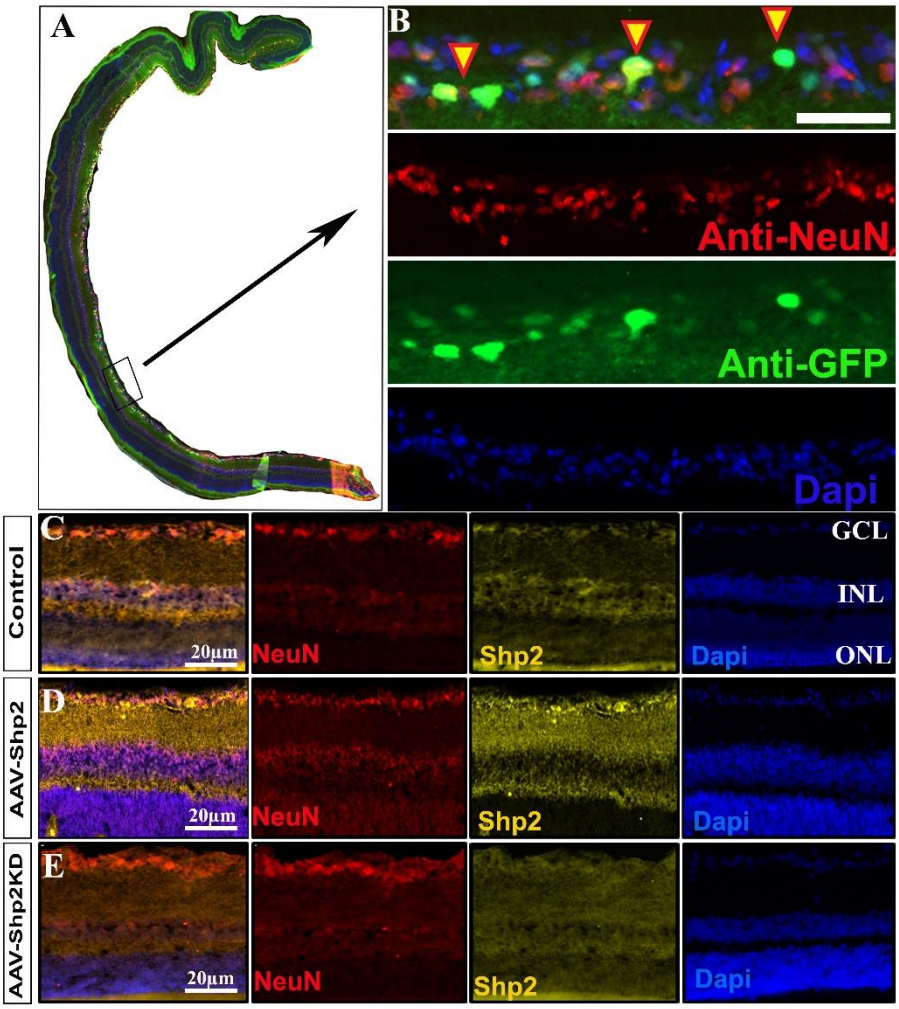

Figure 6.1. Expression of GFP in the inner retina of rat following intravitreal injection. (A) Complete retina immunostaining (B) expression of anti-GFP (green), anti-NeuN (red) and Dapi (blue) to stain nucleus. Expression of Shp2 was detected by anti-Shp2 (yellow) in (C) control, (D) retina expressing Shp2 sequence and (E) shRNA (PTPN11) in the RGCs. Scale 100 µm and 20 µm.

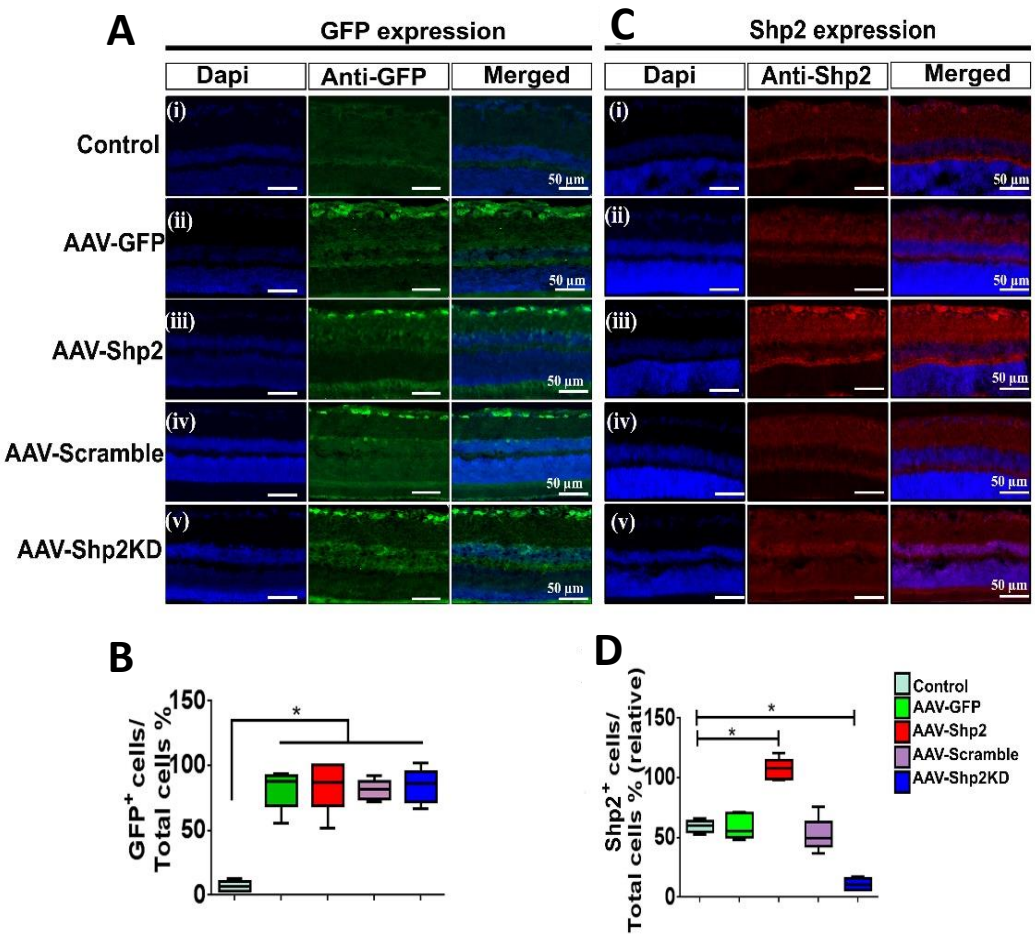

Figure 6.2. Transgene (GFP and Shp2) expression in normal rat eyes under healthy condition. Rat eyes were injected with viral constructs overexpressing and knockdown *Shp2* sequence. GFP alone or GFP co-expressed with scrambled peptide were used as controls (final concentration, 3.4×10^{12}VG/ml). Eyes were enucleated, sectioned, and stained with DAPI, anti-GFP and, anti-Shp2 to evaluate expression of (A) GFP, scale 50 µm (B) proportion of GFP-positive RGCs in the GCL, 8 weeks after rat intravitreal injection. Following intravitreal injection significant increase the expression GFP positive RGCs were observed compared to non-injected and AAV2-GFP injected eyes ($^{*}p<0.0001$; n=12 each). (C) Expression of Shp2. Scale 50 µm (D) proportion of Shp2-positive RGCs is significantly increased in AAV2 expressing Shp2 whereas significant decrease in Shp2 positive GCs was observed in Shp2 knockdown compared to control and AAV2-Scramble injected eyes ($^{*}p<0.0001$; n=12 each).

The transfection efficiency of the Shp2 in ONH region was also assessed with western blot analysis. Blotting and quantitative results for GFP and Shp2 are shown in Figure 6.7. Data are presented as an adjusted ratio of either GFP or Shp2 to Actin. As expected, equal levels of GFP were expressed in rat ONH treated with viral vector. These data show that AAV2 are effective in up-regulating or down-regulating Shp2 in RGCs.

6.3.2 Reduced GCL density and axonal loss in response to Shp2 upregulation

As the BDNF/TrkB signaling plays a critical role in the preservation of inner retinal architecture (Gupta et al., 2014b) and our data suggested negative regulation of TrkB by Shp2 in SH-SY5Y cells (chapter 5), we sought to investigate the impact of Shp2 overexpression in the rat retina. Morphological changes in retinas transduced with different AAV2 constructs were assessed using haematoxylin and eosin staining (H and E) (Figure 6.3 A, D). Assessment of GCL count revealed significant reduction in the GCL density overexpressing Shp2 sequence compared to AAV-GFP control eyes (Figure 6.3 A and B). Also, there was a significant reduction in the thickness of inner plexiform layer (IPL) while inner nuclear layer (INL) showed no remarkable differences compared to GFP control transduced retina (Figure 6.3 C). Retina subjected to Shp2 knockdown and scramble AAV control injected animals revealed no reduction GCL density percentage and retinal layer thickness (Figure 6.3 E and F). Given that ON axons are an extension of RGCs, we focused on assessing changes in ON axonal density to further validate inner retinal changes. Axonal staining was performed using Bielschowsky's silver stain method (You et al., 2014) and alterations in axonal density was evaluated in Shp2 overexpression and knockdown conditions (Figure 6.3 G-L). The results showed significant decline in ON axonal counts in Shp2 upregulated eyes (Figure 6.3 G-I), thereby providing further evidence to support the observations made in the retinal histological analysis (Figure 6.3 A and B). The retinal H and E staining of Shp2 knockdown and scramble sequence control eyes identified no significant loss in the ON axonal count (Figure 6.3 J-L). These observations support the hypothesis that prolonged Shp2 upregulation in RGCs is detrimental to the inner retinal and ON structure.

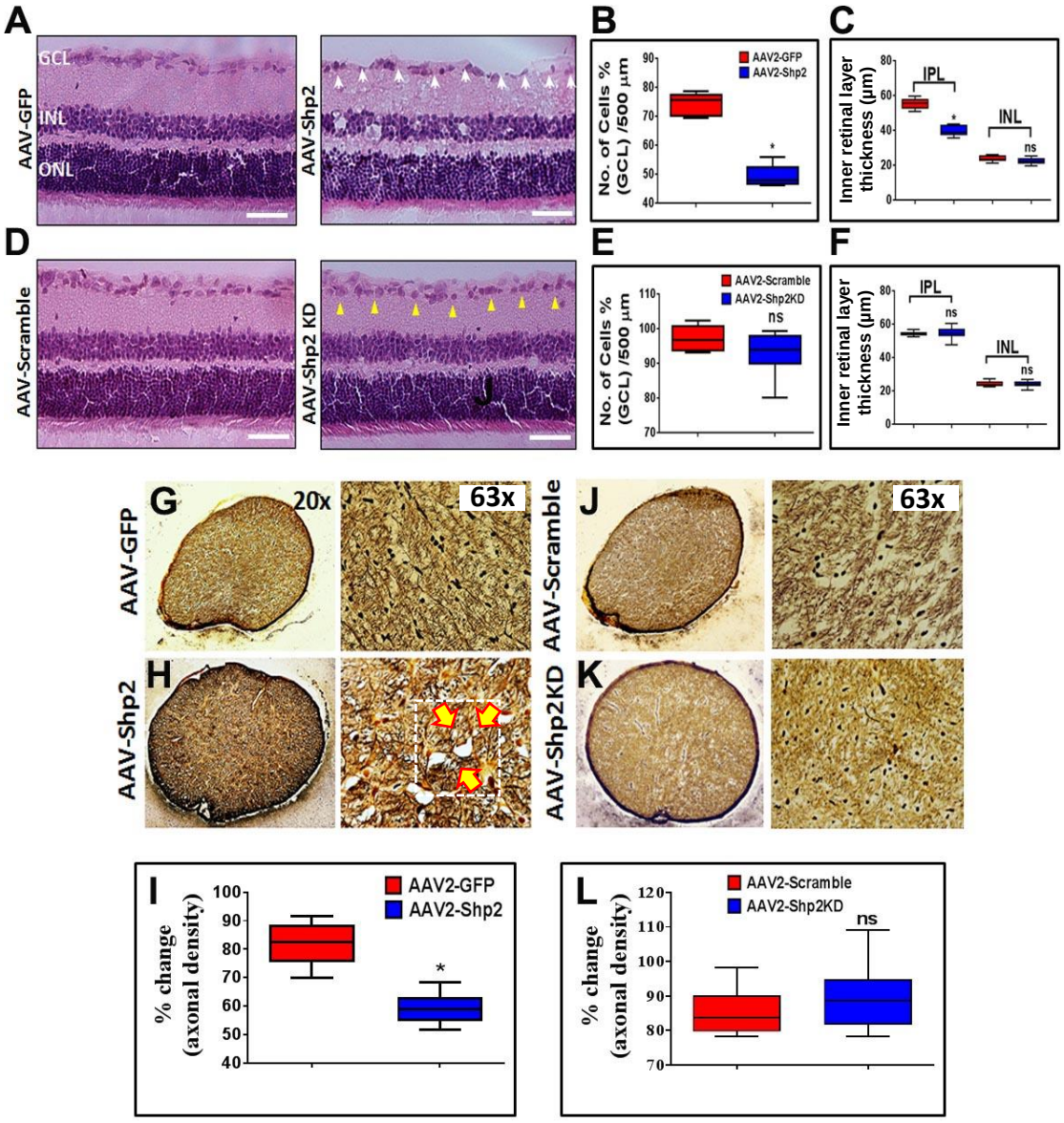

Figure 6.3. Retinal and optic nerve morphometric changes induced by *Shp2* upregulation. (A and D) H and E staining of the rat retinal sections in *Shp2* overexpression and knockdowm conditions respectively. AAV-GFP and scramble treated retina were used as respective controls. Scale 50 µm. (B) Quantification of GCL% density was found significant in Shp2 overexpression retina compared to GFP alone treated animal eyes (*p<0.0001, n=14 in each group). (D) Significant reduction in IPL thickness (*p<0.0001, n=14 in each group), whereas no change in INL thickness was observed in animal retina overexpressing Shp2. No significant difference was noticed in (E) GCL% (F) inner retinal layer thickness % of animal expressing shRNAmir sequence. (G, H) Bielschowsky's silver staining of the ON highlighted loss of axonal density % in *Shp2* overexpression compared to eye (shown in yellow arrow head), left 20x; right 63x. (I) Quantification graph showing significant decrease in percentage change in axonal density (n = 8 per group; *p<0.002). (J, K) Axonal density percentage remain unaffected in *Shp2KD* condition. Left 20x; right 63x. (L) Quantification of optic nerve tissue axonal density percentage (n=8 in each group).

6.3.3 Shp2 upregulation impairs inner retinal electrophysiological response

Given that Shp2 upregulation was associated with inner retinal structural deterioration, we speculated whether these changes translated to functional phenotype and whether animals depicted a structure-function correlation. Towards this end, retinal electrophysiological recordings were carried out in rat RGCs transduced with either of the four AAV2 viral constructs. Effects of Shp2 modulation were evaluated after period of 2 months follow up. Significant decline in pSTR amplitudes was detected in animal eyes overexpressing Shp2 compared to GFP injected and control retina (Figure 6.4 A and B). pSTR predominantly reflects inner retinal activity and its impairment indicates compromised inner retinal function. In contrast, viral vector expressing either shRNAmir or scramble animal eye did not show any remarkable changes in pSTR amplitudes, strongly suggesting preservation of inner retinal micro-environment (Figure 6.4 C and D). These results advocate that Shp2 suppression in the adult rat RGCs although increased TrkB phosphorylation (Figures 6.7 and 6.8), was not associated with a noticeable phenotypic trait. Whole retinal scotopic electrophysiological response (ERG) demonstrated preservation of a-wave amplitudes and latencies indicating that outer retinal function remained largely unaffected in both Shp2 overexpression and knockdown paradigms (Figure 6.4 A-F). A slight reduction in b-wave amplitudes was observed in AAV2 induced Shp2 overexpression eyes, although this loss was statistically not significant (Figure 6.5 A and B). IOP measurements also did not reveal any significant variation in any of the animal groups indicating that AAV injection could not be attributed to IOP changes (Figure 6.6). Thus, consistent with structural findings, electrophysiological measurements support the conclusion that Shp2 upregulation is associated with inner retinal functional deficits.

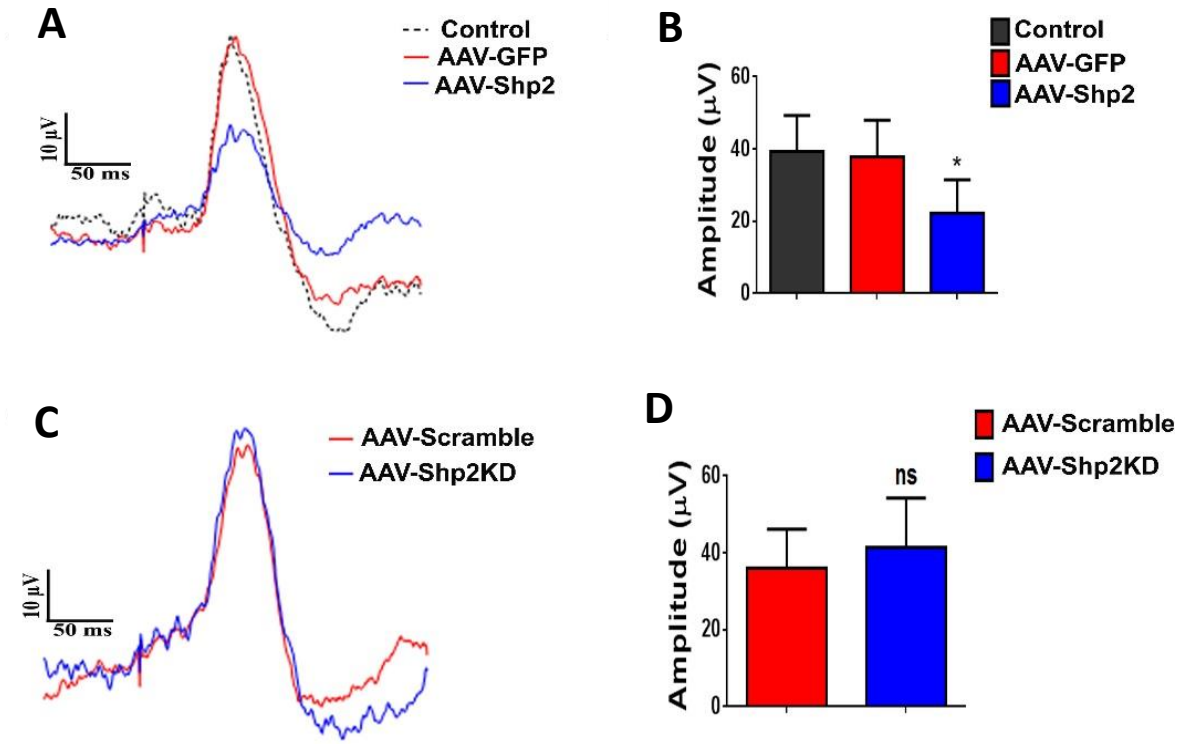

Figure 6.4. Shp2 upregulation in RGCs induces inner retinal functional loss. (A) Average trace of pSTR signal from the Shp2 retinas (blue), GFP expressing (red) and control eyes (black dotted line). The pSTR was evaluated after 2 months of GFP and Shp2 intravitreal injection in rat eyes. (B) Quantification indicates a significantly lowered amplitude of pSTR in the Shp2 compared to the GFP and control eyes (n = 14 per group; *$p < 0.05$). (C) Average traces of pSTR obtained from Shp2KD (blue) treated rat eyes compared to scramble control (red). The pSTR was evaluated after 2 months after scramble and Shp2KD intravitreal injection in rat eyes. (D) Graph indicating no significant change in amplitude either expressing Shp2KD or scramble control sequence (n = 14 in each group).

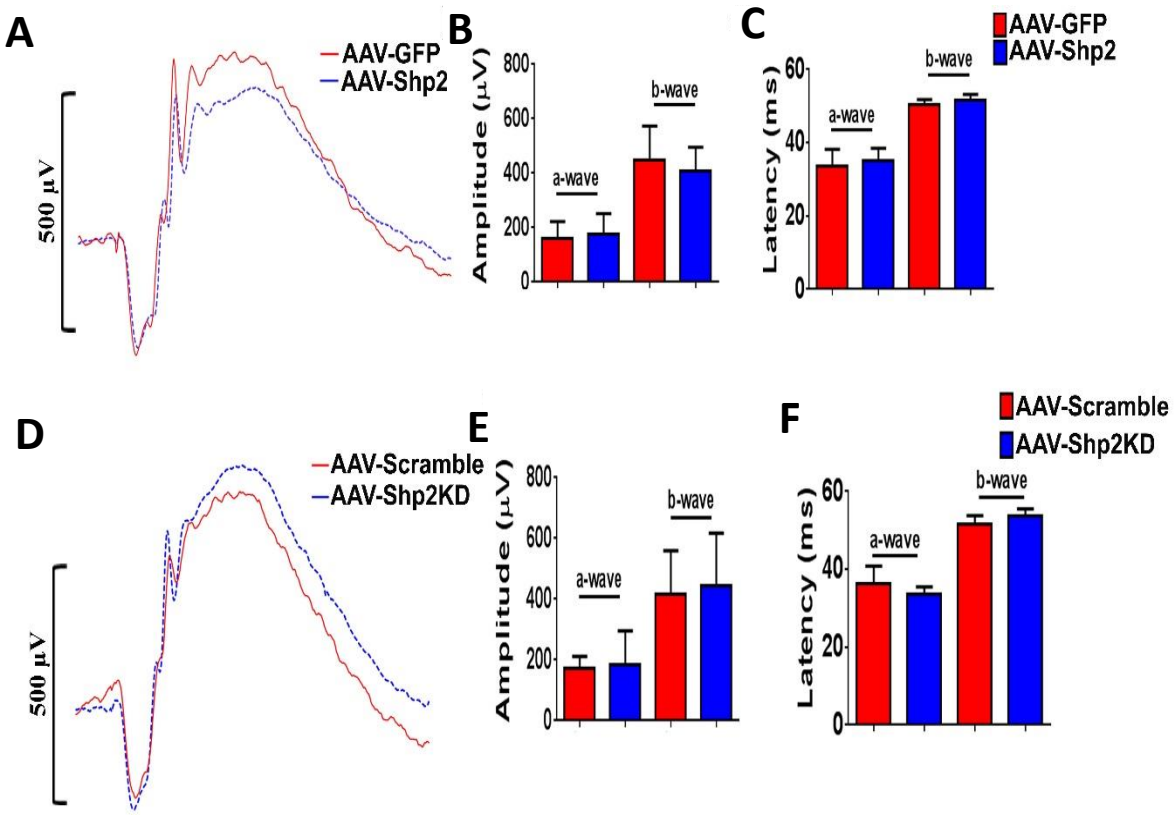

Figure 6.5. Effect of Shp2 overexpression and knock down on scotopic ERG (A) No change in scotopic ERG was recorded in animal injected with viral vector expressing Shp2 sequence. Quantification shows no change in (B) scotopic ERG –a and –b wave amplitude and (C) in latency (D) No change in scotopic ERG was recorded in animal injected with viral vector expressing Shp2KD sequence. Following quantification shows no change in (E) scotopic ERG –a and –b wave amplitude and (F) in latency. GFP and scramble sequence were used as control for Shp2 overexpression and knockdown respectively.

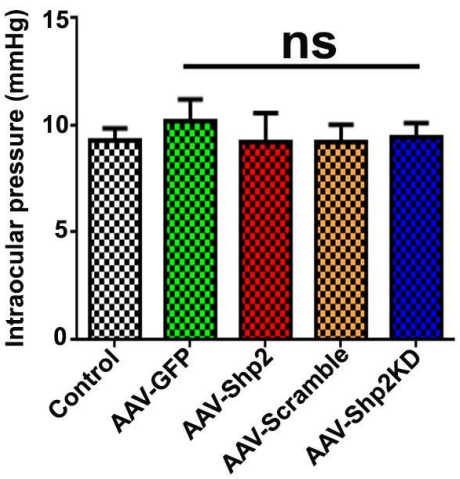

Figure 6.6. No elevation in IOP was noted after AAV injection.

6.3.4 Shp2 has regulatory effects on TrkB phosphorylation

We have demonstrated the effect of Shp2 (PTPN11) modulation on TrkB activity in SH-SY5Y cells *in vitro* (Chapter 5). To recapitulate the results in *in vivo* we have examined the change in TrkB activity upon Shp2 upregulation and down regulation in ONH and in the rat RGCs. As discussed in chapter 5, *Shp2* modulation was achieved by viral construct AAV2 (Figure 5.1) using eGFP and scramble sequence as control for overexpression and knockdown respectively. Immunoblotting of ONH tissue lysates validated protein expression alterations in response to AAV transduction (Figure 6.7 A). Supporting the previous evidence of Shp2 mediated regulation of TrkB actions (Gupta et al., 2012b), we observed that *Shp2* upregulation resulted in reduced TrkB Y^{515} phosphorylation in both ONH and rat RGCs (Figure 6.7 A and 6.8). Conversely, *Shp2* knockdown lead to increased Y^{515} phosphorylation of TrkB compared to the scramble control in both ONH and rat RGCs (Figure 6.7 A and 6.8). Analysis of TrkB expression in retinal tissue revealed that there was no compensatory change in total TrkB protein levels in response to AAV treatment or *Shp2* modulation (Figures 6.7 A and D and 6.8), suggesting that loss of Y^{515} phosphorylation is intervened through the bonafide phosphatase action of Shp2. Similar findings were also reported in neuronal SH-SY5Y cells *in vitro* (Chapter 5, Figure 5.2). Overall, these outcomes implicate the *in-vitro/ in-vivo* correlation that Shp2 phosphatase activity negatively modulates the TrkB phosphorylation.

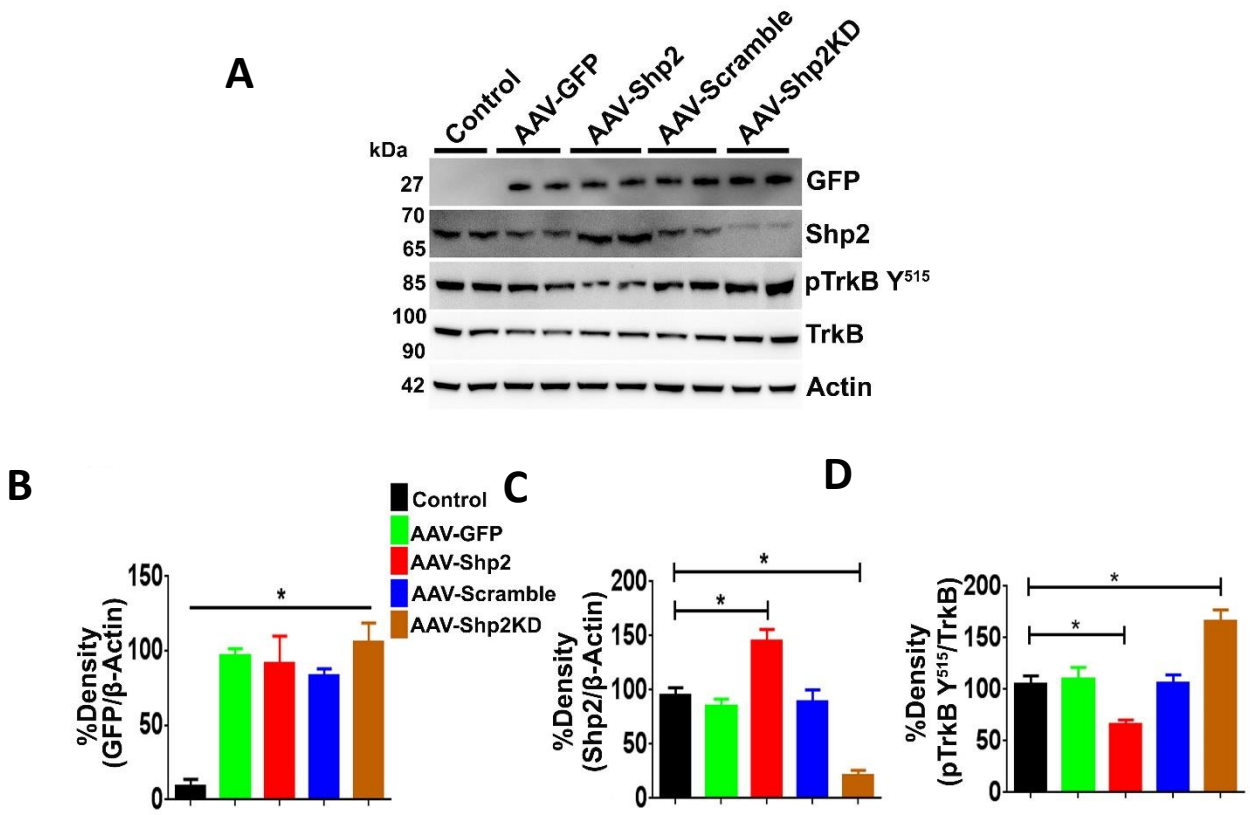

Figure 6.7. *Shp2* modulation negatively affects TrkB Y^{515} phosphorylation in rat ONH (A) Western-blot of AAV transduced ONH lysate for expression of GFP, Shp2, TrkB, pTrkB Y^{515} and actin (loading control) showed similar results in SH-SY5Y cells (Chapter 5, Figure 5.2) that the level of pTrkB Y^{515} is dependent on Shp2 modulation *in vivo*. (B) Densitometric quantification of GFP protein expression in ONH of rat retina injected with four different AAV viral construct (*$p<0.001$; ANOVA; Brown-Forsythe test). (C) Quantification of Shp2 under *Shp2* overexpression and knockdown experiment showed significant changes in Shp2 expression compared to control rat ONH. (*$p<0.02$, *$p<0.006$; student t test). (D) Densitometric analysis of pTrkB Y^{515} in ONH relative to TrkB showed significant decrease in pTrkB Y^{515} in *Shp2* overexpression and significant increase in pTrkB Y^{515} under *Shp2*KD viral construct injected rat retina (*$p<0.02$, *$p<0.02$; student t test). Saline injected, GFP alone and scrambled sequence were used as controls (n=8 in each group), data are mean±SD and value correspond to three independent experiment.

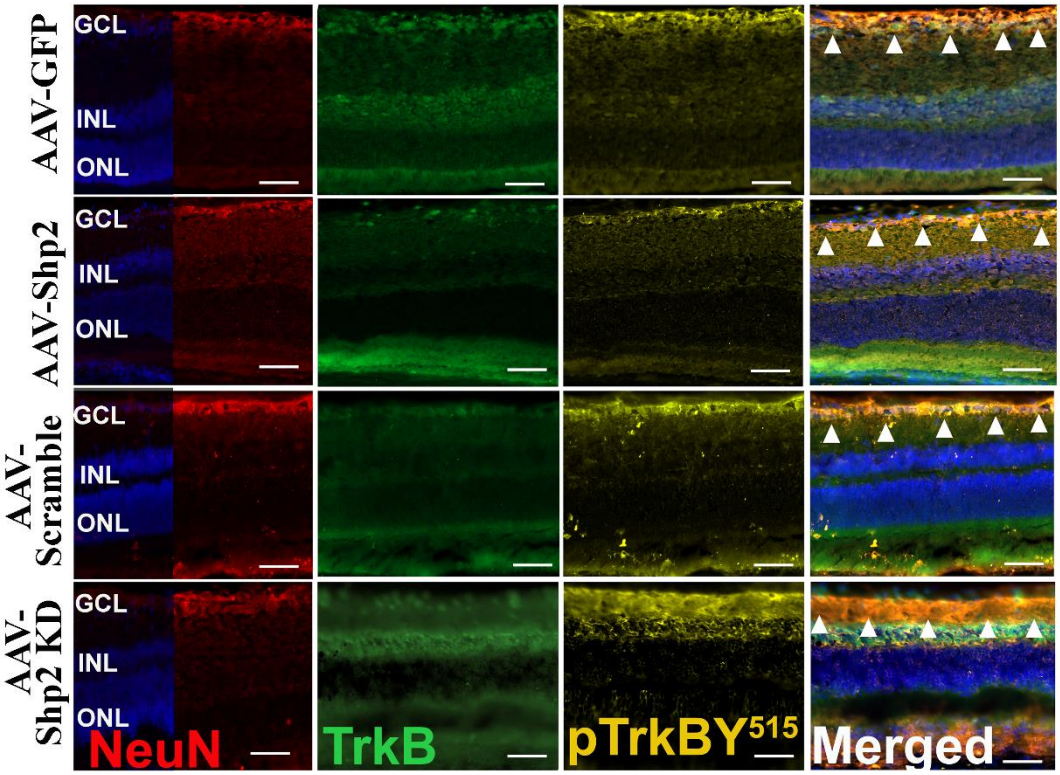

Figure 6.8. Cryosections of rat retina showed expression of RGCs, anti-NeuN (red), anti-TrkB (green) and anti-pTrkB Y^{515} (yellow) expression. Dapi for visualizing cell nuclei as landmark. Note the expression of pTrkB Y^{515} in GCL of Shp2 overexpression and Shp2KD intravitreal injected rat retina (shown in white triangle box). AAV expressing GFP and scramble sequence was used as control. (n=8 in each group, scale 20 µm).

6.3.5 Shp2 upregulation induces neuronal apoptosis and ER stress in retina

Shp2 overexpression was associated with SH-SY5Y cell growth inhibition, significant loss of neurite outgrowth (Chapter 5, Figure 5.11) and increased apoptosis (Chapter 5, Figure 5.9). Further, visible retinal laminar structure in response to *Shp2* overexpression in RGCs (Figure 6.3) demanded investigations into potential effects on cell apoptosis. To delineate Shp2 physiological effects, rat retinas with promoter specific overexpression of *Shp2* in their RGCs were investigated for apoptotic changes and staining revealed TUNEL positive cells in the GCL layer (white arrow). Control, GFP and scramble sequence transduced retinas were used as controls (Figure 6.9). In the control, GFP, scramble and retinas with *Shp2* knocked down RGCs, in line with previous results on structural-functional elucidation,

showed no significant TUNEL staining (Figure 6.9). Upregulation of ER stress markers has been suggested to promote apoptotic changes in several studies (Szegezdi et al., 2006, Sano and Reed, 2013). To evaluate ER stress associated with *Shp2* overexpression, Shp2 overexpressed retinal sections were analyzed for GADD153 expression. As for the effects of *Shp2* modulation on rat RGCs, a significant upregulation of GADD153 immunoreactivity was demonstrated in response to *Shp2* over-expression (Figure 6.10). AAV expressing eGFP alone or scrambled sequence for *Shp2* knockdown were used as controls. *Shp2* suppression, conversely, was not associated with any notable differences in expression of GADD153. Altogether, this experiment demonstrated that whereas *Shp2* upregulation contributed to cell apoptosis and enhanced ER stress, the response was not dependent on the loss of endogenous levels of Shp2 in neurons.

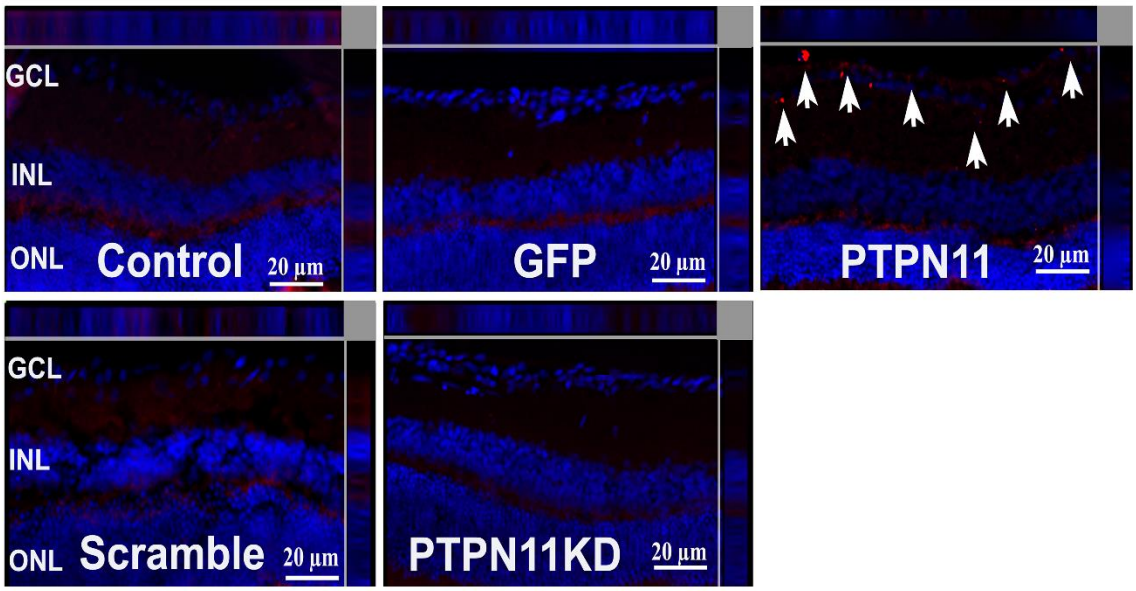

Figure 6.9. *Shp2* upregulation induces cell apoptosis. Rat retinal sections over-expressing *PTPN11 (*or *Shp2)* were immunostained with TUNEL assay kit for apoptotic changes and demonstrated notably increased TUNEL reactivity (red), DAPI (blue). Non-treated, AAV-GFP and AAV-Scramble sequence expressing retinas were used as controls. Scale 20 µm.

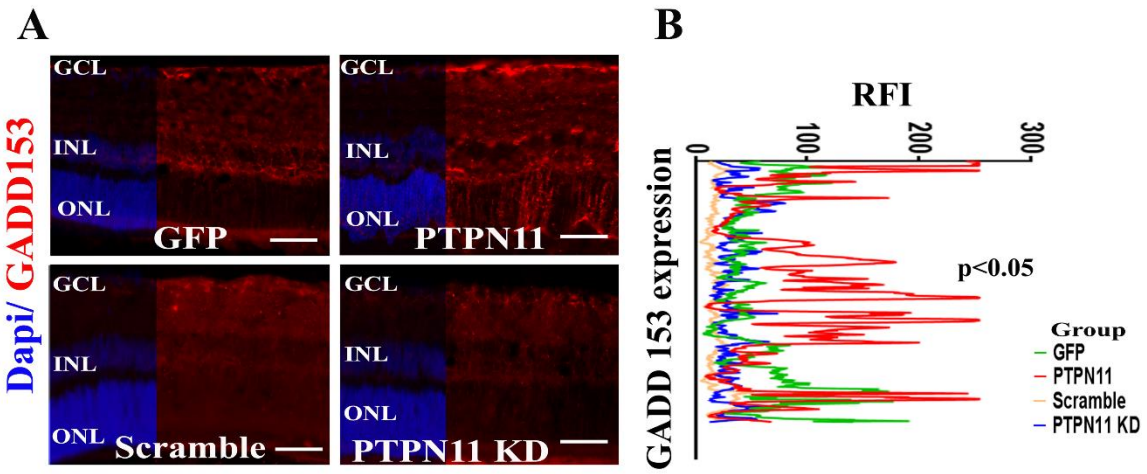

igure 6.10. *PTPN11* (or *Shp2*) upregulation is associated with enhanced ER stress marker response (A) Rat retinal sections subjected to *PTPN11* modulation were stained with ER stress marker GADD153 (red) and Dapi (blue). AAV constructs expressing GFP and scrambled sequence were used as controls. Scale 20 µm. (B) Image J was used to plot relative intensity of immunofluorescence signal in each case (*p<0.05; n=8).

6.4 Discussion

BDNF and its receptor, TrkB, are well expressed in the retina particularly in the ganglion cells and we have shown previously that impairment of this signaling pathway is associated with the inner retinal degenerative phenotype (Gupta et al., 2013a). BDNF and other neurotrophic factors stimulate intracellular TrkB signaling for neuronal survival, morphogenesis, and plasticity (Qian et al., 2017). The sustained dephosphorylation of TrkB obstructs cell revival and additional neuroprotective effects of intrinsic neurotrophic factors like BDNF and NT-4. Our previous findings have suggested that TrkB and Shp2 interact with each other under normal physiological conditions and negatively regulate the phosphorylation activity of TrkB in a cell and tissue dependent manner (Gupta et al., 2012b).

This study established that TrkB activation in the RGCs is regulated by Shp2 actions. *Shp2* upregulation negatively affected the TrkB phosphorylation, while its knockdown enhances

phosphorylation of TrkB at Tyr^{515} involving in the binding of SHC adaptor protein and downstream signaling (Yamada et al., 2001, Easton et al., 2006). Shp2 modulation was further associated with alterations in ER stress response and apoptotic changes. In the RGCs, this lead to loss of cells in GCL and functional impairment. Here, we report that AAV-mediated *Shp2* overexpression in the RGCs and in ONH leads to loss of TrkB activation while *Shp2* knockdown resulted in increased TrkB activation (Figure 6.7 and 6.8). This corresponds with previous reports that Shp2 interacts with TrkB and regulates its activity in culture. This interaction was reported to be mediated through interactions with caveolin (You et al., 1999, Gupta et al., 2012b).

The physiological relevance of changes in *Shp2* expression was established by specifically investigating its role in rat RGCs. We provide evidence that *Shp2* upregulation led to the loss of GCL and IPL and associated diminution of ON axonal density, although its downregulation had no discernible effects on the retinal laminar structure. Cai et al. (2011), demonstrated that *Shp2* ablation in the embryonic stages resulted in severe retinal degenerative phenotype and ON dystrophy (Cai et al., 2011). This variance is likely attributed to pre- and post-natal developmental roles of *Shp2* in the retina and may also be contributed to by promoter-specific differences. *Shp2* has indeed been shown to provide axonal guidance through its Sema4D-induced signaling role and localization in the growth cones of chick embryonic RGCs (Fuchikawa et al., 2009). Shp2 also plays a key role in Ras/Erk signaling in retinal progenitor cells and orchestrates retinal and ON morphogenesis (Cai et al., 2010a). Normal RGCs survival and retinal anatomy in $BDNF^{+/-}$ mice during maturation support the notion that *Shp2* participation in retinal development may be either independent of BDNF signaling or only partially dependent on it and possibly linked to Shp2 adapter functions (Gupta et al., 2014b). Our results do not rule out the possible complementation of Shp2 actions conferred by the interplay of other tyrosine phosphatase

and kinase signaling networks in the adult RGCs. Corresponding to the retinal structural attrition upon *Shp2* upregulation, significant deficits in pSTR amplitudes were observed highlighting a preferential impairment of the inner retinal function. To our knowledge, this is the first report highlighting the pathological association of *Shp2* dysregulation with inner retinal function. Although *Shp2*KD biochemically correlates inversely to the effects of *Shp2* over-expression, no retinal structural or functional phenotypic changes were noticed, which we believe was anticipated due to the post-mitotic nature of the adult retinal neurons.

Shp2 is ubiquitously expressed phosphatase with a multi-substrate target that is implicated in downstream cell signaling pathway of the BDNF stimulated TrkB phosphorylation. Whether Shp2 regulates other pathways that are relevant to neuronal cell survival is yet to be determined. Stimulation of receptor tyrosine kinases comprising TrkB activates the kinase cascade of RAS, c-Raf, MEK, MAPK, AKT and ERK1/2, subsequent to the modulation of transcription of various genes (Murphy and Blenis, 2006, Patapoutian and Reichardt, 2001). BDNF persuades phosphorylation of Shp2 both in neuronal cells and primary cortical neurons (Easton et al., 2006). The neurotransmitter, glutamate and BDNF interact to regulate development and neuroplasticity via Ca^{2+} influx activating kinases and phosphatases that act on a variety of substrates including ion channels and cytoskeletal proteins (Mattson, 2008). However, several proteins required for SH2 domains activation of Shp2 that bind phosphorylated tyrosine motifs (Pawson and Scott, 1997). Tyr^{515} is the important residue of TrkB phosphorylation for binding of SHC adaptor protein and downstream signaling initiation (Minichiello et al., 1998). Suppression of BDNF-stimulated MAPK/ ERK pathway *via* inhibition of Shp2-TrkB interaction using glucocorticoid has also been reported (Kumamaru et al., 2011). Dopamine D_1 receptor and Shp2 interactions trigger the D_1-mediated Erk1/2 signaling in striatal neurons (Fiorentini et al., 2011).

Shp2 is thought to play a multifarious role in interacting with and modulating the activity of its protein substrates (Gupta et al., 2012b). TrkB is a transmembrane receptor tyrosine kinase, whereas Shp2 is an intracellular phosphatase that is localized to the cytoplasm and participate in signal transduction from the cell surface to the nucleus (Gupta et al., 2012b). It is conceivable that the Shp2-TrkB interaction and TrkB receptor dephosphorylation occur after ligand-induced receptor internalization, like epidermal growth factor and platelet-derived growth factor receptors (Gupta et al., 2013a, Yamada et al., 1999). Alternatively, Shp2 interacts with the adapter protein caveolin, Gab, and FRS2/SNT and may recruit Shp2 for TrkB receptor dephosphorylation, as in the case of insulin receptor signaling (Gupta et al., 2012b, Kelly-Spratt et al., 1999). The precise biochemical mechanism by which Shp2 attenuates TrkB signaling needs further investigation.

ER is a sensitive organelle which recognizes disturbances in cellular homeostasis and activates protective signaling cascades to evoke biochemical adaptive responses (Lin et al., 2008). Neuronal ER stress is already established as a key pathway and activates a signaling network to generate the unfolded protein response (UPR) in neurodegenerative diseases (Salminen et al., 2009, Soo et al., 2015). We observed enhanced ER stress response elucidation as indicated by enhanced immunoreactivity of GADD153 ER stress markers in the GCL in retinas overexpressing *Shp2*. Similar modulation of ER stress response caused by *Shp2* changes has previously been reported in liver cells (Agouni et al., 2011) and *Shp2* resulted in enhanced Ca^{2+} from ER in glial cells (Ibanez, 2013). ER stress may induce an inflammatory response *via* different UPR transducers in glaucoma affected RGCs and in other neurodegenerative disorders. Enhanced ER stress has been observed in neurodegenerative disorders of the brain such as Alzheimer's disease. In the retina, increased ER stress has been implicated in macular degeneration, glaucoma and diabetic retinopathy (Zhang et al., 2014). ER stress onset is associated with UPR aimed to restore normal ER

functioning however, prolonged stress and diminished adaptive response is associated with cellular dysfunction and apoptotic cell death (Kim et al., 2008). Accordingly, we observed onset of apoptotic changes (TUNEL positive) associated with *Shp2* overexpression in GCL in the retina *in vivo.* The physiological relevance of Shp2 expression changes in the CNS was demonstrated using GCL of the rat retina.

In conclusion, the present study highlighted that Shp2 overexpression modulated the inner retinal environment and is associated with reduced TrkB activation and enhanced ER stress response. The precise biochemical mechanism by which Shp2 attenuated TrkB signaling in RGCs may needs further investigation. Nevertheless, this study elucidated that TrkB activity is tightly regulated by Shp2 and its pathological activation may form the molecular basis of several retinal disorders like glaucoma and neurodegenerative disorders of the brain.

CHAPTER 7

Shp2 gene therapy is effective in RGC neuroprotection in experimental glaucoma

The abstract of this chapter was presented in ARVO-ASIA 2017, Brisbane, Australia

Nitin Chitranshi, Vivek K Gupta, Yogita Dheer, Stuart L Graham. Adeno-associated virus knockdown of Shp2 phosphatase protect inner retinal structure and function in experimental glaucoma.

Manuscript is under preparation

Abstract

Retinal ganglion cell (RGC) loss and axon damage lead to blindness in glaucoma , therapies that increase RGC and axon survival can be directly relevant to clinical intervention. Activation of tropomyosin-receptor-kinase B (TrkB) receptor by neurotrophic factor is a critical mechanism to promote neuronal cell survival, but in glaucoma TrkB deactivation is augmented through adapter protein, Shp2. In this study we investigated the therapeutic potential of Shp2-TrkB signaling in RGC survival and axonal neuroprotection using an adeno-associated virus serotype 2 (AAV2) to deliver Shp2-shRNAmir in a rodent microbead model of experimental glaucoma. We tested whether knockdown (KD) of Shp2 expression prevents neuronal death and facilitates TrkB signaling in RGCs subject to chronic elevation of intraocular pressure (IOP) in a rodent model. Our data indicate that RGCs exposed to high IOP and treated with AAV2-Shp2KD displayed a significant protection in ganglion cell layer (GCL) density (51.61±3.22% vs 69.38±2.88%, $p<0.003$) and axonal loss (51.42±4.2 vs 75.91±1.84, $p<0.0001$). We also found protective effect of Shp2KD in positive scotopic threshold response (pSTR) amplitude (18.18±3.98µV vs 32.47±4.01µV, $p<0.05$) and increase in phospho-TrkB activity at Thr^{515} in GCL of glaucoma retina (18.18±3.98µV vs 32.47±4.01µV, $p<0.05$). These findings suggest that increased TrkB activation in RGCs attenuates retinal damage in experimental animal model of glaucoma.

7.1 Introduction

RGC axon degeneration and ONH cupping are the important features of glaucoma and eventually lead to permanent blindness. POAG is the most common type of glaucoma (Walland et al., 2012). Elevated IOP is the prominent risk factor in POAG which is most common form but lowering of IOP is not always sufficient to stop the progression of the optic neuropathy (Katz et al., 1990). Therefore, glaucoma is thought to be a neurodegenerative disease, open to therapies (*i.e.* stem cell, gene etc) other than lowering of IOP (Mead et al., 2015, Foldvari and Chen, 2016). While substantial effort has been made to develop neuroprotection agents in the management of glaucoma that prevent retinal neuronal loss or delay disease progression (Gossman et al., 2016). RGC neuroprotective strategies were previously demonstrated using PDGF (Chong et al., 2016), BDNF (Gupta et al., 2014b), magnesium acetyltaurate (Lambuk et al., 2016) and brimonidine (Guo et al., 2015) in rodent models of ocular hypertension, retinal excitotoxicity and optic neuritis (Li et al., 2013a).

Earlier reports have suggested for neurotrophins and their receptors have a protective role in RGCs (Galindo-Romero et al., 2013, Bikbova et al., 2013). BDNF has high affinity to TrkB, the Trk family of receptor tyrosine kinases, is well expressed in RGCs (Gupta et al., 2012b, Ren et al., 2012) and plays a critical role in RGCs degeneration in glaucoma (Cheng et al., 2002). BDNF is produced in the superior colliculus during development of retinocollicular projection and binds to the TrkB receptor in different splice variants TrkB-full length (TrkB-FL) and TrkB-truncated from-1 (TrkB-T1), lacking the C-terminal intracellular kinase domain (Fenner, 2012) and undergoes retrograde transport in microsomal vesicles *via* RGC axons to the cell bodies (Marotte et al., 2004). Exogenous administration of BDNF activates TrkB and transiently BDNF-TrkB activation can rescue RGCs, however subsequent doses

or multiple use of BDNF fail to support long term survival of RGCs which finally become inactive to the defensive impact of BDNF (Cheng et al., 2002, Di Polo et al., 1998).

TrkB sensitivity to BDNF in glaucoma is poorly understood. To maintain adequate equilibrium in the downstream signaling, receptor tyrosine kinase undergoes random phosphorylation and dephosphorylation (Lemmon and Schlessinger, 2010). Therefore, simultaneous dephosphorylation and deactivation of TrkB by an interacting phosphatase may restrain the protective effects of BDNF. One such phosphatase is SH2 domain-containing tyrosine phosphatase-2 (Shp2 or PTPN11), intermediate in neurotrophin induced activation of TrkB under normal and glaucomatous stress (Gupta et al., 2012b). In brain Shp2 regulates neuronal cell differentiation and neuronal plasticity, thereby controls locomotor activity and memory formation (Kusakari et al., 2015). However, negative regulation of Shp2 has been reported in cerebral neuron activation through BDNF in a calcium dependent manner (Rusanescu et al., 2005).

Recent studies on retinal gene delivery using viral vectors has been shown to be effective in protecting structural and functional damage in several ocular diseases (Venkatesh et al., 2013, Bennett et al., 2012, Lau et al., 2000, Wassmer et al., 2017). In addition, it was shown that BDNF-expressing adenoviral vector has the capability to delay RGC death after optic nerve transection (Di Polo et al., 1998). However, the short duration of efficient transgene expression and tendency to induce inflammation are the limitations of viral vector based on adenovirus. Adenoassociated virus (AAV) overcomes adenovirus restrictions and is effectively used in a broad range of host species (Peel and Klein, 2000, Hosel et al., 2017, Chamberlain et al., 2017, Brady et al., 2017).

In continuation to the findings from chapter 6 which demonstrated that long term *Shp2* upregulation in animal RGCs is associated with functional and morphological degenerative

changes in inner retina, we hypothesized that *Shp2* knockdown would be protective in experimental glaucoma. We tested this hypothesis in a microbead injected rat model of glaucoma, previously well established in our lab, creating chronic IOP elevation with consequent specific loss of RGCs in the inner retina (You et al., 2014). We report a marked and statistically significant increase in RGC survival, axonal protection, pSTR improvement and phosphor-TrkB activity after 8 weeks of experimental glaucoma in rats treated with intravitreal AAV-Shp2KD compared with intravitreal AAV-Scramble or control with virus.

7.2 Material and Methods

Used of animals and chemicals are described in chapter 2.

7.2.1 Microbead Injection and IOP measurement

Detailed procedure of microbead injection and IOP measurement is described in chapter 2, *section 2.3.4*.

7.2.2 AAV vectors-Design and packaging

Chapter 2, *section 2.3.2* describes the detailed methodology of viral vector design and packaging of *PTPN11* gene (Shp2) silencing.

7.2.3 AAV2 vectors intravitreal injections

Chapter 2, *section 2.3.3* describes the intravitreal injections of AAV2 expressing mShp2shRNA sequence in detail.

7.2.4 Electroretinography

Electroretinographic (ERG) recordings were performed as described in chapter 2, *section 2.3.6*.

7.2.5 Histology

As described in chapter 2, *section 2.3.7.1*, animal eye and ON were fixed, embedded and section. Animal eye tissue were stained with H & E as described in chapter 2, *section 2.3.7.2*. GCL density and retinal layer thickness were calculated as described in chapter 6, *section 6.2.4*. ON subjected to Bielschowsky's silver staining and axonal density calculation as mentioned in chapter 2, *section 2.3.7.3* and chapter 6, *section 6.2.4*.

7.2.6 SDS PAGE and western blotting

Detailed protocol is mentioned in chapter 2, *section 2.3.8.2*.

7.2.7 Immunofluorescence

Following fixation for 2 hrs in 4%PFA, the eyes and ON were washed incubated in 30% sucrose overnight and embedded in tissue Tek OCT cryostat embedding medium (Sakura Finetek) as described previously (Gupta et al., 2016) in chapter 2, *section 2.3.7.5*.

7.2.8 Statistical Analysis

The ERG/STR amplitudes, fluorescence changes, and retinal thickness differences, axon density in optic nerve were plotted and analyzed using GraphPad Prism software (version 6.0) (GraphPad Software, San Diego, CA). All values with error bars are presented as mean

± SD for given n sizes and compared by Student's t test and two-way ANOVA. The significance was set at $p < 0.05$.

7.3 Results

7.3.1 Intravitreal injection of microbead induced intraocular pressure elevation in animal eyes

A chronic RGC degeneration model was established with repeated microbead injections into the anterior chamber leading to long-lasting increase in IOP were like those seen in previous studies (Feng et al., 2016, Gupta et al., 2012b). Twenty-four SD rats were treated with microbead administration unilaterally. The baseline IOP (mean±standard deviation) before treatment was 9.32±0.17 mmHg, 8.18±0.33 mmHg, 8.17±0.33 mmHg and 9.58±0.23 mmHg in the control, glaucoma, glaucoma+AAV2-scramble and glaucoma+AAV2-Shp2KD treated eyes (n=32), respectively, and IOP is measured using icare TonoLab. With the microbead treatment, the IOP of all treated eyes increased at least 12-13 mmHg from baseline IOP. However, the IOP of some animals returned to normal after 1-2 weeks. The second, third and fourth week microbead treatment was performed on these animals after the first treatment. The resultant IOP was again higher than the baseline and remained elevated during the period of two months. Figure 7.1 shows the average changes in IOP in every group on the control and the animal treated eyes. After microbead treatment, the mean IOP of the microbead injected eyes after 8 weeks in three groups was greater than 18 mmHg (19.84±0.17, 20.78±1.67 and 20.71±1.53) as compared to control. However, there was no significant difference in mean IOP among the three treated groups ($p>0.05$, ANOVA).

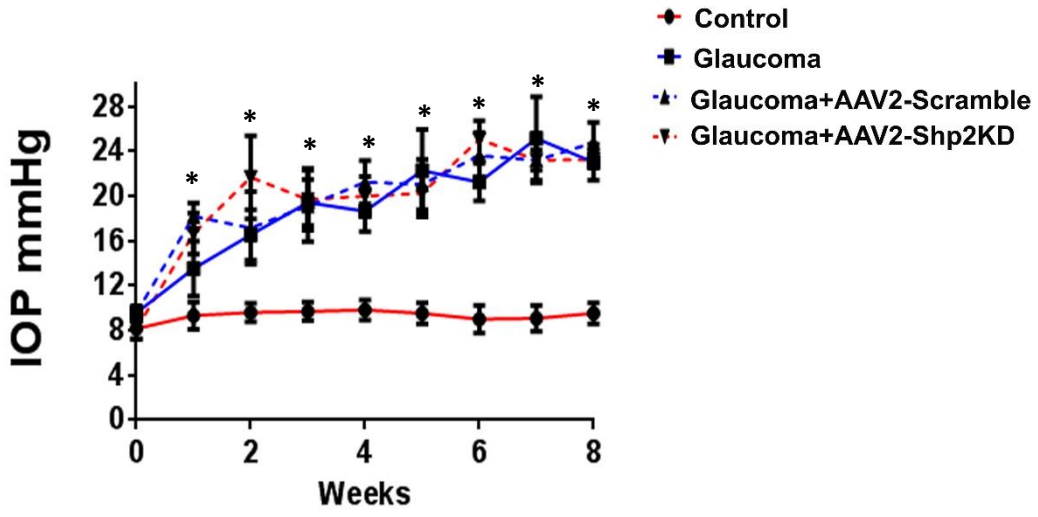

Figure 7.1. Effect of IOP on intravitreal AAV2 injections and microbead injection in rat eyes. IOP changes in rat eyes with repetitive injections of microbeads (8 weeks), a comparable increase in IOP was observed after anterior chamber microbead injections (n=32).

7.3.2 Assessment of transgene expression in experimental glaucoma animal eyes

We investigated the effect of AAV2 to express transgene on intravitreal injection of RGCs in the experimentally induced-glaucoma model. The tropism of AAV2 has been shown to selectively target RGCs in the rodent retina (Cheng et. al 2002; Fisher et al, 2004; Moore et al. 2009). *Shp2* was experimentally downregulated using AAV2 containing a shRNAmir sequence specific to rat mShp2 (AAV2-shRNAmir-Shp2 or AAV2-Shp2KD) (Chapter 2, Figure 2.2). The level of Shp2 was monitored by immunofluorescence in glaucoma retinal sections (Figure 7.2) after AAV2 delivery. No fluorescence detection of GFP was observed in control and microbead injected retinal section (Figure 7.2 A and C). Enhanced GFP fluorescence detection on retinal sections (Figure 7.2 E and G) revealed that AAV2-mediated expression of the target gene in cells mostly located in the retinal ganglion cell layer (RGCL), while a very few were in the inner nuclear layer (INL, Figure 7.2 E, G and yellow arrow).

Immunohistochemistry of retinal sections (Figure7.2 G) showed that most of these GFP^+ cells were RGCs (Xiong and Cepko, 2016, Schmitt et al., 2014) having the size and dendritic morphology of RGCs and possessing an axon. Antibody NeuN was used to stained neuronal cells in GCL. Higher expression of Shp2 fluorescence was detected in glaucoma model as compared to control retinas (Figure 7.2 B, D and F) indicating its higher phosphatase activity in high IOP condition. Suppression of *Shp2* in RGCs was observed in animals exposed to high IOP, as shown in Figure 7.2 H. The transfection efficiency of the target gene was also assessed with western blot analysis, the expression of GFP and Shp2 protein in the ONH region. Blotting and quantitative results for GFP and Shp2 are shown in Figure 7.3. Data are presented as an adjusted ratio of either GFP or Shp2 to Actin. As expected, GFP was expressed in only rat ONH with viral vector transduction. No expression of GFP was detected in control and microbead injected ONH lysates since there is no expression of GFP is normal conditions. Intravitreally knocking down Shp2, the expression levels of Shp2 in optic nerve was radically down-regulated by more than sixfold compared to the control group ($^{**}p<0.01$). These data demonstrate that AAV2 intravitreal injection is effective in down-regulating Shp2 in glaucoma RGCs.

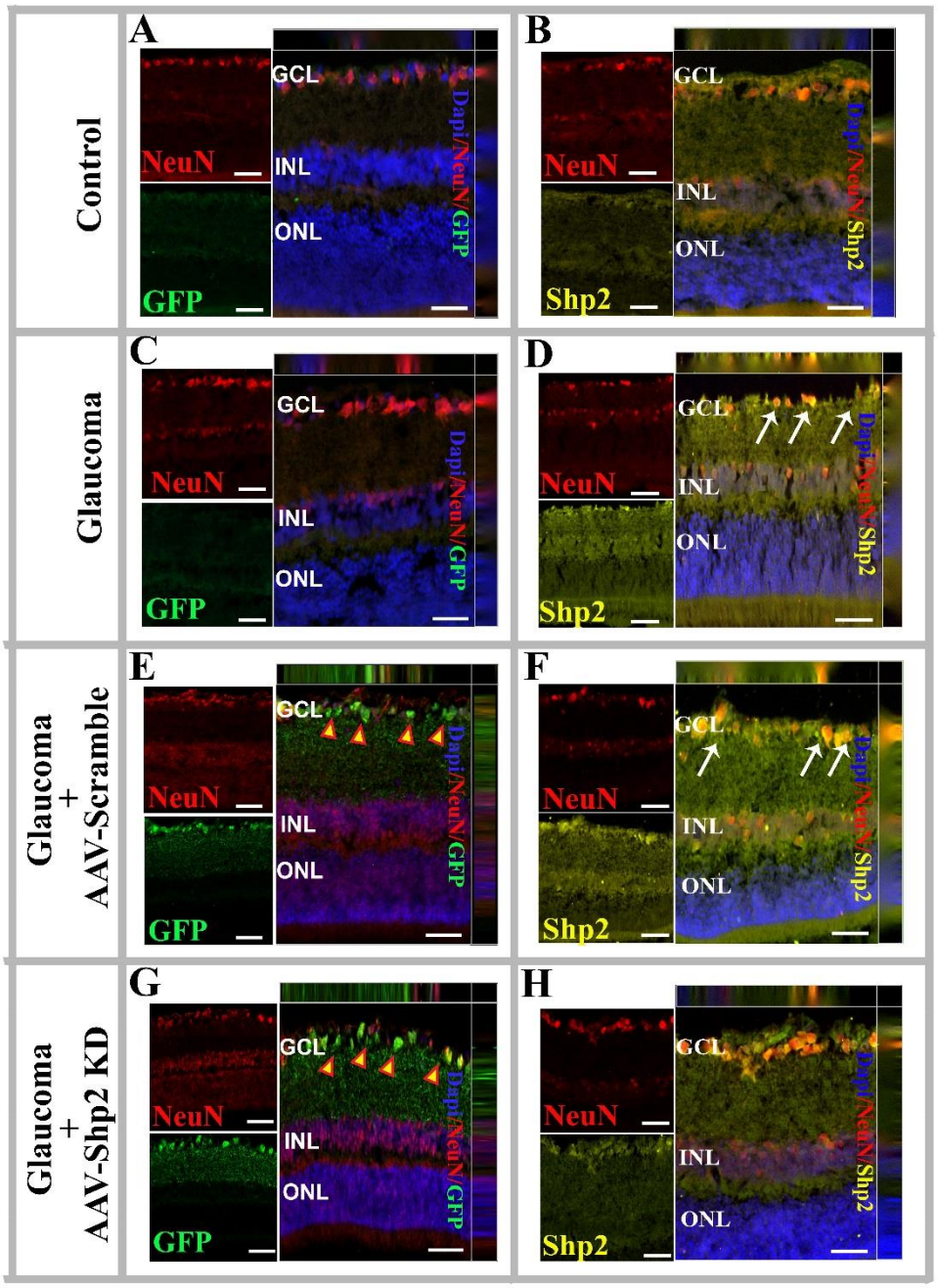

Figure 7.2. Transgene (*GFP* and *Shp2*) expression in animal glaucoma eyes. Rat eyes were injected with viral constructs for Shp2 knock down. GFP co-expressed with scrambled peptide was used as control (final concentration, 3.4×10^{12}GC/ml). Eyes were enucleated, sectioned, and stained with DAPI, anti-GFP and, anti-Shp2 to evaluate expression of GFP and Shp2 respectively. Scale 50 µm. Fluorescent microscopy showing characteristics of GFP^+ transfected cells (in green) (e, g), $NeuN^+$ cells (red) and $Shp2^+$ cells (yellow) (f, h) in a retinal slice. Most GFP^+ transfected cells were in the GCL (red arrow, yellow circle). The white thin cross in each figure indicates the same position (Z axis) of scanning. Scale 50 µm. GCL, ganglion cell layer; INL, inner nuclear layer; ONL, outer nuclear layer.

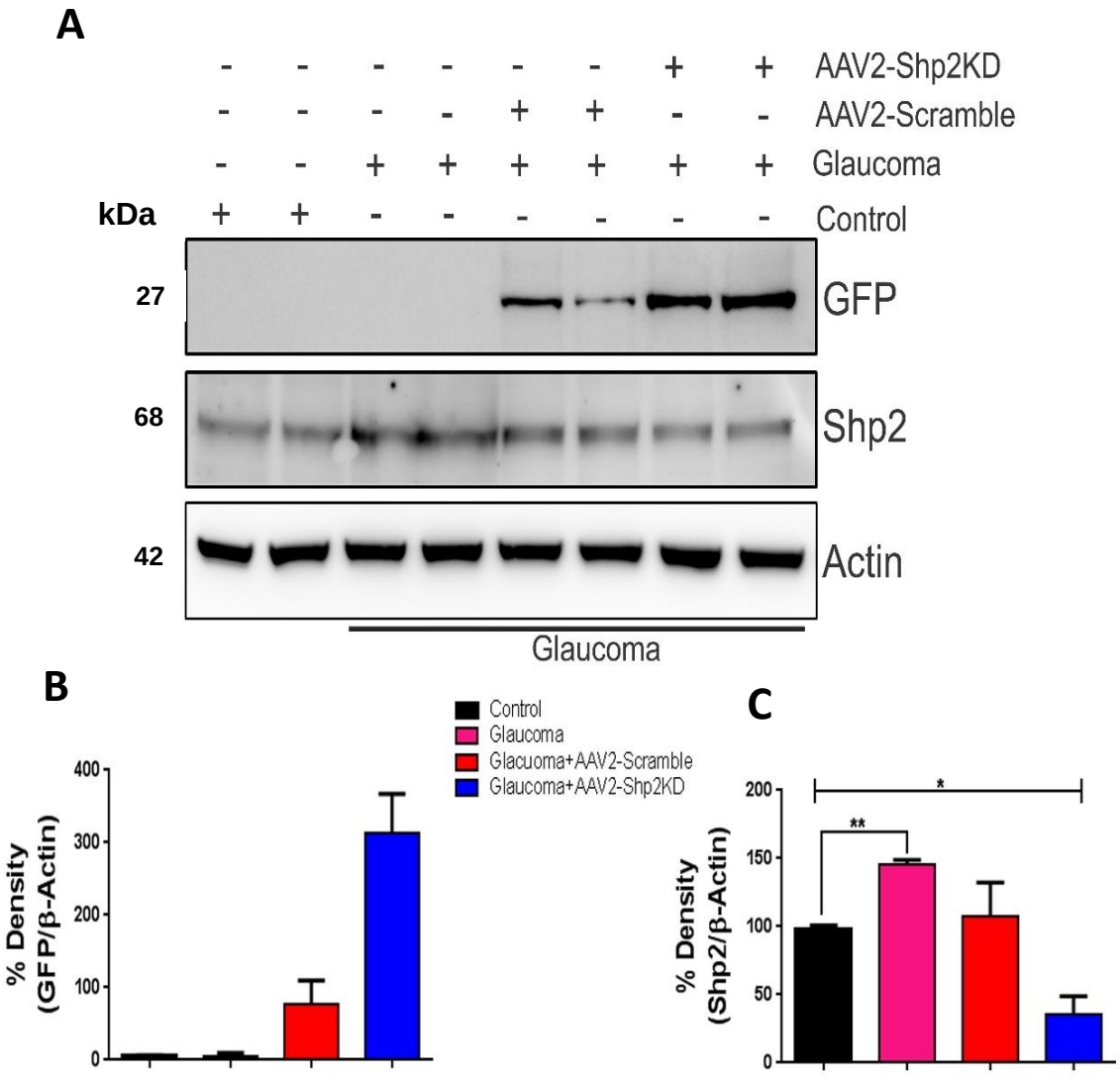

Figure 7.3. GFP and Shp2 expression in control and glaucoma optic nerve head (ONH) lysate (A) Western blot shows GFP and Shp2 expression in AAV treated ONH lysate (B) Densitometry quantification of GFP band shows axonal uptake of AAV viral vector expressing GFP (n=16, $^{*}p<0.05$) (C) Densitometry quantification show significant increase in expression of Shp2 in glaucoma and decreased expression of Shp2 in ONH lysate expressing shRNAmir sequence (n=16, $p<0.05$).

7.3.3 Reduced GCL density and axon loss in response to experiment induced-glaucoma

To evaluate the effect of high IOP we examined histopathologic and morphometric changes 2 months after microbead injection. Ganglion cell counts were made on cross-sectional slides stained with H&E (Igarashi et al., 2016). No attempt was made to distinguish RGCs from displaced amacrine cells or other neuron-like cells, but morphologically distinguishable glial cells and vascular endothelial cells were excluded. The mean number of cells in the RGC layer or section in animals with high IOP was significantly lower than in animals remain untreated (Figure 7.4 A and B, $^{***}p<0.00001$; n=8 in each group; control, 99.34±3.44 cells %; glaucoma, 37.22±2.99 cells %). We have also examined the changes in inner retinal layers by measuring the thickness of inner plexiform layer (IPL) and inner nuclear layer (INL) in microbead injected animal eyes. No significant change was observed in IPL in high IOP compared to non-treated animals (Figure 7.4 C; control vs glaucoma, 79.98±0.85 µm vs 78.63±0.77 µm; n= 8). However, INL thickness was significantly reduced in glaucoma group (32.90±0.36 µm) compared to control group was 35.15±0.36 µm (Figure 7.4 C; $^{***}p<0.0002$; n=8 in each group). Assessment of changes in optic nerve sections using Bielschowsky's silver staining demonstrated a reduction (58.95 ± 2.13%; $^{****}p < 0.0001$) in the axonal density in glaucoma compared to control animals (84.88 ± 1.47%; n = 18) (Figure 7.4 D and E).

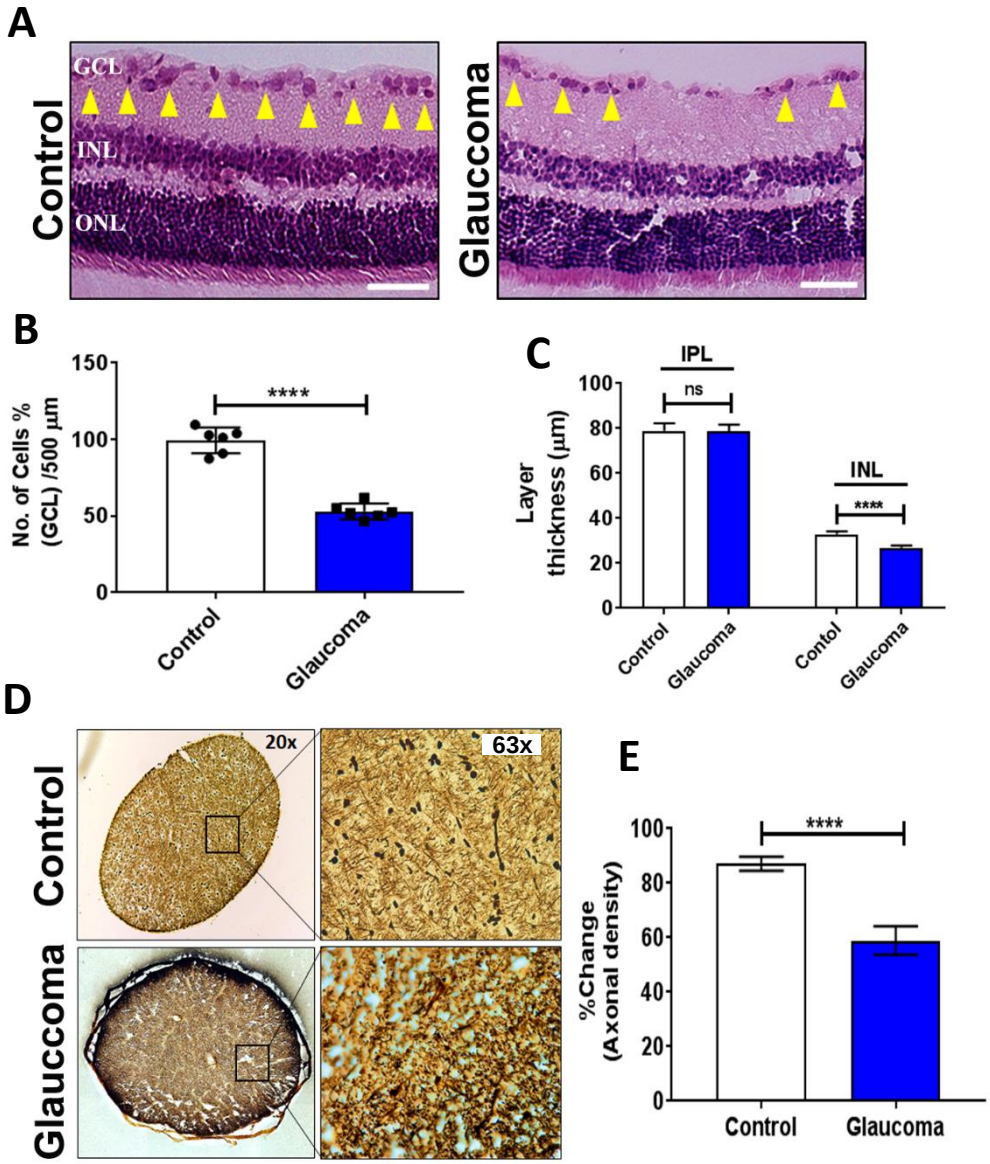

Figure 7.4. Retinal and optic nerve morphometric changes experimentally induced high ocular pressure (A) H and E staining of the rat retinal sections in high ocular pressure. Non-treated treated retinas were used as control. Scale 50 µm. (B) Quantification indicating significant difference was observed in the GCL density in glaucoma rat eyes ($^{*}p<0.0001$; n=16). (C) Retinal thickness demonstrated no-change in IPL under high ocular hypertension eyes compared to control ones where as significant decrease in INL thickness was observed in experimentally induced glaucoma eyes ($^{****}p<0.0002$; n=16) (D) Bielschowsky's silver staining of the control and glaucoma ON. (E) Quantification highlighted loss of axonal density in glaucoma compared to control ($^{****}p<0.0001$; n= 16).

7.3.4 Downregulation of Shp2 protects the GCL and axon loss against experimental glaucoma

Shp2 was knocked down in the rat retina using AAV2-shRNAmir placed in cell specific CAG promoter as under experimental glaucoma model. As mentioned previously, the assessment of GCL and retinal layer thickness was also carried out in glaucoma conditions with viral injection expressing shRNAmir or scramble sequence. AAV2 expressing shRNAmir sequence showed no significant change in IPL but INL thickness was significantly protected compared to AAV2-Scramble treated animal eyes experiencing high IOP (Figure 7.5 A and B; n=8; Glaucoma, IPL, AAV2-Scramble, 80.17±0.70%, AAV2-Shp2KD, 79.60±0.87%, INL, AAV2-Scramble, 26.86±0.28%, AAV2-Shp2KD, 32.47±0.23%). However, experimentally induced-glaucoma in animal eyes receiving AAV2-Scramble sequence showed significant cell loss in GCL density (Figure 7.5 A and B) compared to Shp2 knockdown retinas (Figure 7.5 A and B). GCL density loss occurred in high IOP, decreasing from 63% to 38% in animals subjected to knockdown of *Shp2* and prolonged the damage of retinal integrity by high IOP. Like the observations in cellular degeneration in the GCL, axonal loss in experimental glaucoma was also significantly attenuated by knocking down of *Shp2*. Axonal loss in experimental glaucoma was reduced from 41.05% to 27.14% after Shp2 knockdown in RGCs compared to Scramble treated animals ($p < 0.03$, Figure 7.5 D and E). Overall these experiments confirm that Shp2 plays important role in regulating RGCs and axonal survival in glaucoma.

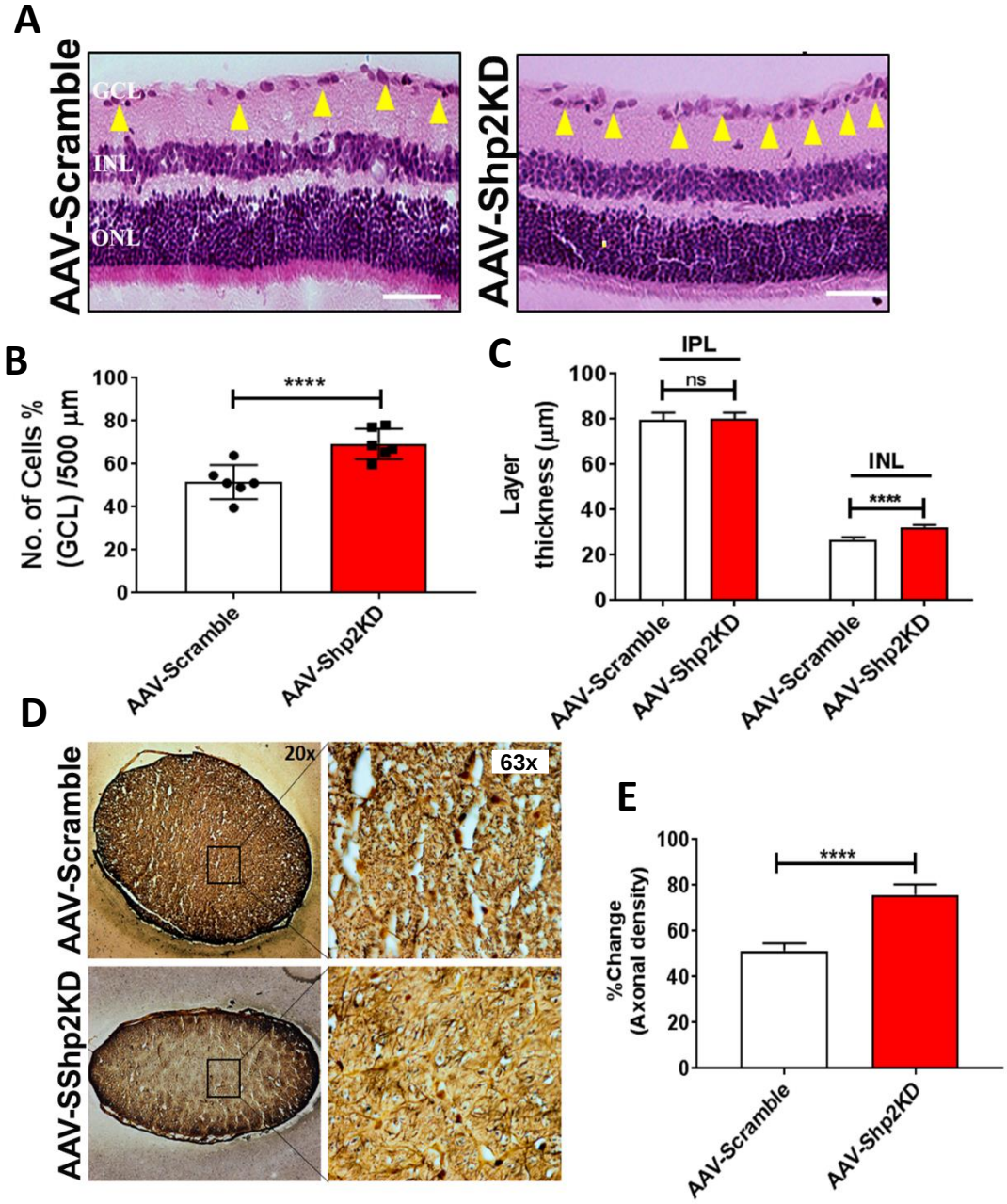

Figure 7.5. Retinal and optic nerve morphometric changes induced by AAV2-Shp2 knockdown in high intraocular pressure (A) H and E staining of the rat retinal sections injected with viral vector expressing shRNAmir in high IOP. AAV2-Scramble treated retinas was used as control in experimental glaucoma model. Scale 50 µm. (B) Quantification indicating significant protection of GCL density in high IOP eyes when treated with AAV2-Shp2 knockdown. AAV2-Scramble injected eyes was used as control in glaucoma eyes ($^{*}p<0.0001$; n=16). (C) Retinal thickness demonstrated no-change in IPL and INL subjected to AAV2-Shp2 knockdown glaucoma eyes. (D) Bielschowsky's silver staining of the ON treated expressing shRNA in animal glaucoma eyes. (E) Quantification highlighted significant axonal density protection in glaucoma eyes subjected to Shp2 knockdown compared to glaucoma eyes expressing shRNA scramble sequence ($^{***}p<0.0001$; n= 18).

7.3.5 Loss of inner retinal function in response to glaucoma

We next compared ERG components recorded from experimental animal model of glaucoma. We focused on pSTRs believed to represent RGCs activity (Yukita et al., 2017). In comparison with healthy eyes (44.54±5.01 µV, n=8), there was a significant, 59% reduction in pSTR amplitude after 8 weeks of microbead injections (18.18±2.88, n=8, $p<0.05$) (Figure 7.6 A and B). However, the amplitude of –a wave and –b wave and latency of the ERG was not significant in either healthy or glaucoma eyes but high IOP alters the spikes of oscillatory potentials (OPs) (Figure 7.6 C-E). Overall, the temporal course of the pSTR reductions correspond to the loss of RGCs in retinas subjected to experimental glaucoma.

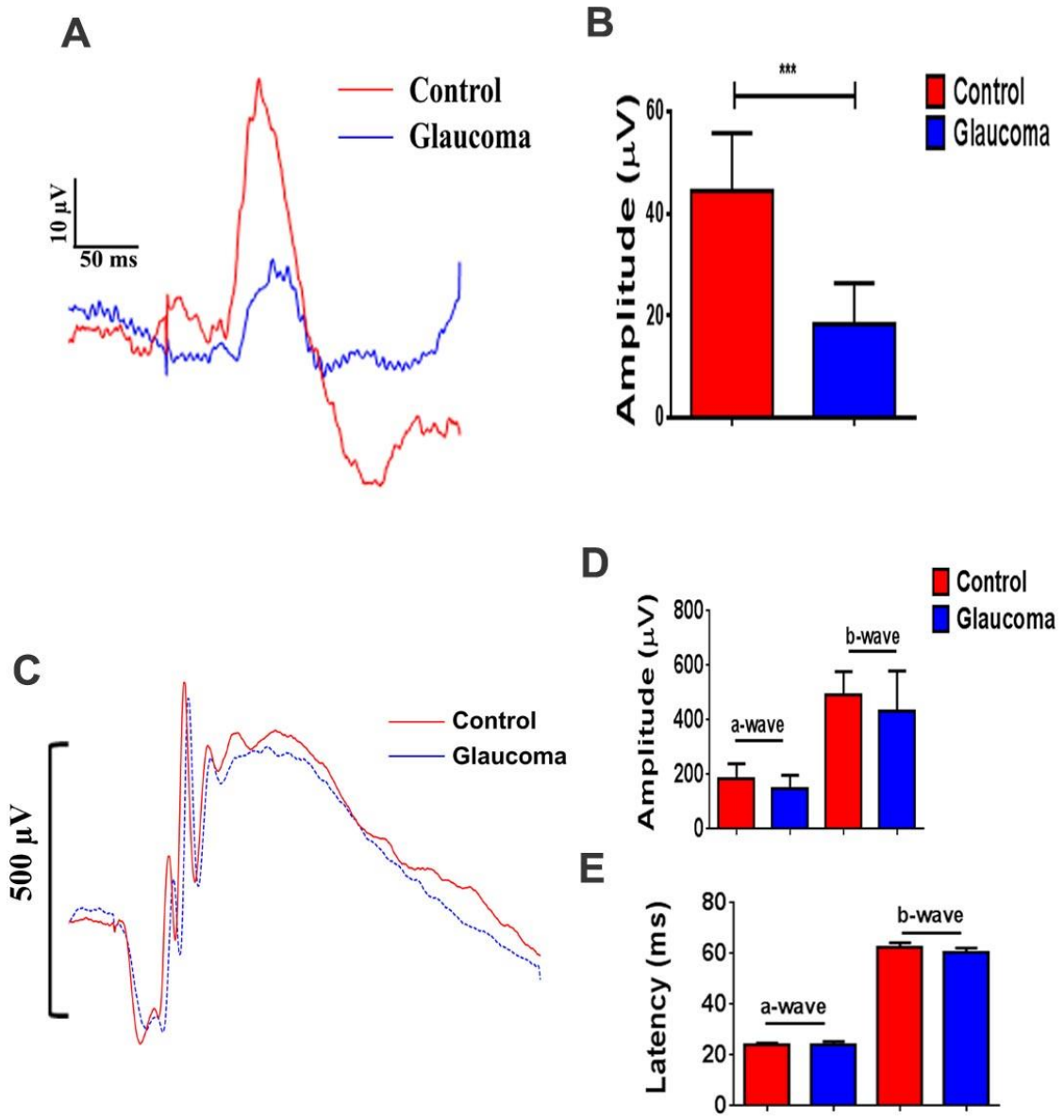

Figure 7.6. Effect of microbead injection on animal electrophysiology (A) Traces of pSTR from control rats and rat exposed to high IOP. (B) Quantification highlighting a decrease in pSTR amplitude in animal exposed to high IOP (n = 16; $^{***}p < 0.0004$). (C) Traces of ERG under control and glaucoma conditions (D) No change in –a wave amplitude but non-significant reduction in –b wave amplitude in animal exposed to high IOP compared to non-treated ones (E) No change in latency –a wave and –b wave under high IOP.

7.3.6 Downregulation of Shp2 is protective against inner retinal functional loss in experimental glaucoma

Corresponding to structural and functional damage that correlated with *Shp2* upregulation in healthy retinas (Chapter 6), we next investigated the therapeutic application of viral gene

therapy by knocking down *Shp2* in experimentally induced glaucoma animal model that exacerbates the severity of these changes. AAV2 viral vector expressing scramble and shRNAmir sequence were injected intravitreally in experimental animal model of glaucoma. Animal eyes were exposed to high IOP (8 weeks) and pSTR electrophysiological recordings were carried out (Figure 7.7). It was expected from our previous studies that exposure of animals to high IOP showed decline in pSTR amplitudes. Glaucoma eyes injected with AAV2-Scramble resulted in a notable decline in the pSTR amplitudes and comparison revealed that there was significantly higher protection in the pSTR amplitudes in glaucoma animals expressing AAV2-Shp2KD viral vector after 8 weeks (Figure 7.7 A and B; AAV2-Scramble, 18.18±3.98 µV; AAV2-Shp2KD, 32.47±4.01 µV; n=12 in each group; $p < 0.05$). The evaluation of the whole retinal scotopic electrophysiological response and quantification of the a- and b-wave amplitudes and latencies indicated no change in normal retina treated with AAV2 viral vector expressing scramble and shRNA sequence (Figure 7.7 C-E), but a slight decline in average b-wave amplitudes in AAV2-Shp2KD animals exposed to high IOP (Figure 7.7 C-E; n = 12). However, these changes were not found to be statistically significant (Figure 7.7). This experiment indicated that Shp2 is playing a more specific role in the preservation of inner retinal function. Overall, these findings highlighted the involvement of Shp2 in RGCs and its genetic knockdown protects inner retinal structural and functional integrity changes on exposure to high IOP.

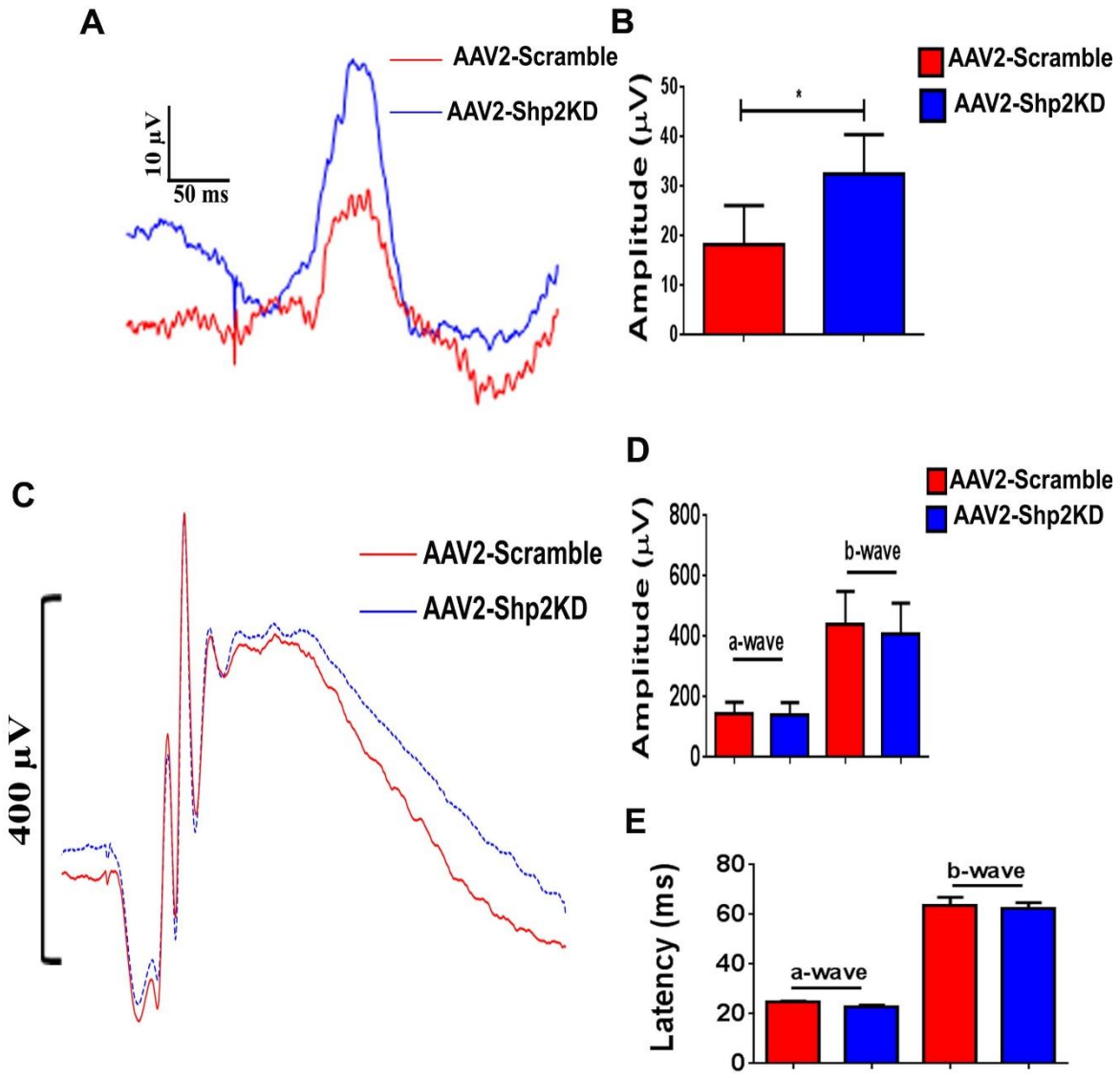

Figure 7.7. Effect of AAV mediated Shp2 KD on electrophysiology under high IOP experimental glaucoma model (A) Traces of pSTR from animal injected with AAV2-Scramble and AAV2-Shp2KD animals exposed to increased IOP. (B) Quantification highlighting a significant protection in pSTR amplitude in high IOP exposed animals subjected to Shp2 knockdown compared to AAV-Scramble ($n = 16$; $^{*}p < 0.05$). (C) Traces of ERG under viral vector expressing shRNA and shRNA scramble sequence in glaucoma conditions. No change in –a wave and –b wave (D) amplitude and (E) latency in high IOP.

7.3.7 Shp2 suppression augments TrkB phosphorylation in inner retina in glaucoma

We have already seen that phosho-TrkB activity was reduced in AAV2-Shp2 overexpression in SHY5Y cells and in rat retina *in vivo* (Chapter 5 and 6). These findings lead us to investigate the TrkB phosphorylation activity in animal RGCs treated with AAV2-Shp2KD

under high IOP. Rat retina sections were subjected to immunochemistry to detect pTrkBY^{515} protein levels. As seen in Figure 7.8, decrease pTrkBY^{515} protein levels was detected in both microbead alone and microbead with AAV2-Scramble administered rat retinas mainly in GCL with activated microglia appear in the INL and outer segment (OS) (Figure 7.8, ii, iii, red arrow). Whereas, truncated and full length TrkB localization in the GCL and inner retinal neurons has been observed in an earlier study (Suzuki et al., 1998, Germana et al., 2010, Kunz et al., 1976). Interestingly, pTrkBY^{515} protein was upregulated prominently in the nerve fiber layer (NFL) and enhanced staining was also observed in GCL and IPL of the glaucoma retina injected with Shp2KD viral vector (Figure 7.8, iv, red arrow). Inset (Figure 7.8, iv) showing higher magnification of RGCs indicated increased staining of pTRkBY^{515} and dendrites growth in activated microglial cells (inset Figure 7.8, iv white arrow). This experiment confirms that Shp2 knockdown rescue the TrkB phosphorylation in high IOP and can be used as neuroprotective strategies for glaucomatous optic neuropathy, other retinal and optic nerve diseases.

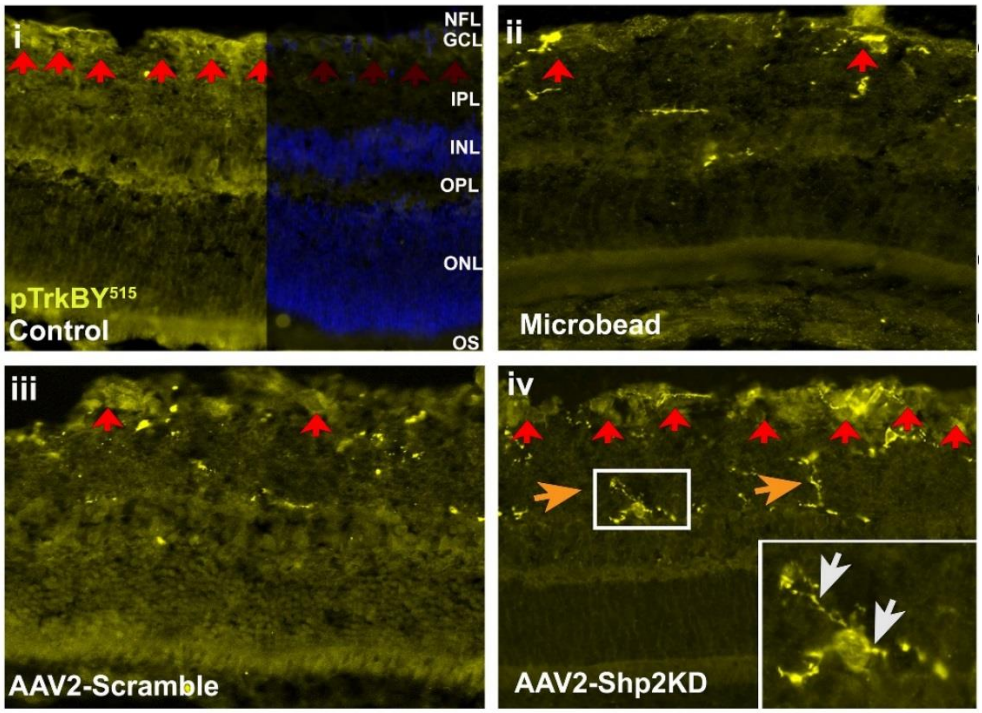

Figure 7.8. Knocking down of Shp2 negatively affects TrkB Y^{515} phosphorylation in rat retina under high intraocular hypertension eyes. Cryosections of rat retina shows expression pTrkB Y^{515} (yellow) expression in (i) control, (ii) glaucoma, (iii) glaucoma+AAV2-Scramble and (iv) glaucoma+AAV2-Shp2KD. Loss of phosphorylated TrkB activity shown with arrow red. Note the high expression of TrkB Y^{515} phosphorylation in GCL, shown in orange arrow and growth of dendrites shown in high magnification (white arrow) (Scale 20 µm).

7.4 Discussion

Glaucoma management comprises mainly of two approaches to lower IOP: either surgery or through pharmaceutical agents that act by dropping aqueous humor formation or increasing the drainage outflow (Goni et al., 2016, Acharya et al., 2016). Despite these treatments, neurodegeneration continues to occur slowly in many cases. Therefore, there is an utmost need for developing new neuroprotective strategies in addition to lowering IOP. Neuroprotection is an important area of glaucoma research, which has made commendable progress in the light of key findings that demonstrate neuroprotective effects in the retina and ON in animal models of optic neuropathy (Li et al., 2016). Neurogenic phosphatase, Shp2, is present in the RGCs and regulates both positively and negatively cell signaling

pathways within the cell and tissue dependent manner (Lemmon and Schlessinger, 2010). In the current study, we modulated the expression of *Shp2* in microbead injected animal model of elevated IOP using intravitreal injection of AAV2 viral vector expressing shRNAmir sequence employed within CMV-CAG hybrid promoter. AAV2 vectors have been shown to be safe and efficacious for use in humans and hold promise for future therapies in several eye diseases (Greenberg et al., 2016, Feuer et al., 2016, Bennett et al., 2016). Shp2 plays an important role during development and differentiation of RGCs, as evidenced in retinal degenerative changes including ON dystrophy in *Shp2*$^{flox/flox}$ mutant mice (Cai et al., 2011). The status of Shp2 in RGCs degeneration as well as its potential role in regulating the neuroprotective action of BDNF-TrkB signaling is largely unclear. In retina, we reported previously that weakening of this signaling pathway is associated with an age related inner retinal degenerative phenotype and exacerbation of experimental glaucoma induced RGC deficits (Gupta et al., 2014b). Shp2 has been shown to be predominantly expressed in the inner retina. Also, the other indirect role of Shp2 is reported to supporting the survival of the photoreceptors through the Muller cells (Cai et al., 2011, Kinkl et al., 2002). We and others have previously demonstrated that Shp2 interacts with TrkB in RGCs and other neuronal cells (Rusanescu et al., 2005).

In this study, we report for the first time that viral vector mediated long term *Shp2* accumulation in animal RGCs and glaucomatous RGCs resemble the similar detrimental effect on RGCs survival. Our findings corroborate with the previous studies that the long term dephosphorylation of TrkB, mediated by the action of Shp2, hampers axonal restoration in the retina (Hollis et al., 2009, Gupta et al., 2012b). Parallel to structural and functional deficit, decline in TrkB phosphorylation form was marked in both Shp2 dysregulation and experimentally induced-glaucoma physiological conditions. These observations confirm the

concept-of-proof that the damaging effect to inner retina in glaucoma is pertained by the action of Shp2 on TrkB activity. Notably, blocking of *Shp2* in RGCs accompanying high IOP rescued TrkB phosphorylation in the ONH and protects the impairment of inner retina structure and electrophysiological function in rat model of induced-glaucoma after 8 weeks. Considerable evidence suggests that this damaging effect was mediated by Shp2 in glaucoma. Initially, no inner retinal damage was observed after AAV-GFP or AAV-Scramble injection, excluding the possibility that the differential survival was mediated by events related to manipulation or penetration to the eye (Chapter 6). Although our recent findings in cell culture showed damaging effects of Shp2 on endoplasmic reticulum (ER) stress response (Chapter 5). Shp2 positively regulates the unfolded protein response (UPR) and upregulation of ER stress and induced cell apoptosis in cell culture and in rat retina (Chapter 5 and 6). Therefore, the neuroprotective function of neurotrophins can be circumvented by Shp2 activation in glaucoma. Collectively, these observations suggest that Shp2 is also involved in the regulation of downstream pathway controlling TrkB activity.

Shp2 is highly expressed in the adult retina and different parts of the brain, including the pituitary gland, olfactory bulb, cerebral cortex, hippocampus, cerebellum and brain stem (Suzuki et al., 1995, Ke et al., 2007). It is also constitutively expressed in mature RGCs, suggestive of its putative role in normal RGC physiology, which is not completely understood. Recently, we demonstrated enhanced interaction of TrkB and Shp2 in RGCs under stress conditions, suggesting that overexpression of Shp2 precedes neurodegenration (Gupta et al., 2012b). Previous studies have shown the failure in delaying RGC death following BDNF gene therapy after optic nerve transfection sensitizes BDNF/TrkB simulations to have any benefit in experimental glaucoma models (Khalin et al., 2015). Hence, with the sustained insult of elevated IOP in the rat glaucoma model, it appears that continuous TrkB activation is important for the beneficial effect. Our results showed that

long term Shp2 knockdown can have substantial benefit on phosphorylation activity of TrkB. Although, Shp2 is produced in the normal adult retina, and even by RGCs themselves, it is likely that progressive glaucoma hyper-phosphorylates adapter protein, caveolin (cav-1) in RGCs and its interaction interrupts the normal levels of Shp2 (Gupta et al., 2012b).

We achieved high levels of RGC transfection after single intravitreal injections of AAV2 vectors with an important element; the use of hybrid CMV-CAG promoter gives us more efficient transfection of retinal neurons, particularly RGCs. Transduction requires not only gene delivery but also efficient translation of transfecting genes into functional protein. The presence of introns associated with a gene of interest can increase expression (Chorev and Carmel, 2012). The results presented show that many neurons were transfected in the RGC layer. It is known that amacrine cells may represent as many as 50% of the RGC layer nuclei in the rat. We show clear evidence that many of the cells expressing transgenes with viral vector are RGCs. Their somal size is larger than the 7-µm diameter of amacrine cells, whereas their dendritic morphology and the presence of an axon shows that they are RGCs. In addition, NeuN positive neurons in RGC layer expressed GFP, indicating that they were not amacrine cells. However, it may be that overexpression of Shp2 by amacrines or other cells of the inner retina is equally effective as a mechanism for increased death of RGCs (Chapter 6). Although we believe that most of the cells expressing the transgene were RGCs, our conclusion that Shp2 knockdown is protective does not depend on exclusive transfection of RGCs in glaucoma.

Clinically, it is relevant to answer one of the important question; whether or not neurotrophins provides long-term protection for RGCs and vision in glaucoma? Comparison of BDNF-mediated neuroprotection between different animal studies is not straightforward due to the variability of the length and degree of IOP elevation used by different investigators, with the result that the same molecular and cellular mechanisms may not be

involved in all studies (Igarashi et al., 2016, Pease et al., 2009). For example, in a rat model of laser-induced experimental glaucoma, RGC loss was significantly reduced by BDNF transfected with AAV vector at 4 weeks' post laser illumination to the trabecular meshwork (Fu and Sretavan, 2010). However, another study suggested that BDNF alone made no significant improvement in axon survival in rats with laser induced glaucoma (Pease et al., 2009). Ren and colleagues showed that the major parameters of the visual evoked potential (VEP) were protected by BDNF at 9 weeks following a transient IOP spike; moreover, visual acuity and contrast sensitivity were well maintained for up to 1 year (Ren et al., 2012, You et al., 2012b). We found that a chronic elevation of IOP produced a gradual decrease of pSTRs amplitude, also the loss in amplitude was similar when Shp2 overexpressed in normal RGCs for longer duration (8 weeks) (Chapter 6). However, knocking-down of Shp2 in high IOP RGCs, the loss of pSTR amplitude was reduced, consistent with previous studies in $BDNF^{+/-}$ mice (Kaplan et al., 1989). The amplitude of pSTRs we measured was the difference between the baseline to the positive peek from the non-filtered waveform and we presume therefore that it corresponds roughly to the intermediate component, which is believed to originate from the inner retina. Taken together, all these results support the notion that Shp2 knockdown exerts long-term protection on RGCs and vision, providing reason to believe that therapies that downregulate Shp2 or engage its signaling pathway should help to preserve vision in glaucoma.

The mechanisms of how Shp2 regulates BDNF/ TrkB signaling in the central nervous system remain unknown. It is important for TrkB to initiate downstream survival pathways after its initial activation. Our findings confirmed that the loss of phosphorylated activity of TrkB in high IOP was activated in glaucoma-induced animal eyes treated with viral vector expressing Shp2-shRNAmir sequence. However, the abundance of $pTrkBY^{515}$ expression in microglial cells was surprising given that expression of the full-length TrkB receptor has previously

been defined in these cells *in vivo* (Spencer-Segal et al., 2011). TrkB ligands such as BDNF may therefore participate in immune functions in the retina, such as retinal inflammation, through direct action on microglial TrkB receptors. An upregulation of BDNF has been identified in cases of brain and retinal inflammation or autoimmunity, but its role in these immune processes is unclear (Tao et al., 2014, Kimura et al., 2016). However, activated microglial cells secrete BDNF *in vitro* and murine microglial BDNF is needed in the neuronal cell for TrkB phosphorylation to maintain synaptic plasticity (Gomes et al., 2013, Parkhurst et al., 2013). Further investigation of the function of microglial TrkB receptors will likely uncover novel mechanisms for neurotrophin regulation of the neuroimmune response. However, more investigations are required to completely unravel the interactions of Shp2 and BDNF/TrkB signaling in neuronal survival mechanisms. Systemic effects of Shp2 modulation may also play a role in neuroprotection.

In summary, BDNF induced TrkB activation is affected in the inner retina and ONH in glaucoma, leading to degenerative changes manifested in the form of decline in inner retinal function and GCL thinning. The involvement of Shp2 in glaucoma is evident from the fact that Shp2 overexpression makes the retinas and ON more susceptible to glaucomatous like damage (Chapter 6). Although we found a protective effect of Shp2 knockdown after 8 weeks of IOP elevation, it is important to demonstrate that the benefit continues over longer periods. We also plan to investigate the molecular mechanism regarding whether other adaptor proteins like cav in Shp2 interaction give similar or additive neuroprotection. Overall, these results support the hypothesis that dephosphorylation of TrkB is mediated by Shp2 more aggressively in glaucoma and its knockdown alters the neuroprotective signaling pathways may be an important mechanism underlying the ganglion cell and optic nerve degenerative changes. In conclusion, our study demonstrated a major neuroprotective effect

of gene therapy in a glaucoma model. Development of gene therapeutic strategies may provide new options for the treatment of patients with glaucoma.

CHAPTER 8

Conclusion and future directions

Retinal and optic nerve degenerative diseases are a heterogeneous group of disorders that have a major impact on society, as the loss of vision brings about a loss in quality of life for patients and increased dependency. Glaucoma is a major cause of world blindness and despite current treatment strategies there is still progression in disease continues. BDNF is an important survival factor for RGC, both during development and in adult life. BDNF binds to TrkB receptor and retrogradely transported to RGC. However, the acute elevation of IOP in animal models shows the retrograde transport of BDNF-TrkB complex is obstructed in ONH. Recent advances have demonstrated the potential of viral gene therapies in some retinal disorders. The advantage of using AAV vectors are their small size, nonpathogenic and easy gene manipulation, which allow us to modify gene expression cell populations in animals.

Presented work in this dissertation demonstrated the molecular insight of the BDNF-TrkB signaling in the neuronal cells and the potential for the gene delivery through viral vector strand displacement mechanism, where single stranded DNA is used for packaging and double-stranded DNA utilized for transcription. Using this mechanism, we have shown the molecular effect of *Shp2* or *PTPN11* modulation in SH-SY5Y cells *in vitro* and in animal RGCs. We have also shown the importance of this approach in AAV-mediated gene therapy treatment specific to RGCs neuroprotection in experimental glaucoma.

The conclusions arising from this PhD thesis include:

1. BDNF/ TrkB signaling plays an important role in regulation of the GSK3β activity both in neuronal cells in culture and in retina *in vivo* (Chapter 3).
2. Identified the molecular interacting residue partner and binding pattern of TrkB receptor with 7,8 DHF, agonist, and CTX-B, antagonist using computational approach (Chapter 4)
3. Induction of *PTPN11* upregulation has detrimental effect on SH-SY5Y cells. Its overexpression negatively regulates the TrkB receptor activity and neurtiogenesis. ER stress upregulation and apoptosis is commonly associated with accumulation of PTPN11 in SH-SY5Y cell culture (Chapter 5).
4. Accumulation of *PTPN11* in SH-SY5Y cell desensitizes TrkB receptor activation on exogenous treatment of BDNF while BDNF directionally regulates the ER stress response in SH-SY5Y cells (Chapter 5).
5. Absence of *PTPN11* in neuronal cell culture shows a beneficial effect on cell survival by activating the TrkB receptor activity, promotes neuritogenesis and eliminate ER stress (Chapter 5).
6. Single injection of AAV viral vector encoding *Shp2* gene under CMV-CAG, hybrid promoter is efficient to transduce rat RGCs *in vivo* (Chapter 6).
7. Long term dysregulation of Shp2 in animal RGCs is associated with inner retinal laminar structural and functional loss. The damage to TrkB receptor activation induces inner retina ER stress and leading to apoptosis (Chapter 6).
8. Establishing molecular cross-talk that Shp2 firmly regulates the BDNF-TrkB receptor interaction activity in SH-SY5Y cells *in vitro* and in RGCs *in vivo* (Chapter 5 and 6).

9. TrkB activation (via downregulation of *Shp2*) is beneficial for RGC survival in animal experimental model of glaucoma. Activation of TrkB in microglial cells may provide the indirect neuroprotection to RGCs exposed to high intraocular pressure and may be involved in secretion of BDNF to support the RGC survival in stress (Chapter 7).

Future directions may include

1. Recruitment of Shp2 to the TrkB receptor is believed to be carried out by the adaptor protein caveolin. As caveolin is highly expressed in RGCs and in glaucoma the caveolin is hyper-phosphorylated. A study investigating interaction of caveolin-Shp2 in BDNF/ TrkB signaling in caveolin knockout mice and animal glaucoma model is being conducted.
2. To extend the molecular gene therapy approach, addition of other neurotrophin factor eg. BDNF gene either alone or in conjugation with *Shp2*-shRNA sequence in AAV2 can be studied to find whether it enhances neuroprotection in optic neuropathy like optic neuritis, glaucoma etc.
3. Multidisciplinary approach of *Shp2*-shRNA capable of neuron regeneration in optic neuropathy animal model can be employed to explore the added mechanism of TrkB-Shp2 interaction.
4. Biochemical investigations to determine the role of Shp2 on TrkB downstream signaling in RGCs survival and apoptosis.
5. To further improve the *proof-of-concept* model, a thorough study on molecular basis of ER stress trafficking within the glaucoma neuronal cells can establish a relationship between TrkB-Shp2-ER stress markers.

6. Implication of TrkB agonist, eg. 7,8 DHF on other tyrosine kinases receptor, like VEGFR1 and VEGFR2, in glaucoma and other retinal diseases.
7. AAV mediated shp2-knockdown can be used in larger number of rodent models of glaucoma as well as clinical trials to evaluate its neuroprotective effect *in vivo.*

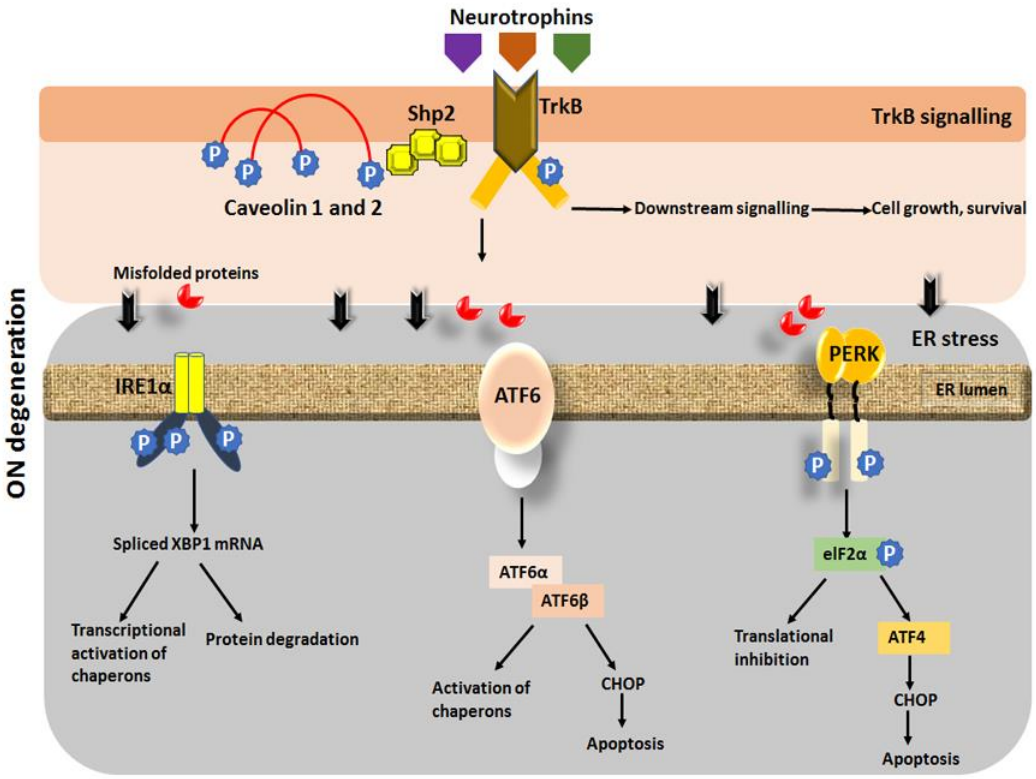

Figure 8.1. Schematic representation of BDNF-TrkB downstream signalling altered by Shp2. Misfolded protein accumulation bring changes in endoplasmic reticulum stress markers (IRE1α, ATF6 and PERK) which are possibly implicated in progression of RGCs axon damage in glaucoma

REFERENCES

ACHARYA, S., ROGERS, P., KRISHNAMOORTHY, R. R., STANKOWSKA, D. L., DIAS, H. V. & YORIO, T. 2016. Design and synthesis of novel hybrid sydnonimine and prodrug useful for glaucomatous optic neuropathy. *Bioorg Med Chem Lett,* 26**,** 1490-4.

ADACHI, M., TAKAHASHI, K., NISHIKAWA, M., MIKI, H. & UYAMA, M. 1996. High intraocular pressure-induced ischemia and reperfusion injury in the optic nerve and retina in rats. *Graefes Arch Clin Exp Ophthalmol,* 234**,** 445-51.

AGARWAL, N., AGARWAL, R., KUMAR, D. M., ONDRICEK, A., CLARK, A. F., WORDINGER, R. J. & PANG, I. H. 2007. Comparison of expression profile of neurotrophins and their receptors in primary and transformed rat retinal ganglion cells. *Mol Vis,* 13**,** 1311-8.

AGAZIE, Y. M. & HAYMAN, M. J. 2003. Molecular mechanism for a role of SHP2 in epidermal growth factor receptor signaling. *Mol Cell Biol,* 23**,** 7875-86.

AGOUNI, A., MODY, N., OWEN, C., CZOPEK, A., ZIMMER, D., BENTIRES-ALJ, M., BENCE, K. K. & DELIBEGOVIC, M. 2011. Liver-specific deletion of protein tyrosine phosphatase (PTP) 1B improves obesity- and pharmacologically induced endoplasmic reticulum stress. *Biochem J,* 438**,** 369-78.

ALUR, R. P., COX, T. A., CRAWFORD, M. A., GONG, X. & BROOKS, B. P. 2008. Optic nerve axon number in mouse is regulated by PAX2. *J AAPOS,* 12**,** 117-21.

ANDERSON, D. R. 2011. Normal-tension glaucoma (Low-tension glaucoma). *Indian J Ophthalmol,* 59 Suppl**,** S97-101.

ANDERSON, M. G., SMITH, R. S., SAVINOVA, O. V., HAWES, N. L., CHANG, B., ZABALETA, A., WILPAN, R., HECKENLIVELY, J. R., DAVISSON, M. & JOHN, S. W. 2001. Genetic modification of glaucoma associated phenotypes between AKXD-28/Ty and DBA/2J mice. *BMC Genet,* 2**,** 1.

ANHOLT, R. R. & CARBONE, M. A. 2013. A molecular mechanism for glaucoma: endoplasmic reticulum stress and the unfolded protein response. *Trends Mol Med,* 19**,** 586-93.

APATACHIOAE, I. & CHISELITA, D. 1999. [Alpha-2 adrenergic agonists in the treatment of glaucoma]. *Oftalmologia,* 47**,** 35-40.

ARAKI, T., YAMADA, M., OHNISHI, H., SANO, S., UETSUKI, T. & HATANAKA, H. 2000. Shp-2 specifically regulates several tyrosine-phosphorylated proteins in brain-derived neurotrophic factor signaling in cultured cerebral cortical neurons. *J Neurochem,* 74**,** 659-68.

AREVALO, J. C., WAITE, J., RAJAGOPAL, R., BEYNA, M., CHEN, Z. Y., LEE, F. S. & CHAO, M. V. 2006. Cell survival through Trk neurotrophin receptors is differentially regulated by ubiquitination. *Neuron,* 50**,** 549-59.

BAKALASH, S., KESSLER, A., MIZRAHI, T., NUSSENBLATT, R. & SCHWARTZ, M. 2003. Antigenic specificity of immunoprotective therapeutic vaccination for glaucoma. *Invest Ophthalmol Vis Sci,* 44**,** 3374-81.

BAMJI, S. X., MAJDAN, M., POZNIAK, C. D., BELLIVEAU, D. J., ALOYZ, R., KOHN, J., CAUSING, C. G. & MILLER, F. D. 1998. The p75 neurotrophin receptor mediates neuronal apoptosis and is essential for naturally occurring sympathetic neuron death. *J Cell Biol,* 140**,** 911-23.

BANFIELD, M. J., NAYLOR, R. L., ROBERTSON, A. G., ALLEN, S. J., DAWBARN, D. & BRADY, R. L. 2001. Specificity in Trk receptor:neurotrophin interactions: the crystal structure of TrkB-d5 in complex with neurotrophin-4/5. *Structure,* 9**,** 1191-9.

BAROT, M., GOKULGANDHI, M. R. & MITRA, A. K. 2011. Mitochondrial dysfunction in retinal diseases. *Curr Eye Res,* 36**,** 1069-77.

BARTKOWSKA, K., TURLEJSKI, K. & DJAVADIAN, R. L. 2010. Neurotrophins and their receptors in early development of the mammalian nervous system. *Acta Neurobiol Exp (Wars),* 70**,** 454-67.

BARTLETT, S. E., REYNOLDS, A. J. & HENDRY, I. A. 1998. Retrograde axonal transport of neurotrophins: differences between neuronal populations and implications for motor neuron disease. *Immunol Cell Biol,* 76**,** 419-23.

BARTZ-SCHMIDT, K. U., THUMANN, G., JONESCU-CUYPERS, C. P. & KRIEGLSTEIN, G. K. 1999. Quantitative morphologic and functional evaluation of the optic nerve head in chronic open-angle glaucoma. *Surv Ophthalmol,* 44 Suppl 1**,** S41-53.

BASAVARAJAPPA, D. K., GUPTA, V. K., DIGHE, R., RAJALA, A. & RAJALA, R. V. 2011. Phosphorylated Grb14 is an endogenous inhibitor of retinal protein tyrosine phosphatase 1B, and light-dependent activation of Src phosphorylates Grb14. *Mol Cell Biol,* 31**,** 3975-87.

BEATTIE, M. S., HARRINGTON, A. W., LEE, R., KIM, J. Y., BOYCE, S. L., LONGO, F. M., BRESNAHAN, J. C., HEMPSTEAD, B. L. & YOON, S. O. 2002. ProNGF induces p75-mediated death of oligodendrocytes following spinal cord injury. *Neuron,* 36**,** 375-86.

BENEDETTI, M., LEVI, A. & CHAO, M. V. 1993. Differential expression of nerve growth factor receptors leads to altered binding affinity and neurotrophin responsiveness. *Proc Natl Acad Sci U S A,* 90**,** 7859-63.

BENNETT, J., CHUNG, D. C. & MAGUIRE, A. 2012. Gene delivery to the retina: from mouse to man. *Methods Enzymol,* 507**,** 255-74.

BENNETT, J., WELLMAN, J., MARSHALL, K. A., MCCAGUE, S., ASHTARI, M., DISTEFANO-PAPPAS, J., ELCI, O. U., CHUNG, D. C., SUN, J., WRIGHT, J. F., CROSS, D. R., ARAVAND, P., CYCKOWSKI, L. L., BENNICELLI, J. L., MINGOZZI, F., AURICCHIO, A., PIERCE, E. A., RUGGIERO, J., LEROY, B. P., SIMONELLI, F., HIGH, K. A. & MAGUIRE, A. M. 2016. Safety and durability of effect of contralateral-eye administration of AAV2 gene therapy in patients with childhood-onset blindness caused by RPE65 mutations: a follow-on phase 1 trial. *Lancet,* 388**,** 661-72.

BERMAN, H., HENRICK, K. & NAKAMURA, H. 2003. Announcing the worldwide Protein Data Bank. *Nat Struct Biol,* 10**,** 980.

BIKADI, Z. & HAZAI, E. 2009. Application of the PM6 semi-empirical method to modeling proteins enhances docking accuracy of AutoDock. *J Cheminform,* 1**,** 15.

BIKBOVA, G., OSHITARI, T. & YAMAMOTO, S. 2013. Neurite regeneration in adult rat retinas exposed to advanced glycation end-products and regenerative effects of neurotrophin-4. *Brain Res,* 1534**,** 33-45.

BINDER, D. K. & SCHARFMAN, H. E. 2004. Brain-derived neurotrophic factor. *Growth Factors,* 22**,** 123-31.

BLANCO, R. E., SOTO, I., DUPREY-DIAZ, M. & BLAGBURN, J. M. 2008. Up-regulation of brain-derived neurotrophic factor by application of fibroblast growth factor-2 to the cut optic nerve is important for long-term survival of retinal ganglion cells. *J Neurosci Res,* 86**,** 3382-92.

BOK, D., YASUMURA, D., MATTHES, M. T., RUIZ, A., DUNCAN, J. L., CHAPPELOW, A. V., ZOLUTUKHIN, S., HAUSWIRTH, W. & LAVAIL, M. M. 2002. Effects of adeno-associated virus-vectored ciliary neurotrophic factor on retinal structure and

function in mice with a P216L rds/peripherin mutation. *Exp Eye Res,* 74**,** 719-35.

BOLAND, M. V., ERVIN, A. M., FRIEDMAN, D., JAMPEL, H., HAWKINS, B., VOLENWEIDER, D., CHELLADURAI, Y., WARD, D., SUAREZ-CUERVO, C. & ROBINSON, K. A. 2012. *Treatment for Glaucoma: Comparative Effectiveness.* Rockville (MD).

BOTHWELL, M. 2016. Recent advances in understanding neurotrophin signaling. *F1000Res,* 5.

BRADY, J. M., BALTIMORE, D. & BALAZS, A. B. 2017. Antibody gene transfer with adeno-associated viral vectors as a method for HIV prevention. *Immunol Rev,* 275**,** 324-333.

BRAVO, R., PARRA, V., GATICA, D., RODRIGUEZ, A. E., TORREALBA, N., PAREDES, F., WANG, Z. V., ZORZANO, A., HILL, J. A., JAIMOVICH, E., QUEST, A. F. & LAVANDERO, S. 2013. Endoplasmic reticulum and the unfolded protein response: dynamics and metabolic integration. *Int Rev Cell Mol Biol,* 301**,** 215-90.

BRESSLER, S. B., QIN, H., BECK, R. W., CHALAM, K. V., KIM, J. E., MELIA, M., WELLS, J. A., 3RD & DIABETIC RETINOPATHY CLINICAL RESEARCH, N. 2012. Factors associated with changes in visual acuity and central subfield thickness at 1 year after treatment for diabetic macular edema with ranibizumab. *Arch Ophthalmol,* 130**,** 1153-61.

BROOKS, A. M. & GILLIES, W. E. 1992. Ocular beta-blockers in glaucoma management. Clinical pharmacological aspects. *Drugs Aging,* 2**,** 208-21.

BUTT, A. M., PUGH, M., HUBBARD, P. & JAMES, G. 2004. Functions of optic nerve glia: axoglial signalling in physiology and pathology. *Eye (Lond),* 18**,** 1110-21.

CAI, Z., FENG, G. S. & ZHANG, X. 2010a. Temporal requirement of the protein tyrosine phosphatase Shp2 in establishing the neuronal fate in early retinal development. *The Journal of neuroscience : the official journal of the Society for Neuroscience,* 30**,** 4110-9.

CAI, Z., FENG, G. S. & ZHANG, X. 2010b. Temporal requirement of the protein tyrosine phosphatase Shp2 in establishing the neuronal fate in early retinal development. *J Neurosci,* 30**,** 4110-9.

CAI, Z., SIMONS, D. L., FU, X. Y., FENG, G. S., WU, S. M. & ZHANG, X. 2011. Loss of Shp2-mediated mitogen-activated protein kinase signaling in Muller glial cells results in retinal degeneration. *Mol Cell Biol,* 31**,** 2973-83.

CAMACHO, C. J. & VAJDA, S. 2001. Protein docking along smooth association pathways. *Proc Natl Acad Sci U S A,* 98**,** 10636-41.

CAMPENOT, R. B. & MACINNIS, B. L. 2004. Retrograde transport of neurotrophins: fact and function. *J Neurobiol,* 58**,** 217-29.

CASACCIA-BONNEFIL, P., CARTER, B. D., DOBROWSKY, R. T. & CHAO, M. V. 1996. Death of oligodendrocytes mediated by the interaction of nerve growth factor with its receptor p75. *Nature,* 383**,** 716-9.

CASTELLO, N. A., NGUYEN, M. H., TRAN, J. D., CHENG, D., GREEN, K. N. & LAFERLA, F. M. 2014. 7,8-Dihydroxyflavone, a small molecule TrkB agonist, improves spatial memory and increases thin spine density in a mouse model of Alzheimer disease-like neuronal loss. *PLoS One,* 9**,** e91453.

CERUTTI, D. S., DUKE, R. E., DARDEN, T. A. & LYBRAND, T. P. 2009. Staggered Mesh Ewald: An extension of the Smooth Particle-Mesh Ewald method adding great versatility. *J Chem Theory Comput,* 5**,** 2322.

CHAMBERLAIN, K., RIYAD, J. M. & WEBER, T. 2017. Cardiac gene therapy with adeno-associated virus-based vectors. *Curr Opin Cardiol*.

CHAPLEAU, C. A., LANE, J., LARIMORE, J., LI, W., POZZO-MILLER, L. & PERCY, A. K. 2013. Recent Progress in Rett Syndrome and MeCP2 Dysfunction: Assessment of Potential Treatment Options. *Future Neurol,* 8.

CHEN, G., FAN, Z., WANG, X., MA, C., BOWER, K. A., SHI, X., KE, Z. J. & LUO, J. 2007. Brain-derived neurotrophic factor suppresses tunicamycin-induced upregulation of CHOP in neurons. *J Neurosci Res,* 85**,** 1674-84.

CHEN, H. & WEBER, A. J. 2001. BDNF enhances retinal ganglion cell survival in cats with optic nerve damage. *Invest Ophthalmol Vis Sci,* 42**,** 966-74.

CHEN, H. Y., LIN, C. L. & KAO, C. H. 2016. Does Migraine Increase the Risk of Glaucoma?: A Population-Based Cohort Study. *Medicine (Baltimore),* 95**,** e3670.

CHEN, S. J., LU, P., ZHANG, W. F. & LU, J. H. 2012. High myopia as a risk factor in primary open angle glaucoma. *Int J Ophthalmol,* 5**,** 750-3.

CHENG, L., SAPIEHA, P., KITTLEROVA, P., HAUSWIRTH, W. W. & DI POLO, A. 2002. TrkB gene transfer protects retinal ganglion cells from axotomy-induced death in vivo. *J Neurosci,* 22**,** 3977-86.

CHITRANSHI, N., GUPTA, S., TRIPATHI, P. K. & SETH, P. K. 2013. New molecular scaffolds for the design of Alzheimer's acetylcholinesterase inhibitors identified using ligand- and receptor-based virtual screening. *Medicinal Chemistry Research,* 22**,** 2328-2345.

CHITRANSHI, N., GUPTA, V., KUMAR, S. & GRAHAM, S. L. 2015. Exploring the Molecular Interactions of 7,8-Dihydroxyflavone and Its Derivatives with TrkB and VEGFR2 Proteins. *Int J Mol Sci,* 16**,** 21087-108.

CHO, S., WOOD, A. & BOWLBY, M. R. 2007. Brain slices as models for neurodegenerative disease and screening platforms to identify novel therapeutics. *Curr Neuropharmacol,* 5**,** 19-33.

CHONG, R. S., OSBORNE, A., CONCEICAO, R. & MARTIN, K. R. 2016. Platelet-Derived Growth Factor Preserves Retinal Synapses in a Rat Model of Ocular Hypertension. *Invest Ophthalmol Vis Sci,* 57**,** 842-52.

CHOREV, M. & CARMEL, L. 2012. The function of introns. *Front Genet,* 3**,** 55.

CHUCAIR-ELLIOTT, A. J., ELLIOTT, M. H., WANG, J., MOISEYEV, G. P., MA, J. X., POLITI, L. E., ROTSTEIN, N. P., AKIRA, S., UEMATSU, S. & ASH, J. D. 2012. Leukemia inhibitory factor coordinates the down-regulation of the visual cycle in the retina and retinal-pigmented epithelium. *J Biol Chem,* 287**,** 24092-102.

CIDECIYAN, A. V., JACOBSON, S. G., BELTRAN, W. A., SUMAROKA, A., SWIDER, M., IWABE, S., ROMAN, A. J., OLIVARES, M. B., SCHWARTZ, S. B., KOMAROMY, A. M., HAUSWIRTH, W. W. & AGUIRRE, G. D. 2013. Human retinal gene therapy for Leber congenital amaurosis shows advancing retinal degeneration despite enduring visual improvement. *Proc Natl Acad Sci U S A,* 110**,** E517-25.

CLAESSON-WELSH, L. 2003. Signal transduction by vascular endothelial growth factor receptors. *Biochem Soc Trans,* 31**,** 20-4.

CLARKE, D. B., BRAY, G. M. & AGUAYO, A. J. 1998. Prolonged administration of NT-4/5 fails to rescue most axotomized retinal ganglion cells in adult rats. *Vision Res,* 38**,** 1517-24.

COHEN-CORY, S. & FRASER, S. E. 1995. Effects of brain-derived neurotrophic factor on optic axon branching and remodelling in vivo. *Nature,* 378**,** 192-6.

COLLIGRIS, B., CROOKE, A., GASULL, X., ESCRIBANO, J., HERRERO-VANRELL, R., BENITEZ-DEL-CASTILLO, J. M., GARCIA-FEIJOO, J. & PINTOR, J. 2012. Recent

patents and developments in glaucoma biomarkers. *Recent Pat Endocr Metab Immune Drug Discov,* 6**,** 224-34.
COMPARISON OF AGE-RELATED MACULAR DEGENERATION TREATMENTS TRIALS RESEARCH, G., MARTIN, D. F., MAGUIRE, M. G., FINE, S. L., YING, G. S., JAFFE, G. J., GRUNWALD, J. E., TOTH, C., REDFORD, M. & FERRIS, F. L., 3RD 2012. Ranibizumab and bevacizumab for treatment of neovascular age-related macular degeneration: two-year results. *Ophthalmology,* 119**,** 1388-98.
CONWAY, B. R. 2009. Color vision, cones, and color-coding in the cortex. *Neuroscientist,* 15**,** 274-90.
CORNEJO, V. H. & HETZ, C. 2013. The unfolded protein response in Alzheimer's disease. *Semin Immunopathol,* 35**,** 277-92.
CRAWLEY, L., ZAMIR, S. M., CORDEIRO, M. F. & GUO, L. 2012. Clinical options for the reduction of elevated intraocular pressure. *Ophthalmol Eye Dis,* 4**,** 43-64.
CUI, Q., TANG, L. S., HU, B., SO, K. F. & YIP, H. K. 2002. Expression of trkA, trkB, and trkC in injured and regenerating retinal ganglion cells of adult rats. *Invest Ophthalmol Vis Sci,* 43**,** 1954-64.
CULLINAN, S. B., ZHANG, D., HANNINK, M., ARVISAIS, E., KAUFMAN, R. J. & DIEHL, J. A. 2003. Nrf2 is a direct PERK substrate and effector of PERK-dependent cell survival. *Mol Cell Biol,* 23**,** 7198-209.
CUNEA, A. & JEFFERY, G. 2007. The ageing photoreceptor. *Vis Neurosci,* 24**,** 151-5.
DANESHVAR, R. 2013. Anti-VEGF Agents and Glaucoma Filtering Surgery. *J Ophthalmic Vis Res,* 8**,** 182-6.
DANIAS, J., SHEN, F., KAVALARAKIS, M., CHEN, B., GOLDBLUM, D., LEE, K., ZAMORA, M. F., SU, Y., BRODIE, S. E., PODOS, S. M. & MITTAG, T. 2006. Characterization of retinal damage in the episcleral vein cauterization rat glaucoma model. *Exp Eye Res,* 82**,** 219-28.
DAVIS, B. M., CRAWLEY, L., PAHLITZSCH, M., JAVAID, F. & CORDEIRO, M. F. 2016. Glaucoma: the retina and beyond. *Acta Neuropathol,* 132**,** 807-826.
DAYA, S., CORTEZ, N. & BERNS, K. I. 2009. Adeno-associated virus site-specific integration is mediated by proteins of the nonhomologous end-joining pathway. *J Virol,* 83**,** 11655-64.
DE REZENDE CORREA, G., SOARES, V. H., DE ARAUJO-MARTINS, L., DOS SANTOS, A. A. & GIESTAL-DE-ARAUJO, E. 2015. Ouabain and BDNF Crosstalk on Ganglion Cell Survival in Mixed Retinal Cell Cultures. *Cell Mol Neurobiol,* 35**,** 651-60.
DEFREITAS, M. F., MCQUILLEN, P. S. & SHATZ, C. J. 2001. A novel p75NTR signaling pathway promotes survival, not death, of immunopurified neocortical subplate neurons. *J Neurosci,* 21**,** 5121-9.
DEKEYSTER, E., GEERAERTS, E., BUYENS, T., VAN DEN HAUTE, C., BAEKELANDT, V., DE GROEF, L., SALINAS-NAVARRO, M. & MOONS, L. 2015. Tackling Glaucoma from within the Brain: An Unfortunate Interplay of BDNF and TrkB. *PLoS One,* 10**,** e0142067.
DEVI, L. & OHNO, M. 2012. 7,8-dihydroxyflavone, a small-molecule TrkB agonist, reverses memory deficits and BACE1 elevation in a mouse model of Alzheimer's disease. *Neuropsychopharmacology,* 37**,** 434-44.
DI POLO, A., AIGNER, L. J., DUNN, R. J., BRAY, G. M. & AGUAYO, A. J. 1998. Prolonged delivery of brain-derived neurotrophic factor by adenovirus-infected Muller cells temporarily rescues injured retinal ganglion cells. *Proc Natl Acad Sci U S A,* 95**,** 3978-83.

DIMOVSKA-JORDANOVA, A. 2012. Neuroprotection in glaucoma--delusion, reality or hope? *Prilozi,* 33**,** 163-73.

DING, Y. Q., LI, X. Y., XIA, G. N., REN, H. Y., ZHOU, X. F., SU, B. Y. & QI, J. G. 2016. ProBDNF inhibits collective migration and chemotaxis of rat Schwann cells. *Tissue Cell,* 48**,** 503-10.

DKHISSI, O., CHANUT, E., WASOWICZ, M., SAVOLDELLI, M., NGUYEN-LEGROS, J., MINVIELLE, F. & VERSAUX-BOTTERI, C. 1999. Retinal TUNEL-positive cells and high glutamate levels in vitreous humor of mutant quail with a glaucoma-like disorder. *Invest Ophthalmol Vis Sci,* 40**,** 990-5.

DOBROWSKY, R. T., WERNER, M. H., CASTELLINO, A. M., CHAO, M. V. & HANNUN, Y. A. 1994. Activation of the sphingomyelin cycle through the low-affinity neurotrophin receptor. *Science,* 265**,** 1596-9.

DOH, S. H., KIM, J. H., LEE, K. M., PARK, H. Y. & PARK, C. K. 2010. Retinal ganglion cell death induced by endoplasmic reticulum stress in a chronic glaucoma model. *Brain Res,* 1308**,** 158-66.

DOMENICI, L., ORIGLIA, N., FALSINI, B., CERRI, E., BARLOSCIO, D., FABIANI, C., SANSO, M. & GIOVANNINI, L. 2014. Rescue of retinal function by BDNF in a mouse model of glaucoma. *PLoS One,* 9**,** e115579.

DUNDAS, J., OUYANG, Z., TSENG, J., BINKOWSKI, A., TURPAZ, Y. & LIANG, J. 2006. CASTp: computed atlas of surface topography of proteins with structural and topographical mapping of functionally annotated residues. *Nucleic Acids Res,* 34**,** W116-8.

EASTON, J. B., MOODY, N. M., ZHU, X. & MIDDLEMAS, D. S. 1999. Brain-derived neurotrophic factor induces phosphorylation of fibroblast growth factor receptor substrate 2. *J Biol Chem,* 274**,** 11321-7.

EASTON, J. B., ROYER, A. R. & MIDDLEMAS, D. S. 2006. The protein tyrosine phosphatase, Shp2, is required for the complete activation of the RAS/MAPK pathway by brain-derived neurotrophic factor. *J Neurochem,* 97**,** 834-45.

EMDADI, A., KONO, Y., SAMPLE, P. A., MASKALERIS, G. & WEINREB, R. N. 1999. Parapapillary atrophy in patients with focal visual field loss. *Am J Ophthalmol,* 128**,** 595-600.

ESIRI, M. M. 2007. The interplay between inflammation and neurodegeneration in CNS disease. *J Neuroimmunol,* 184**,** 4-16.

FEENSTRA, D. J., YEGO, E. C. & MOHR, S. 2013. Modes of Retinal Cell Death in Diabetic Retinopathy. *J Clin Exp Ophthalmol,* 4**,** 298.

FENG, L., CHEN, H., YI, J., TROY, J. B., ZHANG, H. F. & LIU, X. 2016. Long-Term Protection of Retinal Ganglion Cells and Visual Function by Brain-Derived Neurotrophic Factor in Mice With Ocular Hypertension. *Invest Ophthalmol Vis Sci,* 57**,** 3793-802.

FENNER, B. M. 2012. Truncated TrkB: beyond a dominant negative receptor. *Cytokine Growth Factor Rev,* 23**,** 15-24.

FEUER, W. J., SCHIFFMAN, J. C., DAVIS, J. L., PORCIATTI, V., GONZALEZ, P., KOILKONDA, R. D., YUAN, H., LALWANI, A., LAM, B. L. & GUY, J. 2016. Gene Therapy for Leber Hereditary Optic Neuropathy: Initial Results. *Ophthalmology,* 123**,** 558-70.

FIORENTINI, C., MATTANZA, C., COLLO, G., SAVOIA, P., SPANO, P. & MISSALE, C. 2011. The tyrosine phosphatase Shp-2 interacts with the dopamine D(1) receptor and triggers D(1) -mediated Erk signaling in striatal neurons. *J Neurochem,* 117**,** 253-63.

FISCHER, C. V., MANS, V., HORN, M., NAXER, S., KLETTNER, A. & VAN OTERENDORP, C. 2016. The Antiproliferative Effect of Bevacizumab on Human Tenon Fibroblasts Is Not Mediated by Vascular Endothelial Growth Factor Inhibition. *Invest Ophthalmol Vis Sci,* 57**,** 4970-4977.

FOLDVARI, M. & CHEN, D. W. 2016. The intricacies of neurotrophic factor therapy for retinal ganglion cell rescue in glaucoma: a case for gene therapy. *Neural Regen Res,* 11**,** 875-7.

FONSECA, A. C., FERREIRO, E., OLIVEIRA, C. R., CARDOSO, S. M. & PEREIRA, C. F. 2013. Activation of the endoplasmic reticulum stress response by the amyloid-beta 1-40 peptide in brain endothelial cells. *Biochim Biophys Acta,* 1832**,** 2191-203.

FRADE, J. M., BOVOLENTA, P., MARTINEZ-MORALES, J. R., ARRIBAS, A., BARBAS, J. A. & RODRIGUEZ-TEBAR, A. 1997. Control of early cell death by BDNF in the chick retina. *Development,* 124**,** 3313-20.

FRASSETTO, L. J., SCHLIEVE, C. R., LIEVEN, C. J., UTTER, A. A., JONES, M. V., AGARWAL, N. & LEVIN, L. A. 2006. Kinase-dependent differentiation of a retinal ganglion cell precursor. *Invest Ophthalmol Vis Sci,* 47**,** 427-38.

FRENK, J. 2006. Disease control priorities in developing countries. *Salud Publica De Mexico,* 48**,** 522-525.

FRIEDMAN, D. S., WOLFS, R. C., O'COLMAIN, B. J., KLEIN, B. E., TAYLOR, H. R., WEST, S., LESKE, M. C., MITCHELL, P., CONGDON, N., KEMPEN, J. & EYE DISEASES PREVALENCE RESEARCH, G. 2004. Prevalence of open-angle glaucoma among adults in the United States. *Arch Ophthalmol,* 122**,** 532-8.

FU, C. T. & SRETAVAN, D. 2010. Laser-induced ocular hypertension in albino CD-1 mice. *Invest Ophthalmol Vis Sci,* 51**,** 980-90.

FU, P., WU, Q., HU, J., LI, T. & GAO, F. 2016. Baclofen Protects Primary Rat Retinal Ganglion Cells from Chemical Hypoxia-Induced Apoptosis Through the Akt and PERK Pathways. *Front Cell Neurosci,* 10**,** 255.

FU, Q. L., HU, B., LI, X., SHAO, Z., SHI, J. B., WU, W., SO, K. F. & MI, S. 2010. LINGO-1 negatively regulates TrkB phosphorylation after ocular hypertension. *Eur J Neurosci,* 31**,** 1091-7.

FU, Q. L., LI, X., YIP, H. K., SHAO, Z., WU, W., MI, S. & SO, K. F. 2009. Combined effect of brain-derived neurotrophic factor and LINGO-1 fusion protein on long-term survival of retinal ganglion cells in chronic glaucoma. *Neuroscience,* 162**,** 375-82.

FUCHIKAWA, T., NAKAMURA, F., FUKUDA, N., TAKEI, K. & GOSHIMA, Y. 2009. Protein tyrosine phosphatase SHP2 is involved in Semaphorin 4D-induced axon repulsion. *Biochem Biophys Res Commun,* 385**,** 6-10.

GALBIATI, F., VOLONTE, D., GIL, O., ZANAZZI, G., SALZER, J. L., SARGIACOMO, M., SCHERER, P. E., ENGELMAN, J. A., SCHLEGEL, A., PARENTI, M., OKAMOTO, T. & LISANTI, M. P. 1998. Expression of caveolin-1 and -2 in differentiating PC12 cells and dorsal root ganglion neurons: caveolin-2 is up-regulated in response to cell injury. *Proc Natl Acad Sci U S A,* 95**,** 10257-62.

GALGAUSKAS, S., JUODKAITE, G. & TUTKUVIENE, J. 2014. Age-related changes in central corneal thickness in normal eyes among the adult Lithuanian population. *Clin Interv Aging,* 9**,** 1145-51.

GALINDO-ROMERO, C., VALIENTE-SORIANO, F. J., JIMENEZ-LOPEZ, M., GARCIA-AYUSO, D., VILLEGAS-PEREZ, M. P., VIDAL-SANZ, M. & AGUDO-BARRIUSO, M. 2013. Effect of brain-derived neurotrophic factor on mouse axotomized retinal ganglion cells and phagocytic microglia. *Invest Ophthalmol Vis Sci,* 54**,** 974-85.

GARCIA, M., FORSTER, V., HICKS, D. & VECINO, E. 2003. In vivo expression of neurotrophins and neurotrophin receptors is conserved in adult porcine retina in vitro. *Invest Ophthalmol Vis Sci,* 44**,** 4532-41.

GARDNER, B. M. & WALTER, P. 2011. Unfolded proteins are Ire1-activating ligands that directly induce the unfolded protein response. *Science,* 333**,** 1891-4.

GERMANA, A., SANCHEZ-RAMOS, C., GUERRERA, M. C., CALAVIA, M. G., NAVARRO, M., ZICHICHI, R., GARCIA-SUAREZ, O., PEREZ-PINERA, P. & VEGA, J. A. 2010. Expression and cell localization of brain-derived neurotrophic factor and TrkB during zebrafish retinal development. *J Anat,* 217**,** 214-22.

GESSESSE, G. W. & DAMJI, K. F. 2013. Advanced glaucoma: management pearls. *Middle East Afr J Ophthalmol,* 20**,** 131-41.

GOMES, C., FERREIRA, R., GEORGE, J., SANCHES, R., RODRIGUES, D. I., GONCALVES, N. & CUNHA, R. A. 2013. Activation of microglial cells triggers a release of brain-derived neurotrophic factor (BDNF) inducing their proliferation in an adenosine A2A receptor-dependent manner: A2A receptor blockade prevents BDNF release and proliferation of microglia. *J Neuroinflammation,* 10**,** 16.

GOMEZ DEL RIO, M. A., SANCHEZ-REUS, M. I., IGLESIAS, I., POZO, M. A., GARCIA-ARENCIBIA, M., FERNANDEZ-RUIZ, J., GARCIA-GARCIA, L., DELGADO, M. & BENEDI, J. 2013. Neuroprotective Properties of Standardized Extracts of Hypericum perforatum on Rotenone Model of Parkinson's Disease. *CNS Neurol Disord Drug Targets,* 12**,** 665-79.

GONI, F. J., STALMANS, I., DENIS, P., NORDMANN, J. P., TAYLOR, S., DIESTELHORST, M., FIGUEIREDO, A. R. & GARWAY-HEATH, D. F. 2016. Elevated Intraocular Pressure After Intravitreal Steroid Injection in Diabetic Macular Edema: Monitoring and Management. *Ophthalmol Ther,* 5**,** 47-61.

GOSSMAN, C. A., CHRISTIE, J., WEBSTER, M. K., LINN, D. M. & LINN, C. L. 2016. Neuroprotective Strategies in Glaucoma. *Curr Pharm Des,* 22**,** 2178-92.

GRAHAM, J. M., JR., KRAMER, N., BEJJANI, B. A., THIEL, C. T., CARTA, C., NERI, G., TARTAGLIA, M. & ZENKER, M. 2009. Genomic duplication of PTPN11 is an uncommon cause of Noonan syndrome. *Am J Med Genet A,* 149A**,** 2122-8.

GRAY, K. & ELLIS, V. 2008. Activation of pro-BDNF by the pericellular serine protease plasmin. *FEBS Lett,* 582**,** 907-10.

GREENBERG, B., BUTLER, J., FELKER, G. M., PONIKOWSKI, P., VOORS, A. A., POGODA, J. M., PROVOST, R., GUERRERO, J., HAJJAR, R. J. & ZSEBO, K. M. 2016. Prevalence of AAV1 neutralizing antibodies and consequences for a clinical trial of gene transfer for advanced heart failure. *Gene Ther,* 23**,** 313-9.

GRILL-SPECTOR, K. & MALACH, R. 2004. The human visual cortex. *Annu Rev Neurosci,* 27**,** 649-77.

GRIMES, C. A. & JOPE, R. S. 2001. CREB DNA binding activity is inhibited by glycogen synthase kinase-3 beta and facilitated by lithium. *J Neurochem,* 78**,** 1219-32.

GROSSMANN, K. S., WENDE, H., PAUL, F. E., CHERET, C., GARRATT, A. N., ZURBORG, S., FEINBERG, K., BESSER, D., SCHULZ, H., PELES, E., SELBACH, M., BIRCHMEIER, W. & BIRCHMEIER, C. 2009. The tyrosine phosphatase Shp2 (PTPN11) directs Neuregulin-1/ErbB signaling throughout Schwann cell development. *Proc Natl Acad Sci U S A,* 106**,** 16704-9.

GUO, L., MOSS, S. E., ALEXANDER, R. A., ALI, R. R., FITZKE, F. W. & CORDEIRO, M. F. 2005. Retinal ganglion cell apoptosis in glaucoma is related to intraocular pressure and IOP-induced effects on extracellular matrix. *Invest Ophthalmol Vis Sci,* 46**,** 175-82.

GUO, L., SALT, T. E., MAASS, A., LUONG, V., MOSS, S. E., FITZKE, F. W. & CORDEIRO, M. F. 2006. Assessment of neuroprotective effects of glutamate modulation on glaucoma-related retinal ganglion cell apoptosis in vivo. *Invest Ophthalmol Vis Sci,* 47**,** 626-33.

GUO, W., JI, Y., WANG, S., SUN, Y. & LU, B. 2014. Neuronal activity alters BDNF-TrkB signaling kinetics and downstream functions. *J Cell Sci,* 127**,** 2249-60.

GUO, X., NAMEKATA, K., KIMURA, A., NORO, T., AZUCHI, Y., SEMBA, K., HARADA, C., YOSHIDA, H., MITAMURA, Y. & HARADA, T. 2015. Brimonidine suppresses loss of retinal neurons and visual function in a murine model of optic neuritis. *Neurosci Lett,* 592**,** 27-31.

GUO, Z., MOHANTY, U., NOEHRE, J., SAWYER, T. K., SHERMAN, W. & KRILOV, G. 2010. Probing the alpha-helical structural stability of stapled p53 peptides: molecular dynamics simulations and analysis. *Chem Biol Drug Des,* 75**,** 348-59.

GUPTA, N. & YUCEL, Y. H. 2003. Brain changes in glaucoma. *Eur J Ophthalmol,* 13 Suppl 3**,** S32-5.

GUPTA, V., CHITRANSHI, N., YOU, Y., GUPTA, V., KLISTORNER, A. & GRAHAM, S. 2014a. Brain derived neurotrophic factor is involved in the regulation of glycogen synthase kinase 3beta (GSK3beta) signalling. *Biochem Biophys Res Commun,* 454**,** 381-6.

GUPTA, V., YOU, Y., LI, J., GUPTA, V., GOLZAN, M., KLISTORNER, A., VAN DEN BUUSE, M. & GRAHAM, S. 2014b. BDNF impairment is associated with age-related changes in the inner retina and exacerbates experimental glaucoma. *Biochim Biophys Acta,* 1842**,** 1567-78.

GUPTA, V. K., CHITRANSHI, N., GUPTA, V. B., GOLZAN, M., DHEER, Y., WALL, R. V., GEORGEVSKY, D., KING, A. E., VICKERS, J. C., CHUNG, R. & GRAHAM, S. 2016. Amyloid beta accumulation and inner retinal degenerative changes in Alzheimer's disease transgenic mouse. *Neurosci Lett,* 623**,** 52-6.

GUPTA, V. K. & GOWDA, L. R. 2008. Alpha-1-proteinase inhibitor is a heparin binding serpin: molecular interactions with the Lys rich cluster of helix-F domain. *Biochimie,* 90**,** 749-61.

GUPTA, V. K., RAJALA, A., DALY, R. J. & RAJALA, R. V. 2010. Growth factor receptor-bound protein 14: a new modulator of photoreceptor-specific cyclic-nucleotide-gated channel. *EMBO Rep,* 11**,** 861-7.

GUPTA, V. K., RAJALA, A. & RAJALA, R. V. 2012a. Insulin receptor regulates photoreceptor CNG channel activity. *Am J Physiol Endocrinol Metab,* 303**,** E1363-72.

GUPTA, V. K., YOU, Y., GUPTA, V. B., KLISTORNER, A. & GRAHAM, S. L. 2013a. TrkB receptor signalling: implications in neurodegenerative, psychiatric and proliferative disorders. *Int J Mol Sci,* 14**,** 10122-42.

GUPTA, V. K., YOU, Y., KLISTORNER, A. & GRAHAM, S. L. 2012b. Shp-2 regulates the TrkB receptor activity in the retinal ganglion cells under glaucomatous stress. *Biochim Biophys Acta,* 1822**,** 1643-9.

GUPTA, V. K., YOU, Y., LI, J. C., KLISTORNER, A. & GRAHAM, S. L. 2013b. Protective effects of 7,8-dihydroxyflavone on retinal ganglion and RGC-5 cells against excitotoxic and oxidative stress. *J Mol Neurosci,* 49**,** 96-104.

GUPTA, V. K., YOU, Y., LI, J. C., KLISTORNER, A. & GRAHAM, S. L. 2013c. Protective Effects of 7,8-Dihydroxyflavone on Retinal Ganglion and RGC-5 Cells Against Excitotoxic and Oxidative Stress. *Journal of molecular neuroscience : MN,* 49**,** 96-104.

HA, Y., LIU, H., XU, Z., YOKOTA, H., NARAYANAN, S. P., LEMTALSI, T., SMITH, S. B., CALDWELL, R. W., CALDWELL, R. B. & ZHANG, W. 2015. Endoplasmic reticulum stress-regulated CXCR3 pathway mediates inflammation and neuronal injury in acute glaucoma. *Cell Death Dis,* 6**,** e1900.

HAGSTROM, S. A., YING, G. S., PAUER, G. J., STURGILL-SHORT, G. M., HUANG, J., MAGUIRE, M. G. & MARTIN, D. F. 2014. VEGFA and VEGFR2 gene polymorphisms and response to anti-vascular endothelial growth factor therapy: comparison of age-related macular degeneration treatments trials (CATT). *JAMA Ophthalmol,* 132**,** 521-7.

HAN, M. L., LIU, G. H., GUO, J., YU, S. J. & HUANG, J. 2016. Imipramine protects retinal ganglion cells from oxidative stress through the tyrosine kinase receptor B signaling pathway. *Neural Regen Res,* 11**,** 476-9.

HANAFUSA, H., TORII, S., YASUNAGA, T., MATSUMOTO, K. & NISHIDA, E. 2004. Shp2, an SH2-containing protein-tyrosine phosphatase, positively regulates receptor tyrosine kinase signaling by dephosphorylating and inactivating the inhibitor Sprouty. *J Biol Chem,* 279**,** 22992-5.

HANIU, M., TALVENHEIMO, J., LE, J., KATTA, V., WELCHER, A. & ROHDE, M. F. 1995. Extracellular domain of neurotrophin receptor trkB: disulfide structure, N-glycosylation sites, and ligand binding. *Arch Biochem Biophys,* 322**,** 256-64.

HARADA, C., GUO, X., NAMEKATA, K., KIMURA, A., NAKAMURA, K., TANAKA, K., PARADA, L. F. & HARADA, T. 2011. Glia- and neuron-specific functions of TrkB signalling during retinal degeneration and regeneration. *Nat Commun,* 2**,** 189.

HARADA, C., HARADA, T., NAKAMURA, K., SAKAI, Y., TANAKA, K. & PARADA, L. F. 2006. Effect of p75NTR on the regulation of naturally occurring cell death and retinal ganglion cell number in the mouse eye. *Dev Biol,* 290**,** 57-65.

HARADA, T., HARADA, C., KOHSAKA, S., WADA, E., YOSHIDA, K., OHNO, S., MAMADA, H., TANAKA, K., PARADA, L. F. & WADA, K. 2002. Microglia-Muller glia cell interactions control neurotrophic factor production during light-induced retinal degeneration. *J Neurosci,* 22**,** 9228-36.

HARDY, B., DOUGLAS, N., HELMA, C., RAUTENBERG, M., JELIAZKOVA, N., JELIAZKOV, V., NIKOLOVA, I., BENIGNI, R., TCHEREMENSKAIA, O., KRAMER, S., GIRSCHICK, T., BUCHWALD, F., WICKER, J., KARWATH, A., GUTLEIN, M., MAUNZ, A., SARIMVEIS, H., MELAGRAKI, G., AFANTITIS, A., SOPASAKIS, P., GALLAGHER, D., POROIKOV, V., FILIMONOV, D., ZAKHAROV, A., LAGUNIN, A., GLORIOZOVA, T., NOVIKOV, S., SKVORTSOVA, N., DRUZHILOVSKY, D., CHAWLA, S., GHOSH, I., RAY, S., PATEL, H. & ESCHER, S. 2010. Collaborative development of predictive toxicology applications. *J Cheminform,* 2**,** 7.

HARRINGTON, A. W., LEINER, B., BLECHSCHMITT, C., AREVALO, J. C., LEE, R., MORL, K., MEYER, M., HEMPSTEAD, B. L., YOON, S. O. & GIEHL, K. M. 2004. Secreted proNGF is a pathophysiological death-inducing ligand after adult CNS injury. *Proc Natl Acad Sci U S A,* 101**,** 6226-30.

HARRIS, P. A., CHEUNG, M., HUNTER, R. N., 3RD, BROWN, M. L., VEAL, J. M., NOLTE, R. T., WANG, L., LIU, W., CROSBY, R. M., JOHNSON, J. H., EPPERLY, A. H., KUMAR, R., LUTTRELL, D. K. & STAFFORD, J. A. 2005. Discovery and evaluation of 2-anilino-5-aryloxazoles as a novel class of VEGFR2 kinase inhibitors. *J Med Chem,* 48**,** 1610-9.

HAUCK, S. M., KINKL, N., DEEG, C. A., SWIATEK-DE LANGE, M., SCHOFFMANN, S. & UEFFING, M. 2006. GDNF family ligands trigger indirect neuroprotective signaling in retinal glial cells. *Mol Cell Biol,* 26**,** 2746-57.

HAUSER, M. A., ALLINGHAM, R. R., LINKROUM, K., WANG, J., LAROCQUE-ABRAMSON, K., FIGUEIREDO, D., SANTIAGO-TURLA, C., DEL BONO, E. A., HAINES, J. L., PERICAK-VANCE, M. A. & WIGGS, J. L. 2006. Distribution of WDR36 DNA sequence variants in patients with primary open-angle glaucoma. *Invest Ophthalmol Vis Sci,* 47**,** 2542-6.

HAUSWIRTH, W. W., ALEMAN, T. S., KAUSHAL, S., CIDECIYAN, A. V., SCHWARTZ, S. B., WANG, L., CONLON, T. J., BOYE, S. L., FLOTTE, T. R., BYRNE, B. J. & JACOBSON, S. G. 2008. Treatment of leber congenital amaurosis due to RPE65 mutations by ocular subretinal injection of adeno-associated virus gene vector: short-term results of a phase I trial. *Hum Gene Ther,* 19**,** 979-90.

HE, L., WU, Y., LIN, L., WANG, J., CHEN, Y., YI, Z., LIU, M. & PANG, X. 2011. Hispidulin, a small flavonoid molecule, suppresses the angiogenesis and growth of human pancreatic cancer by targeting vascular endothelial growth factor receptor 2-mediated PI3K/Akt/mTOR signaling pathway. *Cancer Sci,* 102**,** 219-25.

HEIJL, A., LESKE, M. C., BENGTSSON, B., HYMAN, L., BENGTSSON, B., HUSSEIN, M. & EARLY MANIFEST GLAUCOMA TRIAL, G. 2002. Reduction of intraocular pressure and glaucoma progression: results from the Early Manifest Glaucoma Trial. *Arch Ophthalmol,* 120**,** 1268-79.

HEMPSTEAD, B. L. 2006. Dissecting the diverse actions of pro- and mature neurotrophins. *Curr Alzheimer Res,* 3**,** 19-24.

HEMPSTEAD, B. L., MARTIN-ZANCA, D., KAPLAN, D. R., PARADA, L. F. & CHAO, M. V. 1991. High-affinity NGF binding requires coexpression of the trk proto-oncogene and the low-affinity NGF receptor. *Nature,* 350**,** 678-83.

HERRERA ABREU, M. T., WANG, Q., VACHON, E., SUZUKI, T., CHOW, C. W., WANG, Y., HONG, O., VILLAR, J., MCCULLOCH, C. A. & DOWNEY, G. P. 2006. Tyrosine phosphatase SHP-2 regulates IL-1 signaling in fibroblasts through focal adhesions. *J Cell Physiol,* 207**,** 132-43.

HETZ, C. 2012. The unfolded protein response: controlling cell fate decisions under ER stress and beyond. *Nat Rev Mol Cell Biol,* 13**,** 89-102.

HEUMANN, R. 1994. Neurotrophin signalling. *Curr Opin Neurobiol,* 4**,** 668-79.

HILDEBRAND, C., REMAHL, S. & WAXMAN, S. G. 1985. Axo-glial relations in the retina-optic nerve junction of the adult rat: electron-microscopic observations. *J Neurocytol,* 14**,** 597-617.

HOLLIEN, J., LIN, J. H., LI, H., STEVENS, N., WALTER, P. & WEISSMAN, J. S. 2009. Regulated Ire1-dependent decay of messenger RNAs in mammalian cells. *J Cell Biol,* 186**,** 323-31.

HOLLIEN, J. & WEISSMAN, J. S. 2006. Decay of endoplasmic reticulum-localized mRNAs during the unfolded protein response. *Science,* 313**,** 104-7.

HOLLIS, E. R., 2ND, JAMSHIDI, P., LOW, K., BLESCH, A. & TUSZYNSKI, M. H. 2009. Induction of corticospinal regeneration by lentiviral trkB-induced Erk activation. *Proc Natl Acad Sci U S A,* 106**,** 7215-20.

HOLMES, K., ROBERTS, O. L., THOMAS, A. M. & CROSS, M. J. 2007. Vascular endothelial growth factor receptor-2: structure, function, intracellular signalling and therapeutic inhibition. *Cell Signal,* 19**,** 2003-12.

HOSEL, M., HUBER, A., BOHLEN, S., LUCIFORA, J., RONZITTI, G., PUZZO, F., BOISGERAULT, F., HACKER, U. T., KWANTEN, W. J., KLOTING, N., BLUHER, M., GLUSCHKO, A., SCHRAMM, M., UTERMOHLEN, O., BLOCH, W., MINGOZZI, F., KRUT, O. & BUNING, H. 2017. Autophagy Determines Efficiency of Liver-directed Gene Therapy with Adeno-associated Viral Vectors. *Hepatology*.

HOSHI, M., TAKASHIMA, A., NOGUCHI, K., MURAYAMA, M., SATO, M., KONDO, S., SAITOH, Y., ISHIGURO, K., HOSHINO, T. & IMAHORI, K. 1996. Regulation of mitochondrial pyruvate dehydrogenase activity by tau protein kinase I/glycogen synthase kinase 3beta in brain. *Proc Natl Acad Sci U S A,* 93**,** 2719-23.

HU, Y. 2016. Axon injury induced endoplasmic reticulum stress and neurodegeneration. *Neural Regen Res,* 11**,** 1557-1559.

HU, Y., CHO, S. & GOLDBERG, J. L. 2010. Neurotrophic effect of a novel TrkB agonist on retinal ganglion cells. *Invest Ophthalmol Vis Sci,* 51**,** 1747-54.

HU, Y., PARK, K. K., YANG, L., WEI, X., YANG, Q., CHO, K. S., THIELEN, P., LEE, A. H., CARTONI, R., GLIMCHER, L. H., CHEN, D. F. & HE, Z. 2012. Differential effects of unfolded protein response pathways on axon injury-induced death of retinal ganglion cells. *Neuron,* 73**,** 445-52.

HU, Y. S., LONG, N., PIGINO, G., BRADY, S. T. & LAZAROV, O. 2013. Molecular mechanisms of environmental enrichment: impairments in Akt/GSK3beta, neurotrophin-3 and CREB signaling. *PLoS One,* 8**,** e64460.

HUANG, E. J. & REICHARDT, L. F. 2003. Trk receptors: roles in neuronal signal transduction. *Annu Rev Biochem,* 72**,** 609-42.

HUANG, W., FILETA, J. B., DOBBERFUHL, A., FILIPPOPOLOUS, T., GUO, Y., KWON, G. & GROSSKREUTZ, C. L. 2005. Calcineurin cleavage is triggered by elevated intraocular pressure, and calcineurin inhibition blocks retinal ganglion cell death in experimental glaucoma. *Proc Natl Acad Sci U S A,* 102**,** 12242-7.

HUANG, Y. Z. & MCNAMARA, J. O. 2010. Mutual regulation of Src family kinases and the neurotrophin receptor TrkB. *J Biol Chem,* 285**,** 8207-17.

HUBERMAN, A. D. 2007. Mechanisms of eye-specific visual circuit development. *Curr Opin Neurobiol,* 17**,** 73-80.

IBANEZ, C. F. 2013. Structure and physiology of the RET receptor tyrosine kinase. *Cold Spring Harb Perspect Biol,* 5.

IBANEZ, C. F. & ANDRESSOO, J. O. 2016. Biology of GDNF and its receptors - Relevance for disorders of the central nervous system. *Neurobiol Dis*.

IBANEZ, C. F. & SIMI, A. 2012. p75 neurotrophin receptor signaling in nervous system injury and degeneration: paradox and opportunity. *Trends Neurosci,* 35**,** 431-40.

IENTILE, R., MACAIONE, V., TELETTA, M., PEDALE, S., TORRE, V. & MACAIONE, S. 2001. Apoptosis and necrosis occurring in excitotoxic cell death in isolated chick embryo retina. *J Neurochem,* 79**,** 71-8.

IGARASHI, T., MIYAKE, K., KOBAYASHI, M., KAMEYA, S., FUJIMOTO, C., NAKAMOTO, K., TAKAHASHI, H., IGARASHI, T., MIYAKE, N., IIJIMA, O., HIRAI, Y., SHIMADA, T., OKADA, T. & TAKAHASHI, H. 2016. Tyrosine triple mutated AAV2-BDNF gene therapy in a rat model of transient IOP elevation. *Mol Vis,* 22**,** 816-26.

ISMAIL, N., ISMAIL, M., FATHY, S. F., MUSA, S. N., IMAM, M. U., FOO, J. B. & IQBAL, S. 2012. Neuroprotective effects of germinated brown rice against hydrogen peroxide induced cell death in human SH-SY5Y cells. *Int J Mol Sci,* 13**,** 9692-708.

JABOIN, J., KIM, C. J., KAPLAN, D. R. & THIELE, C. J. 2002. Brain-derived neurotrophic factor activation of TrkB protects neuroblastoma cells from chemotherapy-induced apoptosis via phosphatidylinositol 3'-kinase pathway. *Cancer Res,* 62**,** 6756-63.

JAMISON, D. T. & MOSLEY, W. H. 1991. Disease-Control Priorities in Developing-Countries - Health-Policy Responses to Epidemiologic Change. *American Journal of Public Health,* 81**,** 15-22.

JANG, S. W., LIU, X., CHAN, C. B., FRANCE, S. A., SAYEED, I., TANG, W., LIN, X., XIAO, G., ANDERO, R., CHANG, Q., RESSLER, K. J. & YE, K. 2010a. Deoxygedunin, a natural product with potent neurotrophic activity in mice. *PLoS One,* 5**,** e11528.

JANG, S. W., LIU, X., YEPES, M., SHEPHERD, K. R., MILLER, G. W., LIU, Y., WILSON, W. D., XIAO, G., BLANCHI, B., SUN, Y. E. & YE, K. 2010b. A selective TrkB agonist with potent neurotrophic activities by 7,8-dihydroxyflavone. *Proc Natl Acad Sci U S A,* 107**,** 2687-92.

JIA, L., CEPURNA, W. O., JOHNSON, E. C. & MORRISON, J. C. 2000. Patterns of intraocular pressure elevation after aqueous humor outflow obstruction in rats. *Invest Ophthalmol Vis Sci,* 41**,** 1380-5.

JIANG, M., PENG, Q., LIU, X., JIN, J., HOU, Z., ZHANG, J., MORI, S., ROSS, C. A., YE, K. & DUAN, W. 2013. Small-molecule TrkB receptor agonists improve motor function and extend survival in a mouse model of Huntington's disease. *Hum Mol Genet,* 22**,** 2462-70.

JIANG, Z. X. & ZHANG, Z. Y. 2008. Targeting PTPs with small molecule inhibitors in cancer treatment. *Cancer Metastasis Rev,* 27**,** 263-72.

JIAO, H., ZHANG, Y., YAN, Z., WANG, Z. G., LIU, G., MINSHALL, R. D., MALIK, A. B. & HU, G. 2013. Caveolin-1 Tyr14 phosphorylation induces interaction with TLR4 in endothelial cells and mediates MyD88-dependent signaling and sepsis-induced lung inflammation. *J Immunol,* 191**,** 6191-9.

JING, G., WANG, J. J. & ZHANG, S. X. 2012. ER stress and apoptosis: a new mechanism for retinal cell death. *Exp Diabetes Res,* 2012**,** 589589.

JO, A., PARK, H., LEE, S. H., AHN, S. H., KIM, H. J., PARK, E. M. & CHOI, Y. H. 2014. SHP-2 binds to caveolin-1 and regulates Src activity via competitive inhibition of CSK in response to H2O2 in astrocytes. *PLoS One,* 9**,** e91582.

JONAS, J. B. & GRUNDLER, A. E. 1997. Correlation between mean visual field loss and morphometric optic disk variables in the open-angle glaucomas. *Am J Ophthalmol,* 124**,** 488-97.

JUNGLAS, B., KUESPERT, S., SELEEM, A. A., STRULLER, T., ULLMANN, S., BOSL, M., BOSSERHOFF, A., KOSTLER, J., WAGNER, R., TAMM, E. R. & FUCHSHOFER, R. 2012. Connective tissue growth factor causes glaucoma by modifying the actin cytoskeleton of the trabecular meshwork. *Am J Pathol,* 180**,** 2386-403.

KANG, M. J. & RYOO, H. D. 2009. Suppression of retinal degeneration in Drosophila by stimulation of ER-associated degradation. *Proc Natl Acad Sci U S A,* 106**,** 17043-8.

KAPLAN, D. R. & MILLER, F. D. 2000. Neurotrophin signal transduction in the nervous system. *Curr Opin Neurobiol,* 10**,** 381-91.

KAPLAN, G., KIESSLING, R., TEKLEMARIAM, S., HANCOCK, G., SHEFTEL, G., JOB, C. K., CONVERSE, P., OTTENHOFF, T. H., BECX-BLEUMINK, M., DIETZ, M. & ET AL. 1989. The reconstitution of cell-mediated immunity in the cutaneous lesions of lepromatous leprosy by recombinant interleukin 2. *J Exp Med,* 169**,** 893-907.

KARKKAINEN, M. J. & PETROVA, T. V. 2000. Vascular endothelial growth factor receptors in the regulation of angiogenesis and lymphangiogenesis. *Oncogene,* 19**,** 5598-605.

KASETTI, R. B., PHAN, T. N., MILLAR, J. C. & ZODE, G. S. 2016. Expression of Mutant Myocilin Induces Abnormal Intracellular Accumulation of Selected Extracellular Matrix Proteins in the Trabecular Meshwork. *Invest Ophthalmol Vis Sci,* 57**,** 6058-6069.

KASS, M. A., HEUER, D. K., HIGGINBOTHAM, E. J., JOHNSON, C. A., KELTNER, J. L., MILLER, J. P., PARRISH, R. K., 2ND, WILSON, M. R. & GORDON, M. O. 2002. The Ocular Hypertension Treatment Study: a randomized trial determines that topical ocular hypotensive medication delays or prevents the onset of primary open-angle glaucoma. *Arch Ophthalmol,* 120**,** 701-13; discussion 829-30.

KATZ, B., WEINREB, R. N., WHEELER, D. T. & KLAUBER, M. R. 1990. Anterior ischaemic optic neuropathy and intraocular pressure. *Br J Ophthalmol,* 74**,** 99-102.

KAUFMAN, P. L. 2017. Latanoprostene bunod ophthalmic solution 0.024% for IOP lowering in glaucoma and ocular hypertension. *Expert Opin Pharmacother,* 18**,** 433-444.

KE, Y., ZHANG, E. E., HAGIHARA, K., WU, D., PANG, Y., KLEIN, R., CURRAN, T., RANSCHT, B. & FENG, G. S. 2007. Deletion of Shp2 in the brain leads to defective proliferation and differentiation in neural stem cells and early postnatal lethality. *Mol Cell Biol,* 27**,** 6706-17.

KELLY-SPRATT, K. S., KLESSE, L. J., MERENMIES, J. & PARADA, L. F. 1999. A TrkB/insulin receptor-related receptor chimeric receptor induces PC12 cell differentiation and exhibits prolonged activation of mitogen-activated protein kinase. *Cell Growth Differ,* 10**,** 805-12.

KHALIN, I., ALYAUTDIN, R., KOCHERGA, G. & BAKAR, M. A. 2015. Targeted delivery of brain-derived neurotrophic factor for the treatment of blindness and deafness. *Int J Nanomedicine,* 10**,** 3245-67.

KILIC, U., KILIC, E., JARVE, A., GUO, Z., SPUDICH, A., BIEBER, K., BARZENA, U., BASSETTI, C. L., MARTI, H. H. & HERMANN, D. M. 2006. Human vascular endothelial growth factor protects axotomized retinal ganglion cells in vivo by activating ERK-1/2 and Akt pathways. *J Neurosci,* 26**,** 12439-46.

KIM, B. S., SAVINOVA, O. V., REEDY, M. V., MARTIN, J., LUN, Y., GAN, L., SMITH, R. S., TOMAREV, S. I., JOHN, S. W. & JOHNSON, R. L. 2001. Targeted Disruption of the Myocilin Gene (Myoc) Suggests that Human Glaucoma-Causing Mutations Are Gain of Function. *Mol Cell Biol,* 21**,** 7707-13.

KIM, H. J., HAN, A. M., SHIM, J. H., YOON, H. H., KWON, H. & KWON, Y. K. 2007. Shp2 is involved in neuronal differentiation of hippocampal precursor cells. *Arch Pharm Res,* 30**,** 750-4.

KIM, I., XU, W. & REED, J. C. 2008. Cell death and endoplasmic reticulum stress: disease relevance and therapeutic opportunities. *Nat Rev Drug Discov,* 7**,** 1013-30.

KIM, M. H. 2003. Flavonoids inhibit VEGF/bFGF-induced angiogenesis in vitro by inhibiting the matrix-degrading proteases. *Journal of cellular biochemistry,* 89**,** 529-38.

KIMURA, A., NAMEKATA, K., GUO, X., HARADA, C. & HARADA, T. 2016. Neuroprotection, Growth Factors and BDNF-TrkB Signalling in Retinal Degeneration. *Int J Mol Sci,* 17.

KINKL, N., HAGEMAN, G. S., SAHEL, J. A. & HICKS, D. 2002. Fibroblast growth factor receptor (FGFR) and candidate signaling molecule distribution within rat and human retina. *Mol Vis,* 8**,** 149-60.

KISS, A. L., TURI, A., MULLER, N., KANTOR, O. & BOTOS, E. 2002. Caveolae and caveolin isoforms in rat peritoneal macrophages. *Micron,* 33**,** 75-93.

KLAASSEN, I., VAN NOORDEN, C. J. & SCHLINGEMANN, R. O. 2013. Molecular basis of the inner blood-retinal barrier and its breakdown in diabetic macular edema and other pathological conditions. *Prog Retin Eye Res,* 34**,** 19-48.

KLOCKER, N., CELLERINO, A. & BAHR, M. 1998. Free radical scavenging and inhibition of nitric oxide synthase potentiates the neurotrophic effects of brain-derived neurotrophic factor on axotomized retinal ganglion cells In vivo. *J Neurosci,* 18**,** 1038-46.

KO, M. L., HU, D. N., RITCH, R. & SHARMA, S. C. 2000. The combined effect of brain-derived neurotrophic factor and a free radical scavenger in experimental glaucoma. *Invest Ophthalmol Vis Sci,* 41**,** 2967-71.

KONTARIDIS, M. I., EMINAGA, S., FORNARO, M., ZITO, C. I., SORDELLA, R., SETTLEMAN, J. & BENNETT, A. M. 2004. SHP-2 positively regulates myogenesis by coupling to the Rho GTPase signaling pathway. *Mol Cell Biol,* 24**,** 5340-52.

KONTARIDIS, M. I., YANG, W., BENCE, K. K., CULLEN, D., WANG, B., BODYAK, N., KE, Q., HINEK, A., KANG, P. M., LIAO, R. & NEEL, B. G. 2008. Deletion of Ptpn11 (Shp2) in cardiomyocytes causes dilated cardiomyopathy via effects on the extracellular signal-regulated kinase/mitogen-activated protein kinase and RhoA signaling pathways. *Circulation,* 117**,** 1423-35.

KRISHNAN, A., FEI, F., JONES, A., BUSTO, P., MARSHAK-ROTHSTEIN, A., KSANDER, B. R. & GREGORY-KSANDER, M. 2016. Overexpression of Soluble Fas Ligand following Adeno-Associated Virus Gene Therapy Prevents Retinal Ganglion Cell Death in Chronic and Acute Murine Models of Glaucoma. *J Immunol,* 197**,** 4626-4638.

KROEBER, M., OHLMANN, A., RUSSELL, P. & TAMM, E. R. 2006. Transgenic studies on the role of optineurin in the mouse eye. *Exp Eye Res,* 82**,** 1075-85.

KROLL, J. & WALTENBERGER, J. 1997. The vascular endothelial growth factor receptor KDR activates multiple signal transduction pathways in porcine aortic endothelial cells. *J Biol Chem,* 272**,** 32521-7.

KRUGER, R. P., AURANDT, J. & GUAN, K. L. 2005. Semaphorins command cells to move. *Nat Rev Mol Cell Biol,* 6**,** 789-800.

KUAN, C. Y., YANG, D. D., SAMANTA ROY, D. R., DAVIS, R. J., RAKIC, P. & FLAVELL, R. A. 1999. The Jnk1 and Jnk2 protein kinases are required for regional specific apoptosis during early brain development. *Neuron,* 22**,** 667-76.

KUMAMARU, E., NUMAKAWA, T., ADACHI, N. & KUNUGI, H. 2011. Glucocorticoid suppresses BDNF-stimulated MAPK/ERK pathway via inhibiting interaction of Shp2 with TrkB. *FEBS Lett,* 585**,** 3224-8.

KUNZ, J., SCHMID, J. & SCHREINER, W. E. 1976. [Contribution to the treatment of threatened abortion]. *Schweiz Med Wochenschr,* 106**,** 1429-35.

KUSAKARI, S., SAITOW, F., AGO, Y., SHIBASAKI, K., SATO-HASHIMOTO, M., MATSUZAKI, Y., KOTANI, T., MURATA, Y., HIRAI, H., MATSUDA, T., SUZUKI, H., MATOZAKI, T. & OHNISHI, H. 2015. Shp2 in forebrain neurons regulates synaptic plasticity, locomotion, and memory formation in mice. *Mol Cell Biol,* 35**,** 1557-72.

LABUTE, P. 2009. Protonate3D: assignment of ionization states and hydrogen coordinates to macromolecular structures. *Proteins,* 75**,** 187-205.

LAMBERT, W. S., CARLSON, B. J., FORMICHELLA, C. R., SAPPINGTON, R. M., AHLEM, C. & CALKINS, D. J. 2017. Oral Delivery of a Synthetic Sterol Reduces Axonopathy and Inflammation in a Rodent Model of Glaucoma. *Front Neurosci,* 11**,** 45.

LAMBROU, F. H., VELA, M. A. & WOODS, W. 1989. Obstruction of the trabecular meshwork by retinal rod outer segments. *Arch Ophthalmol,* 107**,** 742-5.

LAMBUK, L., JAFRI, A. J., ARFUZIR, N. N., IEZHITSA, I., AGARWAL, R., ROZALI, K. N., AGARWAL, P., BAKAR, N. S., KUTTY, M. K., YUSOF, A. P., KRASILNIKOVA, A., SPASOV, A., OZEROV, A. & ISMAIL, N. M. 2016. Neuroprotective Effect of

Magnesium Acetyltaurate Against NMDA-Induced Excitotoxicity in Rat Retina. *Neurotox Res*.
LANGMAN, M. J., LANCASHIRE, R. J., CHENG, K. K. & STEWART, P. M. 2005. Systemic hypertension and glaucoma: mechanisms in common and co-occurrence. *Br J Ophthalmol,* 89**,** 960-3.
LASKOWSKI, R. A. & SWINDELLS, M. B. 2011. LigPlot+: multiple ligand-protein interaction diagrams for drug discovery. *J Chem Inf Model,* 51**,** 2778-86.
LASZLO, C. F. & WU, S. 2009. Old target new approach: an alternate NF-kappaB activation pathway via translation inhibition. *Mol Cell Biochem,* 328**,** 9-16.
LAU, D., MCGEE, L. H., ZHOU, S., RENDAHL, K. G., MANNING, W. C., ESCOBEDO, J. A. & FLANNERY, J. G. 2000. Retinal degeneration is slowed in transgenic rats by AAV-mediated delivery of FGF-2. *Invest Ophthalmol Vis Sci,* 41**,** 3622-33.
LAURIOL, J., JAFFRE, F. & KONTARIDIS, M. I. 2015. The role of the protein tyrosine phosphatase SHP2 in cardiac development and disease. *Semin Cell Dev Biol,* 37**,** 73-81.
LAW, S. K. 2007. First-line treatment for elevated intraocular pressure (IOP) associated with open-angle glaucoma or ocular hypertension: focus on bimatoprost. *Clin Ophthalmol,* 1**,** 225-32.
LE BAIL, J. C., VARNAT, F., NICOLAS, J. C. & HABRIOUX, G. 1998. Estrogenic and antiproliferative activities on MCF-7 human breast cancer cells by flavonoids. *Cancer Lett,* 130**,** 209-16.
LEAVER, S. G., CUI, Q., PLANT, G. W., ARULPRAGASAM, A., HISHEH, S., VERHAAGEN, J. & HARVEY, A. R. 2006. AAV-mediated expression of CNTF promotes long-term survival and regeneration of adult rat retinal ganglion cells. *Gene Ther,* 13**,** 1328-41.
LEBRUN-JULIEN, F., BERTRAND, M. J., DE BACKER, O., STELLWAGEN, D., MORALES, C. R., DI POLO, A. & BARKER, P. A. 2010. ProNGF induces TNFalpha-dependent death of retinal ganglion cells through a p75NTR non-cell-autonomous signaling pathway. *Proc Natl Acad Sci U S A,* 107**,** 3817-22.
LEBRUN-JULIEN, F., MORQUETTE, B., DOUILLETTE, A., SARAGOVI, H. U. & DI POLO, A. 2009. Inhibition of p75(NTR) in glia potentiates TrkA-mediated survival of injured retinal ganglion cells. *Mol Cell Neurosci,* 40**,** 410-20.
LEE, J. & OZCAN, U. 2014. Unfolded protein response signaling and metabolic diseases. *J Biol Chem,* 289**,** 1203-11.
LEE, R., KERMANI, P., TENG, K. K. & HEMPSTEAD, B. L. 2001. Regulation of cell survival by secreted proneurotrophins. *Science,* 294**,** 1945-8.
LEI, K. & DAVIS, R. J. 2003. JNK phosphorylation of Bim-related members of the Bcl2 family induces Bax-dependent apoptosis. *Proc Natl Acad Sci U S A,* 100**,** 2432-7.
LEMMON, M. A. & SCHLESSINGER, J. 2010. Cell signaling by receptor tyrosine kinases. *Cell,* 141**,** 1117-34.
LEVI-MONTALCINI, R. 1987. The nerve growth factor 35 years later. *Science,* 237**,** 1154-62.
LEVKOVITCH-VERBIN, H., WASERZOOG, Y., VANDER, S., MAKAROVSKY, D. & ILIA, P. 2014. Minocycline mechanism of neuroprotection involves the Bcl-2 gene family in optic nerve transection. *Int J Neurosci,* 124**,** 755-61.
LI, H. & LI, C. 2010. Multiple ligand simultaneous docking: orchestrated dancing of ligands in binding sites of protein. *J Comput Chem,* 31**,** 2014-22.
LI, J. C., GUPTA, V. K., YOU, Y., NG, K. W. & GRAHAM, S. L. 2013a. The dynamic response of intraocular pressure and ocular pulse amplitude to acute hemodynamic

changes in normal and glaucomatous eyes. *Invest Ophthalmol Vis Sci,* 54**,** 6960-7.

LI, R. S., TAY, D. K., CHAN, H. H. & SO, K. F. 2006. Changes of retinal functions following the induction of ocular hypertension in rats using argon laser photocoagulation. *Clin Exp Ophthalmol,* 34**,** 575-83.

LI, S., HSU, D. D., WANG, H. & FENG, G. S. 2012a. Dual faces of SH2-containing protein-tyrosine phosphatase Shp2/PTPN11 in tumorigenesis. *Front Med,* 6**,** 275-9.

LI, S., YANG, L., SELZER, M. E. & HU, Y. 2013b. Neuronal endoplasmic reticulum stress in axon injury and neurodegeneration. *Ann Neurol,* 74**,** 768-77.

LI, T., LINDSLEY, K., ROUSE, B., HONG, H., SHI, Q., FRIEDMAN, D. S., WORMALD, R. & DICKERSIN, K. 2016. Comparative Effectiveness of First-Line Medications for Primary Open-Angle Glaucoma: A Systematic Review and Network Meta-analysis. *Ophthalmology,* 123**,** 129-40.

LI, X., MCCLELLAN, M. E., TANITO, M., GARTEISER, P., TOWNER, R., BISSIG, D., BERKOWITZ, B. A., FLIESLER, S. J., WOODRUFF, M. L., FAIN, G. L., BIRCH, D. G., KHAN, M. S., ASH, J. D. & ELLIOTT, M. H. 2012b. Loss of caveolin-1 impairs retinal function due to disturbance of subretinal microenvironment. *J Biol Chem,* 287**,** 16424-34.

LIN, C., WU, M. & DONG, J. 2012. Quercetin-4'-O-beta-D-glucopyranoside (QODG) inhibits angiogenesis by suppressing VEGFR2-mediated signaling in zebrafish and endothelial cells. *PLoS One,* 7**,** e31708.

LIN, J. H., WALTER, P. & YEN, T. S. 2008. Endoplasmic reticulum stress in disease pathogenesis. *Annu Rev Pathol,* 3**,** 399-425.

LINDEN, C. & ALM, A. 1999. Prostaglandin analogues in the treatment of glaucoma. *Drugs Aging,* 14**,** 387-98.

LIU, C., CHAN, C. B. & YE, K. 2016. 7,8-dihydroxyflavone, a small molecular TrkB agonist, is useful for treating various BDNF-implicated human disorders. *Transl Neurodegener,* 5**,** 2.

LIU, X., CHAN, C. B., JANG, S. W., PRADOLDEJ, S., HUANG, J., HE, K., PHUN, L. H., FRANCE, S., XIAO, G., JIA, Y., LUO, H. R. & YE, K. 2010a. A synthetic 7,8-dihydroxyflavone derivative promotes neurogenesis and exhibits potent antidepressant effect. *J Med Chem,* 53**,** 8274-86.

LIU, X., CHAN, C. B., JANG, S. W., PRADOLDEJ, S., HUANG, J., HE, K., PHUN, L. H., FRANCE, S., XIAO, G., JIA, Y., LUO, H. R. & YE, K. 2010b. A Synthetic 7,8-Dihydroxyflavone Derivative Promotes Neurogenesis and Exhibits Potent Antidepressant Effect. *Journal of medicinal chemistry*.

LIU, X., GRISHANIN, R. N., TOLWANI, R. J., RENTERIA, R. C., XU, B., REICHARDT, L. F. & COPENHAGEN, D. R. 2007. Brain-derived neurotrophic factor and TrkB modulate visual experience-dependent refinement of neuronal pathways in retina. *J Neurosci,* 27**,** 7256-67.

LIU, X., OBIANYO, O., CHAN, C. B., HUANG, J., XUE, S., YANG, J. J., ZENG, F., GOODMAN, M. & YE, K. 2014. Biochemical and biophysical investigation of the brain-derived neurotrophic factor mimetic 7,8-dihydroxyflavone in the binding and activation of the TrkB receptor. *J Biol Chem,* 289**,** 27571-84.

LIU, Z. Z., ZHU, L. Q. & EIDE, F. F. 1997. Critical role of TrkB and brain-derived neurotrophic factor in the differentiation and survival of retinal pigment epithelium. *J Neurosci,* 17**,** 8749-55.

LONDON, A., BENHAR, I. & SCHWARTZ, M. 2013. The retina as a window to the brain-from eye research to CNS disorders. *Nat Rev Neurol,* 9**,** 44-53.

LORENZ, U. 2009. SHP-1 and SHP-2 in T cells: two phosphatases functioning at many levels. *Immunol Rev,* 228**,** 342-59.

LU, B., PANG, P. T. & WOO, N. H. 2005. The yin and yang of neurotrophin action. *Nat Rev Neurosci,* 6**,** 603-14.

LUCAS, J. J., HERNANDEZ, F., GOMEZ-RAMOS, P., MORAN, M. A., HEN, R. & AVILA, J. 2001. Decreased nuclear beta-catenin, tau hyperphosphorylation and neurodegeneration in GSK-3beta conditional transgenic mice. *EMBO J,* 20**,** 27-39.

LUO, J. 2009. Glycogen synthase kinase 3beta (GSK3beta) in tumorigenesis and cancer chemotherapy. *Cancer Lett,* 273**,** 194-200.

LUTHER, J. A. & BIRREN, S. J. 2009. Neurotrophins and target interactions in the development and regulation of sympathetic neuron electrical and synaptic properties. *Auton Neurosci,* 151**,** 46-60.

MA, Y. T., HSIEH, T., FORBES, M. E., JOHNSON, J. E. & FROST, D. O. 1998. BDNF injected into the superior colliculus reduces developmental retinal ganglion cell death. *J Neurosci,* 18**,** 2097-107.

MABUCHI, F., SAKURADA, Y., KASHIWAGI, K., YAMAGATA, Z., IIJIMA, H. & TSUKAHARA, S. 2015. Involvement of genetic variants associated with primary open-angle glaucoma in pathogenic mechanisms and family history of glaucoma. *Am J Ophthalmol,* 159**,** 437-44 e2.

MAI, L., JOPE, R. S. & LI, X. 2002. BDNF-mediated signal transduction is modulated by GSK3beta and mood stabilizing agents. *J Neurochem,* 82**,** 75-83.

MAKKERH, J. P., CENI, C., AULD, D. S., VAILLANCOURT, F., DORVAL, G. & BARKER, P. A. 2005. p75 neurotrophin receptor reduces ligand-induced Trk receptor ubiquitination and delays Trk receptor internalization and degradation. *EMBO Rep,* 6**,** 936-41.

MALLICK, J., DEVI, L., MALIK, P. K. & MALLICK, J. 2016. Update on Normal Tension Glaucoma. *J Ophthalmic Vis Res,* 11**,** 204-8.

MANSOUR-ROBAEY, S., CLARKE, D. B., WANG, Y. C., BRAY, G. M. & AGUAYO, A. J. 1994. Effects of ocular injury and administration of brain-derived neurotrophic factor on survival and regrowth of axotomized retinal ganglion cells. *Proc Natl Acad Sci U S A,* 91**,** 1632-6.

MAO, M., BIERY, M. C., KOBAYASHI, S. V., WARD, T., SCHIMMACK, G., BURCHARD, J., SCHELTER, J. M., DAI, H., HE, Y. D. & LINSLEY, P. S. 2004. T lymphocyte activation gene identification by coregulated expression on DNA microarrays. *Genomics,* 83**,** 989-99.

MARCINIAK, S. J., GARCIA-BONILLA, L., HU, J., HARDING, H. P. & RON, D. 2006. Activation-dependent substrate recruitment by the eukaryotic translation initiation factor 2 kinase PERK. *J Cell Biol,* 172**,** 201-9.

MARCINIAK, S. J., YUN, C. Y., OYADOMARI, S., NOVOA, I., ZHANG, Y., JUNGREIS, R., NAGATA, K., HARDING, H. P. & RON, D. 2004. CHOP induces death by promoting protein synthesis and oxidation in the stressed endoplasmic reticulum. *Genes Dev,* 18**,** 3066-77.

MAROTTE, L. R., VIDOVIC, M., WHEELER, E. & JHAVERI, S. 2004. Brain-derived neurotrophic factor is expressed in a gradient in the superior colliculus during development of the retinocollicular projection. *Eur J Neurosci,* 20**,** 843-7.

MARQUIS, R. E. & WHITSON, J. T. 2005. Management of glaucoma: focus on pharmacological therapy. *Drugs Aging,* 22**,** 1-21.

MARTI, H. J., BERNAUDIN, M., BELLAIL, A., SCHOCH, H., EULER, M., PETIT, E. & RISAU, W. 2000. Hypoxia-induced vascular endothelial growth factor expression precedes neovascularization after cerebral ischemia. *Am J Pathol,* 156**,** 965-76.

MARTIN, K. R., KLEIN, R. L. & QUIGLEY, H. A. 2002. Gene delivery to the eye using adeno-associated viral vectors. *Methods,* 28**,** 267-75.

MARTIN, K. R., QUIGLEY, H. A., ZACK, D. J., LEVKOVITCH-VERBIN, H., KIELCZEWSKI, J., VALENTA, D., BAUMRIND, L., PEASE, M. E., KLEIN, R. L. & HAUSWIRTH, W. W. 2003. Gene therapy with brain-derived neurotrophic factor as a protection: retinal ganglion cells in a rat glaucoma model. *Invest Ophthalmol Vis Sci,* 44**,** 4357-65.

MARTINOU, J. C. & YOULE, R. J. 2011. Mitochondria in apoptosis: Bcl-2 family members and mitochondrial dynamics. *Dev Cell,* 21**,** 92-101.

MATTSON, M. P. 2008. Glutamate and neurotrophic factors in neuronal plasticity and disease. *Ann N Y Acad Sci,* 1144**,** 97-112.

MAY, C. A. & LUTJEN-DRECOLL, E. 2002. Morphology of the murine optic nerve. *Invest Ophthalmol Vis Sci,* 43**,** 2206-12.

MCGILL, T. J., PRUSKY, G. T., DOUGLAS, R. M., YASUMURA, D., MATTHES, M. T., NUNE, G., DONOHUE-ROLFE, K., YANG, H., NICULESCU, D., HAUSWIRTH, W. W., GIRMAN, S. V., LUND, R. D., DUNCAN, J. L. & LAVAIL, M. M. 2007. Intraocular CNTF reduces vision in normal rats in a dose-dependent manner. *Invest Ophthalmol Vis Sci,* 48**,** 5756-66.

MEAD, B., BERRY, M., LOGAN, A., SCOTT, R. A., LEADBEATER, W. & SCHEVEN, B. A. 2015. Stem cell treatment of degenerative eye disease. *Stem Cell Res,* 14**,** 243-57.

MEY, J. & THANOS, S. 1993. Intravitreal injections of neurotrophic factors support the survival of axotomized retinal ganglion cells in adult rats in vivo. *Brain Res,* 602**,** 304-17.

MEYER, M., CLAUSS, M., LEPPLE-WIENHUES, A., WALTENBERGER, J., AUGUSTIN, H. G., ZICHE, M., LANZ, C., BUTTNER, M., RZIHA, H. J. & DEHIO, C. 1999. A novel vascular endothelial growth factor encoded by Orf virus, VEGF-E, mediates angiogenesis via signalling through VEGFR-2 (KDR) but not VEGFR-1 (Flt-1) receptor tyrosine kinases. *EMBO J,* 18**,** 363-74.

MIKELBERG, F. S., DRANCE, S. M., SCHULZER, M., YIDEGILIGNE, H. M. & WEIS, M. M. 1989. The normal human optic nerve. Axon count and axon diameter distribution. *Ophthalmology,* 96**,** 1325-8.

MILHAS, D., CLARKE, C. J. & HANNUN, Y. A. 2010. Sphingomyelin metabolism at the plasma membrane: implications for bioactive sphingolipids. *FEBS Lett,* 584**,** 1887-94.

MILLER, J. R. & MOON, R. T. 1996. Signal transduction through beta-catenin and specification of cell fate during embryogenesis. *Genes Dev,* 10**,** 2527-39.

MINCIONE, F., SCOZZAFAVA, A. & SUPURAN, C. T. 2007. The development of topically acting carbonic anhydrase inhibitors as anti-glaucoma agents. *Curr Top Med Chem,* 7**,** 849-54.

MINICHIELLO, L., CASAGRANDA, F., TATCHE, R. S., STUCKY, C. L., POSTIGO, A., LEWIN, G. R., DAVIES, A. M. & KLEIN, R. 1998. Point mutation in trkB causes loss of NT4-dependent neurons without major effects on diverse BDNF responses. *Neuron,* 21**,** 335-45.

MORRIS, G. M., HUEY, R., LINDSTROM, W., SANNER, M. F., BELEW, R. K., GOODSELL, D. S. & OLSON, A. J. 2009. AutoDock4 and AutoDockTools4: Automated docking with selective receptor flexibility. *J Comput Chem,* 30**,** 2785-91.

MORRISON, J., FARRELL, S., JOHNSON, E., DEPPMEIER, L., MOORE, C. G. & GROSSMANN, E. 1995. Structure and composition of the rodent lamina cribrosa. *Exp Eye Res,* 60**,** 127-35.

MURAKAMI, T., HINO, S. I., SAITO, A. & IMAIZUMI, K. 2007. Endoplasmic reticulum stress response in dendrites of cultured primary neurons. *Neuroscience,* 146**,** 1-8.

MURPHY, L. O. & BLENIS, J. 2006. MAPK signal specificity: the right place at the right time. *Trends Biochem Sci,* 31**,** 268-75.

MYSONA, B. A., SHANAB, A. Y., ELSHAER, S. L. & EL-REMESSY, A. B. 2014. Nerve growth factor in diabetic retinopathy: beyond neurons. *Expert Rev Ophthalmol,* 9**,** 99-107.

NAGATA, N., MATSUO, K., BETTAIEB, A., BAKKE, J., MATSUO, I., GRAHAM, J., XI, Y., LIU, S., TOMILOV, A., TOMILOVA, N., GRAY, S., JUNG, D. Y., RAMSEY, J. J., KIM, J. K., CORTOPASSI, G., HAVEL, P. J. & HAJ, F. G. 2012. Hepatic Src homology phosphatase 2 regulates energy balance in mice. *Endocrinology,* 153**,** 3158-69.

NAIR, K. S., COSMA, M., RAGHUPATHY, N., SELLAROLE, M. A., TOLMAN, N. G., DE VRIES, W., SMITH, R. S. & JOHN, S. W. 2016. YBR/EiJ mice: a new model of glaucoma caused by genes on chromosomes 4 and 17. *Dis Model Mech,* 9**,** 863-71.

NAKAMURA, K., MARTIN, K. C., JACKSON, J. K., BEPPU, K., WOO, C. W. & THIELE, C. J. 2006. Brain-derived neurotrophic factor activation of TrkB induces vascular endothelial growth factor expression via hypoxia-inducible factor-1alpha in neuroblastoma cells. *Cancer Res,* 66**,** 4249-55.

NAKANO, N., IKEDA, H. O., HASEGAWA, T., MURAOKA, Y., IWAI, S., TSURUYAMA, T., NAKANO, M., FUCHIGAMI, T., SHUDO, T., KAKIZUKA, A. & YOSHIMURA, N. 2016. Neuroprotective effects of VCP modulators in mouse models of glaucoma. *Heliyon,* 2**,** e00096.

NAMEKATA, K., HARADA, C., GUO, X., KIMURA, A., KITTAKA, D., WATANABE, H. & HARADA, T. 2012. Dock3 stimulates axonal outgrowth via GSK-3beta-mediated microtubule assembly. *J Neurosci,* 32**,** 264-74.

NEEL, B. G., GU, H. & PAO, L. 2003. The 'Shp'ing news: SH2 domain-containing tyrosine phosphatases in cell signaling. *Trends Biochem Sci,* 28**,** 284-93.

NICKELLS, R. W. 1999. Apoptosis of retinal ganglion cells in glaucoma: an update of the molecular pathways involved in cell death. *Surv Ophthalmol,* 43 Suppl 1**,** S151-61.

NISHIGUCHI, K. M., NAKAMURA, M., KANEKO, H., KACHI, S. & TERASAKI, H. 2007. The role of VEGF and VEGFR2/Flk1 in proliferation of retinal progenitor cells in murine retinal degeneration. *Invest Ophthalmol Vis Sci,* 48**,** 4315-20.

NISHIYAMA, K., TRAPP, B. D., IKEZU, T., RANSOHOFF, R. M., TOMITA, T., IWATSUBO, T., KANAZAWA, I., HSIAO, K. K., LISANTI, M. P. & OKAMOTO, T. 1999. Caveolin-3 upregulation activates beta-secretase-mediated cleavage of the amyloid precursor protein in Alzheimer's disease. *J Neurosci,* 19**,** 6538-48.

NOECKER, R. J. 2006. The management of glaucoma and intraocular hypertension: current approaches and recent advances. *Ther Clin Risk Manag,* 2**,** 193-206.

NOGA, O., ENGLMANN, C., HANF, G., GRUTZKAU, A., SEYBOLD, J. & KUNKEL, G. 2003. The production, storage and release of the neurotrophins nerve growth factor, brain-derived neurotrophic factor and neurotrophin-3 by human peripheral eosinophils in allergics and non-allergics. *Clin Exp Allergy,* 33**,** 649-54.

NUMAKAWA, T., SUZUKI, S., KUMAMARU, E., ADACHI, N., RICHARDS, M. & KUNUGI, H. 2010. BDNF function and intracellular signaling in neurons. *Histol Histopathol,* 25**,** 237-58.

O'BRIEN, S. E., BROWN, D. G., MILLS, J. E., PHILLIPS, C. & MORRIS, G. 2005. Computational tools for the analysis and visualization of multiple protein-ligand complexes. *J Mol Graph Model,* 24**,** 186-94.

OKAMOTO, T., SCHLEGEL, A., SCHERER, P. E. & LISANTI, M. P. 1998. Caveolins, a family of scaffolding proteins for organizing "preassembled signaling complexes" at the plasma membrane. *J Biol Chem,* 273**,** 5419-22.

OPPENHEIM, R. W. 1989. The neurotrophic theory and naturally occurring motoneuron death. *Trends Neurosci,* 12**,** 252-5.

ORGUL, S., CIOFFI, G. A., BACON, D. R. & VAN BUSKIRK, E. M. 1996. An endothelin-1-induced model of chronic optic nerve ischemia in rhesus monkeys. *J Glaucoma,* 5**,** 135-8.

ORTEGA, F., PEREZ-SEN, R., MORENTE, V., DELICADO, E. G. & MIRAS-PORTUGAL, M. T. 2010. P2X7, NMDA and BDNF receptors converge on GSK3 phosphorylation and cooperate to promote survival in cerebellar granule neurons. *Cell Mol Life Sci,* 67**,** 1723-33.

OSBORNE, N. N., CASSON, R. J., WOOD, J. P., CHIDLOW, G., GRAHAM, M. & MELENA, J. 2004. Retinal ischemia: mechanisms of damage and potential therapeutic strategies. *Prog Retin Eye Res,* 23**,** 91-147.

OYAMA, T., ABE, H. & USHIKI, T. 2006. The connective tissue and glial framework in the optic nerve head of the normal human eye: light and scanning electron microscopic studies. *Arch Histol Cytol,* 69**,** 341-56.

OZCAN, U., YILMAZ, E., OZCAN, L., FURUHASHI, M., VAILLANCOURT, E., SMITH, R. O., GORGUN, C. Z. & HOTAMISLIGIL, G. S. 2006. Chemical chaperones reduce ER stress and restore glucose homeostasis in a mouse model of type 2 diabetes. *Science,* 313**,** 1137-40.

PAN, X. L., REN, R. J., WANG, G., TANG, H. D. & CHEN, S. D. 2010. The Gab2 in signal transduction and its potential role in the pathogenesis of Alzheimer's disease. *Neurosci Bull,* 26**,** 241-6.

PAP, M. & COOPER, G. M. 1998. Role of glycogen synthase kinase-3 in the phosphatidylinositol 3-Kinase/Akt cell survival pathway. *J Biol Chem,* 273**,** 19929-32.

PARAMASHIVAM, S. K., ELAYAPERUMAL, K., NATARAJAN, B. B., RAMAMOORTHY, M. D., BALASUBRAMANIAN, S. & DHIRAVIAM, K. N. 2015. In silico pharmacokinetic and molecular docking studies of small molecules derived from Indigofera aspalathoides Vahl targeting receptor tyrosine kinases. *Bioinformation,* 11**,** 73-84.

PARIKH, R. S., PARIKH, S. R., NAVIN, S., ARUN, E. & THOMAS, R. 2008. Practical approach to medical management of glaucoma. *Indian J Ophthalmol,* 56**,** 223-30.

PARK, H. & POO, M. M. 2013. Neurotrophin regulation of neural circuit development and function. *Nat Rev Neurosci,* 14**,** 7-23.

PARKHURST, C. N., YANG, G., NINAN, I., SAVAS, J. N., YATES, J. R., 3RD, LAFAILLE, J. J., HEMPSTEAD, B. L., LITTMAN, D. R. & GAN, W. B. 2013. Microglia promote learning-dependent synapse formation through brain-derived neurotrophic factor. *Cell,* 155**,** 1596-609.

PATAPOUTIAN, A. & REICHARDT, L. F. 2001. Trk receptors: mediators of neurotrophin action. *Curr Opin Neurobiol,* 11**,** 272-80.

PAWSON, T., GISH, G. D. & NASH, P. 2001. SH2 domains, interaction modules and cellular wiring. *Trends Cell Biol,* 11**,** 504-11.
PAWSON, T. & SCOTT, J. D. 1997. Signaling through scaffold, anchoring, and adaptor proteins. *Science,* 278**,** 2075-80.
PEASE, M. E., MCKINNON, S. J., QUIGLEY, H. A., KERRIGAN-BAUMRIND, L. A. & ZACK, D. J. 2000. Obstructed axonal transport of BDNF and its receptor TrkB in experimental glaucoma. *Invest Ophthalmol Vis Sci,* 41**,** 764-74.
PEASE, M. E., ZACK, D. J., BERLINICKE, C., BLOOM, K., CONE, F., WANG, Y., KLEIN, R. L., HAUSWIRTH, W. W. & QUIGLEY, H. A. 2009. Effect of CNTF on retinal ganglion cell survival in experimental glaucoma. *Invest Ophthalmol Vis Sci,* 50**,** 2194-200.
PEEL, A. L. & KLEIN, R. L. 2000. Adeno-associated virus vectors: activity and applications in the CNS. *J Neurosci Methods,* 98**,** 95-104.
PEINADO-RAMON, P., SALVADOR, M., VILLEGAS-PEREZ, M. P. & VIDAL-SANZ, M. 1996. Effects of axotomy and intraocular administration of NT-4, NT-3, and brain-derived neurotrophic factor on the survival of adult rat retinal ganglion cells. A quantitative in vivo study. *Invest Ophthalmol Vis Sci,* 37**,** 489-500.
PENG, X., GREENE, L. A., KAPLAN, D. R. & STEPHENS, R. M. 1995. Deletion of a conserved juxtamembrane sequence in Trk abolishes NGF-promoted neuritogenesis. *Neuron,* 15**,** 395-406.
PERDICCHI, A., IESTER, M., SCUDERI, G., AMODEO, S., MEDORI, E. M. & RECUPERO, S. M. 2007. Visual field damage and progression in glaucomatous myopic eyes. *Eur J Ophthalmol,* 17**,** 534-7.
PERNET, V. & DI POLO, A. 2006. Synergistic action of brain-derived neurotrophic factor and lens injury promotes retinal ganglion cell survival, but leads to optic nerve dystrophy in vivo. *Brain,* 129**,** 1014-26.
PERNET, V., HAUSWIRTH, W. W. & DI POLO, A. 2005. Extracellular signal-regulated kinase 1/2 mediates survival, but not axon regeneration, of adult injured central nervous system neurons in vivo. *J Neurochem,* 93**,** 72-83.
PERRY, C. M., MCGAVIN, J. K., CULY, C. R. & IBBOTSON, T. 2003. Latanoprost : an update of its use in glaucoma and ocular hypertension. *Drugs Aging,* 20**,** 597-630.
PETERS, J. C., BHATTACHARYA, S., CLARK, A. F. & ZODE, G. S. 2015. Increased Endoplasmic Reticulum Stress in Human Glaucomatous Trabecular Meshwork Cells and Tissues. *Invest Ophthalmol Vis Sci,* 56**,** 3860-8.
PETERSON, B. B. & DACEY, D. M. 2000. Morphology of wide-field bistratified and diffuse human retinal ganglion cells. *Vis Neurosci,* 17**,** 567-78.
PETROS, T. J., REBSAM, A. & MASON, C. A. 2008. Retinal axon growth at the optic chiasm: to cross or not to cross. *Annu Rev Neurosci,* 31**,** 295-315.
PETSALAKI, E., STARK, A., GARCIA-URDIALES, E. & RUSSELL, R. B. 2009. Accurate prediction of peptide binding sites on protein surfaces. *PLoS Comput Biol,* 5**,** e1000335.
PETTERSEN, E. F., GODDARD, T. D., HUANG, C. C., COUCH, G. S., GREENBLATT, D. M., MENG, E. C. & FERRIN, T. E. 2004. UCSF Chimera--a visualization system for exploratory research and analysis. *J Comput Chem,* 25**,** 1605-12.
PINZON-GUZMAN, C., XING, T., ZHANG, S. S. & BARNSTABLE, C. J. 2015. Regulation of rod photoreceptor differentiation by STAT3 is controlled by a tyrosine phosphatase. *J Mol Neurosci,* 55**,** 152-9.
POLANSKY, J. R., FAUSS, D. J., CHEN, P., CHEN, H., LUTJEN-DRECOLL, E., JOHNSON, D., KURTZ, R. M., MA, Z. D., BLOOM, E. & NGUYEN, T. D. 1997. Cellular pharmacology

and molecular biology of the trabecular meshwork inducible glucocorticoid response gene product. *Ophthalmologica,* 211**,** 126-39.

POLLOCK, G. S., ROBICHON, R., BOYD, K. A., KERKEL, K. A., KRAMER, M., LYLES, J., AMBALAVANAR, R., KHAN, A., KAPLAN, D. R., WILLIAMS, R. W. & FROST, D. O. 2003. TrkB receptor signaling regulates developmental death dynamics, but not final number, of retinal ganglion cells. *J Neurosci,* 23**,** 10137-45.

POLYAK, S. L. 1957. *The vertebrate visual system; its origin, structure, and function and its manifestations in disease with an analysis of its role in the life of animals and in the origin of man, preceded by a historical review of investigations of the eye, and of the visual pathways and centers of the brain,* Chicago, University of Chicago Press.

PRASANNA, S., MANIVANNAN, E. & CHATURVEDI, S. C. 2005. Quantitative structure-activity relationship analysis of 2,3-diaryl indoles as selective cyclooxygenase-2 inhibitors. *J Enzyme Inhib Med Chem,* 20**,** 455-61.

PULA, J. H., TOWLE, V. L., STASZAK, V. M., CAO, D., BERNARD, J. T. & GOMEZ, C. M. 2011. Retinal Nerve Fibre Layer and Macular Thinning in Spinocerebellar Ataxia and Cerebellar Multisystem Atrophy. *Neuroophthalmology,* 35**,** 108-114.

QIAN, M. D., ZHANG, J., TAN, X. Y., WOOD, A., GILL, D. & CHO, S. 2006. Novel agonist monoclonal antibodies activate TrkB receptors and demonstrate potent neurotrophic activities. *J Neurosci,* 26**,** 9394-403.

QIAN, Q., LIU, Q., ZHOU, D., PAN, H., LIU, Z., HE, F., JI, S., WANG, D., BAO, W., LIU, X., LIU, Z., ZHANG, H., ZHANG, X., ZHANG, L., WANG, M., XU, Y., HUANG, F., LUO, B. & SUN, B. 2017. Brain-specific ablation of Efr3a promotes adult hippocampal neurogenesis via the brain-derived neurotrophic factor pathway. *FASEB J*.

QIU, W., WANG, X., ROMANOV, V., HUTCHINSON, A., LIN, A., RUZANOV, M., BATTAILE, K. P., PAI, E. F., NEEL, B. G. & CHIRGADZE, N. Y. 2014. Structural insights into Noonan/LEOPARD syndrome-related mutants of protein-tyrosine phosphatase SHP2 (PTPN11). *BMC Struct Biol,* 14**,** 10.

QUIGLEY, H. A., MCKINNON, S. J., ZACK, D. J., PEASE, M. E., KERRIGAN-BAUMRIND, L. A., KERRIGAN, D. F. & MITCHELL, R. S. 2000. Retrograde axonal transport of BDNF in retinal ganglion cells is blocked by acute IOP elevation in rats. *Invest Ophthalmol Vis Sci,* 41**,** 3460-6.

RAGHUNATH, A. & PERUMAL, E. 2015. Micro-RNAs and their roles in eye disorders. *Ophthalmic Res,* 53**,** 169-86.

RAJ, L. S. M., J, J., I, K., KRISHNA, P. S. & K, A. S. 2014. Molecular Docking Study for Inhibitors of Aggregatibacter actinomycetamcomitans Toxins in Treatment of Aggressive Perioodontitis. *J Clin Diagn Res,* 8**,** ZC48-51.

RAJALA, A., GUPTA, V. K., ANDERSON, R. E. & RAJALA, R. V. 2013. Light activation of the insulin receptor regulates mitochondrial hexokinase. A possible mechanism of retinal neuroprotection. *Mitochondrion,* 13**,** 566-76.

RAPER, S. E., CHIRMULE, N., LEE, F. S., WIVEL, N. A., BAGG, A., GAO, G. P., WILSON, J. M. & BATSHAW, M. L. 2003. Fatal systemic inflammatory response syndrome in a ornithine transcarbamylase deficient patient following adenoviral gene transfer. *Mol Genet Metab,* 80**,** 148-58.

REAGAN, A., GU, X., HAUCK, S. M., ASH, J. D., CAO, G., THOMPSON, T. C. & ELLIOTT, M. H. 2016. Retinal Caveolin-1 Modulates Neuroprotective Signaling. *Adv Exp Med Biol,* 854**,** 411-8.

REICHARDT, L. F. 2006. Neurotrophin-regulated signalling pathways. *Philos Trans R Soc Lond B Biol Sci,* 361**,** 1545-64.

REN, R., LI, Y., LIU, Z., LIU, K. & HE, S. 2012. Long-term rescue of rat retinal ganglion cells and visual function by AAV-mediated BDNF expression after acute elevation of intraocular pressure. *Invest Ophthalmol Vis Sci,* 53**,** 1003-11.

RICHARDS, A., EMONDI, A. A. & ROHRER, B. 2006. Long-term ERG analysis in the partially light-damaged mouse retina reveals regressive and compensatory changes. *Vis Neurosci,* 23**,** 91-7.

ROBIN, A. & GROVER, D. S. 2011. Compliance and adherence in glaucoma management. *Indian J Ophthalmol,* 59 Suppl**,** S93-6.

ROCHTCHINA, E. & MITCHELL, P. 2000. Projected number of Australians with glaucoma in 2000 and 2030. *Clin Exp Ophthalmol,* 28**,** 146-8.

ROH, M., ZHANG, Y., MURAKAMI, Y., THANOS, A., LEE, S. C., VAVVAS, D. G., BENOWITZ, L. I. & MILLER, J. W. 2012. Etanercept, a widely used inhibitor of tumor necrosis factor-alpha (TNF-alpha), prevents retinal ganglion cell loss in a rat model of glaucoma. *PLoS One,* 7**,** e40065.

ROVERE, G., NADAL-NICOLAS, F. M., SOBRADO-CALVO, P., GARCIA-BERNAL, D., VILLEGAS-PEREZ, M. P., VIDAL-SANZ, M. & AGUDO-BARRIUSO, M. 2016. Topical Treatment With Bromfenac Reduces Retinal Gliosis and Inflammation After Optic Nerve Crush. *Invest Ophthalmol Vis Sci,* 57**,** 6098-6106.

RUSANESCU, G., YANG, W., BAI, A., NEEL, B. G. & FEIG, L. A. 2005. Tyrosine phosphatase SHP-2 is a mediator of activity-dependent neuronal excitotoxicity. *EMBO J,* 24**,** 305-14.

SALMINEN, A., KAUPPINEN, A., SUURONEN, T., KAARNIRANTA, K. & OJALA, J. 2009. ER stress in Alzheimer's disease: a novel neuronal trigger for inflammation and Alzheimer's pathology. *J Neuroinflammation,* 6**,** 41.

SANGUINETTI, A. R., CAO, H. & CORLEY MASTICK, C. 2003. Fyn is required for oxidative- and hyperosmotic-stress-induced tyrosine phosphorylation of caveolin-1. *Biochem J,* 376**,** 159-68.

SANO, R. & REED, J. C. 2013. ER stress-induced cell death mechanisms. *Biochim Biophys Acta,* 1833**,** 3460-70.

SAPIEHA, P. S., PELTIER, M., RENDAHL, K. G., MANNING, W. C. & DI POLO, A. 2003. Fibroblast growth factor-2 gene delivery stimulates axon growth by adult retinal ganglion cells after acute optic nerve injury. *Mol Cell Neurosci,* 24**,** 656-72.

SAPPINGTON, R. M., CARLSON, B. J., CRISH, S. D. & CALKINS, D. J. 2010. The microbead occlusion model: a paradigm for induced ocular hypertension in rats and mice. *Invest Ophthalmol Vis Sci,* 51**,** 207-16.

SARFARAZI, M. & REZAIE, T. 2003. Optineurin in primary open angle glaucoma. *Ophthalmol Clin North Am,* 16**,** 529-41.

SAWADA, A., RIVERA, J. A., TAKAGI, D., NISHIDA, T. & YAMAMOTO, T. 2015. Progression to Legal Blindness in Patients With Normal Tension Glaucoma: Hospital-Based Study. *Invest Ophthalmol Vis Sci,* 56**,** 3635-41.

SAYERS, E. W., BARRETT, T., BENSON, D. A., BOLTON, E., BRYANT, S. H., CANESE, K., CHETVERNIN, V., CHURCH, D. M., DICUCCIO, M., FEDERHEN, S., FEOLO, M., FINGERMAN, I. M., GEER, L. Y., HELMBERG, W., KAPUSTIN, Y., LANDSMAN, D., LIPMAN, D. J., LU, Z., MADDEN, T. L., MADEJ, T., MAGLOTT, D. R., MARCHLER-BAUER, A., MILLER, V., MIZRACHI, I., OSTELL, J., PANCHENKO, A., PHAN, L., PRUITT, K. D., SCHULER, G. D., SEQUEIRA, E., SHERRY, S. T., SHUMWAY, M., SIROTKIN, K., SLOTTA, D., SOUVOROV, A., STARCHENKO, G., TATUSOVA, T. A., WAGNER, L., WANG, Y., WILBUR, W. J., YASCHENKO, E. & YE, J. 2011. Database

resources of the National Center for Biotechnology Information. *Nucleic Acids Res,* 39**,** D38-51.
SCHAPER, F., GENDO, C., ECK, M., SCHMITZ, J., GRIMM, C., ANHUF, D., KERR, I. M. & HEINRICH, P. C. 1998. Activation of the protein tyrosine phosphatase SHP2 via the interleukin-6 signal transducing receptor protein gp130 requires tyrosine kinase Jak1 and limits acute-phase protein expression. *Biochem J,* 335 (Pt 3)**,** 557-65.
SCHMEER, C., STRATEN, G., KUGLER, S., GRAVEL, C., BAHR, M. & ISENMANN, S. 2002. Dose-dependent rescue of axotomized rat retinal ganglion cells by adenovirus-mediated expression of glial cell-line derived neurotrophic factor in vivo. *Eur J Neurosci,* 15**,** 637-43.
SCHMITT, H. M., PELZEL, H. R., SCHLAMP, C. L. & NICKELLS, R. W. 2014. Histone deacetylase 3 (HDAC3) plays an important role in retinal ganglion cell death after acute optic nerve injury. *Mol Neurodegener,* 9**,** 39.
SCHNEIDMAN-DUHOVNY, D., INBAR, Y., NUSSINOV, R. & WOLFSON, H. J. 2005. PatchDock and SymmDock: servers for rigid and symmetric docking. *Nucleic Acids Res,* 33**,** W363-7.
SCHWARZ, D. S. & BLOWER, M. D. 2016. The endoplasmic reticulum: structure, function and response to cellular signaling. *Cell Mol Life Sci,* 73**,** 79-94.
SEBASTIANI, A., GOLZ, C., WERNER, C., SCHAFER, M. K., ENGELHARD, K. & THAL, S. C. 2015. Proneurotrophin Binding to P75 Neurotrophin Receptor (P75ntr) Is Essential for Brain Lesion Formation and Functional Impairment after Experimental Traumatic Brain Injury. *J Neurotrauma,* 32**,** 1599-607.
SEIGEL, G. M. 1999. The golden age of retinal cell culture. *Mol Vis,* 5**,** 4.
SEKI, M., TANAKA, T., SAKAI, Y., FUKUCHI, T., ABE, H., NAWA, H. & TAKEI, N. 2005. Muller Cells as a source of brain-derived neurotrophic factor in the retina: noradrenaline upregulates brain-derived neurotrophic factor levels in cultured rat Muller cells. *Neurochem Res,* 30**,** 1163-70.
SHAARAWY, T., FLAMMER, J. & HAEFLIGER, I. O. 2004. Reducing intraocular pressure: is surgery better than drugs? *Eye (Lond),* 18**,** 1215-24.
SHAN, Y., KIM, E. T., EASTWOOD, M. P., DROR, R. O., SEELIGER, M. A. & SHAW, D. E. 2011. How does a drug molecule find its target binding site? *J Am Chem Soc,* 133**,** 9181-3.
SHIBUYA, M. 2006. Vascular endothelial growth factor (VEGF)-Receptor2: its biological functions, major signaling pathway, and specific ligand VEGF-E. *Endothelium,* 13**,** 63-9.
SHIMOKE, K., AMANO, H., KISHI, S., UCHIDA, H., KUDO, M. & IKEUCHI, T. 2004. Nerve growth factor attenuates endoplasmic reticulum stress-mediated apoptosis via suppression of caspase-12 activity. *J Biochem,* 135**,** 439-46.
SIMHA, A., BRAGANZA, A., ABRAHAM, L., SAMUEL, P. & LINDSLEY, K. 2013. Anti-vascular endothelial growth factor for neovascular glaucoma. *Cochrane Database Syst Rev***,** CD007920.
SIMMONS, A. D., NGUYEN, T. K., FOLLIS, J. L. & RIBES-ZAMORA, A. 2014. Using a PyMOL activity to reinforce the connection between genotype and phenotype in an undergraduate genetics laboratory. *PLoS One,* 9**,** e114257.
SIMONELLI, F., MAGUIRE, A. M., TESTA, F., PIERCE, E. A., MINGOZZI, F., BENNICELLI, J. L., ROSSI, S., MARSHALL, K., BANFI, S., SURACE, E. M., SUN, J., REDMOND, T. M., ZHU, X., SHINDLER, K. S., YING, G. S., ZIVIELLO, C., ACERRA, C., WRIGHT, J. F., MCDONNELL, J. W., HIGH, K. A., BENNETT, J. & AURICCHIO, A. 2010. Gene

therapy for Leber's congenital amaurosis is safe and effective through 1.5 years after vector administration. *Mol Ther,* 18**,** 643-50.
SIPPL, C. & TAMM, E. R. 2014. What is the nature of the RGC-5 cell line? *Adv Exp Med Biol,* 801**,** 145-54.
SKARIE, J. M. & LINK, B. A. 2008. The primary open-angle glaucoma gene WDR36 functions in ribosomal RNA processing and interacts with the p53 stress-response pathway. *Hum Mol Genet,* 17**,** 2474-85.
SONDELL, M., SUNDLER, F. & KANJE, M. 2000. Vascular endothelial growth factor is a neurotrophic factor which stimulates axonal outgrowth through the flk-1 receptor. *Eur J Neurosci,* 12**,** 4243-54.
SONG, B. J. & CAPRIOLI, J. 2014. New directions in the treatment of normal tension glaucoma. *Indian J Ophthalmol,* 62**,** 529-37.
SOO, K. Y., HALLORAN, M., SUNDARAMOORTHY, V., PARAKH, S., TOTH, R. P., SOUTHAM, K. A., MCLEAN, C. A., LOCK, P., KING, A., FARG, M. A. & ATKIN, J. D. 2015. Rab1-dependent ER-Golgi transport dysfunction is a common pathogenic mechanism in SOD1, TDP-43 and FUS-associated ALS. *Acta Neuropathol,* 130**,** 679-97.
SOUTHWOOD, C. M., GARBERN, J., JIANG, W. & GOW, A. 2002. The unfolded protein response modulates disease severity in Pelizaeus-Merzbacher disease. *Neuron,* 36**,** 585-96.
SPENCER-SEGAL, J. L., WATERS, E. M., BATH, K. G., CHAO, M. V., MCEWEN, B. S. & MILNER, T. A. 2011. Distribution of phosphorylated TrkB receptor in the mouse hippocampal formation depends on sex and estrous cycle stage. *J Neurosci,* 31**,** 6780-90.
SRIBURI, R., JACKOWSKI, S., MORI, K. & BREWER, J. W. 2004. XBP1: a link between the unfolded protein response, lipid biosynthesis, and biogenesis of the endoplasmic reticulum. *J Cell Biol,* 167**,** 35-41.
SRINIVASAN, B., ROQUE, C. H., HEMPSTEAD, B. L., AL-UBAIDI, M. R. & ROQUE, R. S. 2004. Microglia-derived pronerve growth factor promotes photoreceptor cell death via p75 neurotrophin receptor. *J Biol Chem,* 279**,** 41839-45.
STOLP, H. B. 2013. Neuropoietic cytokines in normal brain development and neurodevelopmental disorders. *Mol Cell Neurosci,* 53**,** 63-8.
STORKEBAUM, E. & CARMELIET, P. 2004. VEGF: a critical player in neurodegeneration. *J Clin Invest,* 113**,** 14-8.
STRAHAN, G. D., KENIRY, M. A. & SHAFER, R. H. 1998. NMR structure refinement and dynamics of the K+-[d(G3T4G3)]2 quadruplex via particle mesh Ewald molecular dynamics simulations. *Biophys J,* 75**,** 968-81.
SUN, L., SIEPMANN, J. I. & SCHURE, M. R. 2006. Conformation and solvation structure for an isolated n-octadecane chain in water, methanol, and their mixtures. *J Phys Chem B,* 110**,** 10519-25.
SURGUCHEVA, I. & SURGUCHOV, A. 2011. Expression of caveolin in trabecular meshwork cells and its possible implication in pathogenesis of primary open angle glaucoma. *Mol Vis,* 17**,** 2878-88.
SUZUKI, A., NOMURA, S., MORII, E., FUKUDA, Y. & KOSAKA, J. 1998. Localization of mRNAs for trkB isoforms and p75 in rat retinal ganglion cells. *J Neurosci Res,* 54**,** 27-37.
SUZUKI, T., MATOZAKI, T., MIZOGUCHI, A. & KASUGA, M. 1995. Localization and subcellular distribution of SH-PTP2, a protein-tyrosine phosphatase with Src homology-2 domains, in rat brain. *Biochem Biophys Res Commun,* 211**,** 950-9.

SZEGEZDI, E., LOGUE, S. E., GORMAN, A. M. & SAMALI, A. 2006. Mediators of endoplasmic reticulum stress-induced apoptosis. *EMBO Rep,* 7**,** 880-5.

TAJIRI, S., YANO, S., MORIOKA, M., KURATSU, J., MORI, M. & GOTOH, T. 2006. CHOP is involved in neuronal apoptosis induced by neurotrophic factor deprivation. *FEBS Lett,* 580**,** 3462-8.

TAKAYASU, Y., TAKEUCHI, K., KUMARI, R., BENNETT, M. V., ZUKIN, R. S. & FRANCESCONI, A. 2010. Caveolin-1 knockout mice exhibit impaired induction of mGluR-dependent long-term depression at CA3-CA1 synapses. *Proc Natl Acad Sci U S A,* 107**,** 21778-83.

TAKIHARA, Y., INATANI, M., HAYASHI, H., ADACHI, N., IWAO, K., INOUE, T., IWAO, M. & TANIHARA, H. 2011. Dynamic imaging of axonal transport in living retinal ganglion cells in vitro. *Invest Ophthalmol Vis Sci,* 52**,** 3039-45.

TANAKA, H., ITO, Y., NAKAMURA, S., SHIMAZAWA, M. & HARA, H. 2009. Involvement of brain-derived neurotrophic factor in time-dependent neurodegeneration in the murine superior colliculus after intravitreal injection of N-methyl-D-aspartate. *Mol Vis,* 15**,** 662-9.

TANSLEY, K. 1956. Comparison of the lamina cribrosa in mammalian species with good and with indifferent vision. *Br J Ophthalmol,* 40**,** 178-82.

TAO, W., CHEN, Q., ZHOU, W., WANG, Y., WANG, L. & ZHANG, Z. 2014. Persistent inflammation-induced up-regulation of brain-derived neurotrophic factor (BDNF) promotes synaptic delivery of alpha-amino-3-hydroxy-5-methyl-4-isoxazolepropionic acid receptor GluA1 subunits in descending pain modulatory circuits. *J Biol Chem,* 289**,** 22196-204.

TATTON, W. G., CHALMERS-REDMAN, R. M. & TATTON, N. A. 2001. Apoptosis and anti-apoptosis signalling in glaucomatous retinopathy. *Eur J Ophthalmol,* 11 Suppl 2**,** S12-22.

TEMPLETON, J. P. & GEISERT, E. E. 2012. A practical approach to optic nerve crush in the mouse. *Mol Vis,* 18**,** 2147-52.

TENG, H. K., TENG, K. K., LEE, R., WRIGHT, S., TEVAR, S., ALMEIDA, R. D., KERMANI, P., TORKIN, R., CHEN, Z. Y., LEE, F. S., KRAEMER, R. T., NYKJAER, A. & HEMPSTEAD, B. L. 2005. ProBDNF induces neuronal apoptosis via activation of a receptor complex of p75NTR and sortilin. *J Neurosci,* 25**,** 5455-63.

THAM, Y. C., LI, X., WONG, T. Y., QUIGLEY, H. A., AUNG, T. & CHENG, C. Y. 2014. Global prevalence of glaucoma and projections of glaucoma burden through 2040: a systematic review and meta-analysis. *Ophthalmology,* 121**,** 2081-90.

THANOS, S., BAHR, M., BARDE, Y. A. & VANSELOW, J. 1989. Survival and Axonal Elongation of Adult Rat Retinal Ganglion Cells. *Eur J Neurosci,* 1**,** 19-26.

THORLEIFSSON, G., WALTERS, G. B., HEWITT, A. W., MASSON, G., HELGASON, A., DEWAN, A., SIGURDSSON, A., JONASDOTTIR, A., GUDJONSSON, S. A., MAGNUSSON, K. P., STEFANSSON, H., LAM, D. S., TAM, P. O., GUDMUNDSDOTTIR, G. J., SOUTHGATE, L., BURDON, K. P., GOTTFREDSDOTTIR, M. S., ALDRED, M. A., MITCHELL, P., ST CLAIR, D., COLLIER, D. A., TANG, N., SVEINSSON, O., MACGREGOR, S., MARTIN, N. G., CREE, A. J., GIBSON, J., MACLEOD, A., JACOB, A., ENNIS, S., YOUNG, T. L., CHAN, J. C., KARWATOWSKI, W. S., HAMMOND, C. J., THORDARSON, K., ZHANG, M., WADELIUS, C., LOTERY, A. J., TREMBATH, R. C., PANG, C. P., HOH, J., CRAIG, J. E., KONG, A., MACKEY, D. A., JONASSON, F., THORSTEINSDOTTIR, U. & STEFANSSON, K. 2010a. Common variants near CAV1 and CAV2 are associated with primary open-angle glaucoma. *Nat Genet,* 42**,** 906-9.

THORLEIFSSON, G., WALTERS, G. B., HEWITT, A. W., MASSON, G., HELGASON, A., DEWAN, A., SIGURDSSON, A., JONASDOTTIR, A., GUDJONSSON, S. A., MAGNUSSON, K. P., STEFANSSON, H., LAM, D. S. C., TAM, P. O. S., GUDMUNDSDOTTIR, G. J., SOUTHGATE, L., BURDON, K. P., GOTTFREDSDOTTIR, M. S., ALDRED, M. A., MITCHELL, P., ST CLAIR, D., COLLIER, D. A., TANG, N., SVEINSSON, O., MACGREGOR, S., MARTIN, N. G., CREE, A. J., GIBSON, J., MACLEOD, A., JACOB, A., ENNIS, S., YOUNG, T. L., CHAN, J. C. N., KARWATOWSKI, W. S. S., HAMMOND, C. J., THORDARSON, K., ZHANG, M., WADELIUS, C., LOTERY, A. J., TREMBATH, R. C., PANG, C. P., HOH, J., CRAIG, J. E., KONG, A., MACKEY, D. A., JONASSON, F., THORSTEINSDOTTIR, U. & STEFANSSON, K. 2010b. Common variants near CAV1 and CAV2 are associated with primary open-angle glaucoma. *Nature Genetics,* 42**,** 906-+.

TIAN, X. F., XIA, X. B., XU, H. Z., XIONG, S. Q. & JIANG, J. 2012. Caveolin-1 expression regulates blood-retinal barrier permeability and retinal neovascularization in oxygen-induced retinopathy. *Clin Exp Ophthalmol,* 40**,** e58-66.

TOPOUZIS, F., MELAMED, S., DANESH-MEYER, H., WELLS, A. P., KOZOBOLIS, V., WIELAND, H., ANDREW, R. & WELLS, D. 2007. A 1-year study to compare the efficacy and safety of once-daily travoprost 0.004%/timolol 0.5% to once-daily latanoprost 0.005%/timolol 0.5% in patients with open-angle glaucoma or ocular hypertension. *Eur J Ophthalmol,* 17**,** 183-90.

TRIFUNOVIC, D., SAHABOGLU, A., KAUR, J., MENCL, S., ZRENNER, E., UEFFING, M., ARANGO-GONZALEZ, B. & PAQUET-DURAND, F. 2012. Neuroprotective strategies for the treatment of inherited photoreceptor degeneration. *Curr Mol Med,* 12**,** 598-612.

TRIP, S. A., SCHLOTTMANN, P. G., JONES, S. J., LI, W. Y., GARWAY-HEATH, D. F., THOMPSON, A. J., PLANT, G. T. & MILLER, D. H. 2006. Optic nerve atrophy and retinal nerve fibre layer thinning following optic neuritis: evidence that axonal loss is a substrate of MRI-detected atrophy. *Neuroimage,* 31**,** 286-93.

TSANG, Y. H., HAN, X., MAN, W. Y., LEE, N. & POON, R. Y. 2012. Novel functions of the phosphatase SHP2 in the DNA replication and damage checkpoints. *PLoS One,* 7**,** e49943.

TSATSOS, M. & BROADWAY, D. 2007. Controversies in the history of glaucoma: is it all a load of old Greek? *Br J Ophthalmol,* 91**,** 1561-2.

TSUI, L., FONG, T. H. & WANG, I. J. 2013. The effect of 3-(5'-hydroxymethyl-2'-furyl)-1-benzylindazole (YC-1) on cell viability under hypoxia. *Mol Vis,* 19**,** 2260-73.

TSURUTA, F., SUNAYAMA, J., MORI, Y., HATTORI, S., SHIMIZU, S., TSUJIMOTO, Y., YOSHIOKA, K., MASUYAMA, N. & GOTOH, Y. 2004. JNK promotes Bax translocation to mitochondria through phosphorylation of 14-3-3 proteins. *EMBO J,* 23**,** 1889-99.

TURNER, B. A., SPARROW, J., CAI, B., MONROE, J., MIKAWA, T. & HEMPSTEAD, B. L. 2006. TrkB/BDNF signaling regulates photoreceptor progenitor cell fate decisions. *Dev Biol,* 299**,** 455-65.

VARMA, D. & SEN, D. 2015. Role of the unfolded protein response in the pathogenesis of Parkinson's disease. *Acta Neurobiol Exp (Wars),* 75**,** 1-26.

VECINO, E., GARCIA-CRESPO, D., GARCIA, M., MARTINEZ-MILLAN, L., SHARMA, S. C. & CARRASCAL, E. 2002. Rat retinal ganglion cells co-express brain derived neurotrophic factor (BDNF) and its receptor TrkB. *Vision Res,* 42**,** 151-7.

VENKATESH, A., MA, S., LANGELLOTTO, F., GAO, G. & PUNZO, C. 2013. Retinal gene delivery by rAAV and DNA electroporation. *Curr Protoc Microbiol,* Chapter 14**,** Unit 14D 4.

VIDAL-SANZ, M., VALIENTE-SORIANO, F. J., ORTIN-MARTINEZ, A., NADAL-NICOLAS, F. M., JIMENEZ-LOPEZ, M., SALINAS-NAVARRO, M., ALARCON-MARTINEZ, L., GARCIA-AYUSO, D., AVILES-TRIGUEROS, M., AGUDO-BARRIUSO, M. & VILLEGAS-PEREZ, M. P. 2015. Retinal neurodegeneration in experimental glaucoma. *Prog Brain Res,* 220**,** 1-35.

VIRDEE, K., BANNISTER, A. J., HUNT, S. P. & TOLKOVSKY, A. M. 1997. Comparison between the timing of JNK activation, c-Jun phosphorylation, and onset of death commitment in sympathetic neurones. *J Neurochem,* 69**,** 550-61.

VOLONTE, D., GALBIATI, F., PESTELL, R. G. & LISANTI, M. P. 2001. Cellular stress induces the tyrosine phosphorylation of caveolin-1 (Tyr(14)) via activation of p38 mitogen-activated protein kinase and c-Src kinase. Evidence for caveolae, the actin cytoskeleton, and focal adhesions as mechanical sensors of osmotic stress. *J Biol Chem,* 276**,** 8094-103.

VRABEC, J. P. & LEVIN, L. A. 2007. The neurobiology of cell death in glaucoma. *Eye (Lond),* 21 Suppl 1**,** S11-4.

WALLAND, M. J., PARIKH, R. S. & THOMAS, R. 2012. There is insufficient evidence to recommend lens extraction as a treatment for primary open-angle glaucoma: an evidence-based perspective. *Clin Exp Ophthalmol,* 40**,** 400-7.

WANG, Q., HERRERA ABREU, M. T., SIMINOVITCH, K., DOWNEY, G. P. & MCCULLOCH, C. A. 2006. Phosphorylation of SHP-2 regulates interactions between the endoplasmic reticulum and focal adhesions to restrict interleukin-1-induced Ca2+ signaling. *J Biol Chem,* 281**,** 31093-105.

WANG, W., ZHANG, G., GU, H., LIU, Y., LAO, J., LI, K. & GUAN, H. 2015a. Role of CtBP2 in the Apoptosis of Retinal Ganglion Cells. *Cell Mol Neurobiol,* 35**,** 633-40.

WANG, X., OLBERDING, K. E., WHITE, C. & LI, C. 2011. Bcl-2 proteins regulate ER membrane permeability to luminal proteins during ER stress-induced apoptosis. *Cell Death Differ,* 18**,** 38-47.

WANG, Y., SHEN, D., WANG, V. M., YU, C. R., WANG, R. X., TUO, J. & CHAN, C. C. 2012. Enhanced apoptosis in retinal pigment epithelium under inflammatory stimuli and oxidative stress. *Apoptosis,* 17**,** 1144-55.

WANG, Y., YAMADA, E., ZONG, H. & PESSIN, J. E. 2015b. Fyn Activation of mTORC1 Stimulates the IRE1alpha-JNK Pathway, Leading to Cell Death. *J Biol Chem,* 290**,** 24772-83.

WANG, Z., WANG, N., HAN, S., WANG, D., MO, S., YU, L., HUANG, H., TSUI, K., SHEN, J. & CHEN, J. 2013. Dietary compound isoliquiritigenin inhibits breast cancer neoangiogenesis via VEGF/VEGFR-2 signaling pathway. *PLoS One,* 8**,** e68566.

WASSMER, S. J., CARVALHO, L. S., GYORGY, B., VANDENBERGHE, L. H. & MAGUIRE, C. A. 2017. Exosome-associated AAV2 vector mediates robust gene delivery into the murine retina upon intravitreal injection. *Sci Rep,* 7**,** 45329.

WEBER, A. J. & ZELENAK, D. 2001. Experimental glaucoma in the primate induced by latex microspheres. *J Neurosci Methods,* 111**,** 39-48.

WEN, R., TAO, W., LI, Y. & SIEVING, P. A. 2012. CNTF and retina. *Prog Retin Eye Res,* 31**,** 136-51.

WIGGS, J. L., KANG, J. H., YASPAN, B. L., MIREL, D. B., LAURIE, C., CRENSHAW, A., BRODEUR, W., GOGARTEN, S., OLSON, L. M., ABDRABOU, W., DELBONO, E., LOOMIS, S., HAINES, J. L., PASQUALE, L. R. & CONSORTIUM, G. 2011. Common

variants near CAV1 and CAV2 are associated with primary open-angle glaucoma in Caucasians from the USA. *Hum Mol Genet,* 20**,** 4707-13.
WILLIAMS, D. L. 2016. Light and the evolution of vision. *Eye (Lond),* 30**,** 173-8.
WOJCIK-GRYCIUK, A., SKUP, M. & WALESZCZYK, W. J. 2015. Glaucoma -state of the art and perspectives on treatment. *Restor Neurol Neurosci,* 34**,** 107-23.
WU, Z., LIN, C., CROWTHER, M., MAK, H., YU, M. & LEUNG, C. K. 2017. Impact of Rates of Change of Lamina Cribrosa and Optic Nerve Head Surface Depths on Visual Field Progression in Glaucoma. *Invest Ophthalmol Vis Sci,* 58**,** 1825-1833.
XIONG, W. & CEPKO, C. 2016. Distinct Expression Patterns of AAV8 Vectors with Broadly Active Promoters from Subretinal Injections of Neonatal Mouse Eyes at Two Different Ages. *Adv Exp Med Biol,* 854**,** 501-7.
YAMADA, M., OHNISHI, H., SANO, S., ARAKI, T., NAKATANI, A., IKEUCHI, T. & HATANAKA, H. 1999. Brain-derived neurotrophic factor stimulates interactions of Shp2 with phosphatidylinositol 3-kinase and Grb2 in cultured cerebral cortical neurons. *J Neurochem,* 73**,** 41-9.
YAMADA, M., SUZUKI, K., MIZUTANI, M., ASADA, A., MATOZAKI, T., IKEUCHI, T., KOIZUMI, S. & HATANAKA, H. 2001. Analysis of tyrosine phosphorylation-dependent protein-protein interactions in TrkB-mediated intracellular signaling using modified yeast two-hybrid system. *J Biochem,* 130**,** 157-65.
YAN, Q., WANG, J., MATHESON, C. R. & URICH, J. L. 1999. Glial cell line-derived neurotrophic factor (GDNF) promotes the survival of axotomized retinal ganglion cells in adult rats: comparison to and combination with brain-derived neurotrophic factor (BDNF). *J Neurobiol,* 38**,** 382-90.
YAN, Z., SUN, X., EVANS, I. A., TYLER, S. R., SONG, Y., LIU, X., SUI, H. & ENGELHARDT, J. F. 2013. Postentry processing of recombinant adeno-associated virus type 1 and transduction of the ferret lung are altered by a factor in airway secretions. *Hum Gene Ther,* 24**,** 786-96.
YANG, L., LI, S., MIAO, L., HUANG, H., LIANG, F., TENG, X., XU, L., WANG, Q., XIAO, W., RIDDER, W. H., 3RD, FERGUSON, T. A., CHEN, D. F., KAUFMAN, R. J. & HU, Y. 2016a. Rescue of Glaucomatous Neurodegeneration by Differentially Modulating Neuronal Endoplasmic Reticulum Stress Molecules. *J Neurosci,* 36**,** 5891-903.
YANG, W., KLAMAN, L. D., CHEN, B., ARAKI, T., HARADA, H., THOMAS, S. M., GEORGE, E. L. & NEEL, B. G. 2006. An Shp2/SFK/Ras/Erk signaling pathway controls trophoblast stem cell survival. *Dev Cell,* 10**,** 317-27.
YANG, X., HONDUR, G. & TEZEL, G. 2016b. Antioxidant Treatment Limits Neuroinflammation in Experimental Glaucoma. *Invest Ophthalmol Vis Sci,* 57**,** 2344-54.
YOSHIDA, H., MATSUI, T., YAMAMOTO, A., OKADA, T. & MORI, K. 2001. XBP1 mRNA is induced by ATF6 and spliced by IRE1 in response to ER stress to produce a highly active transcription factor. *Cell,* 107**,** 881-91.
YOU, M., YU, D. H. & FENG, G. S. 1999. Shp-2 tyrosine phosphatase functions as a negative regulator of the interferon-stimulated Jak/STAT pathway. *Mol Cell Biol,* 19**,** 2416-24.
YOU, Q., BROWN, L. A., MCCLEMENTS, M., HANKINS, M. W. & MACLAREN, R. E. 2012a. Tetradecanoylphorbol-13-acetate (TPA) significantly increases AAV2/5 transduction of human neuronal cells in vitro. *Exp Eye Res,* 97**,** 148-53.

YOU, Y., GUPTA, V. K., LI, J. C., AL-ADAWY, N., KLISTORNER, A. & GRAHAM, S. L. 2014. FTY720 protects retinal ganglion cells in experimental glaucoma. *Invest Ophthalmol Vis Sci,* 55**,** 3060-6.

YOU, Y., THIE, J., KLISTORNER, A., GUPTA, V. K. & GRAHAM, S. L. 2012b. Normalization of visual evoked potentials using underlying electroencephalogram levels improves amplitude reproducibility in rats. *Invest Ophthalmol Vis Sci,* 53**,** 1473-8.

YUKITA, M., OMODAKA, K., MACHIDA, S., YASUDA, M., SATO, K., MARUYAMA, K., NISHIGUCHI, K. M. & NAKAZAWA, T. 2017. Brimonidine Enhances the Electrophysiological Response of Retinal Ganglion Cells through the Trk-MAPK/ERK and PI3K Pathways in Axotomized Eyes. *Curr Eye Res,* 42**,** 125-133.

ZENG, Y., LV, F., LI, L., YU, H., DONG, M. & FU, Q. 2012. 7,8-dihydroxyflavone rescues spatial memory and synaptic plasticity in cognitively impaired aged rats. *J Neurochem,* 122**,** 800-11.

ZHANG, L., HU, Y., SUN, C. Y., LI, J., GUO, T., HUANG, J. & CHU, Z. B. 2010. Lentiviral shRNA silencing of BDNF inhibits in vivo multiple myeloma growth and angiogenesis via down-regulated stroma-derived VEGF expression in the bone marrow milieu. *Cancer Sci,* 101**,** 1117-24.

ZHANG, Q. L., WANG, W., LI, J., TIAN, S. Y. & ZHANG, T. Z. 2015. Decreased miR-187 induces retinal ganglion cell apoptosis through upregulating SMAD7 in glaucoma. *Biomed Pharmacother,* 75**,** 19-25.

ZHANG, S. X., SANDERS, E., FLIESLER, S. J. & WANG, J. J. 2014. Endoplasmic reticulum stress and the unfolded protein responses in retinal degeneration. *Exp Eye Res,* 125**,** 30-40.

ZHANG, Z., TONG, N., GONG, Y., QIU, Q., YIN, L., LV, X. & WU, X. 2011. Valproate protects the retina from endoplasmic reticulum stress-induced apoptosis after ischemia-reperfusion injury. *Neurosci Lett,* 504**,** 88-92.

ZHENG, Y., WONG, T. Y., MITCHELL, P., FRIEDMAN, D. S., HE, M. & AUNG, T. 2010. Distribution of ocular perfusion pressure and its relationship with open-angle glaucoma: the singapore malay eye study. *Invest Ophthalmol Vis Sci,* 51**,** 3399-404.

ZHOU, L., TALEBIAN, A. & MEAKIN, S. O. 2015. The signaling adapter, FRS2, facilitates neuronal branching in primary cortical neurons via both Grb2- and Shp2-dependent mechanisms. *J Mol Neurosci,* 55**,** 663-77.

ZHOU, M., WANG, W., HUANG, W. & ZHANG, X. 2014. Diabetes mellitus as a risk factor for open-angle glaucoma: a systematic review and meta-analysis. *PLoS One,* 9**,** e102972.

ANIMAL RESEARCH AUTHORITY (ARA)

AEC Reference No.: 2012/031-8 **Date of Expiry:** 14 August 2015

Full Approval Duration: *15 August 2012 to 14 August 2015 (36 Months)*

This ARA remains in force until the Date of Expiry (unless suspended, cancelled or surrendered) **and will only be renewed upon receipt of a satisfactory Progress Report before expiry.**

Principal Investigator:
Prof Stuart Graham
Australian School of Advanced Medicine
Macquarie University NSW 2109
0416 060 862
stuart.graham@mq.edu.au

Associate Investigators:

Vivek Gupta	0422 122 996
Yuyi You	0410 384 655
Keith Ng	0404 744 488
Nitin Chitranshi	0432 599 293

In case of emergency, please contact:

the Principal Investigator / Associate Investigator named above

or Manager, CAF: 9850 7780 / 0428 861 163 and **Animal Welfare Officer**: 9850 7758 / 0439 497 383

The above-named are authorised by MACQUARIE UNIVERSITY ANIMAL ETHICS COMMITTEE to conduct the following research:

Title of the project: **Study the Neuro-protective effects of drugs on the retina**

Purpose: **5 - Research : human or animal health and welfare**

Aims: **1. To study the protective effects of 7,8 DHF and Deoxygedunin on the retina under the normal and glaucoma conditions**
2. To study whether the loss of BDNF can be compensated by the administration of either of these compounds

Surgical Procedures category: **4. Minor surgery with recovery**
2. Animal unconscious without recovery

All procedures must be performed as per the AEC-approved protocol, unless stated otherwise by the AEC and/or AWO.

Maximum numbers approved (for the Full Approval Duration):

Species	Strain	Age/Sex/Weight	Total	Supplier/Source
Rats	SD	6-10w/Male/200-500g	66 +12	ARC Perth
Mice	Mixed	4-14w/Both/15-40g	108	Melbourne Brain Centre
		TOTAL	**186**	

Location of research:

Location	*Full street address*
Central Animal Facility	Building F9A, Research Park Drive, Macquarie University NSW 2109

Amendments approved by the AEC since initial approval:

1. *Amendment #1 - Change to experimental design - urethane anaesthesia and surgical procedure prior to euthanasia (Approved December 2012)*
2. *Removal of Jonathan Li from the ARA (Approved by Exec on 2 April 2014, to be ratified at the 17 April 2014 AEC meeting).*
3. *Amendment #2 – Amend number of animals (n=8); technique or procedure (Approved AEC 15 May 2014).*
4. *Amendment #3 – Addition of Mr Nitin Chitranshi as Student (Exec approved 5 June 2014, ratified at the 19 June 2014 AEC meeting).*
5. *Amendment #4 – Amend number of animals(addition of 12 rats), techniques and procedure(Approved by AEC 16 October 2014)*

Conditions of Approval:

1. *The AEC requests that each of the experimental groups are increased to 6 animals (total n=12) to ensure statistical validity (AEC May 2014).*
2. *Approval of Amendment #3 is conditional to Nitin Chitranshi attending the next Working With Research Animals Workshop on Friday, 25 July 2014 in order to appreciate NSW legislation and expectation.*

Being animal research carried out in accordance with the Code of Practice for a recognised research purpose and in connection with animals (other than exempt animals) that have been obtained from the holder of an animal suppliers licence.

Professor Mark Connor (Chair, Animal Ethics Committee) **Approval Date:** 16 October 2014

Adapted from Form C (issued under part IV of the Animal Research Act, 1985)

ANIMAL RESEARCH AUTHORITY (ARA)

MACQUARIE University

AEC Reference No.: 2014/058-4 **Date of Expiry:** 15 January 2016

Full Approval Duration: *15 January 2015 to 31 October 2017*

This ARA remains in force until the Date of Expiry (unless suspended, cancelled or surrendered) **and will only be renewed upon receipt of a satisfactory Progress Report before expiry (see Approval email for submission details).**

Principal Investigator:
Professor Stuart Graham
Australian School of Advanced medicine
Macquarie University, NSW 2109
0416 060 862
Stuart.graham@mq.edu.au

Associate Investigator:
Yuyi You 0410 384 655
Nitin Chitranshi 0432 599 293
Vivek Gupta 0422 122 996

Research Assistant:
Roshana Vander Wall 0401 500 680
Yogita Dheer 0466 576 418

In case of emergency, please contact:
the Principal Investigator / Associate Investigator named above
or Manager, CAF: 9850 7780 / 0428 861 163 and **Animal Welfare Officer**: 9850 7758 / 0439 497 383

The above-named are authorised by MACQUARIE UNIVERSITY ANIMAL ETHICS COMMITTEE to conduct the following research:

Title of the project : To study the cellular signalling pathways in the retina

Purpose: 5 - Research: Human or Animal Health and Welfare

Aims: 1. To study the role of caveolin in the inner retinal structure and function
2. To study the Shp2-caveolin interactions and investigate the effect of Shp2 manipulation in the retina.

Surgical Procedures category: 4 - Minor Surgery With Recovery

All procedures must be performed as per the AEC-approved protocol, unless stated otherwise by the AEC and/or AWO

Maximum numbers approved (for the Full Approval Duration):

Species	Strain	Sex/Age/Weight	Total	Supplier/Source
01 Mus	Caveolin-1 Knock out mice	Any/ 3 week to 4 month old for experimentation	48	2-3 breeder pairs from University of Queensland. Afterwards the animals will be bred at MARS
01 Mus	Caveolin - Wild Type mice	Any/ 3 week to 4 month old for experimentation	48	MARS
01 Mus	Caveolin Heterozygous mice	Any/ 3 week to 4 month old for experimentation	48	MARS
02 Rat	Sprague-Dawley	Male/ 6-12 week/Any	32	ARC Perth
		TOTAL	176	

Location of research:

Location	*Full street address*
FMHS Laboratory	Level 1, F10A, 2 Technology Place, Macquarie University, NSW 2109
MARS	Building F9A, Research Park Drive, Macquarie University, NSW 2109

Amendments approved by the AEC since initial approval: N/A

1. Amendment #1 - Addition of Roshana Vander Wall as Research Assistant (approved at AEC meeting 14 May 2015)
2. Amendment #2 - Addition of Yogita Dheer as Associate Investigator (approved at AEC meeting 14 May 2015)
3. Amendment #3 - Change type of animals – additional 48 Caveolin Heterozygous mice requested (Executive approved. Ratified at AEC meeting 17 September 2015).
4. Amendment #4 - Change number and type of animals – 32 Rats (approved at AEC meeting 17 September 2015).

Conditions of Approval:

1. ***Amendment #1 and #2 approved subject to PI providing additional evidence of experience for both Roshana Vander Wall and Yogita Dheer. Additional evidence provided and approved at 18 June 2015 AEC meeting.***

Being animal research carried out in accordance with the Code of Practice for a recognised research purpose and in connection with animals (other than exempt animals) that have been obtained from the holder of an animal suppliers licence.

Professor Mark Connor (Chair, Animal Ethics Committee) **Approval Date:** 17 September 2015

Adapted from Form C (issued under part IV of the Animal Research Act, 1985)